ROBUST NUMERICAL SCHEMES FOR SINGULARLY PERTURBED BOUNDARY-VALUE PROBLEMS ON ADAPTIVE MESHES

by

Pratibhamoy Das

DEPARTMENT OF MATHEMATICS
INDIAN INSTITUTE OF TECHNOLOGY GUWAHATI
GUWAHATI-781039, INDIA

February, 2013

ROBUST NUMERICAL SCHEMES FOR SINGULARLY PERTURBED BOUNDARY-VALUE PROBLEMS ON ADAPTIVE MESHES

A Thesis Submitted

in Partial Fulfillment of the Requirements

for the Degree of

DOCTOR OF PHILOSOPHY

by

Pratibhamoy Das

(Roll Number: 08612305)

to the

DEPARTMENT OF MATHEMATICS

INDIAN INSTITUTE OF TECHNOLOGY GUWAHATI

February, 2013

DECLARATION

It is certified that the work contained in the thesis titled **"Robust Numerical Schemes for Singularly Perturbed Boundary-Value Problems on Adaptive Meshes"** has been done by me, a student in the Department of Mathematics, Indian Institute of Technology Guwahati under the guidance of Dr. Srinivasan Natesan, Professor, Indian Institute of Technology Guwahati, for the award of Doctor of Philosophy and that this work has not been submitted elsewhere for a degree.

February, 2013

Pratibhamoy Das
Department of Mathematics
Indian Institute of Technology Guwahati

CERTIFICATE

It is certified that the work contained in the thesis titled **"Robust Numerical Schemes for Singularly Perturbed Boundary-Value Problems on Adaptive Meshes"** by **Pratibhamoy Das** (Roll No: 08612305), a student in the Department of Mathematics, Indian Institute of Technology Guwahati, for the award of the degree of Doctor of Philosophy has been carried out under my supervision and this work has not been submitted elsewhere for a degree.

February, 2013

Dr. Srinivasan Natesan
Professor
Department of Mathematics
Indian Institute of Technology Guwahati

Dedicated to

My Parents

Acknowledgement

First and foremost, I would like to express my profound gratitude and heartfelt thanks to my thesis supervisor Prof. Srinivasan Natesan for his guidance during my research. In particular, I would like to thank him for his continuous help, for being an endless source of information and for teaching me the scientific writings. All of this on top of being a genuinely nice person. His patience, encouragement and support from the beginning to the end, enabled me throughout the development of my understanding on the subject. Apart from this, I acknowledge my gratitude to the Indian Institute of Technology, Guwahati for the financial, academic and technical support.

Next, I owe my sincere thanks to the members of my doctoral committee Prof. D.C. Dalal, Prof. R.K. Sinha and Prof. S.N. Bora for the time they invested in reading the manuscript during the progress of this dissertation and commenting on it. I also convey my gratitude to all the faculty members who have offered their help at different stages during my research time.

In addition, I take this opportunity to convey my gratefulness to my friends and co-researchers, specially to the members of my coffee club, Manideepa and Ravi, who gave the early mornings a pleasant start and also Murli for his fake fairy tales about other research scholars during coffee breaks. My senior Kaushik, Jugal and junior Gowrishankar deserve special thank due to their friendly and wonderful company during my research. As a big fan of extra-institutional activities, a huge debt of gratitude is also owed to everyone, specially Supriyo who encouraged me to pursue my interests.

At this juncture I think of my parents whose selfless sacrificial life and their great efforts with pain and tears with continuous support– both spiritually and materially has enabled me to reach the present position in life. The completion of this thesis will mean a lot to them, particularly "seeing more of me". So I dedicate this thesis to my loving parents Phanindra Nath Das and Mitali Das, without whose love, affection and encouragement this work would not have been possible.

Finally, I thank all those who have helped me directly or indirectly in the successful completion of my thesis. Anyone missed in this acknowledgement are also thanked.

February, 2013

Pratibhamoy Das

"Nothing happens until something moves"

—**Albert Einstein**

"We often hear that mathematics consists mainly of 'proving theorems'. Is a writer's job mainly that of 'writing sentences'?"

—**Gian-Carlo Rota**

"The shortest path between two truths in the real domain passes through the complex domain"

—— **Jacques Hadamard**

Abstract

In this thesis, our primary interest is to provide some efficient and higher-order numerical techniques for solving singularly perturbed convection-diffusion and reaction-diffusion boundary-value problems exhibiting boundary layers. These singular perturbation problems (SPPs) are described by differential equations in which the highest-order derivative is multiplied by an arbitrarily small parameter ε (say) known as *singular perturbation parameter*. This leads to the existence of boundary layers which are basically narrow regions in the neighbourhood of the boundary of the domain, where the gradient of the solution becomes steep as the perturbation parameter tends to zero. Due to the appearance of the layer phenomena, it is a challenging task to provide ε-uniform numerical methods. The term 'ε-uniform' refers to identify those numerical methods in which the approximate solution converges to the corresponding exact solution (measured to the supremum norm) independently with respect to the perturbation parameter ε.

The purpose of this thesis is to develop, analyze and improve the ε-uniform numerical methods for solving SPPs. These methods are mainly based on two types of nonuniform meshes. They are the well-known layer resolving piecewise-uniform Shishkin mesh and the equidistributed layer-adapted meshes, which are obtained by moving fixed number mesh points to equidistribute a positive monitor function, depending on the solution or/and its derivatives.

At first, a uniformly convergent hybrid numerical scheme is proposed and analyzed on the equidistributed mesh for singularly perturbed Robin type reaction-diffusion problems. This scheme uses a proper combination of central difference and cubic spline approximation for the second-order derivative. In addition, the proposed hybrid scheme is extended for a system of Robin type reaction-diffusion problems on *apriori* chosen piecewise-uniform Shishkin mesh. In all these cases, the newly proposed hybrid scheme attains almost second-order accuracy. Thereafter, the mesh equidistribution technique is extended for a class of fourth-order ordinary differential equations (ODEs), where the adaptively generated mesh is obtained by equidistribution of a curvature type monitor function. Moreover, we derive theoretically *apriori* monitor function to study the effect of mesh equidistribution for a general singularly perturbed system of reaction-diffusion problems. Next, Richardson extrapolation technique, which improves the first-order accuracy of the standard upwind scheme to second-order convergence is analyzed for singularly perturbed convection-diffusion problems using moving mesh methods. Finally, the equidistribution of a monitor function which works for scalar form of convection-diffusion problem is extended for a system singularly perturbed convection-diffusion problems to obtain an optimal first-order accurate parameter-uniform convergent solution. Extensive numerical experiments are conducted which support all of our theoretical findings. A concise conclusion with possible further work is provided at the end of this thesis.

Contents

NOMENCLATURE

SPP	Singular Perturbation Problem
BVP	Boundary-Value Problem
MBVP	Mixed /or Robin type Boundary-Value Problem
ODE	Ordinary Differential Equation
$\mathbb{R}$	Set of real numbers
ε, ε_m	Singular perturbation parameter
h	Step length
$O(\cdot)$, $o(\cdot)$	Landau order symbols
N	Number of mesh intervals
x, x_i, x_j	Independent variables
h_i, h_j	Mesh width of a nonuniform mesh
C	Generic positive constant independent of ε, h, h_i, x_i
$u(x), u_\varepsilon(x), \boldsymbol{u}(x), \boldsymbol{u}_\varepsilon(x)$	Solution of continuous problem
U_i, U_i^N, U^N, $\boldsymbol{U}_i$, $\boldsymbol{U}_i^N$, $\boldsymbol{U}^N$	Numerical solution
Ω	Open interval $(0, 1)$
$\overline{\Omega}$	Closed interval $[0, 1]$
$\partial\Omega$	Boundary of the domain Ω *i.e.,* $\{0, 1\}$
$\Omega^N, \overline{\Omega}^N$	Discrete domain
$\mathfrak{C}^k(\Omega), \mathfrak{C}^k(\bar{\Omega})$	k times continuously differentiable functions in the respective domain
$\lvert\cdot\rvert$	Absolute value
$\lVert\cdot\rVert$ or $\lVert\cdot\rVert_D$	Supremum norm over the domain D
$\mathcal{L}$,$\mathcal{L}_\varepsilon$, L, $\mathbb{L}$,$\mathfrak{L}$,$\mathbf{L}$	Differential operators
$\mathcal{L}^N$,$\mathcal{L}_\varepsilon^N$, L^N, $\mathbb{L}^N$, $\mathfrak{L}^N$, $\mathbf{L}^N$	Difference operators
M_l, M_r	Continuous mixed boundary operators for left and right boundaries, respectively
M_l^N, M_r^N	Discrete mixed boundary operators for left and right boundaries, respectively
D^+, D^-	Forward and backward difference operators, respectively
δ^2	Central difference operator

$E_{\varepsilon}^{N}, E_{m,\varepsilon}^{N}$	Maximum point-wise errors
E^{N}, E_{m}^{N}	Uniform errors
r^{N}, r_{m}^{N}	Rate of convergence of uniform errors

List of Figures

List of Tables

Chapter 1

Introduction

1.1 Singular Perturbation Problem

Singular perturbation problems (SPPs) are of common occurrence in many branches of applied mathematics and engineering including fluid mechanics, chemical reactor theory, elasticity, gas porous electrodes theory, heat and mass transfer processes in composite materials with small heat conduction or diffusion. These types of problems are typically characterized by an arbitrarily small parameter multiplied with some or all of the highest order terms in the differential equation. For example, one of the most striking examples of SPPs is the Navier-Stokes equation of fluid dynamics

$$\frac{\partial(u^2+p)}{\partial x}+\frac{\partial(uv)}{\partial y}=\frac{1}{Re}\left(\frac{\partial^2 u}{\partial x^2}+\frac{\partial^2 u}{\partial y^2}\right), \tag{1.1.1}$$

with suitable initial and boundary conditions. Here u and v are the velocity components along the x and y directions and p is the pressure. The parameter 'Re' is known as 'Reynolds number'. 'Re' is proportional to the length scale, velocity scale and inversely proportional to the kinematic viscosity of the fluid. For sufficiently large $Re(\gg 1)$, the equation stated in (1.1.1) will be transformed into a singularly perturbed differential equation. The 'continuity equation' for electrons in a steady state scaled model [67] of a one-dimensional semiconductor is another significant example to be noted as a singularly perturbed equation. Several other examples can be found in the books of Miller [57], Morton [59] and Roos et al. [74].

The birth of singular perturbation problems came into picture at the Third International Congress of Mathematicians in Heidelberg in 1904 by Prandtl's seven-page report published in the proceedings [68]. In his innovative work on the subject of *boundary layer theory*, he explained about how a quantity as small as the viscosity of common fluids such as water and air could play a crucial role in determining their flow. In his work, Prandtl proved that the flow about a body can be treated by dividing it into two regions: inside a very thin layer (which he called the boundary layer) in proximity to the body where the frictional effects are prominent, and the remaining as the outside

region. The boundary layer theory became the foundation stone for modern fluid dynamics. The term 'singular perturbation' was first introduced by Friedrichs and Wasow in their paper [32]. Though Prandtl introduced the terminology 'boundary layer', it got much greater generality in the substantial work of Wasow [84].

The singularly perturbed differential equations involving an arbitrarily small parameter ε (say), where $0 < \varepsilon \ll 1$ attract its attention from mathematicians as well as physicists. In general, the analytical solutions of these problems exhibit multi-scale phenomena, *i.e.,* the solutions vary rapidly within the boundary layers and behave smoothly away from the layers. The common approach to study the fundamental nature of the analytical solution as the parameter ε goes to zero is through asymptotic expansion technique. A straightforward asymptotic expansion using an asymptotic sequence of the parameter ε leads to differential equations of lower order than the original differential equation. As a consequence, not all the boundary or initial conditions can be satisfied by the perturbation expansion. The technique for overcoming this difficulty is to combine the straightforward expansion known as *outer expansion,* valid away from the boundary layer with an expansion called the *inner expansion* valid within a layer adjacent to the boundary where the boundary condition is not satisfied. The inner expansion associated within the boundary layer region is expressed in terms of a stretched variable rather than the original independent variable, which takes account of the scale of certain solution derivative terms. The inner and outer expansions are matched over a region located at the edge of the boundary layer using the method of *matched asymptotic expansion.* It should be noticed that before solving the problem, one has to know the location and width of the boundary layer which can be obtained by the *principle of least degeneracy* from Van Dyke [27]. For more details about the asymptotic expansion technique, one can refer the books of Bender and Orszag [11], Bush [13], Miller [57] and O' Malley [65].

Classical computational methods (standard finite difference or finite element or finite volume methods) to SPPs are known to be inadequate on uniform meshes as they require extremely large number of mesh points to produce satisfactory numerical solutions (see [74]). This is due to the presence of steep gradients in the analytical solutions. In this context, careful numerical experiments (see Farrell [29]) show that the classical methods fail to decrease the maximum point-wise error as the mesh is refined, until the mesh size and the perturbation parameter have the same order of magnitude. This contradicts the natural expectation that the error of an acceptable computational method (applicable for regular perturbation problems) decreases when the mesh is refined. For *e.g.*, when the perturbation parameter $\varepsilon = 2^{-20}$ an unexpectedly large number of mesh points are required to achieve an accurate numerical solution. Consequently, the size of system of algebraic equations will be increasing more as the dimension of the problem increases. Hence this incorporates the massive computational cost. This drawback motivates to the

concept of ε-uniform numerical methods; in which the order of convergence and the error constant is independent of the perturbation parameter ε. Throughout this thesis, we focus only on ε-uniform (robust) numerical methods to obtain the approximate solutions.

The construction of ε-uniform numerical methods over the last few decades, can be classified mainly by two different approaches. These approaches are defined as follows.

The first approach substitutes the standard finite difference operator (corresponding to the continuous problem) by a difference operator which reflects the singularly perturbed nature of the differential operator. The modified finite difference operator is referred as *fitted finite difference operator*, which is defined on a standard mesh (very often on uniform mesh). The construction of this difference operator uses a proper choice of the difference coefficients so that some or all of the exponential functions are in the null space of the differential operator. In general, this method is known as *fitted operator method*, which is first introduced by Allen et al. [24] for solving the problem of a viscous fluid flow past a cylinder. It is often possible to obtain ε-uniform numerical method by constructing an appropriately fitted finite difference operator for the problems with regular boundary layers (a boundary layer is said to be of regular type if the characteristics of the reduced equation corresponding to $\varepsilon = 0$ are not parallel to the boundary and the boundary layer is said to be of parabolic type if the characteristics are parallel to the boundary) on uniform meshes. However, in the case of problems with parabolic layers, Shishkin [78] established that no fitted operator method on a uniform mesh exists for such problems. The same result is also introduced by Miller et al. [56] where the modeling of heat transfer in the case of flow over a fat plate with suction of the boundary layer is considered. For more details about the explanation of this method, one can see the books Doolan et al. [26], Miller et al. [55].

The second recognized approach for the construction of ε-uniform numerical method involves the use of standard finite difference operators on special meshes which are condensed towards the boundary or interior layers. Such methods are referred as *fitted mesh methods.* These methods have an extra advantage over the fitted operator methods due to their implementation on the standard operators and their extensions to solve higher-dimensional and nonlinear problems with complicated domain structure. If sufficient *apriori* information about the solution is available, then appropriate meshes can be constructed where the solution accuracy of these methods depend only on the number of meshes and is independent of the perturbation parameter. Otherwise, a newly developed adaptive strategy can be implemented to determine the appropriate grading for obtaining a layer-adapted mesh. This technique uses the equidistribution of a positive monitor function, which defines some error measurement of the numerical solution. This simply means the rearrangement of the meshes so that the error quantity is equally distributed. For example, if we consider the porous medium equation for [30], which can model a gas

bubble spreading in a porous medium [3], we might want to have more points where the mass density is high. Here, the monitor function plays the role of automatic detection of the locations where the mass density /or solution variation is rapid. Now-a-days, this adaptive technique has become a valuable computational technique in the context of singular perturbation theory. Here the importance of the monitor function is to automatically detect the presence of the boundary layers together with their locations, widths and distribute mesh points accordingly. The mesh adaptation techniques, which study the proper movement of a fixed number of mesh points by the equidistribution of a positive monitor function are generally known as *moving mesh methods*.

1.1.1 Adaptive mesh

This thesis mainly focuses on the moving mesh adaptivity, but also discusses alternative approaches. The overview is not only a good introduction to the methods used in the following chapters but, more importantly, puts all approaches together and describing their equivalences and differences. Adaptive mesh methods can be recognized as an efficient tool for differential equations involving multi-scale nature of the solution.

The singular perturbation problems can be classified by two major ways, so called convection-diffusion problems and reaction-diffusion problems. A typical singularly perturbed convection-diffusion problem on $\Omega = (0, 1)$ is of the following form

$$\begin{cases} -\varepsilon u''(x) + a(x)u'(x) + b(x)u(x) = f(x), \quad x \in \Omega, \\ \\ u(0) = u(1) = 0, \end{cases} \tag{1.1.2}$$

where ε $(0 < \varepsilon \ll 1)$ is the singular perturbation parameter. The locations of the boundary and interior layers will depend on the smoothness of the known functions $a(x)$, $b(x)$ and $f(x)$. Let us assume that the given functions $a(x)$, $b(x)$ and $f(x)$ are continuous. Then, the solution of problem (1.1.2) admits one-sided boundary layer if $a(x) > \alpha > 0$ or $a(x) < -\alpha < 0$ on $\overline{\Omega} = [0, 1]$ and interior layers if $a(x)$ changes its sign on $\overline{\Omega}$.

The problem (1.1.2) will be called reaction-dominated if $a(x) = 0$. The solution of singularly perturbed reaction-diffusion problem admits boundary layers at both ends of the boundary if $b(x) > \beta > 0$ on $\overline{\Omega}$. In general, the discontinuity of any given functions $a(x)$, $b(x)$ and $f(x)$ produce interior layers.

If the location and width of the layer are known *apriori*, then these knowledge can be used to construct suitable layer-adapted meshes. The main idea behind the construction of these meshes is to concentrate the computational effort where it is needed most, for example, using a high resolution near the interesting features of the solution (specially where the solution gradients become steep as the perturbation parameter goes to zero)

and a lower resolution for its smooth behaviors.

In this context, Bakhvalov [4] introduced a special nonuniform mesh in 1969 from a continuous strictly decreasing mesh generating function $\lambda : \overline{\Omega} \to [-1, 1]$ where $\lambda(0) = 1$ and $\lambda(1) = -1$. This function is defined as

$$\lambda(s) = \begin{cases} \psi(s), & s \in [0, \tau], \\ \\ \psi'(\tau)(s - \tau) + \psi(\tau), & s \in [\tau, 1], \end{cases}$$

where $\psi(s) = \exp(-\alpha s/\varepsilon)$ and the transition parameter τ, which separates the fine and coarse mesh is defined by the implicit equation

$$\psi'(\tau) = \frac{1 + \psi(\tau)}{1 - \tau}.$$

One of the limitations on Bakhvalov mesh includes that τ cannot be written in closed form from the above nonlinear equation. The complicated construction of this mesh makes it difficult to extend for singularly perturbed partial differential equations. Thereafter, Vulanovic [83] constructed a new mesh in 1983 which can capture the boundary layer.

In 1988, Gartland [33] proposed a graded mesh in which the domain is divided in to three regions. These regions are: inner regions (boundary layer regions) where the mesh is graded exponentially with respect to ε, transition region in which the mesh is changing geometrically from fine to coarse position and the outer region in which the mesh is uniform. The generation of this mesh is also complicated and difficult to extend to higher-dimensions.

In the same year 1988, Shishkin [77] proposed a relatively simpler mesh, which can be extended easily for higher-dimensions. Shishkin defines a piecewise-uniform mesh suitable for problem (1.1.2) with the transition point τ_ε defined as

$$\tau_\varepsilon = \min\left\{\frac{1}{2}, \varepsilon\tau_0 \ln N\right\}, \quad \tau_0 \geq p/\alpha.$$

The piecewise-uniform mesh $\Omega^N = \{x_i\}_{i=0}^N$ is obtained by dividing each of the intervals $[0, \tau_\varepsilon]$ and $[\tau_\varepsilon, 1]$ into $N/2$ equal subintervals. Note that p is an arbitrary positive constant, which defines the order of convergence of the numerical method, for example, $p = 1$ for simple upwind scheme. It should also be noted that this mesh will reduce to a uniform mesh whenever $\varepsilon\tau_0 \ln N > 1/2$, which implies that N is sufficiently large (relative to $1/\varepsilon$). In a similar way, the transition parameter for the reaction-diffusion problem is defined by:

$$\tau_\varepsilon = \min\left\{\frac{1}{4}, \sqrt{\varepsilon}\tau_0 \ln N\right\}, \quad \tau_0 \geq p/\beta,$$

and the piecewise-uniform mesh $\{x_i\}_{i=0}^{N}$ is obtained by dividing each intervals $[0, \tau_\varepsilon]$, $[\tau_\varepsilon, 1-\tau_\varepsilon]$ and $[1-\tau_\varepsilon, 1]$ into $N/4$, $N/2$ and $N/4$ equal subintervals, respectively.

However, these meshes are formulated with the help of *apriori* information about the location and width of the boundary layer. The construction of these meshes are also complicated and highly depends on the shape of the domain. Many physically interesting problems involve the propagation of moving boundaries like wave interaction in the oceans free surface, multi-phase flows in porus media, Hele-Shaw cells in pattern formation with few other nonlinear problems for which the *apriori* information about the exact solutions are not available. Another big concern is the order of accuracy of the numerical methods on these meshes. A finer discretization can be used for numerical simulations to yield better results. But, doubling the resolution becomes increasingly expensive on multidimensional domains. Therefore, it is always necessary to obtain a nonuniform mesh which can retain the accuracy and also improve the efficiency of an existing method by automatically adopting the solution behavior and concentrating mesh points within the regions of interest, from geometry and features of the solution. Mesh refinements is often realized as one of the fundamental way in order to capture the essential physics of the above mentioned problems. In general, the refinement techniques take the following three form (see Bangerth and Rannacher [5]).

h-refinement: This method involves automatic refinement or coarsening the mesh by adding the extra meshes based on *aposteriori* error estimates or local error indicators. This technique captures the geometry of the solution by dividing certain mesh cells into multiple smaller cells and is very popular in finite element context. The main weakness of this is the growth of the computational expense as we add the extra meshes to the regions of interest.

p-refinement: This method involves the adaptive enrichment of the polynomial order. It results a more accurate approximation of the solution by increasing or decreasing the local polynomial degree in each cell.

r-refinement: This method is also known as moving mesh method which uses a fixed number of meshes. These meshes are redistributed at each step in order to track the regions of rapid variation of the solution. The main advantage of this method is that it is not computationally expensive to grab the geometry of the solution. In this dissertation, we shall mainly focus our attention on r-refinement strategy.

A commonly-used technique in adaptive mesh generation is based on the idea of equidistribution. This technique is first introduced by de Boor [22]. It involves the selection of mesh points such that some measurement of the solution error is equalized over each subinterval. A mesh $\Omega^N \equiv \{0 = x_0 < x_1 < \cdots < x_N = 1\}$ is said to be

equidistributed, if

$$\int_{x_{i-1}}^{x_i} M\big(s,u(s)\big)ds = \int_{x_i}^{x_{i+1}} M\big(s,u(s)\big)ds, \quad i=1,\cdots,N-1, \tag{1.1.3}$$

where $M\big(s,u(s)\big)$ is nonnegative L^1–integrable function. This function is also known as a *monitor function* since it defines a measurement of the numerical error. Equivalently, (1.1.3) can be expressed as

$$\int_{x_{i-1}}^{x_i} M\big(s,u(s)\big)ds = \frac{1}{N}\int_0^1 M\big(s,u(s)\big)ds, \quad i=1,\ldots,N. \tag{1.1.4}$$

Mesh equidistribution can also be thought of as a mapping $x = x(\xi)$ from a computational coordinate $\xi \in [0,1]$ to the physical coordinate $x \in [0,1]$ defined by

$$\int_0^{x(\xi)} M\big(s,u(s)\big)ds = \xi\int_0^1 M\big(s,u(s)\big)ds. \tag{1.1.5}$$

It is common to use monitor functions which are bounded away from zero to maintain an appropriate distribution of mesh points throughout the domain. The optimal choice of the monitor function depends on the problem being solved, the numerical discretization being used and the norm of the error that is to be minimized. In practice, the monitor function is often based on simple functions, involving the derivatives of the unknown solution. According to Ren and Russell [72], there are three types of monitor functions available in the literature. They are of arc-length type, combination of gradient and curvature type and based on truncation error or solution residual. Monitor function based on arc-length type is considered by several authors for instance, Huang, Ren and Russell [36], Budd, Huang and Russell [12] to numerically model the areas of high activity (regions where the solution changes rapidly) successfully. For SPPs, this monitor function is examined by Qui et al. [71]. *Aposteriori* error estimate corresponding to this monitor function is also carried out by Kopteva [42] for one-dimensional singularly perturbed convection-diffusion problem. On the other hand, Beckett and Mackenzie [8, 9] proposed another monitor function which is based on the curvature of the solution. This works well for both singularly perturbed convection-diffusion as well as reaction-diffusion problems. Likewise, monitor functions based on the truncation errors or residuals are examined by Chen [18].

Moving mesh methods using mesh equidistribution are often realized as one of the fundamental way in order to capture the essential physics of the solution. The existence and uniqueness of an equidistributing mesh is guaranteed theoretically when a strictly positive monitor function is used. However, it can rarely be found exactly as the integrals of (1.1.3) will be normally approximated. Thus one has to rely on numerical methods to generate the equidistributed mesh. In this purpose, a large number of

methods have been developed in recent past. The first example includes de Boor [22], where the monitor function is approximated by a piecewise constant function. Pryce [69] considered a modified version of de Boors [23] algorithm, where the piecewise linear interpolation was used for the approximation. Other works include the use of Newton's iteration by Linß [47]. The issues related to convergence of de Boor algorithm is considered by Kopteva and Stynes [45] based on upwind finite difference solution of singularly perturbed convection-diffusion problems and by Chadha and Kopteva [16] of singularly perturbed reaction-diffusion problems. It is observed that this algorithm numerically produces better result compared to other modified versions of this. This thesis uses the de Boor algorithm to generate the layer-adapted mesh by the equidistribution of the proposed positive monitor functions.

1.2 Objective and Motivation

The main theme of this thesis revolves around developing, analyzing, improving and optimizing the ε-uniform *fitted mesh methods* for singularly perturbed convection-diffusion as well as reaction-diffusion boundary-value problems on the two kind of nonuniform meshes namely, *apriori* chosen Shishkin mesh and the equidistributed mesh using moving mesh methods. A brief survey of the literature illustrating the motivations behind the present works, carried out in this thesis is presented below.

In the past few years, uniformly convergent numerical methods for singularly perturbed convection-diffusion and reaction-diffusion problems have been considered by several researchers. The literature of approximating the solution by finite difference or finite element or finite volume methods is quite large. One may refer the books of Farrell et al. [29], Miller et al. [55], Morton [59], Roos et al. [74] and the survey articles by Kadalbajoo and Patidar [38] and Kadalbajoo and Reddy [40] for more details. The singularly perturbed partial differential equations also attracted by several authors for example, Clavero et al. [19], Hemker et al. [34], Mukherjee and Natesan [60], Shishkin [79]. A brief survey about the works done in this context can be seen in Kadalbajoo and Patidar [39]. But most of these articles cited above are mainly concentrated on *apriori* chosen Shishkin mesh, whose construction depends on the problem type and its domain structure. Therefore, the necessity of the adaptive mesh by equidistributing a monitor function draws its attention from engineers and mathematicians. In this context, one can see the following articles de Boor [23], Baines et al. [3], Beckett [7], Budd et al. [12], Carey and Dinh [15], Huang et al. [36], Huang and Russell [37], Mohapatra and Natesan [58], Pereyra and Sewell [66] and Pryce [69]. These papers are mainly based on the standard finite difference/element methods in which higher-order schemes or methods are not yet considered. This thesis attempts to consider also higher-order methods

using mesh equidistribution.

In recent past, mesh equidistribution for reaction-diffusion boundary-value problems are considered by a couple of articles, namely, Beckett and Mackenzie [9] and Kopteva et al. [44], where the monitor functions are based on the curvature of the solution. For this problem, a second-order convergence is observed. Further the technique in [9] is extended to obtain higher-order convergence by Beckett and Mackenzie [10] using finite element methods. The current interest is to use the adaptive numerical methods for more general Robin type problems using mesh equidistribution. In this case, Robin or mixed type convection-diffusion boundary-value problems (MBVPs) are first considered by Ansari and Hegarty [2] and Cai and Liu [14] on piecewise-uniform Shishkin mesh. An almost first-order accurate parameter-uniform convergence is observed by them. On the other hand, Robin type reaction-diffusion problem is considered by Natesan and Bawa [62], where a cubic spline based almost second-order hybrid numerical scheme is proposed. This work is also based on piecewise-uniform Shishkin mesh. Therefore, considering the above literature survey, one may still desire to construct an efficient higher-order uniformly convergent numerical scheme for singularly perturbed Robin type reaction-diffusion problems using mesh equidistribution.

Next, designing a low-cost uniformly convergent numerical method for higher-order differential equations is always a desirable task. Generating convergent schemes for higher-order derivatives are a difficult part of this. In this context, a class of singularly perturbed fourth-order ordinary differential equations (ODEs) are considered by several authors for *e.g.*, Shanthi and Ramanujam [75, 76]. Most of these available numerical techniques are constructed either by fitted operators or by the use of reasonable *apriori* information about the solutions on the domain. Therefore, the natural question is: Can we develop a uniformly convergent numerical technique using moving mesh methods by mesh equidistribution, where the complexity of obtaining difference schemes corresponding to the higher-order derivatives will not appear? Many researchers used the finite difference methods for approximating the unweighted derivatives of the solution. Such approximations are essential in certain applications, for example, the normal derivatives are required to compute skin friction coefficients and to calculate the stress intensity factors. In this context, Ervin and Layton [28] considered the approximation for the unweighted derivatives of second-order differential equations outside the boundary layers. Hence, another valid question is the construction of a ε-uniform numerical method which will lead to the convergence of the computed solution and its double derivative for fourth-order ODEs.

The modeling of turbulence in water wave when they interact with current is a complex phenomena and can be described by a system of two singularly perturbed differential equations (see Rodi [73]). In recent years, construction of layer-adapted meshes for sys-

tem of boundary-value problems are attracted by several authors. A variety of uniformly convergent numerical methods for reaction-diffusion as well as for convection-diffusion system of equations are developed on *apriori* chosen piecewise-uniform Shishkin mesh. In this regard, Matthews et al. [54], first examines a uniformly convergent method for system of two reaction-diffusion problems, where only one equation is perturbed. Thereafter, for system of two singularly perturbed reaction-diffusion problems, Madden and Stynes [53] provided an almost first-order uniformly convergent scheme. Linß and Madden [51] improved this analysis to almost second-order convergence for piecewise-uniform Shishkin mesh. Later on, Linß and Madden [52] extended this approach for studying Bakhvalov mesh applied to a general singularly perturbed system of reaction-diffusion problems. These raise the natural question about the possibility of deriving a monitor function from the convergence analysis, whose equidistribution will lead to a layer-adapted mesh for the system of reaction-diffusion problems.

Furthermore, an almost second-order numerical scheme is developed by Bawa and Natesan [6] for singularly perturbed reaction-diffusion problems. The piecewise-uniform Shishkin mesh is considered for their analysis. This scheme is a proper combination of cubic spline and central difference approximation for the second-order derivative. Later on, Natesan and Deb [63] applied the cubic spline based hybrid scheme for a system of two reaction-diffusion problems.Therefore, the common question is to develop a uniformly convergent hybrid scheme for more general system of singularly perturbed Robin type reaction-diffusion problems. It is proved here that the newly proposed scheme converges ε-uniformly with almost second-order accuracy, whereas the standard well-known method *i.e.,* the forward-backward approximation for mixed boundary conditions and the central difference scheme for the differential equation leads to almost first-order convergence on Shishkin mesh.

Finally, we turn our attention to the development of higher-order numerical solution using mesh equidistribution. In this context, the post-processing Richardson extrapolation technique is very well-known to obtain higher-order approximate solution. This technique is recently used for singularly perturbed convection-diffusion boundary-value problems by Natividad and Stynes [64] and for system of convection-diffusion problems by Deb and Natesan [25] on piecewise-uniform Shishkin mesh. Their analysis is based on the truncation error estimate and barrier function technique. This approach is immutably followed by Hemker et al. [70] and Mukherjee and Natesan [61] for singularly perturbed parabolic convection-diffusion problems and in Hemker et al. [35] for singularly perturbed elliptic reaction-diffusion problems. For this purpose, Linß [48] provided a different approach to obtain higher-order convergence on *apriori* chosen Shishkin and Bakhvalov mesh by using stability estimate. In this thesis, we study the possibility of extending the Richardson extrapolation technique to the equidistributed nonuniform

mesh. At the same time, many researchers used the upwind based finite difference methods for the system of singularly perturbed weakly coupled convection-diffusion problems. Arc-length type monitor functions are proposed for the convection-diffusion problems. An extension of this monitor function from the scalar problem to the system of SPPs is done by Linß [50]. But Kopteva et al. [44] observed that this monitor function is not suitable for reaction-diffusion problems. Another monitor function proposed by Beckett and Mackenzie [8, 9] is successfully used by several authors for singularly perturbed convection-diffusion as well as reaction-diffusion problems. This monitor function is based on the derivative of the singular component of the solution. In this thesis, we used this monitor function for a system of singularly perturbed convection-diffusion problems where the proposed monitor function only involves the double derivative of the solution.

1.3 Preliminaries

This section introduces a few basic definitions, notations and conventions which will be used throughout the thesis.

First, we define Ω as a bounded open interval in $\mathbb{R}$ and is considered as $(0, 1)$. For any nonnegative integer k, $\mathcal{C}^k(\Omega)$ denotes the space of all functions, whose derivatives are continuous up to order k on Ω. In the analysis, we use the standard supremum norm $||\cdot||_\infty$ by $||\cdot||_D$ as

$$||g|| = \sup_{\xi \in D} |g(\xi)|,$$

for a function $g(\xi)$ on some domain D. It is a convention that when the domain is obvious or of no particular interest, we simply write $||\cdot||_D$ by $||\cdot||$, *i.e.,* by omitting D. For a vector valued function $\boldsymbol{g}(x) = (g_1, \cdots, g_k)^T \in \mathbb{R}^k$, the supremum norm is defined as

$$||\boldsymbol{g}|| = \sup_{\xi \in D} \Big\{ |g_1(\xi)|, , \cdots, |g_k(\xi)| \Big\}.$$

Another continuous norm will be frequently used for our analysis, which is defined as

$$||g||_* = ||g||_{-1,\infty} = \max_{x \in (0,1)} \left| \int_x^1 g(s) ds \right|.$$

It is easy to observe that $||g||_* \leq ||g||_\infty$. By a similar way as like $||\cdot||_\infty$, this norm can also be defined for vector valued function.

Now, we shall define the following finite difference operators which will be used to discretize the continuous problem in the subsequent chapters. Consider an arbitrary nonuniform mesh Ω^N by

$$\Omega^N \equiv \big\{ 0 = x_0 < x_1 < \cdots < x_N = 1 \big\},$$

where the step sizes are defined as $h_i = x_i - x_{i-1},\ i = 1, \cdots, N$. For a discrete function G_i define the central difference operator as

$$\delta^2 G_i = \frac{(D^+ G_i - D^- G_i)}{\hbar_i},$$

with the forward and backward operators as

$$D^+ G_i = \frac{G_{i+1} - G_i}{h_{i+1}}, \quad \text{and} \quad D^- G_i = \frac{G_i - G_{i-1}}{h_i},$$

respectively, and $DG_i = (G_{i+1} - G_i)/\hbar_i$, where $\hbar_i = (h_i + h_{i+1})/2$. The maximum norm for the discrete function G_i or sometimes denoted as G_i^N on Ω^N is defined as

$$||G|| = \max_{x_i \in \Omega^N} \{|G_i|\}.$$

Similarly, for the vector valued discrete function $\mathbf{G} = (G_1, \cdots, G_k)^T \in \mathbb{R}^k$ the maximum norm is defined by

$$||\mathbf{G}|| = \max_{x_i \in \Omega^N} \{|G_{1,i}|, \cdots, |G_{k,i}|\}.$$

The discrete counterpart of the continuous norm $||\cdot||_*$ on the domain Ω^N will be defined by

$$||v||_{-1,\infty,\Omega^N} = \frac{1}{2}\left(\min_i \left| \sum_{j=i}^{N-1} v_j \hbar_j \right| + \max_i \left| \sum_{j=i}^{N-1} v_j \hbar_j \right| \right).$$

The above norm can also be expressed by the following forms

$$||v||_{-1,\infty,\Omega^N} = \min_{\gamma \in R} \max_{i=0,\cdots,N-1} \left| \sum_{j=i}^{N-1} h_{j+1} v_j - \gamma \right| = \max_{i=0,\cdots,N-1} \left| \sum_{p=i}^{N-1} h_{p+1} v_p \right|. \tag{1.3.1}$$

Throughout this thesis C (sometimes subscripted) denotes a generic positive constant, which is independent of the perturbation parameter ε, the number of mesh intervals N and the mesh points x_i, which can take different values at different places even in the same argument. Note that subscripted C (for *e.g.,* C_1) is a fixed constant.

In the analysis, it is frequently assumed that the perturbation parameter $\varepsilon \leq CN^{-1}$, which is the case of actual interest from practical point of view. In practice, if $\varepsilon \geq CN^{-1}$, then the model problems considered in this thesis are not difficult to solve computationally.

Now, we shall explain the ***Landau's order symbols*** O(big oh) and o (little-oh), which are used throughout the thesis to define the order of convergence of the numerical method. Let $f(\varepsilon)$ and $g(\varepsilon)$ be two real valued functions, where $0 < \varepsilon \ll 1$.

Definition 1.3.1. *The expression $f(\varepsilon) = O(g(\varepsilon))$ as $\varepsilon \to 0$, defines that there exist some positive constants C and ε_0 satisfying $\varepsilon \in (0, \varepsilon_0]$ such that*

$$|f(\varepsilon)| \leq C|g(\varepsilon)|, \quad \varepsilon \to 0.$$

Definition 1.3.2. *The expression* $f(\varepsilon) = o(g(\varepsilon))$ *as* $\varepsilon \to 0$, *defines that*

$$\lim_{\varepsilon \to 0} \frac{f(\varepsilon)}{g(\varepsilon)} = 0.$$

One can refer the book [13] for the further discussions about the above two definitions. The next few definitions will be useful for the explanation of the proposed numerical techniques. These definitions can be seen in the books [29, 74].

Definition 1.3.3. *A sequence of functions* $\delta_n(\varepsilon)$, $n = 0, 1, \cdots$ *is called* ***an asymptotic sequence*** *if for* $n = 0, 1, \cdots$, $\delta_{n+1}(\varepsilon)/\delta_n(\varepsilon) \to 0$, *as* $\varepsilon \to 0$.

Definition 1.3.4. *The sum* $\sum_{n=0}^{m} a_n f_n(\varepsilon)$ *with constants coefficients* a_n *is called* ***an asymptotic series*** *if* $f_n(\varepsilon)$, $n = 0, 1, \cdots, m$ *is an asymptotic sequence.*

The robustness of the proposed numerical methods will be examined by the concept of ε–uniform accuracy.

Definition 1.3.5. ε***–uniform numerical method:*** *Consider a family of mathematical problems parameterized by a parameter* ε, *where* ε *lies in the interval* $0 < \varepsilon \ll 1$. *Assume that each problem has a unique solution defined by* u_ε *and this solution* u_ε *is approximated by a sequence of numerical solution* U_ε, *where* U_ε *is defined on the discrete space* Ω^N *with* N *as the number of mesh intervals. Now the numerical solution* U_ε *is said to converge* ε*–uniformly to the exact solution* u_ε, *if there exist a positive integer* N_0, *positive numbers* C *and* p, *such that*

$$\sup_{0<\varepsilon\ll 1} ||U_\varepsilon - u_\varepsilon|| \leq CN^{-p}, \quad \textit{for all} \quad N \geq N_0,$$

where N_0, C *and* p *are independent of* ε. *Here* p *is called the order of convergence of the numerical method and* C *is called the* ε*–uniform error constant.*

We shall frequently use the maximum norm for our error analysis. This is due to the measurement of the errors from the small part of the domain, where boundary layer occurs. Other norms, specially the root mean square norm fails to capture the local behavior of the errors inside the boundary layer regions. For further discussions on the choice of these norms, one can refer [29].

Definition 1.3.6. *A matrix* $\mathbf{A} = (a_{ij}) \in \mathbb{R}^{k\times k}$ *is said to be an* M*-matrix if* $\mathbf{A}$ *is nonsingular,* $\mathbf{A}^{-1} \geq 0$, $a_{ij} \leq 0$ *for all* $i \neq j$, $1 \leq i, j \leq k$.

1.4 Model Problems

In this thesis, we mainly consider the singular perturbation problems involving the perturbation parameter ε $(0 < \varepsilon \ll 1)$. This parameter is also denoted by the notation ε_l $(0 < \varepsilon_l \ll 1)$ for system of ODEs. Throughout the thesis, all the differential equations are considered in the unit interval $\Omega = (0, 1)$. Here the following six types of model problems are considered.

1.4.1 Singularly perturbed Robin type reaction-diffusion boundary-value problem

Consider the following singularly perturbed Robin type reaction-diffusion problem:

$$\begin{cases} \mathcal{L}_\varepsilon u(x) = -\varepsilon u''(x) + b(x)u(x) = f(x), \quad x \in \Omega, \\ M_l u(0) \equiv \alpha_1 u(0) - \beta_1\sqrt{\varepsilon}u'(0) = \gamma_1, \quad M_r u(1) \equiv \alpha_2 u(1) + \beta_2\sqrt{\varepsilon}u'(1) = \gamma_2. \end{cases} \tag{1.4.1}$$

The functions $b(x)$ and $f(x)$ are assumed to be sufficiently smooth with $\beta^* > b(x) > \beta > 0$ for $x \in \overline{\Omega}$. We also assume that the coefficients of the mixed boundary conditions satisfy $\alpha_k, \beta_k \geq 0$, $\alpha_k + \beta_k > 0$ for $k = 1, 2$ with $\alpha_1 \neq \beta_1\sqrt{b(0)}$. Under these hypotheses, the problem (1.4.1) has a unique solution $u(x)$ which exhibits boundary layers at both ends $x = 0, 1$, Bawa and Natesan [62].

1.4.2 Singularly perturbed fourth-order boundary-value problem

Consider the following form of singularly perturbed two-point boundary-value problem for fourth-order ODE:

$$\begin{cases} \mathrm{L}u(x) = -\varepsilon u^{iv}(x) + b(x)u''(x) - c(x)u(x) = -f(x), \quad x \in \Omega, \\ u(0) = p, \quad u(1) = q, \quad u''(0) = -r, \quad u''(1) = -s. \end{cases} \tag{1.4.2}$$

The continuous functions $b(x)$, $c(x)$ and $f(x)$ are assumed to be sufficiently smooth and $\beta^* > b(x) > \beta > 0$, $0 \geq c(x) \geq -\gamma$, $\gamma > 0$ with $\beta - 2\gamma \geq \eta > 0$, on $\overline{\Omega}$ for some real number η. In general, the ODE (1.4.2) admits a unique solution $u(x) \in \mathcal{C}^4(\Omega) \cap \mathcal{C}^2(\overline{\Omega})$, which has boundary layers at both ends $x = 0, 1$, Shanthi and Ramanujam [75].

1.4.3 Singularly perturbed system of reaction-diffusion problems

Consider the following system of singularly perturbed reaction-diffusion boundary-value problems:

$$\begin{cases} \mathbb{L}\boldsymbol{u}(x) \equiv -\boldsymbol{Eps}\ \boldsymbol{u}''(x) + \ \boldsymbol{B}(x)\boldsymbol{u}(x) = \boldsymbol{f}(x), \quad \text{for} \quad x \in \Omega, \\ \boldsymbol{u}(0) = \boldsymbol{u}(1) = \boldsymbol{0}. \end{cases} \tag{1.4.3}$$

Here $\mathbb{L} = (\mathbb{L}_1, \cdots, \mathbb{L}_k)^T$, $\mathbb{L}_m\boldsymbol{u}(x) = -\varepsilon_m u_m''(x) + \sum_{j=1}^{k} b_{mj}(x)u_m(x)$, $\boldsymbol{Eps} = \text{diag}(\varepsilon_1, \varepsilon_2, \cdots, \varepsilon_k)$, $\boldsymbol{B}(x) = (b_{ij}(x))_{k\times k}$, $\boldsymbol{f}(x) = (f_1(x), f_2(x), \cdots, f_k(x))^T$, and $\boldsymbol{u}(x) = (u_1(x), \cdots, u_k(x))^T$. The diffusion parameters ε_l, $l = 1, \cdots, k$ are of different magnitudes. The matrix $\boldsymbol{B}(x) = (b_{ij}(x))_{i,j=1}^{k}$ is a strictly diagonally dominant L_0–matrix (*i.e.,* off diagonal entries are nonpositive and diagonal entries are positive) satisfying

$$\min_{x\in\overline{\Omega}; m=1,\cdots,k} \left\{ \sum_{j=1}^{k} b_{mj}(x) \right\} \geq \beta > 0,$$

and the elements of the coefficient matrix $\boldsymbol{B}$ and the vector $\boldsymbol{f}$, *i.e.,* $b_{ij}(x), f_i(x)$ are in $\mathfrak{C}^3(\Omega)$ for $i, j = 1, \cdots, k$. In general, the solution components of $\boldsymbol{u}(x)$ of (1.4.3) exhibit boundary layers at both ends $x = 0, 1$, Linß and Madden [52].

1.4.4 Singularly perturbed convection-diffusion problem

Here, we consider the following singularly perturbed convection-diffusion problem:

$$\begin{cases} \mathfrak{L}u(x) \equiv -\varepsilon u''(x) - (a(x)u(x))' = f(x), \quad x \in \Omega, \\ u(0) = 0, \quad u(1) = 0. \end{cases} \tag{1.4.4}$$

The functions $a(x)$ and $f(x)$ are assumed to be in $\mathfrak{C}^2(\Omega)$. We also assume that $a(x)$ has a positive lower bound. In general, the solution $u(x)$ of the problem (1.4.4) possesses a boundary layer at $x = 0$, if $a(x)$ has a positive lower bound, Roos et al. [74].

1.4.5 Singularly perturbed weakly coupled system of convection-diffusion problems

The following system of weakly coupled singularly perturbed convection-diffusion boundary-value problems is considered:

$$\begin{cases} \mathbf{L}\boldsymbol{u}(x) \equiv -\boldsymbol{Eps}\ \boldsymbol{u}''(x) - \boldsymbol{A}(x)\boldsymbol{u}'(x) + \boldsymbol{B}(x)\boldsymbol{u}(x) = \boldsymbol{f}(x), \quad x \in \Omega, \\ \boldsymbol{u}(0) = \boldsymbol{u}(1) = \boldsymbol{0}. \end{cases} \tag{1.4.5}$$

Here $\mathbf{L} = (\mathbf{L}_1, \cdots, \mathbf{L}_k)^T$, where $\mathbf{L}_m \boldsymbol{u}(x) = -\varepsilon_m u_m''(x) - a_{mm}(x)u_m'(x) + \sum_{j=1}^{k} b_{mj}(x)u_m(x)$, and $\boldsymbol{Eps} = \text{diag}(\varepsilon_1, \varepsilon_2, \cdots, \varepsilon_k)$, $\boldsymbol{A}(x) = \text{diag}(a_{11}(x), a_{22}(x), \cdots, a_{kk}(x))$, $\boldsymbol{B}(x) = (b_{ij}(x))_{k\times k}$, $\boldsymbol{f}(x) = (f_1(x), f_2(x), \cdots, f_k(x))^T$, and $\boldsymbol{u}(x) = (u_1(x), \cdots, u_k(x))^T$. The entries of the coefficient matrix $\boldsymbol{A}(x)$ are assumed to be bounded away from $\mathbf{0}$. The matrix $\boldsymbol{B}(x) = (b_{ij}(x))_{i,j=1}^{k}$ is considered to be an L_0-matrix with

$$\min_{x\in\overline{\Omega}; m=1,\cdots,k} \left\{ \sum_{j=1}^{k} b_{mj}(x) \right\} \geq \beta > 0,$$

and the entries of coefficient matrices $\boldsymbol{A}$, $\boldsymbol{B}$, and the vector $\boldsymbol{f}$ *i.e.*, $a_{ii}(x), b_{ij}(x), f_i(x)$ are in $\mathcal{C}^2(\Omega)$ for $i, j = 1, \cdots, k$. In general, the solution components u_l, $l = 1, \cdots, k$, of $\boldsymbol{u}(x)$, exhibit boundary layers at $x = 0$, if $a_{ii}(x)$ has a positive lower bound for all i, Linß [49].

1.4.6 Singularly perturbed system of reaction-diffusion problems with Robin type boundary conditions

Consider the following system of singularly perturbed Robin type reaction-diffusion problems:

$$\begin{cases} \mathcal{L}\boldsymbol{u}(x) \equiv -\boldsymbol{Eps}\ \boldsymbol{u}''(x) + \mathcal{B}(x)\boldsymbol{u}(x) = \boldsymbol{f}(x), \quad x \in \Omega, \\ \\ M_{l_k}\boldsymbol{u}(0) \equiv \alpha_k u_k(0) - \beta_k u_k'(0) = A_k, \quad M_{r_k}\boldsymbol{u}(1) \equiv \gamma_k u_k(1) + \delta_k u_k'(1) = B_k, \quad k = 1, 2, \end{cases} \tag{1.4.6}$$

where $\boldsymbol{Eps} = \text{diag}(\varepsilon_1, \varepsilon_2)$ with

$$\boldsymbol{u}(x) = \begin{pmatrix} u_1(x) \\ u_2(x) \end{pmatrix}, \quad \mathcal{B}(x) = \begin{pmatrix} b_{11}(x) & b_{12}(x) \\ b_{21}(x) & b_{22}(x) \end{pmatrix}, \quad \text{and} \quad \boldsymbol{f}(x) = \begin{pmatrix} f_1(x) \\ f_2(x) \end{pmatrix}.$$

It is assumed that the functions $b_{ij}(x) \in \mathcal{C}^3(\Omega)$ and $f_i(x) \in \mathcal{C}^2(\Omega)$ for $i, j = 1, 2$, and

$$\alpha_k, \beta_k \geq 0, \quad \alpha_k + \beta_k > 0, \quad \gamma_k > 0, \quad \delta_k \geq 0, \quad \text{for} \quad k = 1, 2.$$

We consider, the matrix $\mathcal{B}(x) = \{b_{ij}(x)\}_{i,j=1}^{2}$ is a strictly diagonally dominant L_0–matrix satisfying

$$\min_{x\in\overline{\Omega}} \{b_{11}(x) + b_{12}(x), b_{21}(x) + b_{22}(x)\} > \beta > 0,$$

with $\beta^* \geq |b_{ij}(x)|$ for $1 \leq i, j \leq 2$. In general, the solution of the above system (1.4.6) admits a unique solution $\boldsymbol{u}(x) \in \mathcal{C}^4(\Omega) \cap \mathcal{C}^1(\overline{\Omega})$ whose components exhibit boundary layers at both ends $x = 0, 1$, Chang and Howes [17].

1.5 Outline of the Thesis

This thesis consists of eight chapters. **Chapter** 1 introduces the historical background of the related work done in the field of singular perturbation problems. It also provides the motivation for solving SPPs. A few preliminaries are presented in this chapter, which are used in the later part of the thesis. The rest of the thesis is organized as follows.

Chapter 2 is concerned with the construction of an ε-uniformly convergent efficient numerical scheme for the MBVP (1.4.1) using mesh equidistribution. The mesh is generated by the equidistribution of a positive monitor function involving the second-order derivative of the singular component of the solution. The MBVP is solved first using the central difference approximation for the differential equation with forward-backward approximation at the boundary. It is shown that this approximation leads to the first-order parameter-uniform convergence. The cubic spline approximation for the mixed boundary conditions are proposed to improve the accuracy of the solution. The proposed method leads to second-order accurate solution on the equidistributed mesh.

Chapter 3 deals with the study of a class of fourth-order ODEs of the form (1.4.2) exhibiting boundary layers. The ODE is converted into a system of second-order reaction-diffusion problems where only one equation is perturbed. The idea of adaptive mesh generation discussed in Chapter 2 is extended to solve this system. The mesh is obtained by equidistributing a monitor function involving the solution component of the systems perturbed equation. The stability and error analysis of the numerical solution are carried out which show that the proposed technique provides at least first-order ε-uniform convergence to the computed solution.

Chapter 4 is devoted to the study of moving mesh methods on a general system of singularly perturbed reaction-diffusion problems of the form (1.4.3), where the perturbation parameters are of different magnitudes. The stability of the continuous and discrete solutions with error analysis are provided for this problem. A suitable monitor function is generated from the error analysis. It is proved that the equidistribution of this monitor function provides almost second-order parameter-uniform convergence for singularly perturbed linear and semilinear system of reaction-diffusion problems.

In **Chapter** 5, a post-processing technique is studied to improve the accuracy of the numerical solution obtained by standard upwind scheme for the singularly perturbed convection-diffusion problem (1.4.4). Here, the Richardson extrapolation technique is used to improve the numerical solution on equidistributed mesh. From this procedure, a better approximation of the computed solution is achieved by using the average of two computed solutions. First the BVP (1.4.4) is solved on two adaptive meshes, which are obtained by the equidistribution of two proposed monitor functions respectively. These numerical solutions converge with the rate of $O(N^{-1})$ on the equidistributed

mesh. Thereafter, it is proved that these solutions can be improved to get $O(N^{-2})$ parameter-uniform convergence by the Richardson extrapolation technique.

In **Chapter** 6, we analyze a system of singularly perturbed weakly coupled convection-diffusion boundary-value problems of the form (1.4.5). Here, *apriori* error analysis is used to construct a suitable monitor function from the sufficient condition of uniform convergence. This analysis can be extended to achieve several other monitor functions whose equidistributions will lead to $O(N^{-1})$ convergent solutions. But the proposed monitor function has an advantage that this is working well for a system of singularly perturbed convection-diffusion and reaction-diffusion boundary-value problems. It is shown that the above technique can also be extended for a system of singularly perturbed semilinear convection-diffusion problems to obtain first-order ε-uniform convergence.

A system of singularly perturbed Robin type reaction-diffusion boundary-value problems of the form (1.4.6) is introduced in **Chapter** 7 on a piecewise-uniform Shishkin mesh. This problem is an extension of MBVPs of the form (1.4.1) described in Chapter 2. The error estimates and stability result are established with the help of *apriori* bounds of the solution and its derivatives. It is shown both theoretically and numerically that the standard method, *i.e.,* the forward-backward approximation for the boundary conditions and central difference approximation for the differential equation provides almost first-order parameter-uniform convergence. A higher-order accurate numerical scheme is proposed for this problem, which uses the cubic spline approximation inside the boundary layer regions. This solution is proved to be almost second-order ε-uniform convergent.

Finally, **Chapter** 8 addresses a brief summary of the results by highlighting the contributions made by this thesis. It also provides various ideas for the scope of further investigations on the theoretical findings.

Extensive numerical results are presented to support the theoretical findings and to demonstrate the accuracy of the proposed numerical methods. The computational results for the corresponding examples are demonstrated in the numerical section of each chapter. Suitable graphs and tables are provided in each chapter which validate the analytical results that are derived.

Chapter 2

Higher-Order Parameter-Uniform Convergent Schemes for Robin type Reaction-Diffusion Problems

This chapter proposes a higher-order numerical scheme for singularly perturbed reaction-diffusion problems with Robin boundary conditions. The proposed numerical scheme is a combination of the cubic spline approximation for mixed boundary conditions and the classical central difference approximation for the differential equations at the interior points. The layer-adapted meshes are generated by the equidistribution of a positive monitor function. It is proved that the classical forward-backward approximation for mixed type boundary conditions and the central difference approximation for the differential equation gives first-order parameter-uniform convergence, whereas the proposed scheme involving the cubic spline approximation provides second-order accuracy independent of the perturbation parameter ε, where $\varepsilon \leq N^{-1}$ (N is the number of mesh intervals).

2.1 Introduction

Consider the following singularly perturbed Robin type reaction-diffusion problem:

$$\begin{cases} \mathcal{L}_\varepsilon u(x) = -\varepsilon u''(x) + b(x)u(x) = f(x), \quad x \in \Omega, \\ M_l u(0) \equiv \alpha_1 u(0) - \beta_1 \sqrt{\varepsilon} u'(0) = \gamma_1, \quad M_r u(1) \equiv \alpha_2 u(1) + \beta_2 \sqrt{\varepsilon} u'(1) = \gamma_2, \end{cases} \tag{2.1.1}$$

where ε $(0 < \varepsilon \ll 1)$ is the singular perturbation parameter. Here the functions $b(x)$ and $f(x)$ are assumed to be sufficiently smooth such that $\beta^* > b(x) > \beta > 0$ for $x \in \overline{\Omega}$. It is also assumed that the coefficients of the mixed boundary conditions satisfy $\alpha_k, \beta_k \geq 0$, $\alpha_k + \beta_k > 0$ for $k = 1, 2$ with $\alpha_1 \neq \beta_1 \sqrt{b(0)}$. Then, it immediately follows that the problem (2.1.1) admits a unique solution $u(x) \in \mathcal{C}^2(\Omega) \cap \mathcal{C}^1(\overline{\Omega})$ (see, for e.g, [62, 17]). In general, the solution $u(x)$ may exhibit boundary layers at both ends $x = 0, 1$.

The outline of this chapter is as follows. Section 2.2 provides *apriori* bounds of the solution and its derivatives and introduces a decomposition of the analytical solution into its smooth and singular components. Section 2.3 describes the numerical discretization of (2.1.1), where the mixed type boundary conditions are approximated by the well-known forward-backward scheme (standard method) and the proposed cubic spline scheme (proposed method) respectively. Stability of the discretized operators are also carried out in this section. Section 2.4 studies the truncation error for the smooth and singular components of the numerical solution. Here the main results, a first-order parameter-uniform convergence for the forward-backward approximation and second-order convergence using proposed spline approximation for the mixed boundary conditions are proved using the discrete supremum norm. Finally, Section 2.5 provides the numerical experiments using an adaptive algorithm to verify the theoretical results.

2.2 Bounds of the Solution and Its Derivatives

This section provides *apriori* bounds for the continuous solution of (2.1.1) and its derivatives. A boundary condition of mixed type causes a less severe boundary layer (see [74]). *Apriori* bounds of the solution and its derivatives are taken from [55].

Lemma 2.2.1. *The solution $u(x)$ of (2.1.1) and its derivatives satisfy the following bounds for any prescribed r,*

$$|u^{(k)}(x)| \leq C\big(1+\varepsilon^{-k/2}\mathcal{E}_\varepsilon(x)\big), \quad \text{for } k=0,\cdots,r,$$

where $\mathcal{E}_\varepsilon(x)=\exp(-x\sqrt{\beta/\varepsilon})+\exp(-(1-x)\sqrt{\beta/\varepsilon})$.

We decompose the analytical solution u into two components, the smooth component v and the singular component w such that $u = v + w$. The following lemma provides the derivative bounds for the smooth component v and the singular component w. This lemma is used to estimate the local truncation error associated with the difference schemes for the standard and proposed methods.

Lemma 2.2.2. *The smooth component v satisfying*

$$\begin{cases} \mathcal{L}_\varepsilon v(x) = f(x), \quad x\in\Omega, \\ M_l v(0) = v_1^\varepsilon, \quad M_r v(1) = v_2^\varepsilon, \ \text{with suitable } v_1^\varepsilon, v_2^\varepsilon, \end{cases}$$

and the singular component w satisfying

$$\begin{cases} \mathcal{L}_\varepsilon w(x) = 0, \quad x\in\Omega, \\ M_l w(0) = \gamma_1 - M_l v(0), \quad M_r w(1) = \gamma_2 - M_r v(1), \end{cases}$$

fulfill the following bounds for an arbitrary p:

$$|v^{(k)}(x)| \leq C,$$

and

$$|w^{(k)}(x)| \leq C\varepsilon^{-k/2}\big[\exp(-x\sqrt{b(0)/\varepsilon})+\exp(-(1-x)\sqrt{b(1)/\varepsilon})\big], \quad \textit{for} \quad k=0,\cdots,2p+1.$$

Proof. We shall decompose the smooth component v by the following asymptotic expansion

$$v(x) = \sum_{i=0}^{2p+1} \varepsilon^{i/2} v_i(x) + \varepsilon^{p+1} v^*_{2p+2}(x).$$

Now, substituting the above expansion in (2.1.1) and comparing the coefficients of powers of ε, we get

$$\mathcal{L}_0 v_0(x) = f(x),$$

$$\mathcal{L}_0 v_{2i}(x) = \mathcal{L}_1 v_{2i-2}(x), \quad i = 1,\cdots,p,$$

$$\mathcal{L}_\varepsilon v^*_{2p+2}(x) = \mathcal{L}_1 v_{2p}(x), \quad M_l v^*_{2p+2}(0) = M_r v^*_{2p+2}(1) = 0,$$

where $\mathcal{L}_0 \equiv b(x)I$ and $\mathcal{L}_1 \equiv \dfrac{d^2}{dx^2}$ with $v_{2i+1}(x) = 0$ for all i. Thereafter, following the approach of [55], we obtain

$$|v^{(k)}(x)| \leq C, \text{ for } k = 0,\cdots,2p+1.$$

For finding the derivative bounds of the singular component w, we decompose the singular component into its left-hand singular component w^l and right-hand singular component w^r such that $w = w^r + w^l$, where

$$w^r(x) = \sum_{i=0}^{2p+1} \varepsilon^{i/2} w^r_i(x) + \varepsilon^{p+1} w^{*r}_{2p+2}(x),$$

and

$$w^l(x) = \sum_{i=0}^{2p+1} \varepsilon^{i/2} w^l_i(x) + \varepsilon^{p+1} w^{*l}_{2p+2}(x).$$

Now, we shall use the transformation $\xi = x/\sqrt{\varepsilon}$ to find the derivative bounds of w^l. Using the Taylor's series expansion of $b(\xi\sqrt{\varepsilon})$, it is easy to show that $w^l_i(\xi)$ satisfies

$$\widehat{\mathcal{L}} w^l_0(\xi) = 0,$$

$$\widetilde{M_l} w^l_0(0) = \gamma_1 - M_l v_0(0), \text{ with } \lim_{\xi\to\infty} w^l_0(\xi) = 0, \text{ where } \widetilde{M_l} g(0) \equiv \alpha_1 g(0) - \beta_1 g'(0),$$

$$\widehat{\mathcal{L}} w^l_i(\xi) = -\widehat{\mathcal{L}}^*(w^l_0,\cdots,w^l_{i-1})(\xi),$$

$$\widetilde{M_l} w^l_i(0) = -M_l v_i(0), \text{ with } \lim_{\xi\to\infty} w^l_i(\xi) = 0, \text{ with } i = 1,\cdots,2p+1,$$

and

$$\mathcal{L}_\varepsilon w^{*l}_{2p+2}(x) = -\varepsilon^{-p-1}\mathcal{L}_\varepsilon(w^l_0 + \cdots + \varepsilon^{(2p+1)/2}w^l_{2p+1})(x),$$

$$\widetilde{M}_l w^{*l}_{2p+2}(0) = 0, \quad M_r w^{*l}_{2p+2}(1) = -\varepsilon^{-p-1}M_r(w^l_0 + \cdots + \varepsilon^{(2p+1)/2}w^l_{2p+1})(1),$$

where

$$\widehat{\mathcal{L}} \equiv -\frac{d^2}{d\xi^2} + b(0)I \text{ and } \widehat{\mathcal{L}}^*(w^l_0, \cdots, w^l_{i-1}) = \sum_{t=1}^{i} \frac{\xi^t b^{(t)}(0) w^l_{i-t}}{t!}.$$

Therefore, adopting the technique provided in [55], we have

$$|w^l(0)| < C, \quad |w^l(1)| < C\exp\left(-\sqrt{\frac{b(0)}{\varepsilon}}\right) \text{ and } |w^{l(k)}(x)| < C\varepsilon^{-k/2}\exp\left(-x\sqrt{\frac{b(0)}{\varepsilon}}\right).$$

By a similar way, the bounds for the right-hand singular component and its derivatives can be obtained, which completes the proof of the lemma. ∎

In reality, from the *apriori* analysis, it is observed that the boundary layer phenomena occurs actually from the singular component of the solution. This motivates Beckett and Mackenzie [8, 9] to consider a monitor function involving especially the derivatives of the singular component. Now onwards, we shall only consider the monitor function

$$M(x, u(x)) = \alpha + |w''(x)|^{1/2}, \tag{2.2.1}$$

proposed by Beckett and Mackenzie [8, 9], which works well for both convection-dominated and reaction-dominated problems. It is easy to see that this monitor function is involving the second-order derivative of the singular component w of the solution u. Here, α is a positive constant to be defined later. The constant α appears inside the monitor function is considered to be positive so that there is no mesh starvation outside the layer.

To approximate $w''(x)$, we use the leading order expansion of $w(x)$ from Lemma 2.2.2, which implies that

$$w''(x) \approx \begin{cases} \kappa_1 b(0)\varepsilon^{-1}\exp\left(-x\sqrt{\dfrac{b(0)}{\varepsilon}}\right), & x \in [0, 1/2], \\ \kappa_2 b(1)\varepsilon^{-1}\exp\left(-(1-x)\sqrt{\dfrac{b(1)}{\varepsilon}}\right), & x \in (1/2, 1], \end{cases}$$

where

$$\kappa_1 = \frac{\gamma_1 - [\alpha_1(f/b)(0) - \beta_1(f/b)'(0)]}{\alpha_1 - \beta_1\sqrt{b(0)}}, \quad \text{and} \quad \kappa_2 = \frac{\gamma_2 - [\alpha_2(f/b)(1) - \beta_2(f/b)'(1)]}{\alpha_2 + \beta_2\sqrt{b(1)}}.$$

Hence, we have

$$\int_0^1 |w''(x)|^{1/2}dx \equiv K \approx 2[|\kappa_1|^{1/2} + |\kappa_2|^{1/2}].$$

Substituting the approximate value of $w''(x)$ in the equidistribution principle (1.1.5), we obtain for $x(\xi) \leq 1/2$,

$$\xi\left(\frac{\alpha}{K}+1\right) = \alpha\frac{x(\xi)}{K} + \frac{2|\kappa_1|^{1/2}}{K}\left[1-\exp\left(-\frac{x(\xi)}{2}\sqrt{\frac{b(0)}{\varepsilon}}\right)\right]. \tag{2.2.2}$$

In a similar way, for $x(\xi) > 1/2$, the mapping (1.1.5) leads to

$$(1-\xi)\left(\frac{\alpha}{K}+1\right) = \alpha\frac{(1-x(\xi))}{K} + \frac{2|\kappa_2|^{1/2}}{K}\left[1-\exp\left(-\frac{(1-x(\xi))}{2}\sqrt{\frac{b(1)}{\varepsilon}}\right)\right]. \tag{2.2.3}$$

Considering (1.1.5), as a mapping from the physical coordinates of nonuniform meshes $\{x_i\}_{i=0}^N$ to the computational coordinates of uniform meshes $\{\xi_i = i/N\}_{i=0}^N$, we have from (2.2.2) and (2.2.3),

$$\frac{\alpha x_i}{K} + K_1\left[1-\exp\left(-\frac{x_i}{2}\sqrt{\frac{b(0)}{\varepsilon}}\right)\right] = \frac{i}{N}\left(\frac{\alpha}{K}+1\right), \quad \text{for } x_i \leq 1/2, \tag{2.2.4}$$

and

$$\frac{\alpha(1-x_i)}{K} + K_2\left[1-\exp\left(-\frac{(1-x_i)}{2}\sqrt{\frac{b(1)}{\varepsilon}}\right)\right] = \left(1-\frac{i}{N}\right)\left(\frac{\alpha}{K}+1\right), \quad \text{for } x_i > 1/2, \tag{2.2.5}$$

where

$$K_1 = \frac{|\kappa_1|^{1/2}}{|\kappa_1|^{1/2}+|\kappa_2|^{1/2}} \quad \text{and} \quad K_2 = 1-K_1.$$

It is clear that the final adaptively generated equidistributed meshes x_i will satisfy both the nonlinear algebraic equations (2.2.4) and (2.2.5). The following lemma provides the structure of the mesh distribution and also a choice of α. This choice is motivated from the well-known *apriori* chosen piecewise-uniform Shishkin mesh (see [55]), which can capture the boundary layer with parameter-uniform convergence.

Lemma 2.2.3. *Assume that the nonuniform mesh is generated by assuming $\alpha = K$ in (2.2.4) and (2.2.5), then the mesh points are distributed by the following way*

$$x_{k_l} < 2\sqrt{\frac{\varepsilon}{b(0)}}\ln(N) < x_{k_l+1},$$

and

$$x_{k_r-1} < 1-2\sqrt{\frac{\varepsilon}{b(1)}}\ln(N) < x_{k_r},$$

with

$$k_l = \left[\frac{K_1}{2}(N-1) + \sqrt{\frac{\varepsilon}{b(0)}}N\ln(N)\right],$$
$$k_r = \left[N - \frac{K_2}{2}(N-1) - \sqrt{\frac{\varepsilon}{b(1)}}N\ln(N)\right] + 1,$$

where $[\cdot]$ *denotes the integral part of the inside quantity. Furthermore, we have*

$$\exp\left(\frac{-x_i}{2}\sqrt{\frac{b(0)}{\varepsilon}}\right) \leq CN^{-1}, \quad i \geq k_l - 1, \quad x_i \leq 1/2,$$

$$\exp\left(\frac{-(1-x_i)}{2}\sqrt{\frac{b(1)}{\varepsilon}}\right) \leq CN^{-1}, \quad i \leq k_r, \quad x_i > 1/2.$$

Proof. The proof of this lemma can be obtained from [9]. ∎

More rigorous analysis relating the piecewise-uniform Shishkin mesh with the adaptively generated mesh and their mesh distribution using the asymptotic expansion are addressed in [9]. The following lemma provides an insight of the mesh spacing.

Lemma 2.2.4. *The mesh widths within the boundary layers satisfy*

$$h_i < C\sqrt{\frac{\varepsilon}{b(0)}}, \quad i = 1, \cdots, k_l, \quad \textit{and} \quad h_i < C\sqrt{\frac{\varepsilon}{b(1)}}, \quad i = k_r + 1, \cdots, N,$$

with

$$|h_{i+1} - h_i| \leq Ch_i^2, \quad i = 1, \cdots, k_l - 1,$$

and

$$|h_{i+1} - h_i| \leq Ch_{i+1}^2, \quad i = k_r + 1, \cdots, N - 1.$$

Proof. A general proof for mesh widths inside the boundary layers are provided in Beckett and Mackenzie [9]. However, the convergence analysis using spline approximation for mixed boundary conditions needs more finer estimates for h_1 and h_N. Here, we have established the result according to our requirement. Under the assumption $\alpha = K$, the equidistribution mapping (2.2.4) leads to

$$x_i + K_1\left[1 - \exp\left(-\sqrt{\frac{b(0)}{\varepsilon}}\frac{x_i}{2}\right)\right] = \frac{2i}{N}.$$

This implies that, we have $\dfrac{x_1}{K_1} + 1 - \dfrac{2N^{-1}}{K_1} = \exp\left(-\sqrt{\dfrac{b(0)}{\varepsilon}}\dfrac{x_1}{2}\right)$, for $i = 1$.
Now for any $\overline{x}_1 > x_1$, we obtain from the mapping (2.2.4) that

$$\exp\left(-\sqrt{\frac{b(0)}{\varepsilon}}\frac{\overline{x}_1}{2}\right) = 1 - \frac{2N^{-1}}{K_1},$$

which implies that

$$\overline{x}_1 = 2\sqrt{\frac{\varepsilon}{b(0)}}\ln\left(\frac{N}{N - 2K_1^{-1}}\right).$$

Hence

$$\begin{aligned} h_1 < \overline{x}_1 - x_0 &= 2\sqrt{\frac{\varepsilon}{b(0)}} \ln\left(\frac{N}{N - 2K_1^{-1}}\right) \\ &= -2\sqrt{\frac{\varepsilon}{b(0)}} \ln\left(1 - 2K_1^{-1}N^{-1}\right) \qquad (2.2.6) \\ &< 4\sqrt{\frac{\varepsilon}{b(0)}} K_1^{-1}N^{-1}. \qquad (2.2.7) \end{aligned}$$

In an analogous manner, following the technique provided for the derivation of h_1's bound, we can deduce that

$$h_N < 4\sqrt{\frac{\varepsilon}{b(1)}} K_2^{-1}N^{-1},$$

where the equidistribution mapping (2.2.5) will be used in the analysis. Hence, this completes the proof. ∎

The following lemma provides upper bounds of the mesh spacings throughout the domain.

Lemma 2.2.5. *The mesh widths generated by the equidistribution of monitor function (2.2.1) satisfy*

$$h_i \leq CN^{-1}, \text{ for } i = 1, \cdots, N.$$

Proof. It is easy to observe that the monitor function (2.2.1) satisfies $M(x, u(x)) \geq \alpha = K$. Again, Lemma 2.2.2 implies that $\int_0^1 M(x, u(x))dx \leq C_2$. Therefore, the equidistribution principle (1.1.4) leads to

$$\alpha h_i \leq \int_{x_{i-1}}^{x_i} M(x, u(x))dx = \frac{1}{N}\int_0^1 M(x, u(x))dx \leq C_2 N^{-1} \Rightarrow h_i \leq C_2\alpha^{-1}N^{-1}.$$

Consequently,

$$h_i \leq CN^{-1}.$$ ∎

The next section is devoted for the discretization of the continuous problem (2.1.1) and the stability analysis of the discrete operator. The upper bounds for the mesh spacing provided in the previous lemmas will be used during the stability analysis of the discrete operator.

2.3 Numerical Schemes

This section explicitly describes the well-known classical scheme and the proposed numerical scheme to discretize the Robin type BVP (2.1.1). In the following, we obtain the cubic spline difference scheme, which will be used to approximate mixed type boundary conditions.

2.3.1 Cubic spline difference scheme

In this part, we derive the cubic spline scheme on a general nonuniform mesh $\Omega^N \equiv \{0 = x_0 < x_1 < \cdots < x_N = 1\}$ where step sizes will be defined as $h_i = x_i - x_{i-1},\ i = 1, \cdots, N$. For the known values $u(x_0), u(x_1), \cdots, u(x_N)$ of a function $u(x)$ defined at the nodal points $x_0, x_1, \cdots, x_N$, a cubic spline interpolating polynomial will have the following properties:

(i) $S(x)$ coincides with a polynomial of degree three on each subinterval $[x_i, x_{i+1}],\ i = 0, \cdots, N-1$,

(ii) $S(x) \in \mathcal{C}^2(\overline{\Omega})$,

(iii) $S(x_i) = u(x_i),\ i = 0, \cdots, N$.

The cubic spline can be written in the following form

$$\begin{aligned} S(x) \ &= \frac{(x_{i+1}-x)^3}{6h_{i+1}}\Phi_i + \frac{(x-x_i)^3}{6h_{i+1}}\Phi_{i+1} + \left(u(x_i) - \frac{h_{i+1}^2}{6}\Phi_i\right)\left(\frac{x_{i+1}-x}{h_{i+1}}\right) + \\ &+ \left(u(x_{i+1}) - \frac{h_{i+1}^2}{6}\Phi_{i+1}\right)\left(\frac{x-x_i}{h_{i+1}}\right),\ x_i \le x \le x_{i+1},\ i = 0, \cdots, N-1, \end{aligned} \tag{2.3.1}$$

where $\Phi_i = S''(x_i),\ i = 0, \cdots, N$. From (2.3.1), we can obtain one sided limits of the first-order derivative as

$$S'(x_i-) = \frac{h_i}{6}\Phi_i + \frac{h_i}{3}\Phi_i + \frac{u(x_i) - u(x_{i-1})}{h_i}, \tag{2.3.2}$$

and

$$S'(x_i+) = -\frac{h_{i+1}}{3}\Phi_i - \frac{h_{i+1}}{6}\Phi_{i+1} + \frac{u(x_{i+1}) - u(x_i)}{h_{i+1}}. \tag{2.3.3}$$

Substituting Φ_i from $-\varepsilon\Phi_i + b(x_i)u(x_i) = f(x_i)$ to (2.3.2) and (2.3.3), we get an approximation of the one sided first-order derivatives at both boundary points. Hence, the discretizations of the mixed boundary conditions of (2.1.1) reduce to

$$\begin{cases} \left[\dfrac{3\varepsilon}{h_1}\left(\alpha_1 + \dfrac{\beta_1'}{h_1}\right) + b_0\beta_1'\right]U_0 + \left[\dfrac{-3\varepsilon\beta_1'}{h_1^2} + \dfrac{b_1\beta_1'}{2}\right]U_1 = \beta_1' f_0 + \dfrac{\beta_1'}{2}f_1 + \dfrac{3\varepsilon\gamma_1}{h_1}, \\ \left[\dfrac{-3\varepsilon\beta_2'}{h_N^2} + \dfrac{b_{N-1}\beta_2'}{2}\right]U_{N-1} + \left[\dfrac{3\varepsilon}{h_N}\left(\alpha_2 + \dfrac{\beta_2'}{h_N}\right) + b_N\beta_2'\right]U_N = \beta_2' f_N + \dfrac{\beta_2'}{2}f_{N-1} + \dfrac{3\varepsilon\gamma_2}{h_N}, \end{cases} \tag{2.3.4}$$

where $\beta_k' = \sqrt{\varepsilon}\beta_k$ for $k = 1, 2$ and U_i is the discrete approximation of u at x_i.

2.3.2 Finite difference discretization

To discretize the continuous problem (2.1.1) at the interior mesh points, we consider the classical finite difference approximations on the nonuniform mesh Ω^N.

The first discretized problem uses the central difference scheme for the DE with forward and backward differences for mixed boundary conditions:

Problem 1.

$$\begin{cases} \mathcal{L}_\varepsilon^N U_i \equiv -\varepsilon\delta^2 U_i + b(x_i)U_i = f(x_i), \quad i = 1, \cdots, N-1, \\ M_l^{N,F} U_0 \equiv \alpha_1 U_0 - \beta_1\sqrt{\varepsilon} D^+ U_0 = \gamma_1, \quad M_r^{N,B} U_N \equiv \alpha_2 U_N + \beta_2\sqrt{\varepsilon} D^- U_N = \gamma_2. \end{cases} \tag{2.3.5}$$

In the second problem, the DE is approximated by the central difference scheme and mixed boundary conditions are replaced by the cubic spline approximations:

Problem 2.

$$\begin{cases} \mathcal{L}_\varepsilon^N U_i \equiv -\varepsilon\delta^2 U_i + b(x_i)U_i = f(x_i), \quad i = 1, \cdots, N-1, \\ M_l^{N,Sp} U_0 = 0, \qquad\qquad M_r^{N,Sp} U_N = 0, \end{cases} \tag{2.3.6}$$

where $M_l^{N,Sp}$ and $M_r^{N,Sp}$ denote the spline approximation for the Robin boundary conditions, which are defined by equations in (2.3.4) and will be written as $M_l^{N,Sp}U_0 = 0$, $M_r^{N,Sp}U_N = 0$.

The difference schemes of the above two problems take the following form

$$\mathcal{L}_\varepsilon^N U_i \equiv r_i^- U_{i-1} + r_i^c U_i + r_i^+ U_{i+1} = q_i^- f_{i-1} + q_i^c f_i + q_i^+ f_{i+1}, \quad i = 1, \cdots, N-1, \tag{2.3.7}$$

with the following equations at the boundary points

$$\begin{cases} r_0^c U_0 + r_0^+ U_1 = q_0^- + q_0^c f_0 + q_0^+ f_1, \\ r_N^- U_{N-1} + r_N^c U_N = q_N^- + q_N^c f_{N-1} + q_N^+ f_N, \end{cases} \tag{2.3.8}$$

where, for $i = 1, \cdots, N-1$,

$$r_i^- = \frac{-2\varepsilon}{h_i(h_{i+1}+h_i)}, \quad r_i^c = \frac{2\varepsilon}{h_i h_{i+1}} + b_i, \quad r_i^+ = \frac{-2\varepsilon}{h_{i+1}(h_i + h_{i+1})}, \tag{2.3.9}$$

and for Problem 1

$$\begin{cases} r_0^c = \alpha_1 + \dfrac{\beta_1\sqrt{\varepsilon}}{h_1}, \quad r_0^+ = -\dfrac{\beta_1\sqrt{\varepsilon}}{h_1}, \\ q_0^- = \gamma_1, \quad q_0^c = q_0^+ = 0, \\ r_N^- = -\dfrac{\beta_2\sqrt{\varepsilon}}{h_N}, \quad r_N^c = \alpha_2 + \dfrac{\beta_2\sqrt{\varepsilon}}{h_N}, \\ q_N^- = \gamma_2, \quad q_N^c = q_N^+ = 0, \end{cases} \tag{2.3.10}$$

with for Problem 2

$$\begin{cases} r_0^c = \dfrac{3\varepsilon}{h_1}\left(\alpha_1 + \dfrac{\beta_1\sqrt{\varepsilon}}{h_1}\right) + b_0\beta_1\sqrt{\varepsilon}, \quad r_0^+ = \dfrac{-3\varepsilon\beta_1\sqrt{\varepsilon}}{h_1^2} + \dfrac{b_1\beta_1\sqrt{\varepsilon}}{2}, \\ q_0^- = \dfrac{3\varepsilon\gamma_1}{h_1}, \quad q_0^c = \beta_1\sqrt{\varepsilon}, \quad q_0^+ = \dfrac{\beta_1\sqrt{\varepsilon}}{2}, \\ r_N^- = \dfrac{-3\varepsilon\beta_2\sqrt{\varepsilon}}{h_N^2} + \dfrac{b_{N-1}\beta_2\sqrt{\varepsilon}}{2}, \quad r_N^c = \dfrac{3\varepsilon}{h_N}\left(\alpha_2 + \dfrac{\beta_2\sqrt{\varepsilon}}{h_{N-1}}\right) + b_N\beta_2\sqrt{\varepsilon}, \\ q_N^- = \dfrac{3\varepsilon\gamma_2}{h_N}, \quad q_N^c = \dfrac{\beta_2\sqrt{\varepsilon}}{2}, \quad q_N^+ = \beta_2\sqrt{\varepsilon}. \end{cases} \tag{2.3.11}$$

By solving the system of linear algebraic equations in (2.3.7) with (2.3.8), we obtain the approximate solution U_i, $i = 0, \cdots, N$, of $u(x)$ at the nodal points $x_0, x_1, \cdots, x_N$, for each discretized problem.

The following lemma shows that the stiffness matrices of the discrete operators defined in **Problem 1** and **Problem 2** lead to an M-matrix and hence, it satisfy the discrete comparison principle. As a consequence, the stability of the discrete solution can be obtained.

Lemma 2.3.1. *The stiffness matrices in (2.3.7)-(2.3.8) associated with the discrete operators (2.3.5) and (2.3.6) for the continuous problem (2.1.1) i.e.,*

1. *Forward and backward schemes for mixed type boundary conditions,*
2. *Proposed cubic spline scheme for mixed type boundary conditions, with sufficiently large N satisfying*

$$3 > 2\beta^*\beta^{-1}\log^2(1-\zeta N^{-1}), \quad \textit{where} \quad \zeta = \min\left\{\frac{2}{K_1}, \frac{2}{K_2}\right\}, \tag{2.3.12}$$

enjoy the M-matrix property. Hence, the discrete solution is ε-uniform stable in the maximum norm.

Proof. In this proof, we consider different cases depending on the location of the mesh points $x_i \in \Omega^N$. From the stiffness matrix of the discretized problem (2.3.5) and (2.3.6), it is clear for $i \neq 0, N$, we have

$$r_i^c > 0, \quad r_i^- < 0, \quad r_i^+ < 0,$$

and

$$|r_i^c| - |r_i^-| - |r_i^+| = b_i > \beta.$$

Now, to examine the M-matrix properties at the boundary points $x_0 = 0$ and $x_N = 1$, we shall consider the following two cases:

Case 1: Forward and backward difference schemes for mixed type boundary conditions.

Assuming $\alpha_1, \alpha_2 > 0$, we have $r_0^c > 0$, $r_0^+ < 0$ with

$$|r_0^c| - |r_0^+| = \alpha_1 > 0.$$

Again $r_N^c > 0$, $r_N^- < 0$ with

$$|r_N^c| - |r_N^-| = \alpha_2 > 0,$$

which show that, the stiffness matrix from (2.3.9)-(2.3.10) corresponding to the discrete operator (2.3.5) leads to an M-matrix.

Case 2: Cubic spline scheme for mixed type boundary conditions.

Now observe that $r_0^c = \dfrac{3\varepsilon\alpha_1}{h_1} + \dfrac{3\varepsilon\sqrt{\varepsilon}\beta_1}{h_1^2} + b_0\beta_1\sqrt{\varepsilon} > 0$. Thereafter, employing the bound for h_1 from (2.2.6), we obtain

$$\begin{aligned} r_0^+ = \frac{-3\varepsilon\sqrt{\varepsilon}\beta_1}{h_1^2} + \frac{b_1\beta_1\sqrt{\varepsilon}}{2} &< \frac{\beta_1\sqrt{\varepsilon}}{2h_1^2}[-6\varepsilon + \beta^* h_1^2] \\ &< \frac{\beta_1\sqrt{\varepsilon}}{2h_1^2}\left[-6\varepsilon + \frac{4\varepsilon\beta^*}{\beta}\log^2(1-\zeta N^{-1})\right] \\ &= \frac{\beta_1\varepsilon\sqrt{\varepsilon}}{h_1^2}[-3 + 2\beta^*\beta^{-1}\log^2(1-\zeta N^{-1})] < 0. \end{aligned}$$

Again

$$|r_0^c| - |r_0^+| = \frac{3\varepsilon\alpha_1}{h_1} + \left(b_0 + \frac{b_1}{2}\right)\beta_1\sqrt{\varepsilon} \geq \frac{3\varepsilon\alpha_1}{h_1} + \frac{3\beta\beta_1\sqrt{\varepsilon}}{2} > 0.$$

A similar argument can be given for the case of $i = N$. Therefore, the stiffness matrix from (2.3.9) and (2.3.11) corresponding to the discretized problem (2.3.6) leads to an M-matrix. ∎

Hence, the discrete operators corresponding to Problem 1 and Problem 2 are ε-uniformly stable in the supremum norm.

2.4 Error Analysis

In this section, we study the consistency of the proposed numerical schemes (2.3.5) and (2.3.6). Finally, the ε-uniform convergence of the numerical solutions are analyzed. We decompose the corresponding numerical solution $U(x_i)$, by its smooth and singular components $V(x_i)$ and $W(x_i)$ respectively, *i.e.,*

$$U_i = V_i + W_i, \quad i = 0, \cdots, N,$$

as like the continuous solution $u(x)$. This decomposition will be used to estimate the nodal errors at the interior points. In the following, we provide the decomposed problem

for smooth and singular components $V(x_i)$ and $W(x_i)$ for Problem 1; since for Problem 2, it can be handled in an analogous manner. For Problem 1, the smooth component V satisfies

$$\mathcal{L}_\varepsilon^N V_i = f(x_i), \quad M_l^{N,F} V_0 = -M_l w(0), \quad M_r^{N,B} V_N = -M_r w(1), \tag{2.4.1}$$

and the singular component W satisfies

$$\mathcal{L}_\varepsilon^N W_i = 0, \quad M_l^{N,F} W_0 = \gamma_1 - M_l v(0), \quad M_r^{N,B} W_N = \gamma_2 - M_r v(1). \tag{2.4.2}$$

The nodal error of the numerical solution U_i is obtained by the errors from the smooth component V_i and singular component W_i, using the triangular inequality

$$|U_i - u(x_i)| \leq |V_i - v(x_i)| + |W_i - w(x_i)|. \tag{2.4.3}$$

Let us define the truncation error of the function $g(x)$ at $x = x_i$ as $\tau_i^g = (\mathcal{L}g)(x_i) - L^N g_i$. The error of the numerical solution U is examined by separately analyzing the errors for the smooth component V and the singular component W in the region Ω^N.

2.4.1 Error of the smooth component

The next lemma gives useful estimates for the local truncation errors of the smooth component V.

Lemma 2.4.1. *The truncation errors of the smooth component V, of numerical solution U satisfy*

$$|\tau_i^V| \leq CN^{-2}, \quad \textit{for} \quad i = 1, \cdots, N-1.$$

Proof. By Peano's kernel theorem, the truncation error of V at x_i can be written as

$$\tau_i^V = -\frac{\varepsilon}{h_i + h_{i+1}} \left\{ \frac{1}{h_{i+1}} \int_{x_i}^{x_{i+1}} (s - x_{i+1})^2 v'''(s) ds - \frac{1}{h_i} \int_{x_{i-1}}^{x_i} (s - x_{i-1})^2 v'''(s) \right\}.$$

Hence

$$|\tau_i^V| \leq C\varepsilon (h_i + h_{i+1}) ||v'''(x)||_{(x_{i-1}, x_{i+1})}.$$

Estimating the third-order derivative bound of $v(x)$ from Lemma 2.2.2 and the step length bounds from Lemma 2.2.5, we finally obtain

$$|\tau_i^V| \leq CN^{-2},$$

since $\varepsilon \leq N^{-1}$. ∎

2.4.2 Error of the singular component

The nodal truncation errors corresponding to the singular component W are analyzed to the next two lemmas by considering different cases, depending on the location of the mesh point x_i.

Lemma 2.4.2. *The truncation errors associated with the singular component W satisfy*

$$|\tau_i^W| \leq CN^{-2}, \quad \text{for} \quad i = k_l, \cdots, k_r.$$

Proof. Using the mean-value theorem, it is easy to check that the truncation error for W at x_i satisfies

$$|\tau_i^W| \leq C\varepsilon ||w''(x)||_{[x_{i-1},x_{i+1}]} \leq C \begin{cases} \exp\left(-x_{i-1}\sqrt{\dfrac{b(0)}{\varepsilon}}\right), & x_i \leq 1/2, \\ \exp\left(-(1-x_{i+1})\sqrt{\dfrac{b(1)}{\varepsilon}}\right), & x_i > 1/2. \end{cases}$$

Now invoking Lemma 2.2.3 for $x_i \geq 1/2$ with $k_l \leq i$, we get

$$|\tau_i^W| \leq C \exp\left(-x_{k_l-1}\sqrt{\frac{b(0)}{\varepsilon}}\right) = C\left(\exp\left(-\frac{x_{k_l-1}}{2}\sqrt{\frac{b(0)}{\varepsilon}}\right)\right)^2 \leq CN^{-2}.$$

A similar technique can be adopted for the case $x_i > 1/2$ with $k_r \geq i$. ∎

Lemma 2.4.3. *The truncation errors of the singular component W satisfy the following inequalities*

$$|\tau_i^W| \leq CN^{-2}, \quad \text{for} \quad i = 1, \cdots, k_l - 1, \quad \text{and} \quad i = k_r + 1, \cdots, N-1.$$

Proof. We shall only consider the left-hand part of the boundary layer regions as the right-hand part of the boundary layers can be addressed in an analogous manner. A direct calculation using Taylor's series expansion shows

$$|\tau_i^W| = \frac{\varepsilon |h_i^2 w'''(\xi_i^1) - h_{i+1}^2 w'''(\xi_i^2)|}{3(h_i + h_{i+1})},$$

where $\xi_i^1 \in (x_{i-1}, x_i)$ and $\xi_i^2 \in (x_i, x_{i+1})$. Hence, observing

$$|h_i^2 w'''(\xi_i^1) - h_{i+1}^2 w'''(\xi_i^2)| \leq C(|h_i^2 - h_{i+1}^2||w'''(x_i)| + h_i^2(h_i + h_{i+1})|w^{(iv)}(x_i)|),$$

we can derive

$$\begin{aligned} |\tau_i^W| &\leq C\varepsilon^{-1} h_i^2 \exp\left(-x_i\sqrt{\frac{b(0)}{\varepsilon}}\right) \\ &\leq C\varepsilon^{-1}\left(\int_{x_{i-1}}^{x_i} \exp\left(-\frac{t}{2}\sqrt{\frac{b(0)}{\varepsilon}}\right) dt\right)^2 \\ &\leq C\varepsilon^{-1}\left(\sqrt{\varepsilon}\int_{x_{i-1}}^{x_i} M(t, u(t)) dt\right)^2 \\ &\leq CK^2 N^{-2} \leq CN^{-2}. \end{aligned}$$

∎

Now, we shall proceed to analyze the truncation errors of the solution at boundary points.

Lemma 2.4.4. *The truncation errors of the numerical solution U at the boundary points $x = 0, 1$, for the problem (2.3.5), where the Robin boundary conditions are discretized by the forward and backward approximations satisfy the following estimates*

$$|\tau_i^U| \leq CN^{-1}, \quad for \quad i = 0, N.$$

Proof. Now, using the Taylor's formula with the integral form of remainder and the derivative bounds for v, w as stated in Lemma 2.2.2, we get

$$\begin{aligned}
|\tau_0^U| &= |(\alpha_1 u(0) - \beta_1\sqrt{\varepsilon}u'(0)) - (\alpha_1 U_0 - \beta_1\sqrt{\varepsilon}D^+U_0)| \\
&= \sqrt{\varepsilon}\beta_1|u'(0) - D^+U_0| \\
&\leq \left|\frac{\sqrt{\varepsilon}\beta_1}{h_1}\int_0^{h_1}(t-h_1)u''(t)dt\right| \\
&\leq Ch_1\sqrt{\varepsilon}||u''(x)||_{(x_0,x_1)} \\
&\leq C\sqrt{\varepsilon}N^{-1}\sqrt{\varepsilon}\left[1+\varepsilon^{-1}\mathcal{E}_\varepsilon(x)\right] \leq CN^{-1},
\end{aligned}$$

where the step length inequalities are obtained from Lemma 2.2.5. Finally, following the same approach as like for x_0, one can obtain the truncation error at the end point x_N. This completes the proof. ∎

Lemma 2.4.5. *The truncation errors of the solution U at the boundary points $x = 0, 1$, for the discrete problem (2.3.6), where the Robin boundary conditions are discretized by using the spline approximation from (2.3.4), lead to the following estimates*

$$|\tau_i^U| \leq CN^{-2}, \quad for \quad i = 0, N.$$

Proof. Estimating the solution derivative bound from Lemma 2.2.1, it is straightforward to obtain the following result using the Taylor's expansion that

$$\begin{aligned}
|\tau_0^U| &\leq C\sqrt{\varepsilon}\beta_1\varepsilon h_1^2||u^{(iv)}(x)||_{(x_0,x_1)} \\
&\leq C\beta_1\varepsilon^2\sqrt{\varepsilon}N^{-2}\left[1+\varepsilon^{-2}\mathcal{E}_\varepsilon(x)\right] \\
&\leq C\sqrt{\varepsilon}N^{-2} \\
&\leq CN^{-2}.
\end{aligned}$$

A similar technique can be applied to find the truncation error at the end point x_N, which completes the proof. ∎

Let us mention that we have just found estimates for the local truncation errors which will lead to the main convergence results.

2.4.3 The main convergence results

We now state the main two theorems of this chapter. The following theorem shows that the method (2.3.5) is ε-uniformly first order convergent on the equidistributed mesh.

Theorem 2.4.6. *Let u be the solution of (2.1.1) and U be the discrete solution, obtained by equidistributing the monitor function (2.2.1) with $\alpha = K$, using the discrete operator (2.3.5), where the Robin boundary conditions are discretized by the forward-backward approximation. Then, there exists a constant C, independent of ε and N, such that*

$$||u - U||_{\Omega^N} \leq CN^{-1}.$$

Proof. The M-Matrix criterion shown at Lemma 2.3.1 implies that the inverse of the discrete operator $\mathcal{L}_\varepsilon^N$ corresponding to the continuous operator $\mathcal{L}_\varepsilon$ of Problem 1 is ε-uniformly bounded. Now by invoking the triangle inequality (2.4.3) to the error estimates derived in Lemmas 2.4.1-2.4.4, we can conclude that

$$|u(x_i) - U_i| \leq CN^{-1} \quad \text{for} \quad i = 0, \cdots, N.$$

■

For the model DE (2.1.1), the next theorem provides an improved ε-uniform second-order accurate solution for the method (2.3.6).

Theorem 2.4.7. *Let u be the solution of (2.1.1) and U be the discrete solution, obtained by equidistributing the monitor function (2.2.1) with $\alpha = K$, using the discrete operator (2.3.6) where the Robin boundary conditions are discretized by the proposed spline approximation (2.3.4). Then, for sufficiently large N satisfying*

$$3 > 2\beta^*\beta^{-1}\log^2(1 - \zeta N^{-1}), \quad \textit{where} \quad \zeta = \min\left\{\frac{2}{K_1}, \frac{2}{K_2}\right\},$$

there exists a constant C, independent of ε and N, such that

$$||u - U||_{\Omega^N} \leq CN^{-2}.$$

Proof. From Lemma 2.3.1, it is clear that the matrix associated with the difference operator $\mathcal{L}_\varepsilon^N$ of Problem 2 is an M-matrix. Hence, the inverse of the discrete operator $\mathcal{L}_\varepsilon^N$ is ε-uniformly bounded. As a consequence, using the inequality (2.4.3) with the estimates given by Lemmas 2.4.1-2.4.3 and Lemma 2.4.5, we conclude that

$$|u(x_i) - U_i| \leq CN^{-2}, \quad \text{for} \quad i = 0, \cdots, N.$$

■

The above analysis shows that the well-known forward-backward scheme as well as the proposed spline scheme, for the mixed boundary conditions are uniformly accurate at all the equidistributed meshes. In fact, a uniformly convergent global approximation for the obtained solution can be constructed by forming piecewise linear interpolation of the numerical solution from the following theorem.

Theorem 2.4.8. *The numerical solution U parameter-uniformly converges to the exact solution u of the problem (2.1.1) and satisfies the following global ε-uniform error estimate:*

$$||\overline{U} - u|| \leq CN^{-1},$$

for problem (2.3.5), i.e., the forward-backward approximation to the Robin boundary conditions and the central difference approximation for the differential equation and

$$||\overline{U} - u|| \leq CN^{-2},$$

for problem (2.3.6), i.e., the spline approximation to the Robin boundary conditions and the central difference approximation for the differential equation. Here $\overline{U}$ is the piecewise linear interpolant of U on $\overline{\Omega}$.

Proof. Invoking the triangle inequality to the error estimate, we get

$$||\overline{U} - u|| \leq ||\overline{U} - \overline{u}|| + ||\overline{u} - u||,$$

where $\bar{u}$ is the piecewise linear interpolant of u at the mesh points. Then, the above result can be easily obtained by following the technique provided in [9]. ∎

Remark 2.4.9. *One can notice that the spline approximation for mixed boundary conditions leads to second-order convergence for the problem type (2.1.1), where the boundary conditions are of the following form*

$$M_l u(0) \equiv \alpha_1 u(0) - \beta_1 \sqrt{\varepsilon} u'(0) = \gamma_1, \quad M_r u(1) \equiv \alpha_2 u(1) + \beta_2 \sqrt{\varepsilon} u'(1) = \gamma_2.$$

This analysis can be extended to get convergence (see the proof of Lemma 2.4.5) as well as stability result for a larger class of problems with the Robin boundary conditions

$$M_l u(0) \equiv \alpha_1 u(0) - \beta_1 u'(0) = \gamma_1, \quad M_r u(1) \equiv \alpha_2 u(1) + \beta_2 u'(1) = \gamma_2.$$

Remark 2.4.10. *For the above problem, Natesan and Bawa [62] observed that one can get second-order convergence up to a logarithmic term on apriori chosen piecewise-uniform Shishkin mesh using spline approximation inside the boundary layers. So, the higher-order convergence achieved here is better than [62].*

2.5 Numerical Experiments

This section presents the numerical experiments to confirm the theoretical results explained in the previous section. The generation of the adaptive finite difference solution requires two steps; firstly the equidistributed mesh is to be determined by a mesh generation algorithm and thereafter, the finite difference solution is to be computed on that mesh.

2.5.1 Adaptive mesh generation algorithm

We use the following iterative algorithm to generate a layer-adapted mesh by the equidistributing of the monitor function (2.2.1). An algorithm, similar to this type is applied for singularly perturbed convection-diffusion type problems by Kopteva and Stynes [45] and for singularly perturbed reaction-diffusion problems by Kopteva et al. [44]. Chadha and Kopteva [16] carried out the convergence analysis of this algorithm for singularly perturbed reaction-diffusion problems. Here, our aim is to obtain a mesh that solves the following equidistribution problem

$$M_i h_i = \frac{1}{N}\sum_{j=1}^{N} M_j h_j, \quad \text{for} \quad i = 1, \cdots, N,$$

where M_i is the discrete approximation of the monitor function $M(x, u(x))$ at the subinterval (x_{i-1}, x_i). Observe that instead of solving the discretized equidistribution problem (1.1.4) exactly, it is sufficient that this algorithm can be stopped when the weakly equidistribution principle

$$M_i h_i \leq \frac{C_0}{N}\sum_{j=1}^{N} M_j h_j, \quad \text{for} \quad i = 1, \cdots, N, \tag{2.5.1}$$

is satisfied with a user chosen constant $C_0 > 1$. C_0 will be chosen large enough to get fewer iterations for the convergence of the algorithm. As C_0 approaches to 1, this algorithm results to more accurate solution with many iterations.

Algorithm-

Step 1: Define the initial uniform mesh $\{x^{(0)} : 0 \leq i \leq N,\ x_i^{(0)} = i/N\}$ and go to Step-2 with $p = 0$.

Step 2: Solve the discretized problem $\mathcal{L}_\varepsilon^N U_i^{(p)} = f_i^{(p)}$ with $M_l^N U_0^{(p)} = \gamma_1$ and $M_r^N U_N^{(p)} = \gamma_2$ at the mesh $\{x_i^{(p)} : 0 \leq i \leq N\}$ for $(U_0^{(p)}, \cdots,\ U_N^{(p)})$ and define $h_i^{(p)} = x_i^{(p)} - x_{i-1}^{(p)}$ for $i = 1, \cdots, N$.

Step 3: Find the smooth component $V_i^{(p)}$ of the numerical solution $U_i^{(p)}$, by solving the given DE with $\varepsilon = 0$. Denote the discrete singular component of the solution $U_i^{(p)}$ as $W_i^{(p)} = U_i^{(p)} - V_i^{(p)}$. Find the discretized monitor function

$$\phi_i^{(p)} = \left[\alpha^{(p)} + |\overline{\delta}^2 W_i^{(p)}|^{1/2}\right] \text{ for } i = 1, \cdots, N, \tag{2.5.2}$$

by defining $\overline{\delta}^2 W_i = (\delta^2 W_i + \delta^2 W_{i-1})/2$ with $\overline{\delta}^2 W_1 = \delta^2 W_1$ and $\overline{\delta}^2 W_N = \delta^2 W_{N-1}$ where $\alpha^{(p)} = \sum_{i=1}^{N} h_i |\overline{\delta}^2 W_i|^{1/2}$.

Compute

$$\Phi_j^{(p)} = \sum_{i=1}^{j} h_i^{(p)} \phi_i^{(p)}.$$

Step 4: Choose a constant $C_0 \geq 1$. The stopping criteria for the iterative technique is

$$\frac{\max\limits_{i=1,\ldots,N} h_i^{(p)}\phi_i^{(p)}}{\Phi_N^{(p)}} \leq \frac{C_0}{N}. \tag{2.5.3}$$

If it holds true, then go to Step-6, else continue with Step-5.

Step 5: Generate a new mesh by equidistributing the proposed monitor function using the current computed solution from Step-2 and $\Phi_i^{(p)}$ from Step-3: Set $Y_i^{(p)} = i\Phi_N^{(p)}/N$ for $i = 0, \cdots, N$. Now interpolate $Y_i^{(p)}$to the points $(\Phi_i^{(p)}, x_i^{(p)})$ using the piecewise linear interpolation. Generate a new mesh $x^{(p+1)} \equiv \{0 = x_0^{(p+1)} < x_1^{(p+1)} < \cdots < x_N^{(p+1)} = 1\}$ and return to Step-2.

Step 6: Set $x^* = \{0 = x_0^* < x_1^* < \cdots < x_N^* = 1\} = x^{(p+1)}$ and $U^* = U^{(p+1)}$, where U^* is the desired solution. Stop.

2.5.2 Numerical examples

Here, we present two numerical examples to verify the theoretical results. The maximum point-wise errors and the corresponding rates of convergence are provided for these problems, where the meshes are obtained by the equidistribution of the monitor function (2.2.1).

Example 2.5.1. *Consider the following two-point MBVP:*

$$\begin{cases} -\varepsilon u''(x) + \dfrac{4(1+\sqrt{\varepsilon}(1+x))}{(1+x)^4}u(x) = f(x), \quad x \in \Omega, \\ u(0) - \sqrt{\varepsilon}u'(0) = 2 + \dfrac{6}{1-\exp\left(-1/\sqrt{\varepsilon}\right)}, \quad u(1) + \sqrt{\varepsilon}u'(1) = \dfrac{-2-\exp\left(-1/\sqrt{\varepsilon}\right)}{2(1-\exp\left(-1/\sqrt{\varepsilon}\right))}, \end{cases}$$

with

$$\begin{aligned} f(x) \;=& \frac{-4}{(1+x)^4}\Big[(1+\sqrt{\varepsilon}(1+x)+4\pi^2\varepsilon)\cos(2\pi t) \\ & -2\pi\varepsilon(1+x)\sin(2\pi t) + 3(1+\sqrt{\varepsilon}(1+x))\frac{\exp\left(-1/\sqrt{\varepsilon}\right)}{1-\exp\left(-1/\sqrt{\varepsilon}\right)}\Big], \end{aligned}$$

where $t = 2x/(x+1)$.

Here the mixed boundary conditions are chosen in such a way that the exact solution of this problem becomes

$$u = -\cos(2\pi t) + 3\frac{\exp(-t/\sqrt{\varepsilon}) - \exp(-1/\sqrt{\varepsilon})}{1-\exp(-1/\sqrt{\varepsilon})}.$$

The maximum point-wise error and the rate of convergence are calculated by using the exact solution. The maximum point-wise error is obtained by

$$E_\varepsilon^N = \max_{x_i \in \Omega^N} |U_\varepsilon^N(x_i) - u(x_i)|,$$

where $u(x_i)$ denotes the exact solution and $U_\varepsilon^N(x_i)$ is the numerical solution at the point x_i, with N number of mesh intervals. The uniform error for each fixed N is obtained by taking the maximum over wide range of ε, say from the set S, namely

$$E^N = \max_{\varepsilon \in S} E_\varepsilon^N.$$

The parameter robust rate of convergence is calculated by the usual way

$$p^N = \log_2 \left(\frac{E^N}{E^{2N}} \right).$$

Example 2.5.2. *Consider the singularly perturbed MBVP:*

$$\begin{cases} -\varepsilon u''(x) + u(x) = -\cos^2(\pi x) - 2\varepsilon\pi^2 \cos(2\pi x), \quad x \in \Omega, \\ u(0) - 2\sqrt{\varepsilon}u'(0) = 1, \quad u(1) + 3\sqrt{\varepsilon}u'(1) = 0. \end{cases}$$

As the exact solution for Example 2.5.2 is not available, therefore, the accuracy of its numerical solution will be computed using the double mesh principle. This principle is defined as follows:

For any fixed value of N, the maximum point-wise error E_ε^N of the numerical solution $U(x_i)$ will be calculated by

$$E_\varepsilon^N = \max_i |U_\varepsilon^N(x_i) - \widetilde{U}_\varepsilon^{2N}(x_i)|,$$

where U_ε^N is the numerical solution at x_i with N number of intervals and $\widetilde{U}_\varepsilon^{2N}$ is the numerical solution at x_i, on a mesh obtained by bisecting the original mesh with $2N$ number of mesh intervals. The uniform error for each fixed N and the corresponding parameter-uniform rate of convergence are calculated by the following formulas

$$E^N = \max_{\varepsilon \in S} E_\varepsilon^N, \quad \text{and} \quad p^N = \log_2 \left(\frac{E^N}{E^{2N}} \right).$$

For both of these problems, adaptively generated meshes are constructed using the constant $C_0 = 1.12$, in the algorithm and the set S is defined as

$$S = \left\{ \varepsilon | \varepsilon = 1, 2^{-2}, \cdots, 2^{-40} \right\}.$$

Table 2.1 displays the maximum ε-uniform errors and the corresponding orders of convergence for Example 2.5.1, where the standard forward-backward approximation is used to discretize the Robin boundary conditions. Table 2.2 clearly shows that the proposed higher-order scheme which involves the cubic spline approximation for the mixed boundary conditions increases the orders of convergence from $O(N^{-1})$ to $O(N^{-2})$. Similar behavior is observed for Example 2.5.2, where Tables 2.3 and 2.4 display the

Table 2.1: *Uniform errors and orders of convergence with forward and backward approx. for mixed boundary conditions for Example 2.5.1.*

$\varepsilon \in S$	Number of intervals N						
	64	128	256	512	1024	2048	4096
E^N	2.9895e-1	1.4626e-1	7.2314e-2	3.5994e-2	1.7954e-2	8.9664e-3	4.4807e-3
p^N	1.0313	1.0162	1.0065	1.0035	1.0017	1.0008	-

Table 2.2: *Uniform errors and orders of convergence obtained using spline approx. for mixed boundary conditions for Example 2.5.1.*

$\varepsilon \in S$	Number of intervals N						
	64	128	256	512	1024	2048	4096
E^N	5.0900e-3	1.2696e-3	3.1841e-4	8.0216e-5	2.0094e-5	5.0358e-6	1.2601e-6
p^N	2.0033	1.9954	1.9889	1.9971	1.9965	1.9987	-

maximum ε-uniform errors and the corresponding orders of convergence for the standard method and the proposed method respectively.

From both the numerical experiments, it is observed that the assumption (2.3.12) is merely a necessary condition to obtain the stable numerical solution although we know that the assumption (2.3.12) stated in Lemma 2.3.1 will be satisfied as N increases. This approves the stability conditions computationally.

As a complement of these observations, Figures 2.1 and 2.2 display the plot of N versus the maximum point-wise errors in the logarithmic scale for Examples 2.5.1 and 2.5.2 respectively. The monotonically decreasing behavior of the maximum point-wise errors can be observed from these two figures, as N increases. These two graphs indeed show the comparison between the two schemes. From the log-log plots, one can conclude that the standard method provides first-order accuracy whereas the proposed method is second-order accurate. We have also shown the maximum point-wise errors E_ε^N as a function of N and ε in Figures 2.3 and 2.4 (observe also the error scale). The parameter-uniform convergence can be ensured from these error graphs, as N increases.

Table 2.3: *Uniform errors and orders of convergence with forward and backward approx. for mixed boundary conditions for Example 2.5.2.*

$\varepsilon \in S$	Number of intervals N						
	64	128	256	512	1024	2048	4096
E^N	8.2336e-2	4.0936e-2	2.0416e-2	1.0196e-2	5.0951e-3	2.5468e-3	1.2732e-3
p^N	1.0082	1.0036	1.0017	1.0008	1.0004	1.0002	-

Table 2.4: *Uniform errors and orders of convergence obtained using spline approx. for mixed boundary conditions for Example 2.5.2.*

$\varepsilon \in S$	Number of intervals N						
	64	128	256	512	1024	2048	4096
E^N	8.3652e-4	1.9349e-4	4.6383e-5	1.1343e-5	2.8032e-6	6.9671e-7	1.7369e-7
p^N	2.1122	2.0606	2.0319	2.0166	2.0085	2.0040	-

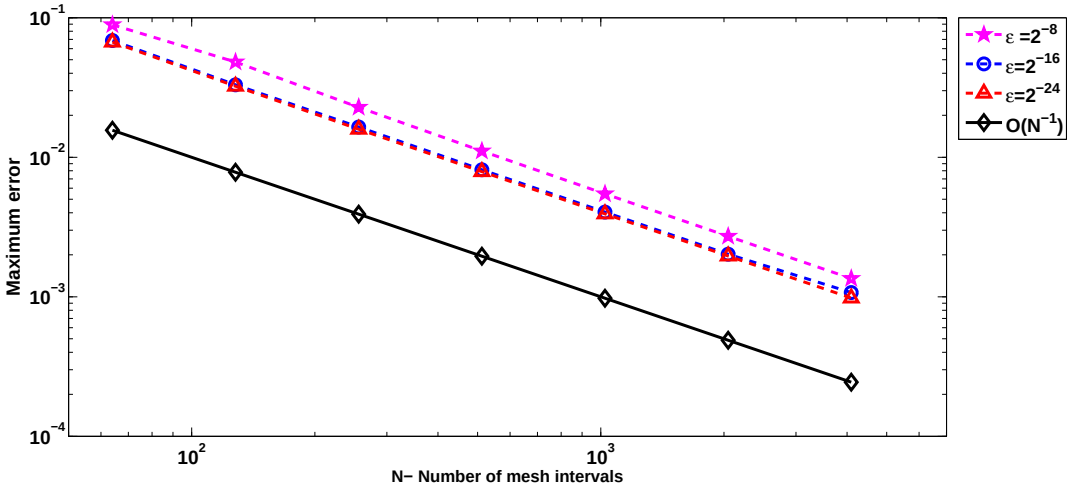

(a) For Problem 1

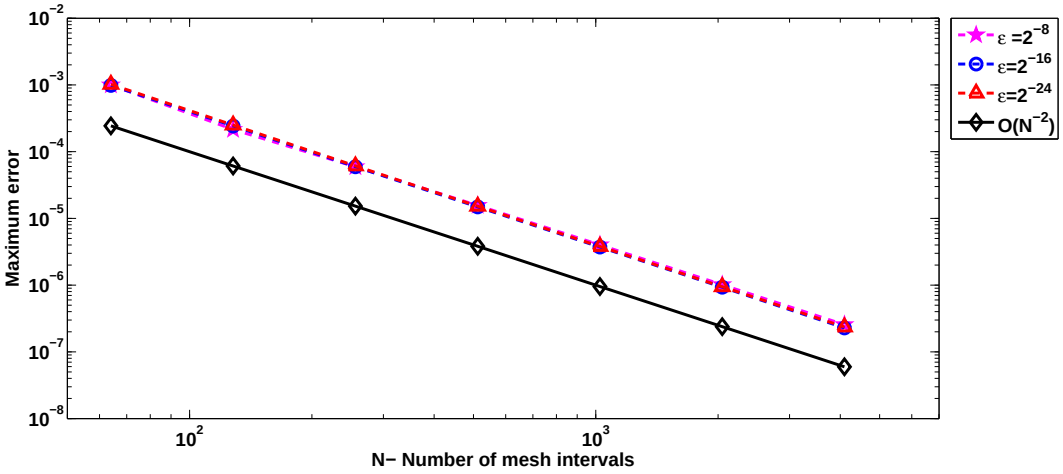

(b) For Problem 2

Figure 2.1: *Loglog plot of the maximum point-wise errors for Example 2.5.1.*

2.6 Conclusions

In this chapter, two parameter uniform numerical methods are considered to solve a class of singularly perturbed Robin type reaction-diffusion problems. The problem is discretized by the well-known forward-backward approximation to the mixed bound-

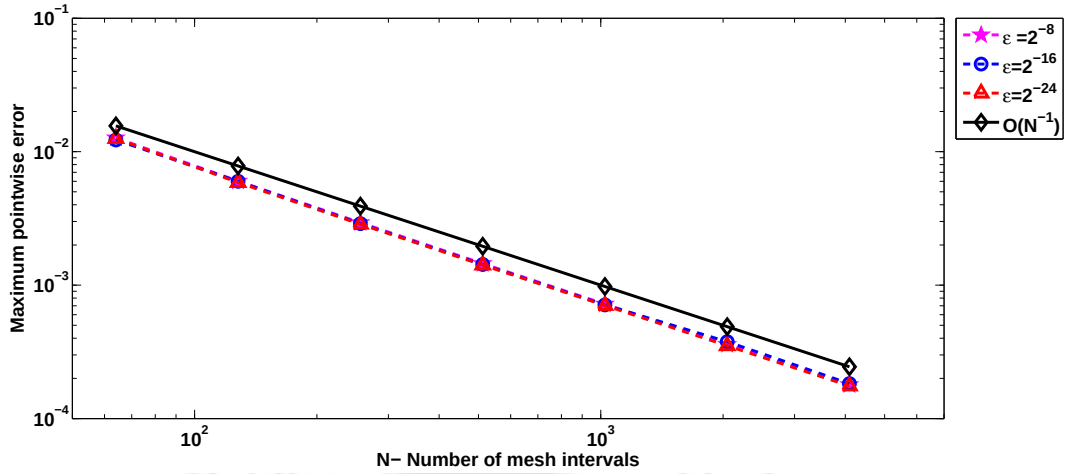

(a) For Problem 1

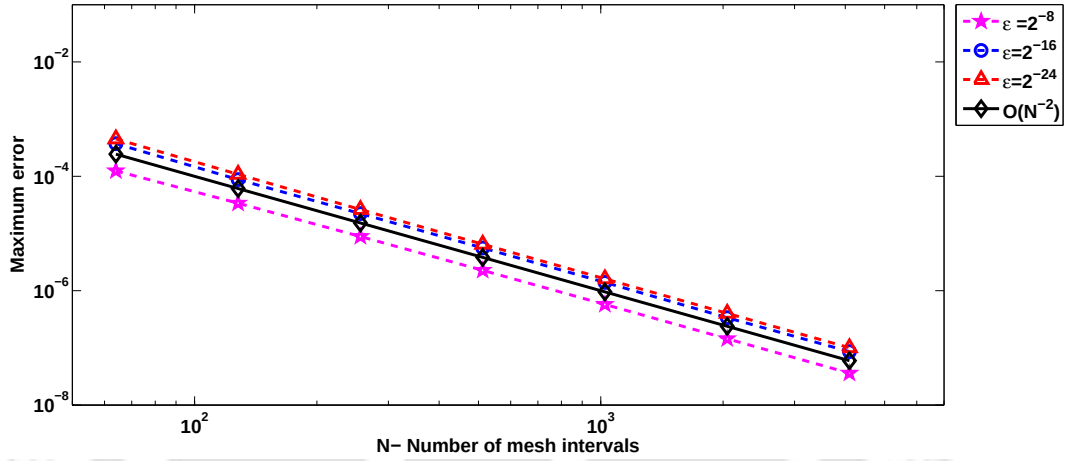

(b) For Problem 2

Figure 2.2: *Loglog plot of the maximum point-wise errors for Example 2.5.2.*

ary conditions and the central difference approximation for the differential equation at the interior meshes. It is shown that this scheme provides first-order convergence. A higher-order uniformly convergent scheme is constructed which is a combination of the central difference scheme for the differential equation at the interior meshes and the cubic spline approximation for the Robin boundary conditions. It has been shown both theoretically and computationally that the newly proposed scheme is of second-order uniformly convergent.

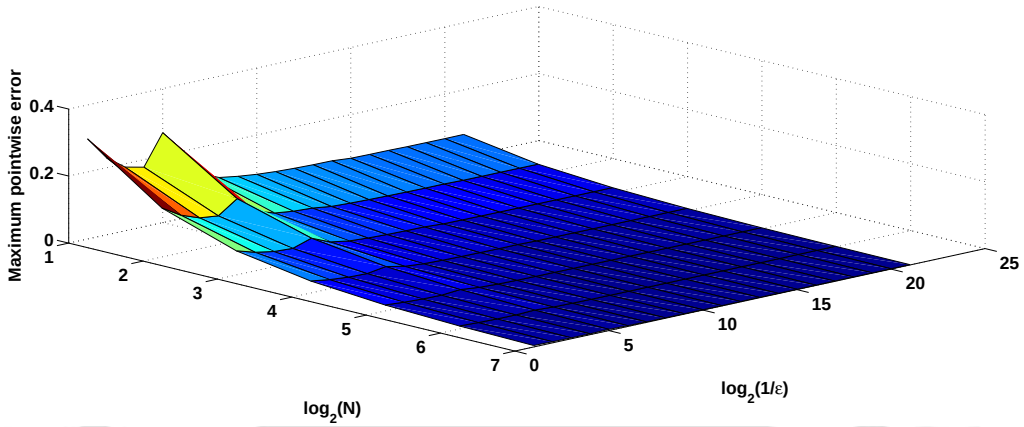

(a) For Problem 1

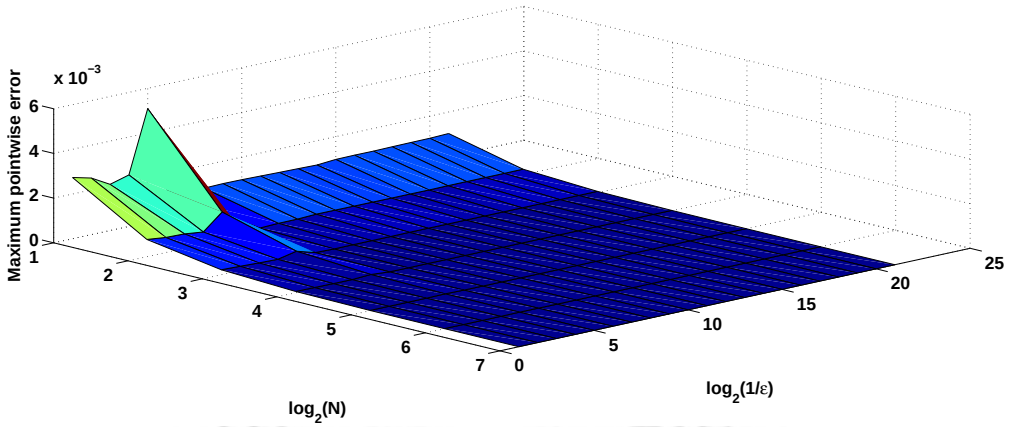

(b) For Problem 2

Figure 2.3: *Maximum point-wise errors as a function of N and ε for Example 2.5.1.*

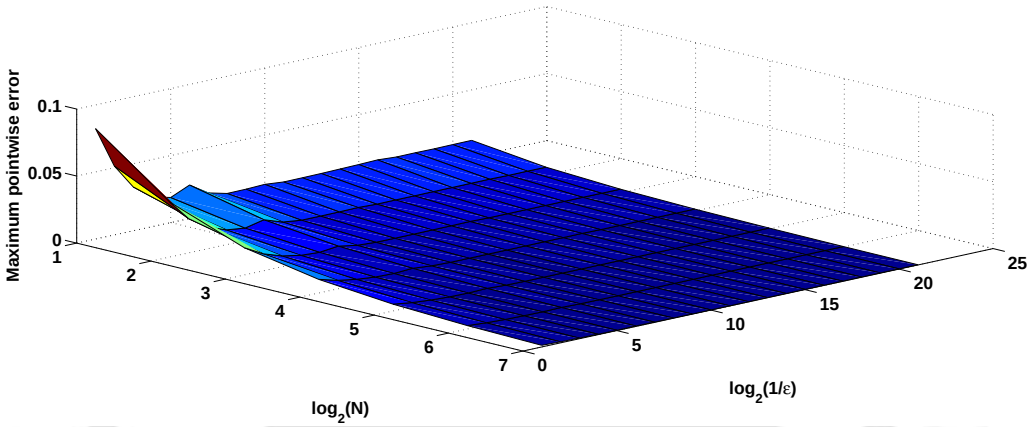

(a) For Problem 1

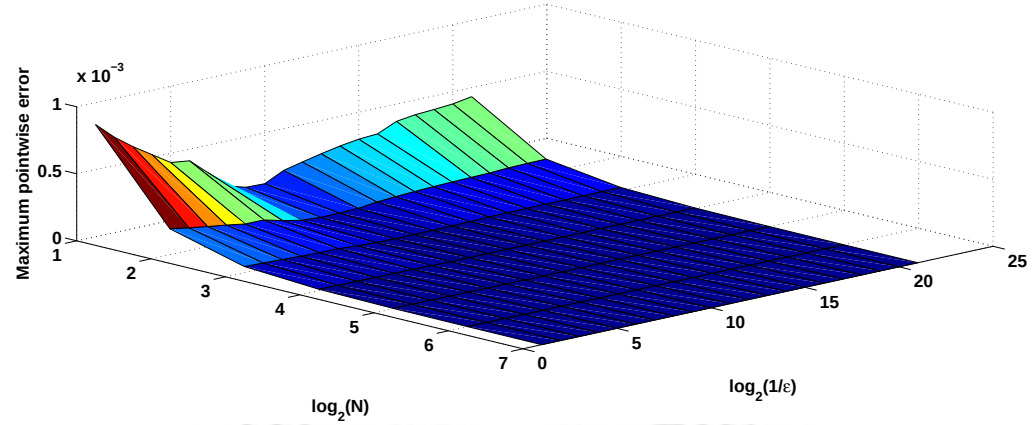

(b) For Problem 2

Figure 2.4: *Maximum point-wise errors as a function of N and ε for Example 2.5.2.*

Chapter 3

Mesh Adaptation for A Class of Singularly Perturbed Fourth-Order Ordinary Differential Equations

This chapter presents the study of a singularly perturbed boundary-value problem of fourth-order ODE on adaptively generated equidistributed mesh. The solution of this problem exhibits boundary layers. To solve these SPPs, we transform the ODE into a coupled system of singularly perturbed ODEs subject to suitable boundary conditions. The classical central difference scheme is used to discretize the system of BVPs on a nonuniform mesh which is generated by the equidistribution of a positive monitor function. We show that the proposed technique provides first-order accuracy independent of the perturbation parameter.

3.1 Introduction

Consider the following singularly perturbed two-point boundary-value problem for fourth-order ODEs of the form:

$$\begin{cases} \mathrm{L}u(x) \equiv -\varepsilon u^{iv}(x) + b(x)u''(x) - c(x)u(x) = -f(x), \quad x \in \Omega, \\ u(0) = p, \quad u(1) = q, \quad u''(0) = -r, \quad u''(1) = -s, \end{cases} \tag{3.1.1}$$

where ε $(0 < \varepsilon \ll 1)$ is the singular perturbation parameter. We assume that the functions $b(x)$, $c(x)$ and $f(x)$ are sufficiently smooth satisfying $\beta^* > b(x) > \beta > 0$ and $0 \geq c(x) \geq -\gamma$, $\gamma > 0$ with $\beta - 2\gamma \geq \eta > 0$, for $x \in \overline{\Omega}$ where η is a real number. Under these assumptions posed on the coefficients in (3.1.1), the BVP (3.1.1) admits a unique solution $u(x) \in \mathcal{C}^4(\Omega) \cap \mathcal{C}^2(\overline{\Omega})$ (see, for e.g, [75]).

The outline of this chapter is as follows: Section 3.2 describes the conversion of the given fourth-order differential equation into a system of second-order ODEs. The stability of the continuous solution and its decomposition into its smooth and singu-

lar components, with their derivative bounds are also introduced here. An adaptively generated mesh is constructed by equidistributing the proposed monitor function at the end of this section. Section 3.3 outlines the numerical discretization of the transformed system of second-order ODEs and the stability of its discrete solution. The truncation error analysis for the smooth and singular components of the numerical solution are introduced in Section 3.4. The main result, the first-order parameter-uniform convergence of the numerical solution is obtained in this section, using the discrete supremum norm. Finally, Section 3.5 conducts the numerical experiments using an adaptive algorithm to show the effectiveness of the preferred monitor function.

3.2 Derivative Bounds and the Solution Decomposition

In this section, we transform the given BVP (3.1.1) into the following system of second-order differential equations

$$\boldsymbol{L}\boldsymbol{u}(x) = \boldsymbol{f}(x) \Leftrightarrow \begin{cases} L_1\boldsymbol{u}(x) \equiv -u_1''(x) - u_2(x) = 0, \quad x \in \Omega, \\ L_2\boldsymbol{u}(x) \equiv -\varepsilon u_2''(x) + c(x)u_1(x) + b(x)u_2(x) = f(x), \\ u_1(0) = p, \quad u_1(1) = q, \quad u_2(0) = r, \quad u_2(1) = s, \end{cases} \tag{3.2.1}$$

where $\boldsymbol{u}(x) = (u_1(x), u_2(x))^T$, $\boldsymbol{L} = (L_1,\ L_2)^T$ and $\boldsymbol{f}(x) = (0, f(x))^T$.

Now onwards, we consider only the system of equations (3.2.1). The following maximum principle for the solution of (3.2.1) is useful to prove the stability result of the exact solution $u(x)$ of (3.1.1).

Lemma 3.2.1. *Let $\boldsymbol{u}(x)$ be a smooth function satisfying (3.2.1). Assume $\boldsymbol{L}\boldsymbol{u}(x) \geq 0$ in Ω and $\boldsymbol{u}(0) \geq 0,\ \boldsymbol{u}(1) \geq 0$, then $\boldsymbol{u}(x) \geq 0$, for all $x \in \overline{\Omega}$.*

Proof. The proof of this lemma follows from [75]. ∎

An immediate consequence of the above maximum principle is the following stability estimate of the solution $\boldsymbol{u}(x)$.

Lemma 3.2.2. *[75] The solution $\boldsymbol{u}(x)$ of the boundary-value problem (3.2.1) satisfies*

$$\|\boldsymbol{u}\| \ \leq C \max\left\{\|\boldsymbol{u}(0)\|, \|\boldsymbol{u}(1)\|, \max_{x\in\overline{\Omega}} \|\boldsymbol{f}(x)\|\right\}, \quad \text{for all} \quad x \in \overline{\Omega}. \tag{3.2.2}$$

The next two lemmas provide the bounds for the continuous solution and its derivatives of (3.2.1).

Lemma 3.2.3. *The solution components of* $\boldsymbol{u}(x)$ *of* (3.2.1) *and its derivatives satisfy the following bounds for any prescribed* r,

$$|u_1^{(k)}(x)| \leq C\big(1+\varepsilon^{1-k/2}\mathcal{E}_\varepsilon(x)\big),$$

$$|u_2^{(k)}(x)| \leq C\big(1+\varepsilon^{-k/2}\mathcal{E}_\varepsilon(x)\big), \quad \textit{for } k=0,\cdots,r,$$

where $\mathcal{E}_\varepsilon(x) = \exp(-x\sqrt{\beta/\varepsilon}) + \exp(-(1-x)\sqrt{\beta/\varepsilon})$.

Proof. The proof of this lemma is given in [75]. ∎

We decompose the analytical solution $\boldsymbol{u}$ into two components, the smooth component $\boldsymbol{v}$ and the singular component $\boldsymbol{w}$ such that $\boldsymbol{u}=\boldsymbol{v}+\boldsymbol{w}$. Bounds for the smooth and singular components will be used for the convergence analysis. The following lemma provides the derivative bounds of the smooth component $\boldsymbol{v}$ and the singular component $\boldsymbol{w}$.

Lemma 3.2.4. *For the smooth component* $\boldsymbol{v}=(v_1,v_2)^T$ *satisfying*

$$\begin{cases} \boldsymbol{L}\boldsymbol{v}(x) = \boldsymbol{f}(x), \quad x\in\Omega, \\ \boldsymbol{v}(0) = (u_1(0),(f(0)-c(0)u_1(0))/b(0))^T, \quad \boldsymbol{v}(1) = (u_1(1),(f(1)-c(1)u_1(1))/b(1))^T, \end{cases}$$

and the singular component $\boldsymbol{w}=(w_1,w_2)^T$ *satisfying*

$$\begin{cases} \boldsymbol{L}\boldsymbol{w}(x) = 0, \quad x\in\Omega, \\ \boldsymbol{w}(0) = \boldsymbol{u}(0)-\boldsymbol{v}(0), \quad \boldsymbol{w}(1) = \boldsymbol{u}(1)-\boldsymbol{v}(1), \end{cases}$$

the following bounds hold true

$$|v_1^{(k)}(x)| \leq C, \quad |v_2^{(k)}(x)| \leq C(1+\varepsilon^{(2-k)/2}), \ \textit{for } k=0,\cdots,4, \tag{3.2.3}$$

and

$$|w_1(x)| \leq C, \ |w_1'(x)| \leq C\varepsilon,$$

$$|w_1^{(k)}(x)| \leq C\varepsilon^{1-k/2}\big(\exp(-x\sqrt{b(0)/\varepsilon}) + \exp(-(1-x)\sqrt{b(1)/\varepsilon})\big), \ \textit{for } k=2,3,4,$$

$$|w_2^{(k)}(x)| \leq C\varepsilon^{-k/2}\big(\exp(-x\sqrt{b(0)/\varepsilon}) + \exp(-(1-x)\sqrt{b(1)/\varepsilon})\big), \ \textit{for } k=0,\cdots,4. \tag{3.2.4}$$

Proof. To find the derivative bounds of the smooth component $\boldsymbol{v}(x)$ and the singular component $\boldsymbol{w}(x)$ of the solution $\boldsymbol{u}(x)$ of (3.2.1), the asymptotic expansion technique provided in Matthews et al. [54] will be used. For the smooth component $\boldsymbol{v}$, we use the

asymptotic expansion $\boldsymbol{v}(x) = \boldsymbol{v}_0(x) + \varepsilon \boldsymbol{v}_1(x)$, with $\boldsymbol{v}_1(0) = 0$ and $\boldsymbol{v}_1(1) = 0$. Hence the leading order term $\boldsymbol{v}_0(x)$ of $\boldsymbol{v}(x) = (\boldsymbol{v}_{01}(x) + \varepsilon \boldsymbol{v}_{11}(x), \boldsymbol{v}_{02}(x) + \varepsilon \boldsymbol{v}_{21}(x))^T$ satisfies

$$-v_{01}'' - v_{02} = 0, \quad \text{with} \quad v_{01}(0) = u_1(0), \quad v_{01}(1) = u_2(1),$$

$$c(x)v_{01} + b(x)v_{02}(x) = 0.$$

Following the method of proof given by Matthews et al. [54], we can obtain the derivative bounds in (3.2.3).

Now, for the singular component $\boldsymbol{w}(x)$, we shall decompose it as $\boldsymbol{w}(x) = \boldsymbol{w}^l(x) + \boldsymbol{w}^r(x)$ such that

$$\begin{cases} \boldsymbol{L}\boldsymbol{w}^l(x) = 0, \quad x \in \Omega, \\ \boldsymbol{w}^l(0) = \boldsymbol{w}(0), \quad \boldsymbol{w}^l(1) = 0, \end{cases} \quad \text{and} \quad \begin{cases} \boldsymbol{L}\boldsymbol{w}^r(x) = 0, \quad x \in \Omega, \\ \boldsymbol{w}^r(0) = 0, \quad \boldsymbol{w}^r(1) = \boldsymbol{w}(1). \end{cases}$$

Let us introduce the asymptotic expansions for the left-hand singular component $\boldsymbol{w}^l = (w_1^l, w_2^l)^T$ and the right-hand singular component $\boldsymbol{w}^r = (w_1^r, w_2^r)^T$ as

$$w_s^l(x) = w_{0s}^l(x) + \sqrt{\varepsilon} w_{1s}^l(x) + \varepsilon w_{2s}^l(x) + \cdots,$$

and

$$w_s^r(x) = w_{0s}^r(x) + \sqrt{\varepsilon} w_{1s}^r(x) + \varepsilon w_{2s}^r(x) + \cdots,$$

where $s = 1, 2$. To find the derivative bounds of $\boldsymbol{w}^l$, we shall use the transformation $\xi = x/\sqrt{\varepsilon}$. Using the Taylor series expansions of $b(\xi\sqrt{\varepsilon})$ and $c(\xi\sqrt{\varepsilon})$, comparing the orders of ε terms, it is easy to obtain that $\boldsymbol{w}^l(\xi)$ satisfies

$$w_{01}^l = 0,$$

$$\hat{L} w_{02}^l(\xi) = 0, \; w_{02}^l(0) = r - v_{02}(0) \text{ with } \lim_{\xi \to \infty} w_{02}^l(\xi) = 0, \text{ where } \hat{L} \equiv -\frac{d^2}{d\xi^2} + b(0)I,$$

and so on. In a similar way, $\boldsymbol{w}^r(\xi)$ satisfies

$$w_{01}^r = 0,$$

$$\hat{L} w_{02}^r(\xi) = 0, \quad w_{02}^r(1) = s - v_{02}(1), \text{ with } \lim_{\xi \to -\infty} w_{02}^l(\xi) = 0,$$

and so on. Therefore, from [75] and [54], we have $|w_1^l(x)| < C, |w_2^l(0)| < C$, $|w_2^l(1)| < C\exp(-b(0)/\varepsilon)$ and $|w_2^{l\,(p)}(x)| \leq C\varepsilon^{-p/2} \exp\left(-x\sqrt{\dfrac{b(0)}{\varepsilon}}\right)$. By a similar way, using the asymptotic expansion technique and Lemma 3.2.3, we can obtain the other derivative bounds including the bounds of the right-hand side of the boundary layer. This completes the proof of this lemma. ∎

Lemma 3.2.5. *Let the zeroth-order asymptotic expansion of the solution* $\boldsymbol{u}$ *be defined as* $\boldsymbol{u}_{as} = \boldsymbol{v}_0 + \boldsymbol{w}_0$, *then the following estimate holds true*

$$\|\boldsymbol{u} - \boldsymbol{u}_{as}\| \leq C\sqrt{\varepsilon}.$$

Proof. The proof of this lemma is given by Shanthi and Ramanujam [75]. ∎

From now onwards, we shall concentrate only on the zeroth-order expansion as $0 < \varepsilon \ll 1$. In reality, *apriori* analysis of the solution behavior suggests that the boundary layer phenomena occurs from the singular component of the solution. It is easy to observe that the second equation of $\boldsymbol{L}$ is only having the perturbation parameter. Therefore, we shall consider the monitor function as

$$M(x, \boldsymbol{u}(x)) = \alpha + |w_2''(x)|^{1/2}, \tag{3.2.5}$$

involving the second-order derivative of the singular component w_2 of the solution u_2 of (3.2.1). Here, α is a positive constant to be defined later.

To approximate $w_2''(x)$, we use the leading order expansion of $\boldsymbol{w}(x)$ from Lemma 3.2.4, which implies that

$$w_2''(x) \approx \begin{cases} \kappa_1 b(0)\varepsilon^{-1} \exp\left(-x\sqrt{\dfrac{b(0)}{\varepsilon}}\right), & x \in [0, 1/2], \\ \kappa_2 b(1)\varepsilon^{-1} \exp\left(-(1-x)\sqrt{\dfrac{b(1)}{\varepsilon}}\right), & x \in (1/2, 1], \end{cases}$$

where

$$\kappa_1 = -(r - v_{02}(0)), \quad \text{and} \quad \kappa_2 = -(s - v_{02}(1)).$$

Hence, we have

$$\int_0^1 |w_2''(x)|^{1/2} dx \equiv K \approx 2[|\kappa_1|^{1/2} + |\kappa_2|^{1/2}].$$

It is easy to observe that substitution of the approximate value of $w_2''(x)$ in the equidistribution principle (1.1.5) will lead to the algebraic equations of the form (2.2.4) and (2.2.5) obtained in Chapter 2 . Hence, the final adaptively generated equidistributed meshes x_i, will satisfy both the nonlinear algebraic equations (2.2.4) and (2.2.5). Therefore, Lemmas 2.2.3 and 2.2.4 can be used to overview the structure of the mesh distribution and for the choice of α.

The following lemma provides upper bounds of the mesh spacings throughout the domain.

Lemma 3.2.6. *The mesh widths generated by the equidistribution of monitor function (3.2.5) satisfies*

$$h_i \leq CN^{-1}, \text{ for } i = 1, \cdots, N.$$

Proof. It is clear that the monitor function (3.2.5) satisfies $M(x, \boldsymbol{u}(x)) \geq \alpha = K$. Again, the derivative estimates from Lemma 3.2.4 imply $\int_0^1 M(x, \boldsymbol{u}(x))dx \leq C_1$. Therefore, from the definition of equidistribution principle (1.1.4), we have

$$\alpha h_i \leq \int_{x_{i-1}}^{x_i} M(x, \boldsymbol{u}(x))dx = \frac{1}{N}\int_0^1 M(x, \boldsymbol{u}(x))dx \leq C_1 N^{-1} \Rightarrow h_i \leq C_1 \alpha^{-1} N^{-1}.$$

This implies that

$$h_i \leq CN^{-1}.$$

■

3.3 Discretized Problem

This section is devoted for the discretization of the continuous problem (3.2.1) and the stability analysis of the discrete operator.

3.3.1 Finite difference discretization

The classical finite difference approximations on the nonuniform mesh Ω^N will be considered to discretize the continuous problem (3.2.1). The discretized problem corresponding to the continuous operator (3.2.1) is defined as to find $\boldsymbol{U} = (U_1, U_2)^T$ satisfying

$$\boldsymbol{L}^N \boldsymbol{U}_i = \boldsymbol{f}_i \Leftrightarrow \begin{cases} L_1^N \boldsymbol{U}_i \equiv -\delta^2 U_{1,i} - U_{2,i} = 0, \\ L_2^N \boldsymbol{U}_i \equiv -\varepsilon\delta^2 U_{2,i} + c_i U_{1,i} + b_i U_{2,i} = f_i, \quad i = 1, \cdots, N-1, \\ U_{1,0} = p, \quad U_{1,N} = q, \quad U_{2,0} = r, \quad U_{2,N} = s, \end{cases} \tag{3.3.1}$$

where $\boldsymbol{L}^N = (L_1^N, L_2^N)^T$ is the discrete operator corresponding to the continuous operator $\boldsymbol{L}$ and $\boldsymbol{f}_i = (0, f_i)^T$. By solving the system of linear algebraic equations in (3.3.1), we obtain the approximate solution $\boldsymbol{U}$ of $\boldsymbol{u}(x)$ at the nodal points $x_0, x_1, \cdots, x_N$.

The discrete operator $\boldsymbol{L}^N$ satisfies the following comparison principle. As a consequence, we get a stable discrete solution.

Lemma 3.3.1. *Let $(\mathbf{Z}_0, \cdots, \mathbf{Z}_N)$ be a mesh function for the discrete solution $\boldsymbol{Z}$, which has two components Z_1 and Z_2, with $\mathbf{Z}_0 \geq 0$, $\mathbf{Z}_N \geq 0$. Now assume that $(\boldsymbol{L}^N \mathbf{Z})_i \geq 0$, for $i = 1, \cdots, N-1$. Then $\mathbf{Z}_i \geq 0$, for all $i = 0, \cdots, N$.*

Proof. Let us define

$$\gamma = \max\left\{ \max_i\big(-Z_{1,i}\big), \quad \max_i\big(-Z_{2,i}\big) \right\}.$$

Now assume that our conclusion is not true. Then $\gamma > 0$ and also

$$Z_{1,i} + \gamma \geq 0, \quad Z_{2,i} + \gamma \geq 0, \text{ for } i = 0, \cdots, N.$$

Case 1: Let $Z_{1,i} + \gamma = 0$, for some $i = k$. Then for $\boldsymbol{S} = (1,1)^T$, we have

$$\begin{aligned} 0 &< (L_1^N(\boldsymbol{Z} + \gamma \boldsymbol{S}))_k \\ &= -\delta^2(Z_{1,k} + \gamma) - (Z_{2,k} + \gamma) \\ &< 0, \end{aligned}$$

which is a contradiction.

Case 2: Now let $Z_{2,i} + \gamma = 0$, for some $i = k$. Then

$$\begin{aligned} 0 &< (L_2^N(\boldsymbol{Z} + \gamma \boldsymbol{S}))_k \\ &= -\varepsilon\delta^2(Z_{2,k} + \gamma) + c_k(Z_{1,k} + \gamma) + b_k(Z_{2,k} + \gamma) \\ &< 0, \end{aligned}$$

which is a contradiction, follows from $c_k < 0$. Hence the result follows. ∎

An immediate consequence of the discrete maximum principle is the following discrete stability result.

Lemma 3.3.2. *If $\boldsymbol{U}_i = (U_{1,i}, U_{2,i})$, $0 \le i \le N$ is any discrete mesh function satisfying the problem (3.3.1), then*

$$\|\boldsymbol{U}\| \le C \max\{\|\boldsymbol{U}_0\|, \|\boldsymbol{U}_N\|, \|\boldsymbol{L}^N \boldsymbol{U}_i\|\}. \tag{3.3.2}$$

Proof. The proof of this lemma can be seen in Shanthi and Ramanujam [75]. ∎

3.4 Error Analysis

This section studies the ε-uniform convergence of the discrete solution for the problem (3.3.1). For the error analysis, we decompose the corresponding numerical solution $\boldsymbol{U}$, by its smooth and singular components $\boldsymbol{V}$ and $\boldsymbol{W}$ respectively, *i.e.,* $\boldsymbol{U} = \boldsymbol{V} + \boldsymbol{W}$ satisfying

$$\begin{cases} \boldsymbol{L}^N \boldsymbol{V}_i = \boldsymbol{f}_i, & i = 1, \cdots, N-1, \\ \boldsymbol{V}_0 = \boldsymbol{v}(0), \quad \boldsymbol{V}_N = \boldsymbol{v}(1), \end{cases}$$

and

$$\begin{cases} \boldsymbol{L}^N \boldsymbol{W}_i = 0, & i = 1, \cdots, N-1, \\ \boldsymbol{W}_0 = \boldsymbol{w}(0), \quad \boldsymbol{W}_N = \boldsymbol{w}(1). \end{cases}$$

The error of the numerical solution $\boldsymbol{U}$ is examined by separately analyzing the errors of the smooth component $\boldsymbol{V}$ and the singular component $\boldsymbol{W}$ in the region Ω^N, *i.e.,* from the inequality

$$||\boldsymbol{U}_i - \boldsymbol{u}(x_i)|| \le ||\boldsymbol{V}_i - \boldsymbol{v}(x_i)|| + ||\boldsymbol{W}_i - \boldsymbol{w}(x_i)||. \tag{3.4.1}$$

To carry out the error analysis, a similar argument provided in Beckett and Mackenzie [9] will be used. For the smooth component $\boldsymbol{V}$, we have from Lemma 3.2.3 and Lemma 3.2.6,

$$|L_1^N(\boldsymbol{V}-\boldsymbol{v})(x_i)| = |(L_1 - L_1^N)\boldsymbol{v}(x_i)| \leq C(h_i + h_{i+1})||v_1'''(x)||_{(x_{i-1},x_{i+1})} \leq CN^{-1},$$

and

$$|L_2^N(\boldsymbol{V}-\boldsymbol{v})(x_i)| = |(L_2 - L_2^N)\boldsymbol{v}(x_i)| \leq C\varepsilon(h_i + h_{i+1})||v_2'''(x)||_{(x_{i-1},x_{i+1})} \leq CN^{-2},$$

since $\sqrt{\varepsilon} \ll N^{-1}$. Hence, we have

$$||\boldsymbol{L}^N(\boldsymbol{V}-\boldsymbol{v})(x_i)|| \leq CN^{-1}. \tag{3.4.2}$$

Now we analyze the error of the singular component for $i = k_l, \cdots, k_r$. The error of the singular component $\boldsymbol{W}$ satisfies

$$|L_1^N(\boldsymbol{W}-\boldsymbol{w})(x_i)| \leq C|(\delta^2 w_1 - w_1'')(x_i)| \leq C|w_1''(x)|_{[x_{i-1},x_{i+1}]},$$

$$|L_2^N(\boldsymbol{W}-\boldsymbol{w})(x_i)| \leq C\varepsilon|(\delta^2 w_2 - w_2'')(x_i)| \leq C\varepsilon|w_2''(x)|_{[x_{i-1},x_{i+1}]}.$$

Hence, the derivative bounds of $\boldsymbol{v}$, $\boldsymbol{w}$ from Lemma 3.2.4 imply that

$$||\boldsymbol{L}^N(\boldsymbol{W}-\boldsymbol{w})(x_i)|| \leq C \begin{cases} \exp\left(-x_{i-1}\sqrt{\dfrac{b(0)}{\varepsilon}}\right), & x_i \leq 1/2, \\ \exp\left(-(1-x_{i+1})\sqrt{\dfrac{b(1)}{\varepsilon}}\right), & x_i > 1/2. \end{cases}$$

By using Lemma 2.2.3 for $x_i \geq 1/2$ with $k_l \leq i$, we get

$$||\boldsymbol{L}^N(\boldsymbol{W}-\boldsymbol{w})(x_i)|| \leq C\exp\left(-x_{k_l-1}\sqrt{\frac{b(0)}{\varepsilon}}\right) = C\left(\exp\left(-\frac{x_{k_l-1}}{2}\sqrt{\frac{b(0)}{\varepsilon}}\right)\right)^2 \leq CN^{-2}.$$

In a similar manner, the case $x_i > 1/2$ with $k_r \geq i$ can be carried out. Hence for $i = k_l, \cdots, k_r$,

$$||\boldsymbol{L}^N(\boldsymbol{W}-\boldsymbol{w})(x_i)|| \leq CN^{-2}. \tag{3.4.3}$$

Now, let us consider the truncation error estimate for $i = 1, \cdots, k_l - 1$ and $i = k_r + 1, \cdots, N-1$. It is enough to consider only the left-hand part of the boundary layer regions as the right-hand part of the boundary layers can be derived in an analogous manner. A direct calculation by using Taylor's series expansion shows that

$$|L_2^N(\boldsymbol{W}-\boldsymbol{w})(x_i)| = \frac{\varepsilon|h_i^2 w_2'''(\xi_i^1) - h_{i+1}^2 w_2'''(\xi_i^2)|}{3(h_i + h_{i+1})},$$

where $\xi_i^1 \in (x_{i-1}, x_i)$ and $\xi_i^2 \in (x_i, x_{i+1})$. Again

$$|h_i^2 w_2'''(\xi_i^1) - h_{i+1}^2 w_2'''(\xi_i^2)| \leq C(|h_i^2 - h_{i+1}^2||w_2'''(x_i)| + h_i^2(h_i + h_{i+1})|w_2^{(iv)}(x_i)|).$$

This inequality will be satisfied by the truncation error estimate obtained from $|L_1^N(\boldsymbol{W}-\boldsymbol{w})(x_i)|$. Hence an application of Lemma 2.2.4 gives

$$\begin{aligned}
||\boldsymbol{L}^N(\boldsymbol{W}-\boldsymbol{w})(x_i)|| &\leq C\varepsilon^{-1}h_i^2 \exp\left(-x_i\sqrt{\frac{b(0)}{\varepsilon}}\right) \\
&\leq C\varepsilon^{-1}\left(\int_{x_{i-1}}^{x_i} \exp\left(-\frac{t}{2}\sqrt{\frac{b(0)}{\varepsilon}}\right)dt\right)^2 \\
&\leq C\varepsilon^{-1}\left(\sqrt{\varepsilon}\int_{x_{i-1}}^{x_i} M(x,\boldsymbol{u}(x))dt\right)^2 \\
&\leq CK^2N^{-2} \leq CN^{-2}.
\end{aligned}$$

Therefore, for $i = 1, \cdots, k_l - 1$ and $i = k_r + 1, \cdots, N-1$, we have

$$||\boldsymbol{L}^N(\boldsymbol{W}-\boldsymbol{w})(x_i)|| \leq CN^{-2}. \tag{3.4.4}$$

This completes the proof. ∎

Combining the above error estimates for the smooth component $\boldsymbol{V}(x_i)$ and the singular component $\boldsymbol{W}(x_i)$, we can obtain the main convergence result for the computed solution $\boldsymbol{U}(x_i)$.

3.4.1 The main convergence result

We now state the main theorem of this chapter. The following theorem shows that the method (3.3.1) is uniformly first-order convergent on the equidistributed mesh.

Theorem 3.4.1. *Let $\boldsymbol{u}$ be the solution of (3.2.1) and $\boldsymbol{U}$ be the solution of the discrete operator (3.3.1), on a mesh obtained by equidistributing the monitor function (3.2.5) with $\alpha = K$. Then, there exists a constant C, independent of ε and N, such that*

$$||\boldsymbol{u} - \boldsymbol{U}||_{\Omega^N} \leq CN^{-1}.$$

Proof. Lemma 3.3.2 implies that the inverse of the discrete operator $\boldsymbol{L}^N$ corresponding to the continuous operator $\boldsymbol{L}$ is ε-uniformly bounded. By using the triangle inequality (3.4.1), from (3.4.2)-(3.4.4) we obtain that

$$||\boldsymbol{u}(x_i) - \boldsymbol{U}_i|| \leq ||\boldsymbol{V}_i - \boldsymbol{v}(x_i)|| + ||\boldsymbol{W}_i - \boldsymbol{w}(x_i)|| \leq CN^{-1} \text{ for } i = 0, \cdots, N.$$ ∎

It should be noted that the solution component u_1 of the solution $\boldsymbol{u}(x) = (u_1, u_2)^T$ of (3.2.1) is the original solution of the problem (3.1.1). Hence, we actually obtained a uniformly convergent numerical solution U_1 of problem (3.1.1) from (3.3.1).

The above analysis shows that the discrete solution the corresponding to the continuous solution is ε-uniformly convergent at all the equidistributed meshes. In fact, the following theorem shows that the uniformly convergent numerical solution U_1 can be extended to the whole domain $\overline{\Omega}$ using the piecewise linear interpolation.

Theorem 3.4.2. *If the numerical solution $\boldsymbol{U}$ uniformly converges to the exact solution $\boldsymbol{u}$ of the problem (3.2.1) at all mesh points, then we have the following global ε-uniform error estimate:*

$$||\overline{\boldsymbol{U}} - \boldsymbol{u}|| \leq CN^{-1},$$

for problem (3.3.1), where $\overline{\boldsymbol{U}}$ is the piecewise linear interpolant of $\boldsymbol{U}$ on $\overline{\Omega}^N$.

Proof. Using the triangle inequality, we get

$$||\overline{\boldsymbol{U}} - \boldsymbol{u}|| \leq ||\overline{\boldsymbol{U}} - \overline{\boldsymbol{u}}|| + ||\overline{\boldsymbol{u}} - \boldsymbol{u}||,$$

where $\overline{\boldsymbol{u}}$ is the piecewise linear interpolant of $\boldsymbol{u}$ at the mesh points. Then, the above result can be easily obtained by following the technique provided in [9]. ∎

3.5 Numerical Results

This section computationally verifies the theoretical results obtained in the previous section. Here, we provide two numerical examples where the mesh is equidistributed by the monitor function (3.2.5).

Example 3.5.1. *Consider the following fourth-order BVP:*

$$\begin{cases} -\varepsilon u^{iv}(x) + (6 - x^2)u''(x) + 2u(x) = -(10x + 1), \quad x \in \Omega, \\ u(0) = 1, \quad u(1) = 1, \quad u''(0) = -1, \quad u''(1) = -1. \end{cases} \tag{3.5.1}$$

Example 3.5.2. *Consider the two-point BVP:*

$$\begin{cases} -\varepsilon u^{iv}(x) + 5\exp(1 - x)u''(x) + (1 + x^3)u(x) = -2\exp(x), \quad x \in \Omega, \\ u(0) = 1, \quad u(1) = 1, \quad u''(0) = -1, \quad u''(1) = -1. \end{cases} \tag{3.5.2}$$

Exact solution for these examples are not available. So the accuracy of its numerical solution will be computed by using the double mesh principle as described in Chapter 2. The generation of the adaptive finite difference solution requires two steps; firstly the equidistributed mesh has to be determined by a mesh generation algorithm and thereafter, the finite difference solution has to be computed on that mesh. For the numerical experiments of these problems, we take ε from the set

$$S = \{\varepsilon | \varepsilon = 1, 2^{-2}, \cdots, 2^{-30}\},$$

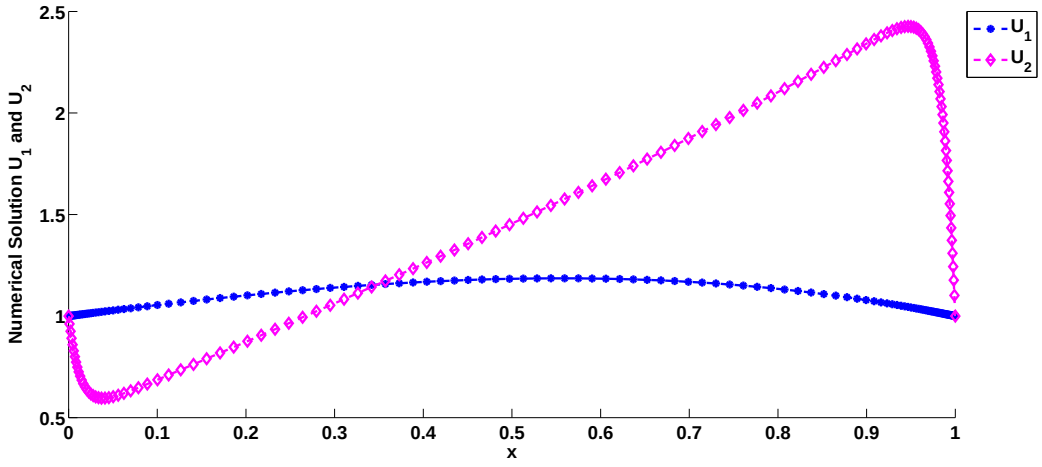

Figure 3.1: *Numerical solutions U_1 and U_2 (for u_1 and $u_2(= -u_1'')$) for $N = 128$ and $\varepsilon = 2^{-10}$ for Example 3.5.1.*

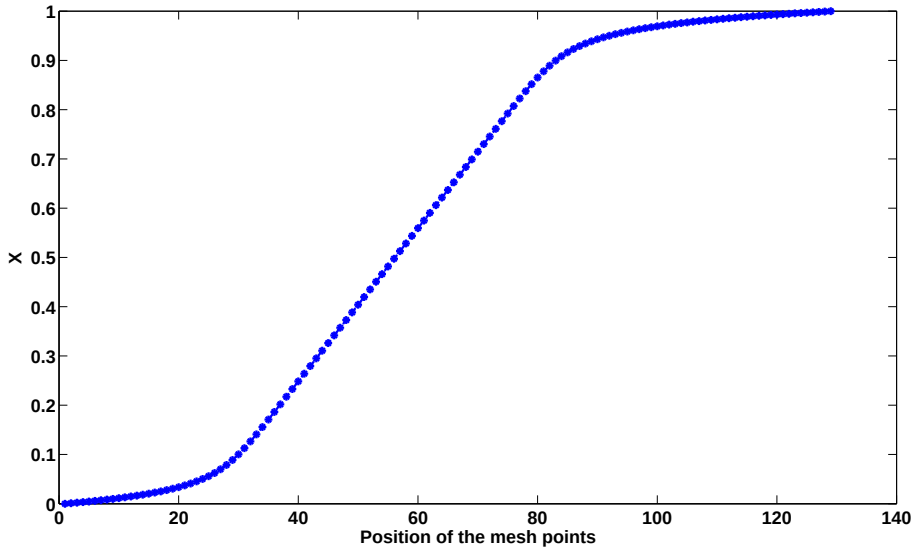

Figure 3.2: *Mesh density towards the boundary layers for $N = 128$ and $\varepsilon = 2^{-10}$ for Example 3.5.1.*

Table 3.1: *Uniform errors and orders of convergence of the numerical solution for Example 3.5.1.*

$\varepsilon \in S$	Number of intervals N						
	64	128	256	512	1024	2048	4096
E^N	2.5352e-5	6.3728e-6	1.5948e-6	3.9877e-7	9.9691e-8	2.4920e-8	6.2277e-9
r^N	1.9921	1.9986	1.9997	2.0000	2.0002	2.0005	-

Table 3.2: *Uniform errors and orders of convergence of the solutions second-order derivative approximation for Example 3.5.1.*

$\varepsilon \in S$	Number of intervals N						
	64	128	256	512	1024	2048	4096
E^N	1.0393e-3	2.4878e-4	6.0628e-5	1.4973e-5	3.7128e-6	9.2333e-7	2.3051e-7
r^N	2.0627	2.0368	2.0176	2.0118	2.0076	2.0020	-

and the adaptively generated mesh is constructed using the constant $C_0 = 1.2$, in the adaptive algorithm described as in Chapter 2.

The maximum ε-uniform errors E^N and the corresponding orders of convergence r^N of the computed solution U are displayed in Table 3.1 for Example 3.5.1. It should be noted that, we reduce both Examples 3.5.1 and 3.5.2 to the system of differential equations of the form (3.2.1), for obtaining the numerical solution. Hence, we demonstrate the uniform errors and orders of convergence for the double derivatives of the solution $u(x)$ in Table 3.2. One can see that the rate of convergence of the computed solution for this problem is almost two. This shows that the first-order convergence of the smooth component is not producing enough difference to the convergence of the solution. This is because that the convergence of the singular component of the solution is exactly two. The computed solution plot shown in Figure 3.1 suggests that the boundary layers appearing in the solution are not so steep, whereas its double derivative has steep boundary layers for this problem. The density of the adaptively generated final mesh towards the boundary layers, can be observed from Figure 3.2, which shows the effec-

Table 3.3: *Uniform errors and orders of convergence of the numerical solution for Example 3.5.2.*

$\varepsilon \in S$	Number of intervals N						
	64	128	256	512	1024	2048	4096
E^N	1.8627e-5	4.6700e-6	1.1877e-6	3.0296e-7	7.5970e-8	1.9042e-8	4.7872e-9
r^N	1.9959	1.9753	1.9709	1.9956	1.9963	1.9919	-

Table 3.4: *Uniform errors and orders of convergence of the solutions second-order derivative approximation for Example 3.5.2.*

$\varepsilon \in S$	Number of intervals N						
	64	128	256	512	1024	2048	4096
E^N	6.5799e-4	1.6165e-4	3.9048e-5	9.5836e-6	2.3783e-6	5.9454e-7	1.4835e-7
r^N	2.0252	2.0496	2.0266	2.0107	2.0001	2.0028	-

tiveness of our preferred monitor function. Both the figures are drawn with the number of mesh intervals $N = 128$ and the perturbation parameter $\varepsilon = 2^{-10}$. Tables 3.3 and 3.4 corresponding to the Example 3.5.2 observed a similar behavior as like Example 3.5.1.

3.6 Conclusion

A parameter-uniform numerical scheme for a class of fourth-order ODE is presented in this chapter. To solve the ODE, we reduce the problem into a system of ODEs. An adaptively generated nonuniform mesh is constructed by equidistributing a monitor function involving the second-order derivative of the singular component of the solution. The adaptive mesh obtained via the equidistribution does not require any *apriori* information about the location of the boundary layer and its width. It is shown that the standard central difference approximation on this mesh produces first-order ε-uniform convergence. Numerical experiments show that the proposed monitor function can be successfully applied to the fourth-order ODEs of the form (3.1.1) to get parameter-uniform convergence, which supports the theoretical result.

Chapter 4

Apriori Error Estimate for Singularly Perturbed System of Reaction-Diffusion Boundary-Value Problems

This chapter studies the problem of determining an appropriate grading of a mesh for a system of coupled singularly perturbed reaction-diffusion ODEs having diffusion parameters of different magnitudes. These small parameters give rise to boundary layers. The central difference scheme on adaptively generated mesh is used to discretize the problem where the mesh equations are derived using an equidistribution principle. A suitable *apriori* monitor function is obtained in the error estimate which will lead to parameter-uniform convergence. Utilizing this monitor function, it is shown that the method converges uniformly in the discrete supremum norm for linear and semilinear system of reaction-diffusion BVPs.

4.1 Introduction

Consider the following system of singularly perturbed reaction-diffusion boundary-value problems

$$\begin{cases} \mathbb{L}\boldsymbol{u}(x) \equiv -\boldsymbol{Eps}\ \boldsymbol{u}''(x) + \ \boldsymbol{B}(x)\boldsymbol{u}(x) = \boldsymbol{f}(x), \quad x \in \Omega, \\ \\ \boldsymbol{u}(0) = \boldsymbol{u}(1) = \boldsymbol{0}, \end{cases} \tag{4.1.1}$$

where $\mathbb{L} = (\mathbb{L}_1, \cdots, \mathbb{L}_k)^T$, $\boldsymbol{Eps} = \text{diag}(\varepsilon_1, \varepsilon_2, \cdots, \varepsilon_k)$, $\boldsymbol{B}(x) = (b_{ij}(x))_{k\times k}$, $\boldsymbol{f}(x) = (f_1(x), f_2(x), \cdots, f_k(x))^T$ and $\boldsymbol{u}(x) = (u_1(x), \cdots, u_k(x))^T$.

Assume that the matrix $\boldsymbol{B} = (b_{ij})_{i,j=1}^k$ is an L_0-matrix (*i.e.,* off-diagonal entries are nonpositive and diagonal entries are positive) with

$$\min_{x\in\overline{\Omega}; m=1,\cdots,k} \left\{ \sum_{j=1}^{k} b_{mj}(x) \right\} \geq \beta > 0. \tag{4.1.2}$$

It will be assumed that the entries of the coefficient matrix $\boldsymbol{B}(x)$ and the vector $\boldsymbol{f}(x)$, *i.e.,* $b_{ij}(x), f_i(x)$ are in $\mathcal{C}^3(\Omega)$ for $i, j = 1, \cdots, k$.

The outline of this chapter is as follows: Section 4.2 relates the analytical solution bound for the system of equations with the scalar reaction-diffusion problems and provides a stability bound for the solution of (4.1.1). Then, in Section 4.3 the discretization of (4.1.1) is described with the discrete stability bound of the numerical solution. Further, an heuristic argument is provided to obtain a suitable monitor function through *apriori* error analysis, which can be equidistributed to achieve proper layer-adapted mesh. A system of semilinear reaction-diffusion problem is introduced in Section 4.4. For numerical experiments, an adaptive algorithm is used in Section 4.5 to show that the rate of convergence predicted by our analysis holds true in practice. Finally in Section 4.6, we provide a concise conclusion.

4.2 Continuous Problem

In this section, the stability property of the analytical solution $\boldsymbol{u}(x)$ of (4.1.1) is discussed. We start by recalling the stability of the scalar operator, which is used to derive the stability of the solution $\boldsymbol{u}(x)$. The following lemma (see for *e.g.,* [44]) provides the stability estimate of general scalar operator.

Lemma 4.2.1. *Suppose the coefficients of the following reaction-diffusion problem*

$$\begin{cases} \hat{L}v \equiv -\varepsilon v''(x) + b(x)v(x) = f(x), \ \text{for } x \in \Omega, \\ \\ v(0) = 0, \quad v(1) = 0, \end{cases} \tag{4.2.1}$$

are such that $b(x), f(x) \in \mathcal{C}^2(\Omega)$ *with* $\varepsilon > 0, b(x) \geq \beta > 0$ *for all* $x \in \overline{\Omega}$. *Then, for any* $v \in \mathcal{C}^2(\Omega) \cap \mathcal{C}(\overline{\Omega})$, *the following stability estimate holds true*

$$||v|| \leq \left|\left|\frac{f}{b}\right|\right|.$$

Now, the stability for the components of the solution $\boldsymbol{u}(x)$ will be discussed with the help of the above lemma.

Lemma 4.2.2. *Let* $\boldsymbol{u}$ *be the solution of (4.1.1) and assume the coupling matrix* $\boldsymbol{B}$ *satisfy the* L_0*-matrix condition (4.1.2). Then*

$$||u_m|| \leq \sum_{l=1}^{k} (\Upsilon^{-1})_{ml} \left|\left|\frac{f_l}{b_{ll}}\right|\right|,$$

where the $k \times k$ *matrix* $\Upsilon = \Upsilon(\boldsymbol{B}) = (\gamma_{ml})_{k\times k}$ *is such that*

$$\gamma_{ml} = -\left|\left|\frac{b_{ml}}{b_{mm}}\right|\right|, \ \text{for } m \neq l \ \text{and } \gamma_{mm} = 1.$$

Proof. An equation from the system (4.1.1) can be written as

$$-\varepsilon_m u_m'' + b_{mm}u_m = f_m - \sum_{l=1,l\neq m}^{k} b_{ml}u_l, \quad \text{for } m = 1, \cdots, k. \tag{4.2.2}$$

From the definition of L_0-matrix, Lemma 4.2.1 yields

$$||u_m|| - \sum_{l=1,l\neq m}^{k} \left\| \frac{b_{ml}}{b_{mm}} \right\| ||u_l|| \leq \left\| \frac{f_m}{b_{mm}} \right\|, \quad m = 1, \cdots, k.$$

Now, if the matrix Υ is assumed to be inverse monotone *i.e.,* $\Upsilon^{-1} \geq 0$, then

$$||u_m|| + \sum_{l=1,l\neq m}^{k} \gamma_{ml}||u_l|| \leq \left\| \frac{f_m}{b_{mm}} \right\|, \quad m = 1, \cdots, k.$$

The matrix $\boldsymbol{B}$ is assumed to be an L_0-matrix from (4.1.2). So Υ will be inverse monotone. Hence, we can write

$$||u_m|| \leq \sum_{l=1}^{k} (\Upsilon^{-1})_{ml} \left\| \frac{f_l}{b_{ll}} \right\|,$$

from which the desired result follows. ∎

As a consequence, the stability of the continuous solution $\boldsymbol{u}(x)$ can be obtained. The above technique will also be used for the error analysis. It should be noted that one can directly compute the inverse of the matrix Υ from the definition of Υ. Its sign pattern for the condition of inverse monotonicity can also be checked. Therefore, to get the stable solution of (4.1.1), the L_0-matrix condition is not necessary for the matrix $\boldsymbol{B}$.

4.3 Finite Difference Scheme

This section is devoted for the discretization of the continuous problem (4.1.1). Monitor function generated by the error analysis is also derived in this section, which will lead to the uniform convergence.

Here, we shall consider the standard finite difference approximation on a nonuniform mesh $\Omega^N \equiv \{0 = x_0 < x_1 < \cdots < x_N = 1\}$, where the step sizes are defined by $h_{i+1} = x_{i+1} - x_i,\ i = 0, \cdots, N-1$. Let us define $\boldsymbol{U}$ as the discrete approximation of the continuous solution $\boldsymbol{u}(x)$. Therefore, by denoting $\boldsymbol{U}_i = \boldsymbol{U}(x_i)$, the discretized problem of (4.1.1) is defined as follows: Find $\boldsymbol{U}_1, \cdots, \boldsymbol{U}_{N-1}$ satisfying

$$\begin{cases} (\mathbb{L}^N \boldsymbol{U})_i \equiv -\boldsymbol{Eps}\ (\delta^2 \boldsymbol{U})_i + \boldsymbol{B}_i \boldsymbol{U}_i = \boldsymbol{f}_i, \quad i = 1, \cdots, N-1, \\ \boldsymbol{U}_0 = 0, \quad \boldsymbol{U}_N = 0, \end{cases} \tag{4.3.1}$$

where $(\mathbb{L}^N \boldsymbol{U})_i = ((\mathbb{L}_1^N \boldsymbol{U})_i, \cdots, (\mathbb{L}_k^N \boldsymbol{U})_i)^T$ with $(\mathbb{L}_m^N \boldsymbol{U})_i = -\varepsilon_m \delta^2 U_{m,i} + \sum_{j=1}^{k} b_{mj,i} U_{m,i}$ and $\boldsymbol{f}_i = (f_{1,i}, \cdots, f_{k,i})^T$. The discrete operator $\mathbb{L}^N$ in (4.3.1) corresponding to the continuous operator $\mathbb{L}$ in (4.1.1) satisfies the following comparison principle. As a consequence, we get a stable discrete solution.

Lemma 4.3.1. *If two mesh functions $\boldsymbol{V}$ and $\boldsymbol{W}$, where $\mathbf{V}_i = (V_{1,i}, \cdots, V_{k,i})$ and $\mathbf{W}_i = (W_{1,i}, \cdots, W_{k,i})$ satisfy $(\mathbb{L}^N \boldsymbol{V})_i \geq (\mathbb{L}^N \boldsymbol{W})_i$, for $i = 1, \cdots, N-1$, with $\boldsymbol{V}_0 \geq \boldsymbol{W}_0$ and $\boldsymbol{V}_N \geq \boldsymbol{W}_N$, then $\boldsymbol{V}_i \geq \boldsymbol{W}_i$, for $i = 1, \cdots, N-1$.*

Proof. It is easy to see that the matrix associated with the discrete operator $\boldsymbol{L}^N$ is an M-matrix. Hence the required result follows. ∎

To carry out the error analysis of the discrete solution $\boldsymbol{U}$ of (4.3.1), we shall take the help of the stability result for the discretized scalar equation of (4.2.1). Define the difference operator corresponding to the scalar equation (4.2.1) as

$$\begin{cases} (\hat{L}^N v)_i \equiv -\varepsilon[\delta^2 v]_i + b_i v_i = f_i, \text{ for } i = 1, \cdots, N-1, \\ \\ v_0 = v_N = 0. \end{cases} \tag{4.3.2}$$

The scalar difference operator (4.3.2) satisfies the following discrete maximum principle.

Lemma 4.3.2. *If the mesh function v_i satisfies $v_0 \geq 0$, $v_N \geq 0$ with $\hat{L}^N v_i \geq 0$. Then $v_i \geq 0$.*

Proof. Let us assume that $v_p = \min_i v_i$ for some p, such that $v_p < 0$. Then from (4.3.2),

$$(\hat{L}^N v)_p = -\frac{\varepsilon}{\hbar_p}\left(\frac{v_{p+1} - v_p}{h_p} - \frac{v_p - v_{p-1}}{h_{p-1}}\right) + b_p v_p < 0,$$

which is a contradiction. Hence the result follows. ∎

As a consequence of the above lemma, the following stability estimate for the scalar operator can be achieved.

Lemma 4.3.3. *If the mesh function v_i satisfies (4.3.2), then*

$$||v||_{\Omega^N} \leq \left|\left|\frac{\hat{L}^N v}{b}\right|\right|_{\Omega^N}.$$

Proof. Taking the barrier function $\Phi_i^{\pm} = \max_i \left|(\hat{L}^N v_i)/b_i\right| \pm v_i$, it is easy to observe that $\Phi_0^{\pm} = \Phi_N^{\pm} = 0$ and $\hat{L}^N \Phi_i^{\pm} \geq 0$ from the assumption $b(x) \geq \beta$. Hence the above maximum principle implies that $\Phi_i^{\pm} \geq 0$ for $i = 0(1)N$. Therefore, we have $|v_i| \leq \max_i \left|(\hat{L}^N v_i)/b_i\right|$, from which the required result follows. ∎

In other words, the discrete maximum principle implies that

$$||v||_{\Omega^N} \leq \frac{||f||_{\infty}}{\beta}. \tag{4.3.3}$$

It can also be seen from Kopteva et al. [44] that the discrete solution v of (4.3.2) satisfies the following inequality

$$||v||_{\Omega^N} \leq C\varepsilon^{-1/2}||f||_{-1,\infty}. \tag{4.3.4}$$

Let $\boldsymbol{E} = \boldsymbol{u} - \boldsymbol{U}$ denotes the error of the discrete solution for the discrete problem (4.3.1), where $E_{m,i} = u_{m,i} - U_{m,i}$, $m = 1(1)k$, $i = 0(1)N$, *i.e.*, $\boldsymbol{E} \in (\mathbb{R}^{N+1})^k$. Now, introducing the operator $(\hat{L}_m^N Y)_i \equiv \varepsilon_m(\delta^2 Y)_i + b_{mm,i}Y_i$, we split the error into two parts $\boldsymbol{E} = \aleph + \Re$, such that

$$(\hat{L}_m^N \aleph_m)_i = (\mathbb{L}_m^N \boldsymbol{E})_i, \quad i = 1, \cdots, N-1, \quad \aleph_{m,0} = \aleph_{m,N} = 0, \quad m = 1, \cdots, k,$$

and

$$(\hat{L}_m^N \Re_m)_i = -\sum_{l=1, l\neq m}^{k} b_{ml,i}E_{l,i}, \quad i = 1, \cdots, N-1, \quad \Re_{m,0} = \Re_{m,N} = 0, \quad m = 1, \cdots, k.$$

Invoking the triangle inequality with Lemma 4.3.3, it follows, from the previous decomposition that

$$||E_m||_{\Omega^N} \leq ||\aleph_m||_{\Omega^N} + ||\Re_m||_{\Omega^N} \leq ||\aleph_m||_{\Omega^N} + \sum_{l=1, l\neq m}^{k} \left\| \frac{b_{ml}}{b_{mm}} \right\|_{\Omega^N} ||E_l||_{\Omega^N}, \quad m = 1, \cdots, k.$$

Consequently,

$$||E_m||_{\Omega^N} - \sum_{l=1, l\neq m}^{k} \left\| \frac{b_{ml}}{b_{mm}} \right\|_{\Omega^N} ||E_l||_{\Omega^N} \leq ||\aleph_m||_{\Omega^N}.$$

Hence, using the inverse monotonicity of Υ (Lemma 4.2.2), we get

$$||E_m||_{\Omega^N} \leq \sum_{l=1}^{k} (\Upsilon^{-1})_{ml} ||\aleph_l||_{\Omega^N}, \text{ for } m = 1, \cdots, k.$$

Therefore, from $\boldsymbol{E} = \boldsymbol{u} - \boldsymbol{U}$, we can write that

$$||\boldsymbol{u} - \boldsymbol{U}||_{\Omega^N} \leq C||\aleph||_{\Omega^N}, \tag{4.3.5}$$

where the components of $\aleph$ are the solutions of

$$(\hat{L}_m^N \aleph_m)_i = \varepsilon_m(\delta^2 u_m - u_m'')_i, \text{ for } i = 1, \cdots, N-1, \quad \aleph_{m,0} = \aleph_{m,N} = 0, \quad m = 1, \cdots, k.$$

since $(\mathbb{L}_m^N \boldsymbol{E})_i = (\mathbb{L}_m^N \boldsymbol{u})_i - (\mathbb{L}_m^N \boldsymbol{U})_i = \varepsilon_m(\delta^2 u_m - u_m'')_i$. For further analysis, we shall use the procedure provided by Kopteva et al. [44] used for scalar reaction-diffusion problem.

For $i = 1, \cdots, N-1$, a straight forward calculation provided in [44] shows that

$$\varepsilon_m(\delta^2 u_m - u_m'')_i = \frac{\sqrt{\varepsilon_m}}{6} D\big(\sqrt{\varepsilon_m} h_i^2 u_m'''(\xi_{m,i})\big) + K_m \varepsilon_m \hbar_i^2 u_m^{(4)}(\eta_{m,i}), \tag{4.3.6}$$

where $\xi_{m,i} \in (x_{i-1}, x_i)$ and $\eta_{m,i} \in (x_{i-1/2}, x_{i+1/2})$, with $x_{i-1/2} = x_i - h_i/2$ and K_m's are constants. Here the component $\aleph_m$ can be written as a sum of two mesh functions such that each term corresponds to one of the terms appearing in the right-hand side of (4.3.6). Now, we apply the relation (4.3.4) to the first term and (4.3.3) to the second term of the right-hand side of (4.3.6), to obtain

$$||\aleph_m||_{\Omega^N} \leq C \max_i \max_{x\in[x_{i-1},x_i]} \sqrt{\varepsilon_m} h_i^2 |u_m'''(x)| + C \max_i \max_{x\in[x_{i-1/2},x_{i+1/2}]} \varepsilon_m \hbar_i^2 \left|u_m^{(4)}(x)\right|.$$

Here, we have used a similar technique provided in [44] to obtain the bound of $\aleph_m$. Next, differentiating each equation in (4.1.1) two times, and using the components of $\boldsymbol{f}(x)$ *i.e.*, $f_m(x) \in \mathcal{C}^2(\Omega)$, we obtain that

$$||\aleph_m||_{\Omega^N} \leq C \Bigg\{ \max_i \max_{x\in[x_{i-1},x_i]} \sqrt{\varepsilon_m} h_i^2 |u_m'''(x)| + \max_i \max_{x\in[x_{i-1/2},x_{i+1/2}]} \hbar_i^2 \left[1 + \sum_{j=1}^{k} |(b_{mj}u_j)''(x)|\right] \Bigg\}.$$

Hence, we have

$$||\aleph||_{\Omega^N} \leq C \Bigg\{ \max_i \max_{x\in[x_{i-1},x_i]} h_i^2 \sum_{l=1}^{k} \sqrt{\varepsilon_l} |u_l'''(x)| + \max_i \max_{x\in[x_{i-1/2},x_{i+1/2}]} \hbar_i^2 \sum_{l=1}^{k} \left[1 + \sum_{j=1}^{k} |(b_{lj}u_j)''(x)|\right] \Bigg\}. \tag{4.3.7}$$

Therefore, from equation (4.3.5), we can state the following theorem.

Theorem 4.3.4. *If $\boldsymbol{u}$ is the solution of (4.1.1) and $\boldsymbol{U}$ is the numerical solution obtained from (4.3.1), then we have the following error estimate*

$$||\boldsymbol{u} - \boldsymbol{U}||_{\Omega^N} \leq C \Bigg\{ \max_i \max_{x\in[x_{i-1},x_i]} h_i^2 \sum_{l=1}^{k} \sqrt{\varepsilon_l} |u_l'''(x)| + \max_i \max_{x\in[x_{i-1/2},x_{i+1/2}]} \hbar_i^2 \sum_{l=1}^{k} \left[1 + \sum_{j=1}^{k} |(b_{lj}u_j)''(x)|\right] \Bigg\}, \tag{4.3.8}$$

where C is a constant, independent of the perturbation parameters ε_l and the number of mesh intervals N.

From the above expression, the monitor function, which needs to be equidistributed to construct a layer-adapted mesh is quite clear. Observe that, for a truly adaptive algorithm, the monitor function has to be approximated from the numerical solution. The procedure of generating the adaptive mesh can be done by computing a solution (say $\boldsymbol{U}$) on a primarily chosen mesh (say uniform mesh) and then, by constructing a

new layer-adapted mesh, which will equidistribute the approximate monitor function $\widehat{M}(x, \boldsymbol{u}(x))$. For the analysis provided here, we shall be using a piecewise constant function $\widehat{M}(x, \boldsymbol{u}(x))$ to approximate the monitor function $M(x, \boldsymbol{u}(x))$. Hence the discretized equidistribution principle for (1.1.3) will take the following form

$$\widehat{M}_i h_i = \frac{1}{N} \sum_{j=1}^{N} \widehat{M}_j h_j, \quad \text{for} \quad i = 1, \cdots, N, \tag{4.3.9}$$

where $\widehat{M}_i$ is the discrete approximation of the monitor function $M(x, \boldsymbol{u}(x))$ at the subinterval (x_{i-1}, x_i). Another way to express (4.3.9) is $h_i \widehat{M}_i = h_j \widehat{M}_j$, where $\widehat{M}_i$ can be defined as $\widehat{M}_i = (M_i + M_{i-1})/2$. It should be noted that to obtain the equidistributed mesh x_i with the corresponding numerical solution $\boldsymbol{U}_i$, which is not known *apriori* one need to solve both (4.3.1) and (4.3.9) simultaneously for $(x_i, \boldsymbol{U}_i)$. Hence the intermediate meshes obtained through adaptive algorithm are nonlinearly linked to the computed solution $\boldsymbol{U}_i$ by (4.3.9).

The monitor function appearing in the right-hand side expression of the *apriori* error estimate (4.3.7) will be discretized by the following way

$$||\aleph||_{\Omega^N} \leq C \max_i \left\{ h_i^2 \sum_{l=1}^{k} \sqrt{\varepsilon_l} |(\delta^3 U_l)_i| + \hbar_i^2 \sum_{l=1}^{k} \left[1 + \sum_{j=1}^{k} |(\delta^2 (b_{lj} U_j))_i| \right] \right\}, \tag{4.3.10}$$

where $(\delta^3 U)_i = (D^- \delta^2 U)_i$. Here, we can use an optimal four point formula derived in Fornberg [31] for the discretization of the second-order derivative at the end points x_0 and x_N. In adaptive mesh generation, Beckett and Mackenzie [8, 9] carried out an error analysis for computed solution, where the mesh is obtained by equidistributing the exact solution. For their numerical experiment, they have used an heuristic argument for the discretization of their proposed monitor function. Our discretization of the monitor function for the system of equations is motivated from the discretization assumption of Kopteva et al. [44] on scalar reaction-diffusion problems, for which a corresponding *aposteriori* error analysis (see Kopteva [43]) is available and can be extended for system of equations. It should be noted that these error estimates involved the maximum norm which is strong enough to capture appropriate boundary layers.

Equidistribution of some quantity involving solution and its derivatives to select a layer-adapted mesh corresponds to the use of a transformation of the given equation, so that the transformed equation has equal error distribution on the uniform mesh with same number of mesh points. This implies to some extent the errors of the numerical solution are distributed uniformly through out the domain, *i.e.,* on the equidistributed mesh the errors appearing in the right-hand side of (4.3.10) will be independent of i. In other words, this implies that one can aim to have

$$||\aleph||_{\Omega^N} \leq C \max_i h_i^2 \sum_{l=1}^{k} \left\{ \sqrt{\varepsilon_l} |(\delta^3 U_l)_i| + \left[1 + \sum_{j=1}^{k} |(\delta^2 (b_{lj} U_j))_i| \right] \right\}, \tag{4.3.11}$$

to be independent of i.

It is easy to see from (4.3.11) that the discrete monitor function in normalized form is

$$M_i = 1 + \sum_{l=1}^{k} \frac{\varepsilon_l^{1/4} |(\delta^3 U_l)_i|^{1/2} + \sum_{j=1}^{k} |(\delta^2 (b_{lj} U_j))_i|^{1/2}}{\Lambda_l}, \tag{4.3.12}$$

where $\Lambda_m = \max_i |U_{m,i}|^{1/2}$, whose continuous counterpart is

$$M(x, \boldsymbol{u}(x)) = 1 + \sum_{l=1}^{k} [\varepsilon_l^{1/4} |u_l'''(x)|^{1/2} + \sum_{j=1}^{k} |(b_{lj}(x) u_j(x))''|^{1/2}].$$

4.4 Semilinear Reaction-Diffusion System

Consider the following singularly perturbed system of reaction-diffusion equations

$$\begin{cases} \mathbb{L}\boldsymbol{u} \equiv -\boldsymbol{Eps}\ \boldsymbol{u}_{xx}(x) + \ \boldsymbol{f}(x, \boldsymbol{u}(x)) = 0, \quad \text{for} \quad x \in \Omega, \\ \\ \boldsymbol{u}(0) = \boldsymbol{u}(1) = 0, \end{cases} \tag{4.4.1}$$

where $\boldsymbol{f}(x, \boldsymbol{u}(x)) = (f_1(x, \boldsymbol{u}(x)), \cdots, f_k(x, \boldsymbol{u}(x)))^T$. Here $f_m(x, \boldsymbol{u}(x))$ can be a nonlinear function of $\boldsymbol{u}(x)$ and the notation $\boldsymbol{u}_{xx}(x)$ is used instead of $\boldsymbol{u}''(x)$ for the sake of convenience. We shall assume that

$$\frac{\partial f_m}{\partial u_l}(x, \boldsymbol{u}(x)) \leq 0, \quad m \neq l, \quad \sum_{l=1}^{k} \frac{\partial f_m}{\partial u_l}(x, \boldsymbol{u}(x)) \geq \beta > 0, \quad m = 1 \cdots, k, \tag{4.4.2}$$

on $(x, \boldsymbol{u}(x)) \in \overline{\Omega} \times \mathbb{R}^k$. Assume that the reduced problem, which is defined by setting $\boldsymbol{Eps} = \boldsymbol{0}$ in (4.4.1), has a unique solution in $\overline{\Omega}$. Under this assumption, the system of BVP (4.4.1) admits a unique solution in $\overline{\Omega}$. Chang and Howes [17] studied the theoretical aspects corresponding to the semilinear system of reaction-diffusion problems.

To obtain the numerical solution of the system (4.4.1), the well-known Newton's quasi-linearization technique will be used. This technique allows to linearize the system into a sequence of linear problems, whose solutions $\boldsymbol{u}^{(p)}(x)$ with a proper initial guess $\boldsymbol{u}^{(0)}$ will converge to the original solution $\boldsymbol{u}(x)$. For each fixed nonnegative integer p, define $\boldsymbol{u}^{(p+1)}(x)$ to be the solution of the linear problem

$$\begin{cases} \overline{\mathbb{L}}\boldsymbol{u}^{(p+1)} \equiv -\boldsymbol{Eps}\ \boldsymbol{u}_{xx}^{(p+1)}(x) + \boldsymbol{J}\boldsymbol{u}^{(p+1)}(x) = \boldsymbol{F}(x), \quad \text{for} \quad x \in \Omega, \\ \\ \boldsymbol{u}^{(p+1)}(0) = \boldsymbol{u}^{(p+1)}(1) = 0. \end{cases} \tag{4.4.3}$$

The Jacobian matrix is given by

$$\boldsymbol{J}(x) = \begin{pmatrix} \dfrac{\partial f_1(x, \boldsymbol{u}^{(p)}(x))}{\partial u_1} & \cdots & \dfrac{\partial f_1(x, \boldsymbol{u}^{(p)}(x))}{\partial u_k} \\ \vdots & \ddots & \vdots \\ \dfrac{\partial f_k(x, \boldsymbol{u}^{(p)}(x))}{\partial u_1} & \cdots & \dfrac{\partial f_k(x, \boldsymbol{u}^{(p)}(x))}{\partial u_k} \end{pmatrix}_{k \times k},$$

and $\boldsymbol{F}(x, \boldsymbol{u}^{(p)}(x)) = \boldsymbol{J}(x)\boldsymbol{u}^{(p)}(x) - \boldsymbol{f}(x, \boldsymbol{u}^{(p)}(x))$. It is easy to see that the Jacobian matrix $\boldsymbol{J}(x)$ satisfies all the conditions of an L_0- matrix defined in (4.1.2). If the initial guess $\boldsymbol{u}^{(0)}(x)$ is sufficiently close to the solution $\boldsymbol{u}(x)$, then following the proof of [26], one can show that the sequence $\boldsymbol{u}^{(p+1)}(x)$ converges to the solution $\boldsymbol{u}(x)$. The solution of the associated reduced problem can be taken as an initial guess $\boldsymbol{u}^{(0)}(x)$. Since, for each fixed p the system (4.4.3) is a linear system of the form (4.1.1), the adaptive procedure explained in the Section 4.3 can be applied to generate a layer-adapted mesh. This solution will converge uniformly to the exact solution. We use the following criteria

$$|\boldsymbol{u}^{(p+1)}(x_i) - \boldsymbol{u}^{(p)}(x_i)| \leq Tol, \quad x_i \in \Omega^N, \quad p \geq 0,$$

for the convergence of the Newton's quasi-linearization technique. Here, *Tol* denotes the user chosen tolerance.

4.5 Numerical Experiments

This section computationally verifies the appropriateness of the proposed monitor function appeared in the theoretical error estimate. We considered the well-known de Boor algorithm to generate the adaptive mesh.

4.5.1 Adaptive mesh generation algorithm

The following iterative algorithm will be used for equidistributing the proposed monitor function (4.3.12). Similar algorithm is applied to system of convection-diffusion type problems by Linß [50] and for scalar reaction-diffusion problems by Kopteva et al. [44]. For scalar reaction-diffusion problems, Chadha and Kopteva [16] carried out the convergence analysis of this algorithm. We shall use this algorithm to generate layer-adapted meshes by extending it for system of equations. Our main aim is to construct a mesh that solves the equidistribution problem (4.3.9). Observe that instead of solving the discretized equidistribution problem (4.3.9) for (1.1.3) exactly, it is sufficient that this algorithm can be stopped when the weakly equidistribution principle

$$\widehat{M}_i h_i \leq \frac{C_0}{N} \sum_{j=1}^{N} \widehat{M}_j h_j, \quad \text{for} \quad i = 1, \cdots, N, \tag{4.5.1}$$

satisfied with a user chosen constant $C_0 > 1$. C_0 will be chosen large enough to get fewer iterations for the convergence of the algorithm.

Algorithm-

Step 1: Define the initial uniform mesh $\{x^{(0)} : 0 \leq i \leq N,\ x_i^{(0)} = i/N\}$ and go to Step 2 with $p = 0$.

Step 2: Solve $\boldsymbol{L}^N \boldsymbol{U}_i^{(p)} = \mathbf{f}_i^{(p)}$ with $\boldsymbol{U}_0^{(p)} = \boldsymbol{u}(0)$ and $\boldsymbol{U}_N^{(p)} = \boldsymbol{u}(1)$ at the mesh $\{x^{(p)} : 0 \leq i \leq N\}$ for $\boldsymbol{U}_i^{(p)} = (U_{1,i}^{(p)}, \cdots, U_{k,i}^{(p)})$ and define $h_{i+1}^{(p)} = x_{i+1}^{(p)} - x_i^{(p)}$.

Step 3: Find the discretized monitor function M_i defined in (4.3.12) for $i = 1, \cdots, N-1$, where at the end points x_0 and x_N, we use an optimal four point formula from Fornberg [31] to discretize the second-order derivative. Define $\widehat{M}_i = (M_i^{(p)} + M_{i-1}^{(p)})/2$ for $i = 1, \cdots, N$, by setting $M_0^{(p)} = M_1^{(p)}$ and $M_N^{(p)} = M_{N-1}^{(p)}$.

Compute

$$\Phi_j^{(p)} = \sum_{i=1}^{j} h_i^{(p)} \widehat{M}_i^{(p)}.$$

Step 4: Choose a constant $C_0 > 1$. The stopping criteria for the iterative technique is

$$\frac{\max\limits_{i=1,\ldots,N} h_i^{(p)} \widehat{M}_i^{(p)}}{\Phi_N^{(p)}} \leq \frac{C_0}{N}.$$

If it holds true, then go to Step 6, else continue with Step 5.

Step 5: Generate a new mesh by equidistributing the proposed monitor function using the current computed solution from Step 2 and $\Phi_j^{(p)}$ from Step 3: Set $Y_i^{(p)} = i\Phi_N^{(p)}/N$ for $i = 0, \cdots, N$. Now interpolate $Y_i^{(p)}$to the points $(\Phi_i^{(p)}, x_i^{(p)})$ using the piecewise linear interpolation. Generate a new mesh $x^{(p+1)} \equiv \{0 = x_0^{(p+1)} < x_1^{(p+1)} < \cdots < x_N^{(p+1)} = 1\}$ and return to Step 2.

Step 6: Set $x^* = \{0 = x_0^* < x_1^* < \cdots < x_N^* = 1\} = x^{(p+1)}$ and $\boldsymbol{U}^* = \boldsymbol{U}^{(p+1)}$, where $\boldsymbol{U}^*$ is the desired solution. Stop.

4.5.2 Numerical examples

To accomplish the results of our theoretical findings, we have numerically studied the component of the error estimator by considering three test problems. For these problems the maximum uniform errors and the corresponding rates of convergence are demonstrated through tables.

Example 4.5.1. *Consider the coupled system of reaction-diffusion BVPs:*

$$\begin{cases} -\varepsilon_1 u_1''(x) + (5+2x)u_1(x) + (x-2)u_2(x) = -4-4x, \quad x \in \Omega, \\ -\varepsilon_2 u_2''(x) - 2u_1(x) + (4-x^2)u_2(x) = 2x^2 - 12, \\ u_1(0) = u_1(1) = u_2(0) = u_2(1) = 0. \end{cases}$$

Example 4.5.2. *Consider the coupled system of singularly perturbed reaction-diffusion BVPs:*

$$\begin{cases} -\varepsilon_1 u_1''(x) + 2(x+1)^2 u_1(x) - (1+x^3)u_2(x) = 2\exp(x), \quad x \in \Omega, \\ -\varepsilon_2 u_2''(x) - 2\cos\left(\frac{\pi x}{4}\right) u_1(x) + 2.2\exp(1-x)u_2(x) = 10x+1, \\ u_1(0) = u_1(1) = u_2(0) = u_2(1) = 0. \end{cases}$$

Example 4.5.3. *Consider the following semilinear system of reaction-diffusion problems:*

$$\begin{cases} -\varepsilon_1 u_1'' + u_1 - 1 - (1-u_1)^3 + \exp(u_1 - u_2) = 0, \quad x \in \Omega, \\ -\varepsilon_2 u_2'' + u_2 - 0.5 - (0.5-u_2)^5 + \exp(u_2 - u_1) = 0, \\ u_1(0) = u_1(1) = u_2(0) = u_2(1) = 0. \end{cases}$$

Exact solution for these examples are not available. The accuracy of their numerical solutions would be computed using the double mesh principle as described in Chapter 2. For the numerical experiments, we took ε_1 and ε_2 from the set

$$S = \{\varepsilon = (\varepsilon_1, \varepsilon_2) | \varepsilon_1 = 1, 2^{-2}, \cdots, 2^{-30}; \varepsilon_2 = 1, 2^{-2}, \cdots, 2^{-30}\},$$

and the adaptively generated mesh is constructed by taking $C_0 = 1.4$, in the algorithm.

Table 4.1: *Uniform errors and orders of convergence of U_1 for Example 4.5.1.*

$(\varepsilon_1, \varepsilon_2) \in S$	Number of intervals N						
	64	128	256	512	1024	2048	4096
E_1^N	1.430e-2	4.087e-3	8.564e-4	1.275e-4	2.622e-5	6.4948e-6	1.311e-6
r_1^N	1.8069	2.2550	2.7473	2.2818	2.0137	2.3084	-

Table 4.2: *Uniform errors and orders of convergence of U_2 for Example 4.5.1.*

$(\varepsilon_1, \varepsilon_2) \in S$	Number of intervals N						
	64	128	256	512	1024	2048	4096
E_2^N	3.492e-2	9.740e-3	2.119e-3	4.128e-4	9.322e-5	1.319e-5	3.565e-6
r_2^N	1.8422	2.2005	2.3598	2.1470	2.8203	1.8884	-

For the first two examples, we display the uniform errors and the corresponding rates of convergence respectively in the maximum norm in tables. In Table 4.1 and Table 4.2, the uniform errors and the corresponding orders of convergence of the numerical solution

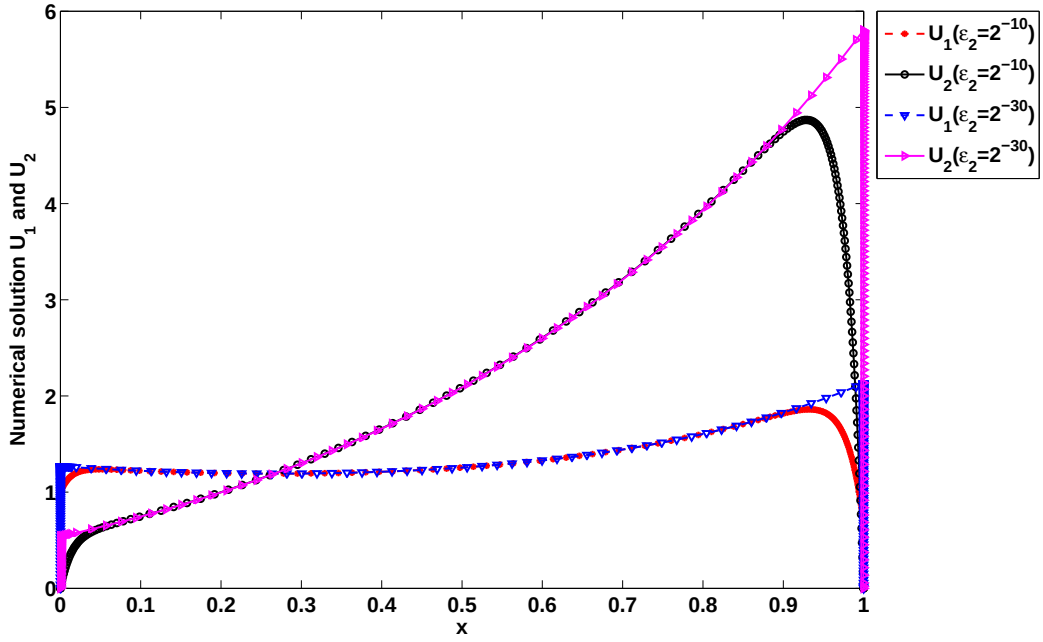

Figure 4.1: *Numerical solutions U_1 and U_2 for $N = 256$, $\varepsilon_1 = 2^{-30}$ and $\varepsilon_2 = 2^{-10}, 2^{-30}$ for Example 4.5.2.*

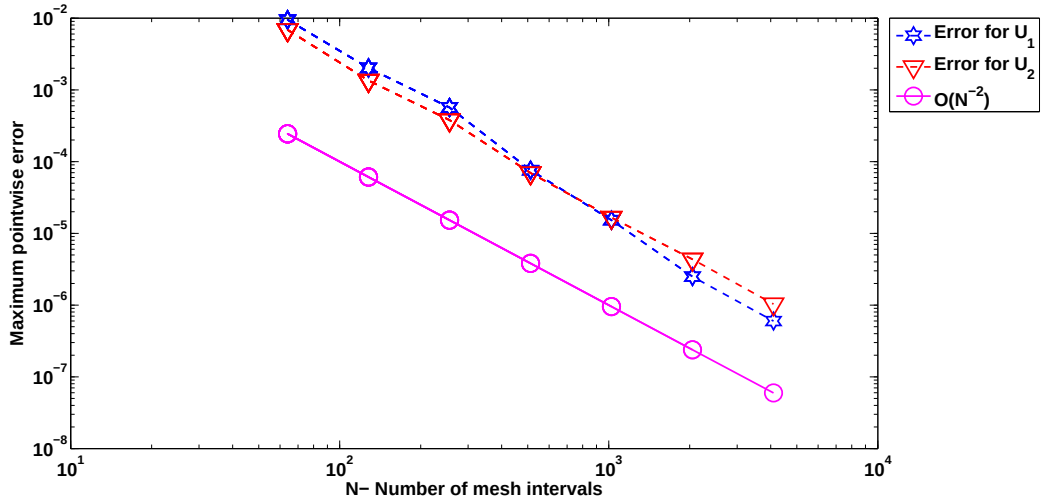

Figure 4.2: *Loglog plot of the maximum point-wise errors for Example 4.5.1 for $\varepsilon_1 = 2^{-20}$ and $\varepsilon_2 = 2^{-30}$.*

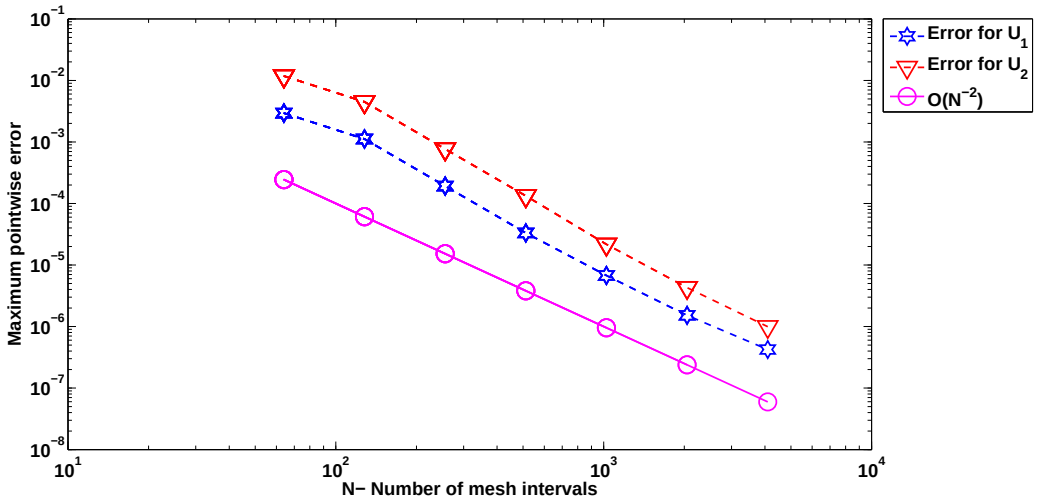

Figure 4.3: *Loglog plot of the maximum point-wise errors for Example 4.5.2 for* $\varepsilon_1 = 2^{-30}$ *and* $\varepsilon_2 = 2^{-20}$.

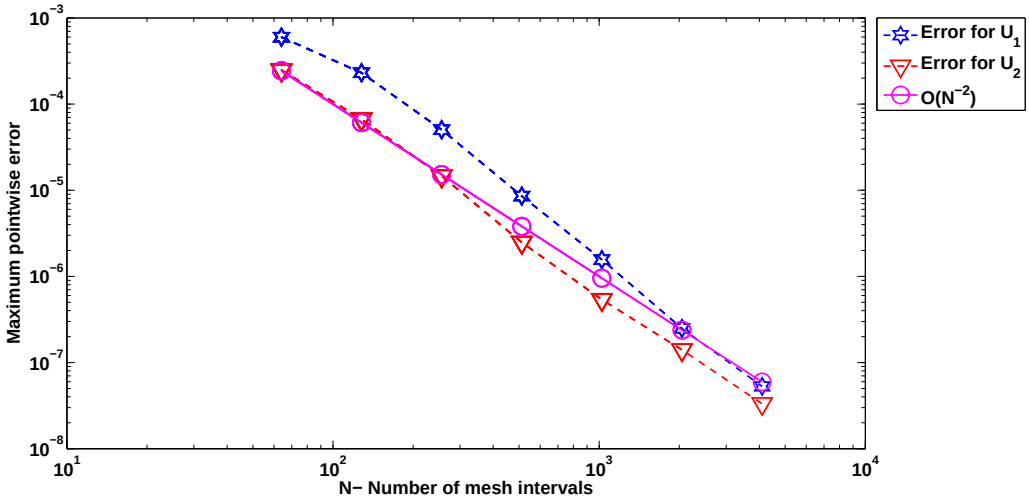

Figure 4.4: *Loglog plot of the maximum point-wise errors for Example 4.5.3 for* $\varepsilon_1 = 2^{-20}$ *and* $\varepsilon_2 = 2^{-30}$.

Table 4.3: *Uniform errors and orders of convergence of U_1 for Example 4.5.2.*

$(\varepsilon_1, \varepsilon_2) \in S$	Number of intervals N						
	64	128	256	512	1024	2048	4096
E_1^N	7.205e-3	1.846e-3	4.476e-4	8.225e-5	1.519e-5	3.122e-6	6.674e-7
r_1^N	1.9644	2.0444	2.4442	2.4365	2.2828	2.2260	-

Table 4.4: *Uniform errors and orders of convergence of U_2 for Example 4.5.2.*

$(\varepsilon_1, \varepsilon_2) \in S$	Number of intervals N						
	64	128	256	512	1024	2048	4096
E_2^N	2.372e-2	5.724e-3	1.365e-3	2.788e-4	5.692e-5	9.582e-6	1.977e-6
r_2^N	2.0510	2.0674	2.2921	2.2924	2.5706	2.2767	-

components $U_1(x)$ and $U_2(x)$ are presented respectively for Example 4.5.1. A similar observation is noticed for Example 4.5.2 in Tables 4.3 and 4.4.

From these tables, it is easy to see that the errors are robust with respect to the perturbation parameters ε_l and converge to 0 as the number of intervals N increases. Some variations in the numerical result, from actual theoretical findings is expected, because instead of solving the equidistribution problem (1.1.3) and (4.3.9) exactly, we have solved the weakly equidistribution problem (4.5.1) with $C_0 = 1.4$. Although the errors are more uniform for smaller values of C_0, but the improvements are insignificant. Observe that a similar kind of result with weakly equidistribution principle (4.5.1) is obtained by Kopteva et al. [44], Linß [50] and also by Das and Natesan [21].

In Figure 4.1, the computed solutions are plotted for Example 4.5.2. From this graph, the mesh movement using the equidistribution technique can be noticed to capture the boundary layer, as ε_2 decreases. This figure also indicates the steepness of the solution components U_1 and U_2 towards the boundary points (which are also the region of boundary layers) as ε_2 decreases. In Figure 4.3, the maximum point-wise errors versus number of mesh intervals is plotted for this example. This figure is drawn in logarithmic scale for $\varepsilon_1 = 2^{-30}$ and $\varepsilon_2 = 2^{-20}$. Graphically this also shows that the computed errors are decreasing approximately with the rate of $O(N^{-2})$ as the number of intervals N increases. Similar observations are demonstrated in Figure 4.2 and Figure 4.4, where approximately second-order convergence is achieved for Example 4.5.1 and Example 4.5.3 respectively with $\varepsilon_1 = 2^{-20}$, $\varepsilon_2 = 2^{-30}$.

To show the effectiveness of the adaptively generated mesh, we considered a system of semilinear reaction-diffusion equations in Example 4.5.3. The quasi-linearization procedure defined in Section 4.4 is used to compute the numerical solution with tolerance 10^{-8}. The uniform errors and the corresponding rates of convergence given in Table 4.5

and Table 4.6 suggest that the proposed monitor function also works well for system of semilinear reaction-diffusion problems.

Table 4.5: *Uniform errors and orders of convergence of U_1 for Example 4.5.3.*

$(\varepsilon_1, \varepsilon_2) \in S$	Number of intervals N						
	64	128	256	512	1024	2048	4096
E_1^N	2.079e-3	5.417e-4	1.120e-4	2.012e-5	4.426e-6	7.248e-7	1.467e-7
r_1^N	1.9405	2.2737	2.4766	2.1849	2.61047	2.3040	-

Table 4.6: *Uniform errors and orders of convergence of U_2 for Example 4.5.3.*

$(\varepsilon_1, \varepsilon_2) \in S$	Number of intervals N						
	64	128	256	512	1024	2048	4096
E_2^N	1.507e-3	4.345e-4	9.771e-5	2.016e-5	3.415e-6	4.994e-7	9.393e-8
r_2^N	1.7941	2.15307	2.2767	2.5616	2.7738	2.4105	-

4.6 Conclusion

In this chapter, a layer-adapted mesh is constructed for system of singularly perturbed reaction-diffusion problems by equidistribution principle. It is found that the equidistribution of the monitor function generated from the *apriori* analysis leads to a uniformly accurate numerical solution for singularly perturbed system of differential equations. It automatically detects the presence and location of the boundary layers and their widths. Numerical experiments are performed on mesh adaption, which seem to work well for obtaining uniformly convergent numerical solution of system of linear and semilinear reaction-diffusion BVPs.

Chapter 5

Richardson Extrapolation Technique for Singularly Perturbed Convection-Diffusion Problems on Adaptively Generated Mesh

This chapter deals with the study of obtaining higher-order convergent numerical solution for singularly perturbed convection-diffusion problems on the equidistributed mesh. A post-processing Richardson extrapolation technique is used to improve the accuracy of the parameter-uniform computed solution. Here the adaptively generated mesh is obtained by the equidistribution of a positive monitor function. It is shown that the extrapolation technique can be used to improve the ε-uniform accuracy of the simple upwinding scheme from $O(N^{-1})$ to $O(N^{-2})$ in the discrete maximum norm, where N is the number of mesh intervals.

5.1 Introduction

Consider the following singularly perturbed convection-diffusion problem:

$$\begin{cases} \mathfrak{L}u(x) \equiv -\varepsilon u''(x) - (a(x)u(x))' = f(x), \quad x \in \Omega, \\ \\ u(0) = 0, \quad u(1) = 0, \end{cases} \tag{5.1.1}$$

where ε $(0 < \varepsilon \ll 1)$ is the singular perturbation parameter. It will be assumed that $a(x)$ and $f(x)$ are in $\mathcal{C}^2(\Omega)$. Under these assumptions, the BVP (5.1.1) admits a unique solution $u(x) \in \mathcal{C}^4(\Omega) \cap \mathcal{C}(\overline{\Omega})$. In general, the solution $u(x)$ of (5.1.1) exhibits a boundary layer at $x = 0$, if $a(x)$ has a positive lower bound.

In this chapter, the following two monitor functions will be used for the error analysis

$$M\big(x, u(x)\big) = 1 + |u''(x)|^{1/2}, \text{ and } M\big(x, w(x)\big) = 1 + |w''(x)|^{1/2}. \tag{5.1.2}$$

Here $u(x)$ is the solution of (5.1.1) and $w(x)$ is the singular component of the solution $u(x)$.

The outline of this chapter is as follows: In Section 5.2, the derivative bounds of the analytical solution $u(x)$ of (5.1.1) is introduced. Its decomposition into the smooth and singular components and their derivatives bounds are established in this section. The stability of the continuous solution is also provided here. A finite difference discretization of the continuous problem (5.1.1) and the stability of the discrete solution is introduced in Section 5.3. Section 5.4 is devoted to study the detailed error analysis. Also, two monitor functions are generated from the error analysis, which will lead to the first-order parameter-uniform convergence on the equidistributed mesh. Richardson extrapolation technique is used at the end of this section, where the error is improved to second-order accuracy by equidistributing the proposed monitor functions. Finally, Section 5.5 provides numerical experiments to support the theoretical findings using an adaptive algorithm.

5.2 Solution Decomposition and Derivative Bounds

This section presents the standard *apriori* bounds of the analytical solution of (5.1.1) and its derivatives. For the analysis presented here, we assume that $a(x) = a$, constant in (5.1.1) such that $a \gg \varepsilon > 0$. The next lemma provides *apriori* bounds of the solution and its derivatives.

Lemma 5.2.1. *The solution $u(x)$ of (5.1.1) and its derivatives satisfy the following bounds for any prescribed r,*

$$|u^{(k)}(x)| \leq C\big(1 + \varepsilon^{-k}\exp(-ax/\varepsilon)\big), \quad \text{for } k = 0, \cdots, r.$$

Proof. The proof of this lemma can be seen in [41]. ∎

To establish the parameter-uniform properties of the numerical methods, we shall decompose the analytic solution u into two components, the smooth component v and the singular component w such that $u = v + w$. The following lemma provides an insight about the derivative bounds of the smooth component v and the singular component w.

Lemma 5.2.2. *The smooth component $v(x)$ of the solution $u(x)$ of (5.1.1) satisfying*

$$\begin{cases} \mathfrak{L}v(x) = f(x), \quad x \in \Omega, \\ v(0) = v_\varepsilon, \quad v(1) = 0, \quad \text{with a suitable} \quad v_\varepsilon \end{cases}$$

admits the following bound

$$|v^{(k)}(x)| \leq C, \quad \text{for } k = 0, \cdots, r, \text{ and any prescribed } r,$$

while the singular component $w(x)$ *satisfying*

$$\begin{cases} \mathfrak{L}w(x) = 0, \quad x \in \Omega, \\ \\ w(0) = -v(0), \quad w(1) = 0, \end{cases}$$

is of the form $w(x) = A + B\exp(-ax/\varepsilon)$, *where*

$$A = \frac{v(0)\exp(-a/\varepsilon)}{1-\exp(-a/\varepsilon)}, \quad B = \frac{-v(0)}{1-\exp(-a/\varepsilon)}.$$

Proof. To obtain the derivative bounds for the smooth component $v(x)$, consider the decomposition

$$v(x) = \sum_{i=0}^{r+1} \varepsilon^i v_i(x), \text{ with } v(1) = 0.$$

Now, comparing the powers of ε, we get

$$-av_0'(x) = f(x), \quad v_0(1) = 0,$$

$$-av_i'(x) = v_{i-1}''(x), \quad v_i(1) = 0, \quad i = 1, \cdots, r,$$

$$\mathfrak{L}v_{r+1}(x) = v_r''(x), \quad v_{r+1}(1) = 0, \quad v_{r+1}(0) = u(0) = 0.$$

Since the last equation is similar to (5.1.1), Lemma 5.2.1 can be used to bound the term $v_{r+1}(x)$. Combining the derivative bounds of each component, we obtain the required bound. A direct calculation from

$$\mathfrak{L}w(x) = 0, \quad w(0) = -v(0), \quad w(1) = 0,$$

leads to

$$w(x) = A + B\exp(-ax/\varepsilon), \quad \text{with} \quad A = \frac{v(0)\exp(-a/\varepsilon)}{1-\exp(-a/\varepsilon)}, \quad B = \frac{-v(0)}{1-\exp(-a/\varepsilon)},$$

which proves the lemma. ∎

The continuous operator $\mathfrak{L}$ defined in (5.1.1) enjoys the following stability property

$$||v||_{\infty,\overline{\Omega}} \leq 2a^{-1}||\mathfrak{L}v||_{*,\overline{\Omega}}, \quad \text{for all } v \text{ with } \quad v(0) = v(1). \tag{5.2.1}$$

This result is obtained by Andreev [1], using the Green's function associated with the operator $\mathfrak{L}$.

5.3 Discretization of the Continuous Problem

In this section, the discretization of the continuous problem (5.1.1) is introduced. To discretize (5.1.1), we shall consider the following upwind finite difference problem

$$\begin{cases} [\mathfrak{L}^N U]_i \equiv -\varepsilon[D^+D^-U]_i - [D^+(aU)]_i = f_i, \quad \text{for} \quad i = 1, \cdots, N-1, \\ \\ U_0 = U_N = 0. \end{cases} \tag{5.3.1}$$

The discrete operator $\mathfrak{L}^N$ corresponding to the continuous operator $\mathfrak{L}$ satisfies the following stability property

$$||U||_{\infty,\Omega^N} \leq 2a^{-1}||\mathfrak{L}^N U||_{*,\Omega^N}, \quad \text{for all} \quad U \in R_0^{N+1}, \tag{5.3.2}$$

(see Andreev [1] and Kopteva [42]), where

$$||U||_{*,\Omega^N} = ||U||_{-1,\infty,\Omega^N} = \max_{i=0,\cdots,N-1} \left| \sum_{p=i}^{N-1} h_{p+1} U_p \right|. \tag{5.3.3}$$

5.4 Error Analysis

In this section, the standard error analysis involving the monitor functions given in (5.1.2) are presented. These monitor functions are generated from the error expansion. First, we provide a technical lemma, which is used for the proof of ε-uniform error estimate.

Lemma 5.4.1. *Consider the following continuous problem*

$$\mathfrak{L}\phi = \Phi', \quad x \in \Omega, \qquad \phi(0) = 0, \quad \phi(1) = 0. \tag{5.4.1}$$

Here $\Phi(x)$ is a piecewise continuously differentiable function where the differentiation can be understood in the distributional sense. If $\phi(x) \in \mathcal{C}^2(\Omega)$, then it satisfies the following equality

$$\sum_{p=i}^{N-1} h_{p+1}[\mathfrak{L}^N \phi]_p = \varepsilon([D^-\phi]_i - \phi'_{i-0}) - \varepsilon([D^-\phi]_N - \phi'_{N-0}) + \Phi_{N-0} - \Phi_{i-0}.$$

Proof. This result can be obtained by integrating the continuous problem (5.4.1) and the discrete problem (5.3.1) over the interval $(x_i, 1)$ and combining them (see Linß [48]). ∎

From this lemma, we can obtain the truncation error estimate of the numerical solution U of (5.3.1). This error becomes

$$\sum_{p=i}^{N-1} h_{p+1}[\mathfrak{L}^N(u-U)]_p = \varepsilon([D^-u]_i - u'_{i-0}) - \varepsilon([D^-u]_N - u'_{N-0}) + \int_{x_i}^{1} f(x)dx - \sum_{p=i}^{N-1} h_{p+1} f_p.$$

Thus, using the discrete norm defined in (5.3.3), we have

$$||\mathfrak{L}^N(u-U)||_{*,\Omega^N} \leq 2\varepsilon \max_{i=1,\cdots,N} |[D^-u]_i - u'_{i-0}| + \max_{i=0,\cdots,N-1} \left| \int_{x_i}^{1} f(x)dx - \sum_{p=i}^{N-1} h_{p+1} f_p \right|. \tag{5.4.2}$$

One can observe that the terms appearing in the right-hand side of the truncation error bound will provide at most first-order convergence. In fact, with the help of discrete stability estimate (5.3.2), it is proved in Linß [46] that

$$\begin{aligned} ||u-U||_{*,\Omega^N} &\leq C \max_{i=1,\cdots,N} \int_{x_{i-1}}^{x_i} \Big(1+\varepsilon^{-1}\exp(-ax/2\varepsilon)\Big)dx \\ &\leq C \max_{i=1,\cdots,N} \int_{x_{i-1}}^{x_i} \Big(1+|w''(x)|^{1/2}\Big)dx. \end{aligned}$$

Here, we have used Lemma 5.2.2. From this expression, it is clear that the equidistribution principle (1.1.3) of the monitor function $M(x, w(x))$ leads to a first-order convergent solution of (5.3.1). A similar technique is used in the convergence analysis of Beckett and Mackenzie [8, 9] and also in Pereyra and Sewell [66].

Now onwards, for the sake of convenience, the left-hand derivative of $u(x)$ at x_i will be denoted by u'_i instead of u'_{i-0}. To improve the accuracy of the numerical solution, we have to eliminate the first-order dominating terms from the expression (5.4.2). This can be achieved by introducing the extrapolation technique. Assume that $\chi(x)$, the leading term of the error expansion be the solution of the following problem

$$\mathfrak{L}\chi = \Lambda', \quad \chi(0)=\chi(1)=0, \quad \text{with} \quad \Lambda(x) = \frac{\varepsilon h(x)u''(x)}{2} - \int_x^1 h(t)f'(t)dt, \tag{5.4.3}$$

where

$$h(x) = x - x_{p-1}, \quad \text{on} \quad x \in (x_{p-1}, x_p).$$

Then, using Lemma 5.4.1, we have

$$\begin{aligned} \sum_{p=i}^{N-1} h_{p+1}[\mathfrak{L}^N(u-\chi-U)]_p &= \varepsilon([D^-u]_i - u'_i + \frac{h_i}{2}u''_i) - \varepsilon([D^-u]_N - u'_N + \frac{h_N}{2}u''_N) + \\ &\int_{x_i}^1 \Big(f(x)-h(x)f'(x)\Big)dx - \sum_{p=i}^{N-1} h_{p+1}f_p + \\ &\varepsilon([D^-\chi]_N - \chi'_N) - \varepsilon([D^-\chi]_i - \chi'_i). \end{aligned} \tag{5.4.4}$$

From the above equality, it can be noted that the expressions involving $u(x)$ and $f(x)$ appearing in the right-hand side of (5.4.4) are of second-order. Third expression involving $\chi(x)$ is also of second-order, as the leading error $\chi(x)$ itself is first-order.

Now we shall analyze each term of the error expression appearing in (5.4.4), separately. This will give us an insight to the place, where the monitor functions and the given BVP (5.1.1) are used. Observe that, the given equation (5.1.1) implies that $|u'| \leq C[1+\varepsilon|u''|]$. Again, differentiating equation (5.1.1) and assuming $u \in \mathcal{C}^3(\Omega)$, we get $\varepsilon u''' = -f' - a''u - 2a'u' - au''$, which implies that $|\varepsilon u'''| \leq C[1+|u''|]$.

Now, consider the first term of the right-hand side expression in (5.4.4). Noting the above observations, Taylor series expansion with integral form of remainder yields

$$\begin{aligned}
\varepsilon\left([D^-u]_i - u_i' + \frac{h_i}{2}u_i''\right) &= \frac{\varepsilon}{2h_i}\left|\int_{x_{i-1}}^{x_i}(x-x_{i-1})^2u'''(x)dx\right| \\
&\leq \frac{C}{2h_i}\int_{x_{i-1}}^{x_i}(x-x_{i-1})^2[1+|u''(x)|]dx \\
&\leq C\max_{[x_{i-1},x_i]}h_i^2[1+|u''(x)|] \\
&\leq C\max_{[x_{i-1},x_i]}h_i^2[1+|w''(x)|] \\
&\leq C\max_{[x_{i-1},x_i]}h_i^2[1+|w''(x)|^{1/2}]^2, \qquad (5.4.5)
\end{aligned}$$

where Lemma 5.2.2 is used. Again Taylor series expansion yields

$$f(s) = f_{i-1} + (s-x_{i-1})f'(s) - \int_{x_{i-1}}^{s}(x-x_{i-1})f''(x)dx.$$

Integrating the above expression over (x_{i-1}, x_i), it leads to

$$\int_{x_{i-1}}^{x_i}(f(x)-(x-x_{i-1})f'(x))dx - h_if_{i-1} = -\int_{x_{i-1}}^{x_i}\int_{x_{i-1}}^{s}(x-x_{i-1})f''(x)dxds.$$

Since $f(x) \in \mathcal{C}^2(\Omega)$, we have

$$\begin{aligned}
&\left|\int_{x_{i-1}}^{x_i}(f(x)-(x-x_{i-1})f'(x))dx - h_if_{i-1}\right| \\
&\leq \int_{x_{i-1}}^{x_i}\int_{x_{i-1}}^{s}(x-x_{i-1})|f''(x)|dxds \\
&\leq Ch_i^3. \qquad (5.4.6)
\end{aligned}$$

Hence,

$$\begin{aligned}
&\left|\int_{x_i}^{1}\Big(f(x)-h(x)f'(x)\Big)dx - \sum_{p=i+1}^{N}h_pf_{p-1}\right| \\
&\leq \sum_{p=i+1}^{N}\left|\int_{x_{p-1}}^{x_p}(f(x)-(x-x_{p-1})f'(x))dx - h_pf_{p-1}\right| \\
&\leq C\sum_{p=i+1}^{N}h_p^3 \leq C\max_p h_p^2\sum_{p=i+1}^{N}h_p \leq C\max_i h_i^2 \\
&\leq C\max_i\max_{[x_{i-1},x_i]}h_i^2[1+|w''(x)|^{1/2}]^2. \qquad (5.4.7)
\end{aligned}$$

Now, to bound the fifth term of the right-hand side expression in (5.4.4), we need the derivative bound of the leading error term $\chi(x)$. The following technical lemma is very useful to derive the derivative bounds of $\chi(x)$.

Lemma 5.4.2. *Let $x \in (x_{i-1}, x_i)$. Then, we have*

$$h(x)(1+\varepsilon^{-1}\exp(-ax/2\varepsilon)) \leq \int_{x_{i-1}}^{x} \Big(1+\varepsilon^{-1}\exp(-at/2\varepsilon)\Big)dt.$$

Proof. It is easy to check that the difference between the two functions appearing in either sides of the above inequality is monotonic in the interval (x_{i-1}, x_i). ∎

The following lemma provides the derivative estimates of $\chi(x)$.

Lemma 5.4.3. *Assume that $a(x), f(x) \in \mathcal{C}^2(\Omega)$. Then the solution of (5.4.3) and its derivatives satisfy*

$$|\chi^{(p)}(x)| \leq C\big(1+\varepsilon^{-p}\exp(-ax/2\varepsilon)\big)\max_{i=1,\cdots,N}\int_{x_{i-1}}^{x_i}\Big(1+\varepsilon^{-1}\exp(-at/2\varepsilon)\Big)dt, \quad \textit{for} \quad p=0,1,$$

and

$$\begin{aligned}\varepsilon|\chi''(x)| \;&\leq\; C\big(1+\varepsilon^{-1}\exp(-ax/2\varepsilon)\big)\max_{i=1,\cdots,N}\int_{x_{i-1}}^{x_i}\Big(1+\varepsilon^{-1}\exp(-at/2\varepsilon)\Big)dt\\ &\quad +h(x)(1+\varepsilon^{-1}\exp(-ax/\varepsilon)), \quad \textit{for} \quad x\in\Omega-\Omega^N. \end{aligned} \tag{5.4.8}$$

Proof. The proof of this lemma is given by Linß [48]. ∎

Now, the first derivative bound of $\chi(x)$ and the mean-value theorem yield

$$\begin{aligned}\varepsilon([D^-\chi]_i-\chi_i') \;&=\; \varepsilon\left|\frac{\chi_i-\chi_{i-1}}{h_i}-\chi_i'\right|\\ &\leq\; \varepsilon\max_{(x_{i-1},x_i)}|\chi'(x)|\\ &\leq\; C\max_{i=1,\cdots,N}\int_{x_{i-1}}^{x_i}\Big(1+\varepsilon^{-1}\exp(-ax/2\varepsilon)\Big)dx\\ &\leq\; C\max_{i=1,\cdots,N}\int_{x_{i-1}}^{x_i}\Big(1+|w''(x)|^{1/2}\Big)dx.\end{aligned}$$

This implies that the proposed technique will lead to first-order convergence if the function $M(x, w(x))$ is equidistributed as a monitor function. Nevertheless, we can improve the convergence rate by using the second-order derivative bound of $\chi(x)$ from Lemma

5.4.3. Again, Taylor series expansion with integral form of the remainder leads to

$$\begin{aligned}
\varepsilon([D^-\chi]_i - \chi_i') &= \frac{\varepsilon}{h_i}\left|\int_{x_{i-1}}^{x_i}(x-x_{i-1})\chi''(x)dx\right| \\
&\leq \frac{C}{h_i}\int_{x_{i-1}}^{x_i} h^2(x)\Big(1+\varepsilon^{-1}\exp(-ax/\varepsilon)\Big)dx \\
&\quad + \frac{C}{h_i}\max_{i=1,\cdots,N}\int_{x_{i-1}}^{x_i}\Big(1+\varepsilon^{-1}\exp(-ax/2\varepsilon)\Big)dx \times \\
&\quad \int_{x_{i-1}}^{x_i}(x-x_{i-1})\Big(1+\varepsilon^{-2}\exp(-ax/2\varepsilon)\Big)dx \\
&= I_1 + I_2.
\end{aligned}$$

Here

$$\begin{aligned}
I_1 &= \frac{C}{h_i}\int_{x_{i-1}}^{x_i} h^2(x)\Big(1+\varepsilon^{-1}\exp(-ax/\varepsilon)\Big)dx \\
&\leq C\int_{x_{i-1}}^{x_i}(x-x_{i-1})dx + \int_{x_{i-1}}^{x_i}(x-x_{i-1})\varepsilon^{-2}\exp(-ax/\varepsilon)dx.
\end{aligned}$$

Now, we shall use the following identity [66]: For any positive monotonically decreasing function $\psi(x)$ defined on $[a,b]$ and arbitrary $k \in \mathbb{N}^+$, we have

$$\int_a^b \psi(t)(t-a)^{(k-1)}dt \leq \frac{1}{k}\left[\int_a^b \psi(t)^{1/k}dt\right]^k.$$

Hence, the above identity for $k=2$ implies that

$$\begin{aligned}
I_1 &\leq Ch_i^2 + C\left[\int_{x_{i-1}}^{x_i}\Big(\varepsilon^{-1}\exp(-ax/2\varepsilon)\Big)dx\right]^2 \\
&\leq Ch_i^2 + C\left[\int_{x_{i-1}}^{x_i}\Big(1+\varepsilon^{-1}\exp(-ax/2\varepsilon)\Big)dx\right]^2 \\
&\leq Ch_i^2 + C\left[\max_{i=1,\cdots,N}\int_{x_{i-1}}^{x_i}\Big(1+|w''(x)|^{1/2}\Big)dx\right]^2.
\end{aligned}$$

A similar technique used to derive the bound for I_1 can be applied to get

$$\begin{aligned}
I_2 &= \frac{C}{h_i}\max_{i=1,\cdots,N}\int_{x_{i-1}}^{x_i}\Big(1+\varepsilon^{-1}\exp(-ax/2\varepsilon)\Big)dx \times \\
&\quad \int_{x_{i-1}}^{x_i}(x-x_{i-1})\Big(1+\varepsilon^{-1}\exp(-ax/2\varepsilon)\Big)dx \\
&\leq C\left[\max_{i=1,\cdots,N}\int_{x_{i-1}}^{x_i}\Big(1+|w''(x)|^{1/2}\Big)dx\right]^2.
\end{aligned}$$

It should be noted that $\max\limits_i \max\limits_{[x_{i-1},x_i]} h_i^2[1+|w''(x)|^{1/2}]^2$ is the discrete analogue of continuous form of the error estimate $\left[\max\limits_{i=1,\cdots,N}\int_{x_{i-1}}^{x_i}\Big(1+|w''(x)|^{1/2}\Big)dx\right]^2$. From these two

expressions, it is clear that the monitor function which is being equidistributed to obtain the error estimate is $M\big(x, w(x)\big) = 1 + |w''(x)|^{1/2}$, where $w(x)$ is the singular component of the solution $u(x)$.

Henceforth, combining all these above estimates, it is clear from the equality (5.4.4) that

$$||\mathfrak{L}^N(u - \chi - U)||_{*,\Omega^N} \leq C \max_i \max_{[x_{i-1},x_i]} h_i^2[1 + |w''(x)|^{1/2}]^2. \tag{5.4.9}$$

Hence, the stability estimate (5.3.2) implies that

$$||u - \chi - U||_{*,\Omega^N} \leq C \max_i \max_{[x_{i-1},x_i]} h_i^2[1 + |w''(x)|^{1/2}]^2. \tag{5.4.10}$$

The key idea of Richardson extrapolation is to provide better numerical approximation of the exact solution, by considering an average of the numerical solutions in two embedded meshes. To explain this method, let us define a mesh $\bar{\Omega}^N \equiv \{0 = \bar{x}_0 < \bar{x}_1 < \cdots < \bar{x}_{2N} = 1\}$, which is obtained by bisecting the original mesh Ω^N with the step size $\bar{h}_i = \bar{x}_i - \bar{x}_{i-1}$. Now consider the discrete problem

$$\begin{cases} [\bar{\mathfrak{L}}^N \bar{U}]_i \equiv -\varepsilon[D^+D^-\bar{U}]_i - [D^+(\bar{a}\bar{U})]_i = \bar{f}_i, \quad \text{for} \quad i = 1, \cdots, 2N-1, \\ \bar{U}_0 = \bar{U}_N = 0. \end{cases} \tag{5.4.11}$$

Extrapolation technique will be used to improve the solutions at the points $x_i \in \Omega^N$, with the help of $\bar{U}$. As like (5.3.2), the stability estimate of the solution $\bar{U}$ implies that

$$||\bar{v}||_{\infty,\Omega^N} \leq 2a^{-1} \max_{i=1,\cdots,N-1} \left| \sum_{p=2i}^{2N-1} \bar{h}_{p+1}[\bar{\mathfrak{L}}^N \bar{v}]_p \right|, \quad \text{where} \quad \bar{v} \in R_0^{2N+1}. \tag{5.4.12}$$

Hence, following the derivation technique to obtain the expression (5.4.4), we deduce that

$$\begin{aligned} \sum_{p=2i}^{2N-1} \bar{h}_{p+1}[\bar{\mathfrak{L}}^N(\bar{u} - \frac{\bar{\chi}}{2} - \bar{U})]_p &= \varepsilon([D^-\bar{u}]_{2i} - \bar{u}'_{2i} + \frac{h_i}{4}u''_i) - \varepsilon([D^-\bar{u}]_{2N} - \bar{u}'_{2N} + \frac{h_N}{4}u''_N) \\ &\quad + \int_{x_i}^{1} \left(f(x) - \frac{h(x)}{2} f'(x) \right) dx - \sum_{p=2i}^{2N-1} \bar{h}_{p+1}\bar{f}_p \\ &\quad + \frac{\varepsilon}{2}\Big([D^-\bar{\chi}]_{2N} - \bar{\chi}'_{2N} \Big) - \frac{\varepsilon}{2}\Big([D^-\bar{\chi}]_{2i} - \bar{\chi}'_{2i} \Big), \end{aligned} \tag{5.4.13}$$

where $\bar{h}_{2i} = h_i/2$ for $i = 1, \cdots, N-1$. The procedure of bounding the first and fifth terms of (5.4.4) can be extended to find the bounds of the corresponding terms in (5.4.13). Hence, we shall be considering only the expressions involving $f(x)$.

Denoting $f_{p+1/2} = f(x_p + x_{p+1})/2$, observe that

$$\begin{aligned}
&\int_{x_p}^{x_{p+1}} \left(f(x) - \frac{h(x)}{2} f'(x) \right) dx - \bar{h}_{2p+1}\bar{f}_{2p} - \bar{h}_{2p+2}\bar{f}_{2p+1} \\
&= \int_{x_p}^{x_{p+1}} \left(f(x) - \frac{h(x)}{2} f'(x) \right) dx - \frac{h_{p+1}}{2}(f_p + f_{p+1/2}) \\
&= \frac{1}{2}\left[\int_{x_p}^{x_{p+1}} (f(x) - h(x)f'(x))dx - h_{p+1}f_p \right] + \frac{1}{2}\left[\int_{x_p}^{x_{p+1}} f(x)dx - h_{p+1}f_{p+1/2} \right].
\end{aligned} \tag{5.4.14}$$

The first term of the above expression is bounded from (5.4.6), *i.e.*,

$$\left| \int_{x_p}^{x_{p+1}} (f(x) - h(x)f'(x))dx - h_{p+1}f_p \right| \leq Ch_{p+1}^3.$$

To bound the second term, the Taylor series expansion of $f(x)$ with respect to the point $x_{p+1/2}$, up to second-order derivative implies that

$$\left| \int_{x_p}^{x_{p+1}} f(x)dx - h_{p+1}f_{p+1/2} \right| \leq Ch_{p+1}^3.$$

By combining the above two inequalities, we get

$$\int_{x_i}^{1} \left(f(x) - \frac{h(x)}{2} f'(x) \right) dx - \sum_{p=2i}^{2N-1} \bar{h}_{p+1}\bar{f}_p \leq C \max_i h_i^2 \leq C \max_i \max_{[x_{i-1},x_i]} h_i^2 [1 + |w''(x)|^{1/2}]^2.$$

Hence, the stability estimate for the discrete operator (5.4.11) leads to

$$||u - \frac{\chi}{2} - \bar{U}||_{\infty,\Omega^N} \leq C \max_i \max_{[x_{i-1},x_i]} h_i^2 [1 + |w''(x)|^{1/2}]^2. \tag{5.4.15}$$

Now, we are in a position to define the extrapolated solution. Let U_{extp} be the solution obtained through Richardson extrapolation, which is defined as

$$U_{i,extp} = 2\bar{U}_{2i} - U_i, \quad \text{for} \quad i = 0, \cdots, N. \tag{5.4.16}$$

Then, from the triangle inequality, we have

$$\begin{aligned}
\|u - U_{extp}\|_{\infty,\Omega^N} &= \|(2u - \chi - 2\bar{U}) - (u - \chi - U)\|_{\infty,\Omega^N} \\
&\leq 2\|u - \frac{1}{2}\chi - \bar{U}\|_{\infty,\Omega^N} + \|u - \chi - U\|_{\infty,\Omega^N}.
\end{aligned} \tag{5.4.17}$$

Therefore, by combining (5.4.10) and (5.4.15) in (5.4.17), we get

$$\|u - U_{extp}\|_{\infty,\Omega^N} \leq C \max_i \max_{[x_{i-1},x_i]} h_i^2 [1 + |w''(x)|^{1/2}]^2. \tag{5.4.18}$$

Note that the error estimator appearing in the right-hand side of the above expression depends on the singular component $w(x)$ of the solution $u(x)$. In reality, from the

apriori analysis, it is observed that the boundary layer phenomena occurs actually from the singular component of the solution. Assuming sufficient smoothness of the given data $a(x)$ and $f(x)$, it should also be noted that the derivatives of the decomposed solution's smooth component $v(x)$ can be uniformly bounded irrespective of the perturbation parameter ε from Lemma 5.2.2. This fact can be used to get a proper error estimator to improve the numerical solution, which can avoid of finding the singular component of the solution at the time of generating a new mesh through equidistribution. Now observe that the solution decomposition and Lemma 5.2.2 lead to

$$|w''(x)| \leq |u''(x)| + |v''(x)| \leq C[1 + |u''(x)|].$$

Hence the expression (5.4.18) reduces to

$$\|u - U_{extp}\|_{\infty,\Omega^N} \leq C \max_i \max_{[x_{i-1},x_i]} h_i^2 [1 + |u''(x)|^{1/2}]^2. \tag{5.4.19}$$

Therefore, we can state the main theorem of this chapter as follows.

Theorem 5.4.4. *If u is the solution of the convection-diffusion problem (5.1.1) and U_{extp} is the extrapolated solution obtained through Richardson extrapolation formula (5.4.16), then we have*

$$\|u - U_{extp}\|_{\infty,\Omega^N} \leq C \max_i \max_{[x_{i-1},x_i]} h_i^2 [1 + |u''(x)|^{1/2}]^2, \tag{5.4.20}$$

where C is independent of the perturbation parameter ε and the number of mesh intervals N.

5.5 Numerical Experiments

This section presents two numerical examples to confirm the theoretical findings. For these two text problems, layer-adapted meshes are obtained by the equidistribution of two monitor functions stated in (5.1.2).

Example 5.5.1. *Consider the following singularly perturbed two-point BVP:*

$$\begin{cases} -\varepsilon u''(x) - u'(x) + 2u(x) = \exp(x-1), \quad x \in \Omega, \\ \\ u(0) = 0, \quad u(1) = 0. \end{cases}$$

The exact solution of this problem is

$$u(x) = c_1 \exp(m_1 x) + c_2 \exp(m_2 x) - \exp(x-1)/(\varepsilon(1-m_1)(1-m_2)),$$

where

$$c_2 = \frac{1 - \exp(-1 + m_1)}{(1-m_1)(1-m_2)\varepsilon(\exp(m_2) - \exp(m_1))}, \quad \text{and}$$

$$c_1 = -c_2 + \frac{\exp(-1)}{\varepsilon(1-m_1)(1-m_2)},$$

with $m_1 = (-1 + \sqrt{1+8\varepsilon})/2\varepsilon, \quad m_2 = (-1 - \sqrt{1+8\varepsilon})/2\varepsilon.$

Example 5.5.2. *Consider the singularly perturbed convection-diffusion BVP:*

$$\begin{cases} \varepsilon u''(x) + ((1 + x(1-x))u(x))' = \exp(x), \quad x \in \Omega, \\ u(0) = 0, \quad u(1) = 0. \end{cases}$$

For these two problems, we take ε from the set S defined as

$$S = \left\{\varepsilon | \varepsilon = 2^{-2}, \cdots, 2^{-30}\right\},$$

and for the numerical computation, the adaptively generated meshes are constructed using the constants $C_0 = 1.6$ and $C_0 = 1.7$, respectively in the adaptive algorithm described in Chapter 2.

Table 5.1: *Improved uniform errors and orders of convergence using the monitor function $M(x, w(x))$ for Example 5.5.1.*

Extrapolation	Number of intervals N						
	64	128	256	512	1024	2048	4096
Before	8.764e-3	4.046e-3	1.945e-3	9.611e-4	4.807e-4	2.471e-4	1.201e-4
	1.1151	1.0570	1.0169	0.9996	0.9600	1.0409	-
After	1.712e-4	3.371e-5	7.728e-6	2.372e-6	5.187e-7	1.495e-7	3.262e-8
	2.3446	2.1250	1.7041	2.1932	1.7942	2.1966	-

Table 5.2: *Improved uniform errors and orders of convergence using the monitor function $M(x, u(x))$ for Example 5.5.1.*

Extrapolation	Number of intervals N						
	64	128	256	512	1024	2048	4096
Before	1.041e-2	4.547e-3	2.210e-3	1.110e-3	5.227e-4	2.823e-4	1.344e-4
	1.1951	1.0439	0.9913	1.0858	0.8887	1.0711	-
After	3.041e-4	5.880e-5	1.496e-5	3.951e-6	8.354e-7	2.592e-7	5.372e-8
	2.3706	1.9744	1.9209	2.2418	1.6882	2.2706	-

For Examples 5.5.1 and 5.5.2, we displayed the maximum uniform errors and the corresponding rates of convergence row-wise respectively, using maximum norm. In Table 5.1, we presented the uniform errors for Example 5.5.1 before and after extrapolation where the mesh is obtained by the equidistribution of the monitor function $M(x, w(x))$. From Table 5.2, one can see that there is strong correlation between the two monitor functions $M(x, w(x))$ and $M(x, u(x))$. In fact, Table 5.2 suggests that one can use

$M(x, u(x))$ as a monitor function to get better convergence rate, in order to avoid the reduced problem (*i.e.,* by taking $\varepsilon = 0$) solving each time. It should also be noted that the derivatives of the smooth component of the solution $u(x)$ are uniformly bounded from Lemma 5.2.2. A similar observation is noticed for Example 5.5.2, where the uniform errors and the corresponding rates of convergence are displayed in Table 5.3 and Table 5.4 for the two monitor functions $M(x, w(x))$ and $M(x, u(x))$ respectively. To discretize the second-order derivative appearing in the monitor function, we have used the same operator, which is used to discretize the second-order derivative of the differential equation. However, it is observed that the central difference approximation for second-order derivative term does not change the theoretical findings as depicted in Tables 5.5 and 5.6.

For the above two examples, extrapolation technique has improved the order of convergence from first-order to second-order. A rapidly decreasing behavior of ε-uniform errors after extrapolation can be noticed for these two problems, as N increases. Some variations in the numerical results from actual theoretical findings is expected, since instead of solving the equidistribution problem (1.1.3) exactly, we have solved the weakly equidistribution problem (2.5.1) for $C_0 = 1.6$ and $C_0 = 1.7$, respectively. Although the errors are more uniform for smaller values of C_0, but the improvements are insignificant. Observe that a similar kind of result with weakly equidistribution principle (2.5.1) is obtained by Kopteva et al. [44] and also by Das and Natesan [21].

The proposed improvement can be compared with the results obtained by Natividad and Stynes [64], where a second-order up to a logarithmic factor is achieved through the extrapolation technique on Shishkin meshes. As like us, Linß [48] obtained a similar result with *apriori* chosen Shishkin and Bakhvalov meshes for Example 5.5.1. But the plus point of adaptive technique with the monitor function $M(x, u(x))$ is that it does not need any *apriori* information about the location and width of the boundary layer.

In Figure 5.1 and Figure 5.2, we have plotted the maximum point-wise errors versus number of mesh intervals for Example 5.5.1 and Example 5.5.2. These figures are drawn in logarithmic scale for $\varepsilon = 2^{-30}$, with $M(x, u(x))$ as a monitor function. Graphically these also suggest that the computed errors are decreasing with the rate of $O(N^{-1})$ and $O(N^{-2})$ approximately before and after extrapolation.

5.6 Conclusion

In this chapter, a post-processing technique is considered to obtain higher-order convergent numerical approximate solution for convection-diffusion SPPs on adaptively generated mesh. First, a monitor function is generated from the error analysis, which provides first-order convergence for the discrete solution. This monitor function is a variant of

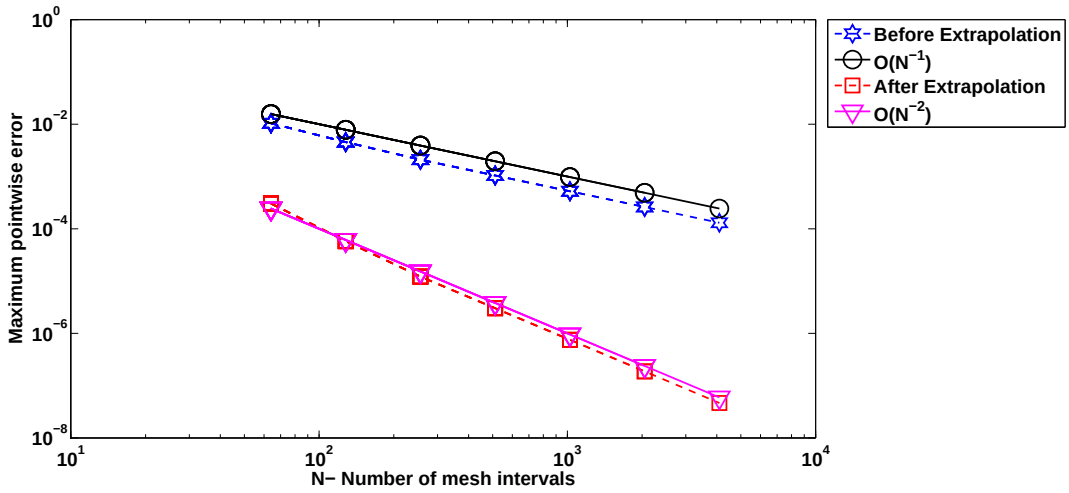

Figure 5.1: *Loglog plot of the maximum point-wise errors before and after extrapolation for Example 5.5.1 for* $\varepsilon = 2^{-30}$ *with the monitor function* $M(x, u(x))$.

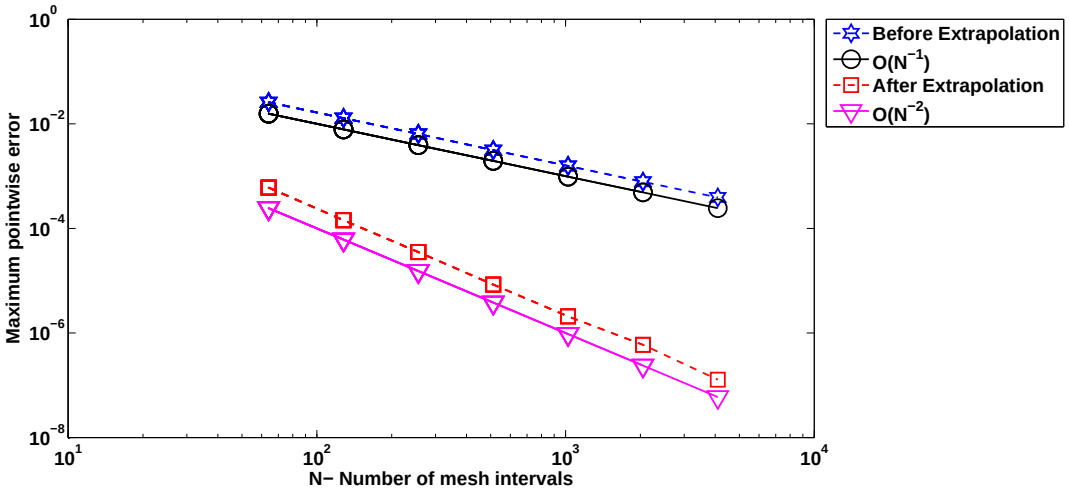

Figure 5.2: *Loglog plot of the maximum point-wise errors before and after extrapolation for Example 5.5.2 for* $\varepsilon = 2^{-30}$ *with the monitor function* $M(x, u(x))$.

the monitor function proposed by Beckett and Mackenzie [8, 9], where the constant (α in (2.2.1)) is chosen appropriately from their error analysis. Using this monitor function, it is shown that the Richardson extrapolation technique can be used to obtain higher-order (in this case second-order) convergence on equidistributed nonuniform mesh. Though the analysis provided here is for a simple model problem, it gives us a useful insight about one possible way (using post-processing technique) to obtain a higher-order convergent solution.

Table 5.3: *Improved uniform errors and orders of convergence using the monitor function $M(x, w(x))$ for Example 5.5.2.*

Extrapolation	Number of intervals N						
	64	128	256	512	1024	2048	4096
Before	3.555e-2	1.553e-2	7.538e-3	3.758e-3	1.871e-3	9.350e-4	4.673e-4
	1.1948	1.0428	1.0040	1.0061	1.0009	1.0005	-
After	7.368e-4	1.515e-4	3.057e-5	8.056e-6	1.873e-6	5.352e-7	1.307e-7
	2.2821	2.3089	1.9241	2.1044	1.8073	2.0335	-

Table 5.4: *Improved uniform errors and orders of convergence using the monitor function $M(x, u(x))$ for Example 5.5.2.*

Extrapolation	Number of intervals N						
	64	128	256	512	1024	2048	4096
Before	3.101e-2	1.281e-2	6.336e-3	3.194e-3	1.567e-3	8.224e-4	3.967e-4
	1.2752	1.0161	0.9884	1.0274	0.9298	1.0518	-
After	9.039e-4	1.435e-4	3.695e-5	1.019e-5	2.184e-6	6.824e-7	1.727e-7
	2.6547	1.9576	1.8587	2.2219	1.6784	1.9823	-

Table 5.5: *Improved uniform errors and orders of convergence for the central difference approx. to the second-order derivative term of the monitor function $M(x, u(x))$ for Example 5.5.1.*

Extrapolation	Number of intervals N						
	64	128	256	512	1024	2048	4096
Before	1.182e-2	4.582e-3	2.125e-3	1.084e-3	5.240e-4	2.823e-4	1.344e-4
	1.3677	1.1087	0.9714	1.0482	0.8923	1.0711	-
After	3.891e-4	5.878e-5	1.259e-5	3.951e-6	8.354e-7	2.592e-7	5.372e-8
	2.7266	2.2229	1.6722	2.2418	1.6882	2.2706	-

Table 5.6: *Improved uniform errors and orders of convergence for the central difference approx. to the second-order derivative term of the monitor function $M(x, u(x))$ for Example 5.5.2.*

Extrapolation	Number of intervals N						
	64	128	256	512	1024	2048	4096
Before	2.898e-2	1.277e-2	6.342e-3	3.164e-3	1.569e-3	8.224e-4	3.967e-4
	1.1826	1.0097	1.0034	1.0120	0.9316	1.0518	-
After	7.848e-4	1.434e-4	3.701e-5	1.019e-5	2.184e-6	6.824e-7	1.920e-7
	2.4518	1.9546	1.8608	2.2219	1.6784	1.8291	-

Chapter 6

Robust Numerical Method for System of Singularly Perturbed Convection-Diffusion Boundary-Value Problems

This chapter analyzes the numerical solution of a system of singularly perturbed weakly coupled convection-diffusion differential equations having diffusion parameters of different magnitudes. These small parameters give rise to boundary layers. An upwind based finite difference scheme is used to get several suitable monitor functions whose equidistribution will lead to the layer-adapted meshes. A monitor function which works well for both singularly perturbed scalar convection-diffusion and reaction diffusion problems is extended for a system of weakly coupled convection-diffusion problems. Utilizing this preferred monitor function, it is observed that the discrete solution is first-order uniformly convergent for linear and semilinear system of BVPs.

6.1 Introduction

Consider the following system of weakly coupled (coupled through the reaction terms) singularly perturbed convection-diffusion BVPs:

$$\begin{cases} \mathbf{L}\boldsymbol{u} \equiv \ -\boldsymbol{Eps}\ \boldsymbol{u}''(x) - \boldsymbol{A}(x)\boldsymbol{u}'(x) + \boldsymbol{B}(x)\boldsymbol{u}(x) = \boldsymbol{f}(x),\ x \in \Omega, \\ \boldsymbol{u}(0) = \boldsymbol{u}(1) = \boldsymbol{0}, \end{cases} \tag{6.1.1}$$

where $\mathbf{L} = (\mathbf{L}_1, \cdots, \mathbf{L}_k)^T$, $\boldsymbol{Eps} = \text{diag}(\varepsilon_1, \varepsilon_2, \cdots, \varepsilon_k)$, $\boldsymbol{A}(x) = \text{diag}(a_{11}(x), a_{22}(x), \cdots, a_{kk}(x))$, $\boldsymbol{B}(x) = (b_{ij}(x))_{k\times k}$, $\boldsymbol{f}(x) = (f_1(x), f_2(x), \cdots, f_k(x))^T$ and $\boldsymbol{u}(x) = (u_1(x), \cdots, u_k(x))^T$.

Without loss of generality, we shall assume that $\min\left\{a_{11}(x), a_{22}(x), \cdots, a_{kk}(x)\right\} \geq \alpha > 0$. The matrix $\boldsymbol{B} = (b_{ij})_{i,j=1}^{k}$ is considered as an L_0-matrix (*i.e.,* off diagonal entries are nonpositive and diagonal entries are positive) with

$$\min_{x\in\overline{\Omega}; m=1,\cdots,k} \left\{ \sum_{j=1}^{k} b_{mj}(x) \right\} \geq \beta > 0. \tag{6.1.2}$$

It will be assumed that the entries of the coefficient matrices $\boldsymbol{A}(x)$, $\boldsymbol{B}(x)$ and the vector $\boldsymbol{f}(x)$, *i.e.,* $a_{ii}(x)$, $b_{ij}(x)$, $f_i(x)$ are in $\mathcal{C}^2(\Omega)$ for $i, j = 1, \cdots, k$.

The outline of this chapter is as follows: In Section 6.2, the analytical solution bound of the system of equations (6.1.1) is derived using the solution bound of the scalar form of the convection-diffusion problem. Bounds of the continuous solution derivatives are also provided here. Then, in Section 6.3, an upwind scheme is used for the numerical discretization of (6.1.1). Stability bound of the discrete solution is also provided in this section. The first-order uniform convergence using the proposed monitor function is derived here from a sufficient condition of uniform convergence using the discrete supremum norm. In Section 6.4, a semilinear system of singularly perturbed convection-diffusion problem is considered. Finally, Section 6.5 conducts the numerical experiments using an adaptive algorithm to show that the rate of convergence predicted by theoretical analysis holds true in practice.

6.2 Continuous Problem and Solution Bounds

This section provides the stability property of the analytical solution $\boldsymbol{u}$ of (6.1.1). We start by recalling the stability of the scalar convection-diffusion operator, which will be used to derive the stability of the solution $\boldsymbol{u}$. The following lemma (see for *e.g.,* [55]) provides the stability estimate of the general scalar operator.

Lemma 6.2.1. *Assume the coefficients of*

$$\begin{cases} -\varepsilon u'' - a(x)u' + b(x)u = f(x), \quad \text{for} \quad x \in \Omega, \\ \\ u(0) = u(1) = 0, \end{cases} \tag{6.2.1}$$

satisfies $a(x), b(x) \in \mathcal{C}(\Omega)$ with $\varepsilon > 0, a(x) \geq \alpha > 0, b(x) \geq \beta > 0$ for all $x \in \overline{\Omega}$. Then, for any $u \in \mathcal{C}^2(\Omega) \cap \mathcal{C}(\overline{\Omega})$, we have the following stability estimate

$$||u|| \leq \min\left\{ \left\| \frac{f}{a} \right\|, \left\| \frac{f}{b} \right\| \right\}.$$

Now, with the help of above lemma the stability for each component of $\boldsymbol{u}$ is addressed here.

Lemma 6.2.2. *Let $\boldsymbol{u}$ be the solution of (6.1.1) and assume that the coupling matrix $\boldsymbol{B}$ satisfy the L_0-matrix condition (6.1.2). Then*

$$||u_m|| \leq \sum_{l=1}^{k} (\Upsilon^{-1})_{ml} \min\left\{\left\|\frac{f_l}{a_{ll}}\right\|, \left\|\frac{f_l}{b_{ll}}\right\|\right\},$$

where the $k \times k$ matrix $\Upsilon = \Upsilon(\boldsymbol{A},\boldsymbol{B}) = (\gamma_{ml})_{k\times k}$ is such that

$$\gamma_{ml} = -\min\left\{\left\|\frac{b_{ml}}{b_{mm}}\right\|, \left\|\frac{b_{ml}}{a_{mm}}\right\|\right\}, \text{ for } m \neq l \text{ and } \gamma_{mm} = 1.$$

Proof. A single equation from (6.1.1) can be written as

$$-\varepsilon_m u_m'' - a_{mm}u_m' + b_{mm}u_m = f_m - \sum_{l=1, l\neq m}^{k} b_{ml}u_l, \text{ for } m = 1, \cdots, k. \tag{6.2.2}$$

Under the condition of L_0-matrix, Lemma 6.2.1 yields

$$||u_m|| - \sum_{l=1, l\neq m}^{k} \min\left\{\left\|\frac{b_{ml}}{b_{mm}}\right\|, \left\|\frac{b_{ml}}{a_{mm}}\right\|\right\} ||u_l|| \leq \min\left\{\left\|\frac{f_m}{a_{mm}}\right\|, \left\|\frac{f_m}{b_{mm}}\right\|\right\}, \quad m = 1, \cdots, k.$$

Now define a $k \times k$ matrix $\Upsilon = \Upsilon(\boldsymbol{A}, \boldsymbol{B}) = (\gamma_{ml})_{k\times k}$ such that

$$\gamma_{ml} = -\min\left\{\left\|\frac{b_{ml}}{b_{mm}}\right\|, \left\|\frac{b_{ml}}{a_{mm}}\right\|\right\}, \text{ for } m \neq l \text{ and } \gamma_{mm} = 1.$$

If we assume Υ to be inverse monotone *i.e.,* $\Upsilon^{-1} \geq 0$, then

$$||u_m|| + \sum_{l=1, l\neq m}^{k} \gamma_{ml}||u_l|| \leq \min\left\{\left\|\frac{f_m}{a_{mm}}\right\|, \left\|\frac{f_m}{b_{mm}}\right\|\right\}, \quad m = 1, \cdots, k.$$

The matrix $\boldsymbol{B}$ is assumed to be an L_0-matrix from (6.1.2). Therefore, Υ will be inverse monotone. Hence, we get the required stability bound. ∎

As a consequence the stability of the continuous solution $\boldsymbol{u}(x)$ can be obtained. It should be noted that, one can directly compute the inverse of the matrix Υ from the definition of Υ. Its sign pattern for the condition of inverse monotonicity can also be checked. Therefore, in order to get the stable solution of (6.1.1), the L_0-matrix condition is not necessary for the matrix $\boldsymbol{B}$. The following theorem provides the derivative estimates of the solution $\boldsymbol{u}$.

Theorem 6.2.3. *Under the assumptions from (6.1.2), the solution $\boldsymbol{u}$ of the system (6.1.1) and its derivatives satisfy the following bounds for $x \in \overline{\Omega}$,*

$$|u_m^{(n)}| \leq C\left[1 + \varepsilon_m^{-n}\exp\left(-\frac{\alpha_m x}{\varepsilon_m}\right)\right], \text{ where } a_{mm}(x) \geq \alpha_m, \text{ for } n = 0, 1, \text{ and}$$

$$|u_m^{(2)}| \leq C\left[1 + \sum_{p=1}^{k} \varepsilon_p^{-2}\exp\left(-\frac{\alpha_p x}{\varepsilon_p}\right)\right], \text{ where } a_{pp}(x) \geq \alpha_p, \text{ for } m, p = 1, \cdots, k.$$

Proof. The bounds of the solution $\boldsymbol{u}$ and its first-order derivative are given by Linß [49], where a standard technique, provided in Kellog and Tsan [41] for scalar operators is used. The proof provided in Zhongdi [85] can be extended to bound the solutions second-order derivative. ∎

6.3 Upwind Finite Difference Scheme

This section is devoted for the discretization of the continuous problem. Monitor functions generated by the error analysis are also derived in this section, which can be equidistributed to obtain layer-adapted meshes.

6.3.1 Discrete problem

Here, we shall consider the finite difference approximation of (6.1.1) on a nonuniform mesh $\Omega^N \equiv \{0 = x_0 < x_1 < \cdots < x_N = 1\}$. Let us define $\boldsymbol{U}$ be the discrete approximation of the continuous solution $\boldsymbol{u}(x)$. Therefore, by denoting $\boldsymbol{U}_i = \boldsymbol{U}(x_i)$, the discretized problem of (6.1.1) is defined as follows: Find $\boldsymbol{U}_1, \cdots, \boldsymbol{U}_{N-1}$ satisfying

$$\begin{cases} [\mathbf{L}^N \boldsymbol{U}]_i \equiv \boldsymbol{f}_i, \quad \text{for} \quad i = 1, 2, \cdots, N-1, \\ \boldsymbol{U}_0 = \boldsymbol{U}_N = 0, \end{cases}$$

i.e., find $U_{m,1}, \cdots, U_{m,N-1}$, for $m = 1, \cdots, k$ satisfying

$$\begin{cases} [\mathbf{L}_m^N \boldsymbol{U}]_i \equiv [\Lambda_m^N U_m]_i + \sum_{l=1, l\neq m}^{k} b_{ml} U_{l;i} = f_{m;i}, \quad \text{with} \quad i = 1, 2, \cdots, N-1, \\ U_{m,0} = U_{m,N} = 0, \end{cases} \tag{6.3.1}$$

where $\mathbf{L}^N = (\mathbf{L}_1^N, \mathbf{L}_2^N, \cdots, \mathbf{L}_k^N)^T$ is the discrete analogue of $\mathbf{L}$ and

$$[\Lambda_m^N v]_i \equiv -\varepsilon_m D^+ D^- v_i - a_{mm;i} D^+ v_i + b_{mm;i} v_i.$$

In a similar way, if a_{mm} is negative, then the upwind scheme will be defined as

$$[\Lambda_m^N v]_i \equiv -\varepsilon_m D^- D^+ v_i - a_{mm;i} D^- v_i + b_{mm;i} v_i.$$

This discrete solution satisfies the following stability result (see for *e.g., [49, 1]*).

Lemma 6.3.1. *Under the conditions of an L_0-matrix (6.1.2), we have*

$$||v||_{\Omega^N} \leq \left\| \frac{\Lambda_m^N v}{b_{mm}} \right\|_{\Omega^N}, \ \textit{for } v \in \mathbb{R}^{N+1},$$

and

$$||v||_{\Omega^N} \leq C ||\Lambda_m^N v||_{-1,\infty,\Omega^N} = C \min_{V: D^+ V = \Lambda_m^N v} ||V||_{\Omega^N}. \tag{6.3.2}$$

Let $\boldsymbol{E} = \boldsymbol{u} - \boldsymbol{U}$ be the error of the discrete solution obtained by the finite difference scheme (6.3.1), where $E_{m,i} = u_{m,i} - U_{m,i},\ m = 1(1)k,\ i = 0(1)N$, *i.e.,* $\boldsymbol{E} \in (\mathbb{R}^{N+1})^k$. We divide the error $\boldsymbol{E}$ in two components $\aleph$, $\Re$ such that $\boldsymbol{E} = \aleph + \Re$ satisfies

$$[\Lambda_m^N \aleph_m]_i = [\mathbf{L}_m^N(\boldsymbol{U} - \boldsymbol{u})]_i, \quad i = 1, 2, \cdots, N-1, \quad \aleph_{m,0} = \aleph_{m,N} = 0, \quad m = 1, 2, \cdots, k, \tag{6.3.3}$$

and

$$[\Lambda_m^N \Re_m]_i = -\sum_{l=1, l\neq m}^{k} b_{ml,i} E_{l;i}, \quad i = 1, 2, \cdots, N-1, \quad \Re_{m,0} = \Re_{m,N} = 0, \quad m = 1, 2, \cdots, k. \tag{6.3.4}$$

From Lemma 6.3.1, it follows that

$$||E_m||_{\Omega^N} \leq ||\aleph_m||_{\Omega^N} + ||\Re_m||_{\Omega^N} \leq ||\aleph_m||_{\Omega^N} + \sum_{l=1, l\neq m}^{k} \left\| \frac{b_{ml}}{b_{mm}} \right\|_{\Omega^N} ||E_l||_{\Omega^N}, \quad m = 1, 2, \cdots, k,$$

which leads to

$$||\boldsymbol{U} - \boldsymbol{u}||_{\Omega^N} \leq C||\aleph||_{\Omega^N}. \tag{6.3.5}$$

Now, using the stability inequality from Lemma 6.2.2 for the discrete solution together with the solution bound from Theorem 6.2.3, it is easy to derive the following lemma.

Lemma 6.3.2. *The solution of (6.3.3) i.e., the components $\aleph_m$ of the term $\aleph$ satisfy*

$$||\aleph_m||_{\Omega^N} \leq C \max_{i=1,\cdots,N} \int_{x_{i-1}}^{x_i} \left[1 + \sum_{m=1}^{k} |u_m'(x)|\right] dx,$$

where C is independent of the perturbation parameters ε_m and the number of mesh intervals N.

Proof. This result is proved in Linß [49]. ∎

Hence, the inequality (6.3.5) reduces to the following result.

Theorem 6.3.3. *Let $\boldsymbol{u}$ be the solution of the system (6.1.1) and $\boldsymbol{U}$ be the finite difference approximate solution of (6.3.1), then we have*

$$||\boldsymbol{u} - \boldsymbol{U}||_{\Omega^N} \leq C \max_{i=1,\cdots,N} \int_{x_{i-1}}^{x_i} \left[1 + \sum_{m=1}^{k} |u_m'(x)|\right] dx,$$

where C is independent of the perturbation parameters ε_m and the number of mesh intervals N.

The next theorem provides a sufficient condition for choosing appropriate monitor functions, whose equidistributions will lead to the layer-adapted meshes.

Theorem 6.3.4. *Assume that there exist positive constants C_1, C_2 and C_3 independent of the perturbation parameters ε_m, such that a monitor function $M(x, \boldsymbol{u}(x))$ satisfies*

$$\int_{x_{i-1}}^{x_i} \left[1 + \sum_{m=1}^{k} |u'_m(x)|\right] dx \leq C_1 \int_{x_{i-1}}^{x_i} M(x, \boldsymbol{u}(x))dx, \text{ for } i = 1, \cdots, N, \tag{6.3.6}$$

$$\int_0^1 M(x, \boldsymbol{u}(x))dx \leq C_2, \tag{6.3.7}$$

and

$$M(x, \boldsymbol{u}(x)) \geq C_3. \tag{6.3.8}$$

Then

$$||\boldsymbol{U} - \boldsymbol{u}||_{\Omega^N} \leq CN^{-1},$$

where C is independent of the perturbation parameters ε_m and the number of mesh intervals N.

Proof. Note that from the definition of equidistribution principle (1.1.4), we have

$$C_3 h_i \leq \int_{x_{i-1}}^{x_i} M(x, \boldsymbol{u}(x))dx = \frac{1}{N} \int_0^1 M(x, \boldsymbol{u}(x))dx \leq C_2 N^{-1} \Rightarrow h_i \leq C_2 C_3^{-1} N^{-1}.$$

Now using (6.3.6)-(6.3.8) with the equidistribution principle (1.1.4), we obtain

$$\begin{aligned} ||\aleph_m||_{\Omega^N} &\leq C \max_i \int_{x_{i-1}}^{x_i} \left[1 + \sum_{m=1}^{k} |u'_m(x)|\right] dx \\ &\leq C \int_{x_{i-1}}^{x_i} M(x, \boldsymbol{u}(x))dx \leq CN^{-1} \int_0^1 M(x, \boldsymbol{u}(x))dx \leq CN^{-1}. \end{aligned}$$

Hence, the inequality (6.3.5) leads to

$$||\boldsymbol{U} - \boldsymbol{u}||_{\Omega^N} \leq CN^{-1}.$$

■

Now consider the following monitor function

$$M(x, \boldsymbol{u}(x)) = 1 + \sum_{m=1}^{k} |u''_m|^{1/2}. \tag{6.3.9}$$

This monitor function is a generalized form of the monitor function proposed by Beckett and Mackenzie [8] for scalar case of (6.1.1), where the solution u is decomposed into two components the so called smooth component v and the singular component w. In reality, from the *apriori* analysis, it is observed that the boundary layer phenomena occurs actually from the singular component of the solution. It should also be noted that the second-order derivative of the smooth component v is bounded. This motivates them to consider a monitor function involving especially derivatives of the singular component. This monitor function works well also for reaction-diffusion type problems [9].

Now, our aim is to show that the above monitor function, where the solution is not decomposed into its singular component satisfies all conditions of Theorem 6.3.4. To show this observe that Theorem 6.2.3 with $\alpha = \min_m \alpha_m$ implies

$$\begin{aligned} |u_m''(x)|^{1/2} &\leq C\bigg[1 + \sum_{p=1}^{k} \varepsilon_p^{-2} \exp\bigg(-\frac{\alpha x}{\varepsilon_p}\bigg)\bigg]^{1/2} \\ &\leq C\bigg[\max\bigg(1, \varepsilon_p^{-2}\exp\bigg(-\frac{\alpha x}{\varepsilon_p}\bigg)\bigg)\bigg]^{1/2}, \text{ for } p = 1, 2, \cdots, k, \end{aligned}$$

where we have used the fact that for any n positive functions $g_1, g_2, \cdots, g_n$, we get

$$\bigg(\sum_{p=1}^{n} g_p\bigg)^{1/2} \leq \sqrt{n}\bigg[\max_p(g_p)\bigg]^{1/2}.$$

Note that

$$\int_0^1 \bigg[\varepsilon_p^{-2}\exp\bigg(-\frac{\alpha x}{\varepsilon_p}\bigg)\bigg]^{1/2} dx = \frac{\alpha}{2}\bigg[1 - \exp\bigg(-\frac{\alpha}{2\varepsilon_p}\bigg)\bigg] < \beta_p \quad \text{(say)}.$$

Therefore,

$$\int_0^1 M(x, \boldsymbol{u}(x))dx \leq \max(1, \beta_p) = C_2 \quad \text{(say)}.$$

Thus the condition (6.3.7) is satisfied. Now, from the equation (6.2.2), we have

$$u_m' = \frac{1}{a_{mm}}\bigg[-\varepsilon_m u_m'' + \sum_{l=1}^{k} b_{ml}u_l - f_m\bigg].$$

Hence, it follows from Lemma 6.2.2 that

$$|u_m'| \leq C[\varepsilon_m|u_m''| + 1].$$

Thereafter, it is enough to show that

$$\sum_{m=1}^{k} \varepsilon_m|u_m''| \leq C\sum_{m=1}^{k} |u_m''|^{1/2}.$$

From the given equation (6.2.2), we can write

$$|\varepsilon_m u_m^{''}| \leq C\bigg[1 + \varepsilon_m^{-1}\exp\bigg(\frac{-\alpha_m x}{\varepsilon_m}\bigg)\bigg]. \tag{6.3.10}$$

Now we shall show that $\varepsilon_m|u_m''| \leq C|u_m''|^{1/2}$. Assuming that $u_m'' \neq 0$, the inequality (6.3.10) leads to

$$\begin{aligned} |\varepsilon_m u_m''|^{1/2} &\leq C\bigg[1 + \varepsilon_m^{-1}\exp\bigg(-\frac{\alpha_m x}{\varepsilon_m}\bigg)\bigg]^{1/2} \\ &\leq \sqrt{2}C\bigg[\max\bigg(1, \varepsilon_m^{-1}\exp\bigg(-\frac{\alpha_m x}{\varepsilon_m}\bigg)\bigg)\bigg]^{1/2}. \end{aligned}$$

So

$$\varepsilon_m|u_m''|^{1/2} \leq C\sqrt{\varepsilon_m}\left[\max\left(1, \varepsilon_m^{-1}\exp\left(-\frac{\alpha_m x}{\varepsilon_m}\right)\right)\right]^{1/2} \leq C.$$

Hence, we have

$$\varepsilon_m|u_m''| \leq C|u_m''|^{1/2}.$$

Therefore, we obtain

$$\begin{aligned}
||\aleph_m||_{\Omega^N} &\leq C \max_{i=1,\cdots,N}\int_{x_{i-1}}^{x_i}\left[1+\sum_{m=1}^{k}|u_m'(x)|\right]dx \\
&\leq C \max_{i=1,\cdots,N}\int_{x_{i-1}}^{x_i}\left[1+\sum_{m=1}^{k}\varepsilon_m|u_m''(x)|\right]dx \\
&\leq C \max_{i=1,\cdots,N}\int_{x_{i-1}}^{x_i}\left[1+\sum_{m=1}^{k}|u_m''(x)|^{1/2}\right]dx,
\end{aligned}$$

i.e.,

$$\max_{i=1,\cdots,N}\int_{x_{i-1}}^{x_i}\left[1+\sum_{m=1}^{k}|u_m'(x)|\right]dx \leq C\int_{x_{i-1}}^{x_i} M(x,\boldsymbol{u}(x))dx.$$

Again, we have

$$1 \leq M(x,\boldsymbol{u}(x)).$$

Thus, conditions (6.3.6) and (6.3.8) are satisfied. Hence, Theorem 6.3.4 implies that

$$||\boldsymbol{U}-\boldsymbol{u}||_{\Omega^N} \leq CN^{-1}.$$

Now, we state the main result of this chapter.

Theorem 6.3.5. *Let $\boldsymbol{u}$ be the solution of (6.1.1) and $\boldsymbol{U}$ be the numerical solution of the discretized problem (6.3.1), on the mesh Ω^N, which is obtained by equidistributing the monitor function (6.3.9). Then there exists a constant C, independent of N and ε, such that*

$$\|\boldsymbol{u}-\boldsymbol{U}\|_{\Omega^N} \leq CN^{-1}.$$

Another commonly used error function is the arc-length type monitor function, where the errors are equidistributed using the arc-length of the solution. This function was formerly used by Kopteva [45] for scalar form of convection-diffusion problems. Thereafter, Linß [50] extended it for a system of convection-diffusion problems, by

$$M_{arc}(x,\boldsymbol{u}(x)) = \left(1+\sum_{m=1}^{k}|u_m'(x)|^2\right)^{1/2}.$$

Using the inequality $\left(\sum_{i=1}^{k} g_i\right) \leq \sqrt{2}\left(\sum_{i=1}^{k} g_i^2\right)^{1/2}$ for positive real numbers g_i, one can also verify (6.3.6)-(6.3.8), for this monitor function with lower bound $\sqrt{2}$. It is also

observed by Kopteva et al. [44] that the monitor function $M_{arc}(x, \boldsymbol{u}(x))$ will not yield parameter-uniform convergence for singularly perturbed reaction-diffusion problems.

A well-known *apriori* chosen mesh known as Bakhvalov mesh (see [74]) can be constructed to provide the parameter-uniform convergence for singularly perturbed system of coupled convection-diffusion problems (see for *e.g.,* Linß [49, 50]) by equidistributing the monitor function

$$M_{ba}(x) = \max\left\{1, K_m\varepsilon_m^{-1}\exp\left(\frac{\alpha_m x}{\varepsilon_m}\right)\right\},$$

where K_ms are user chosen constants. Appropriateness of this monitor function from Theorem 6.3.4 can be verified by using the bounds of the solution u_m from Theorem 6.2.3 to Theorem 6.3.3. Therefore, the layer-adapted mesh obtained by the equidistribution of $M_{ba}(x)$ will provide the first-order parameter uniform convergence.

6.4 Semilinear Convection-Diffusion System

Consider the following singularly perturbed system of semilinear convection-diffusion problems

$$\begin{cases} \mathbf{L}\boldsymbol{u} \equiv -\boldsymbol{Eps}\ \boldsymbol{u}_{xx}(x) - \boldsymbol{A}(x)\boldsymbol{u}_x(x) + \ \boldsymbol{f}(x, \boldsymbol{u}(x)) = 0, \quad \text{for} \quad x \in \Omega, \\ \boldsymbol{u}(0) = \boldsymbol{u}(1) = 0, \end{cases} \tag{6.4.1}$$

where $\boldsymbol{f}(x, \boldsymbol{u}) = (f_1(x, \boldsymbol{u}), \cdots, f_k(x, \boldsymbol{u}))^T$. Here, $f_m(x, \boldsymbol{u})$ can involve nonlinear terms of $\boldsymbol{u}$ and the notations $\boldsymbol{u}_x$, $\boldsymbol{u}_{xx}$ are used instead of $\boldsymbol{u}'$ and $\boldsymbol{u}''$ respectively, for the sake of convenience. We shall assume that

$$\frac{\partial f_m}{\partial u_l}(x, \boldsymbol{u}) \le 0, \quad m \ne l, \quad \sum_{l=1}^{k} \frac{\partial f_m}{\partial u_l}(x, \boldsymbol{u}) \ge \beta > 0, \quad m = 1 \cdots, k, \tag{6.4.2}$$

on $(x, \boldsymbol{u}) \in \overline{\Omega} \times \mathbb{R}^k$. Assume that the reduced problem, which is defined by setting $\mathbf{Eps} = \mathbf{0}$ in (6.4.1), has a unique solution in $\overline{\Omega}$. Under this assumption, the system of BVP (6.4.1) admits a unique solution in $\overline{\Omega}$. Chang and Howes [17] studied the theoretical aspects corresponding to the semilinear system of convection-diffusion problems.

To obtain the numerical solution of the system (6.4.1), the well-known Newton's quasilinearization technique is used. This technique allows us to linearize the system into a sequence of linear problems, whose solutions $\boldsymbol{u}^{(p)}$ with a proper initial guess $\boldsymbol{u}^{(0)}$ will converge to the original solution $\boldsymbol{u}$. For each fixed nonnegative integer p define $\boldsymbol{u}^{(p+1)}$ to be the solution of the linear problem

$$\begin{cases} \overline{\mathbf{L}}\boldsymbol{u}^{(p+1)} \equiv -\boldsymbol{Eps}\ \boldsymbol{u}_{xx}^{(p+1)}(x) - \boldsymbol{A}(x)\boldsymbol{u}_x^{(p+1)}(x) + \boldsymbol{J}(x)\boldsymbol{u}^{(p+1)}(x) = \boldsymbol{F}(x, \boldsymbol{u}^{(p)}(x)), \\ \boldsymbol{u}^{(p+1)}(0) = \boldsymbol{u}^{(p+1)}(1) = 0, \quad \text{for } x \in \Omega, \end{cases} \tag{6.4.3}$$

for $p = 0, 1, \cdots$. Here $\boldsymbol{J}(x)$ is the Jacobian matrix which is given by

$$\boldsymbol{J}(x) = \begin{pmatrix} \dfrac{\partial f_1(x, \boldsymbol{u}^{(p)})}{\partial u_1} & \cdots & \dfrac{\partial f_1(x, \boldsymbol{u}^{(p)})}{\partial u_k} \\ \vdots & \ddots & \vdots \\ \dfrac{\partial f_k(x, \boldsymbol{u}^{(p)})}{\partial u_1} & \cdots & \dfrac{\partial f_k(x, \boldsymbol{u}^{(p)})}{\partial u_k} \end{pmatrix}_{k \times k},$$

and $\boldsymbol{F}(x, \boldsymbol{u}^{(p)}) = \boldsymbol{J}(x)\boldsymbol{u}^{(p)}(x) - \boldsymbol{f}(x, \boldsymbol{u}^{(p)}(x))$. It is easy to see that the Jacobian matrix $\boldsymbol{J}(x)$ satisfies all the conditions of an L_0- matrix defined in (6.1.2). If the initial guess $\boldsymbol{u}^{(0)}$ is sufficiently close to the solution $\boldsymbol{u}$, then following the proof of [26], one can show that the sequence $\boldsymbol{u}^{(p+1)}$ converges to the solution $\boldsymbol{u}$. The solution of the associated reduced problem can be taken as an initial guess $\boldsymbol{u}^{(0)}(x)$. Since, for each fixed p the system (6.4.3) is a linear system of the form (6.1.1) the mesh generation procedure by equidistributing the proposed monitor function explained in Section 6.3 can be applied to generate a layer-adapted mesh. The obtained solution will converge uniformly to the continuous solution. We use the following criteria

$$|\boldsymbol{u}^{(p+1)}(x_i) - \boldsymbol{u}^{(p)}(x_i)| \leq Tol, \quad x_i \in \overline{\Omega}, \quad p \geq 0,$$

for the convergence of iterative quasi-linearization technique. Here, *Tol* denotes the user chosen tolerance.

6.5 Numerical Experiments

This section computationally verifies the theoretical results obtained in the previous section. For the numerical examples, we use the equidistribution technique to the proposed monitor function

$$M\big(x, \boldsymbol{u}(x)\big) = 1 + \sum_{m=1}^{k} |u_m''(x)|^{1/2}.$$

Algorithm 2.5.1 (stated in Chapter 2) is adapted for the generation of the equidistributed mesh and the corresponding adaptive finite difference solution.

Example 6.5.1. *Consider the singularly perturbed system of convection-diffusion problems:*

$$\begin{cases} -\varepsilon_1 u_1''(x) - u_1'(x) + 2u_1(x) - u_2(x) = f_1(x), \quad x \in \Omega, \\ -\varepsilon_2 u_2''(x) - 2u_2'(x) - u_1(x) + 4u_2(x) = f_2(x), \\ u_1(0) = u_1(1) = u_2(0) = u_2(1) = 0, \end{cases}$$

where $f_1(x)$ and $f_2(x)$ are chosen such a way, that the exact solution is given by

$$\begin{cases} u_1(x) = & \dfrac{1-\exp(-x/\varepsilon_1)}{1-\exp(-1/\varepsilon_1)} + \dfrac{1-\exp(-x/\varepsilon_2)}{1-\exp(-1/\varepsilon_2)} - 2\sin\dfrac{\pi}{2}x, \\ u_2(x) = & \dfrac{1-\exp(-x/\varepsilon_2)}{1-\exp(-1/\varepsilon_2)} - x\exp(x-1). \end{cases}$$

Example 6.5.2. *Consider the following system of convection-diffusion problems:*

$$\begin{cases} -\varepsilon_1 u_1''(x) + (5-x^2)u_1'(x) + (4+x)u_1(x) - u_2(x) = 2\exp(x), \quad x \in \Omega, \\ -\varepsilon_2 u_2''(x) - 6u_2'(x) - 2u_1(x) + (4-x)u_2(x) = 10x + 1, \\ u_1(0) = u_1(1) = u_2(0) = u_2(1) = 0. \end{cases}$$

Example 6.5.3. *Consider the semilinear system of convection-diffusion differential equations:*

$$\begin{cases} -\varepsilon_1 u_1'' - 2(x+1)^2 u_1' + u_1 - 1 - (1-u_1)^3 + \exp(u_1 - u_2) = 0, \quad x \in \Omega, \\ -\varepsilon_2 u_2'' - 5u_2' + u_2 - 0.5 - (0.5-u_2)^5 + \exp(u_2 - u_1) = 0, \\ u_1(0) = u_1(1) = u_2(0) = u_2(1) = 0. \end{cases}$$

The uniform errors E_m^N, $m = 1, 2$, of the numerical solution U_1 and U_2, for each fixed N and the corresponding parameter-uniform rates of convergence r_m^N are calculated by the formulas described in Chapter 2.

For the numerical experiments of all the test problems, we take ε_1 and ε_2 from the set

$$S = \{\varepsilon = (\varepsilon_1, \varepsilon_2) | \varepsilon_1 = 1, 2^{-2}, \cdots, 2^{-22}; \varepsilon_2 = 1, 2^{-2}, \cdots, 2^{-22}\},$$

and the adaptively generated mesh is constructed by taking $C_0 = 1.9$ in the adaptive algorithm described in Chapter 2. Here, we have used the central difference approximation to discretize the second-order derivative involved in the proposed monitor function (6.3.9).

In Table 6.1 and Table 6.2, we presented the uniform errors and the corresponding orders of convergence of the numerical solution components U_1 and U_2, respectively for Example 6.5.1, which clearly indicates that the proposed method is ε-uniform first-order accurate. A similar result was observed by Linß [50] for strongly coupled system of convection-diffusion problems using the arc-length type monitor function. The theoretical results obtained in this thesis, is also reflected for Example 6.5.2 as depicted in Table 6.3 and Table 6.4. These tables demonstrate the uniform errors and the corresponding first-order convergence of the solution components U_1 and U_2, respectively, where the double mesh principle is used to find errors and rates of convergence.

To show the effectiveness of the proposed monitor function, a numerical example is provided for a system of semilinear convection-diffusion problems in Example 6.5.3. Numerical results obtained for uniform errors and orders of convergence from Table 6.5 and Table 6.6 approve our theoretical findings for semilinear system of differential equations with $Tol = 10^{-8}$. In Figures 6.1-6.3, the maximum point-wise errors versus number of mesh intervals are demonstrated for Example 6.5.1, Example 6.5.2 and Example 6.5.3, respectively. These figures are drawn in logarithmic scale for $\varepsilon_1 = 2^{-22}$, $\varepsilon_2 = 2^{-16}$; $\varepsilon_1 = 2^{-10}$, $\varepsilon_2 = 2^{-22}$ and $\varepsilon_1 = 2^{-18}$, $\varepsilon_2 = 2^{-22}$ respectively. Graphically these also suggest that the computed errors are decreasing with the rate of $O(N^{-1})$ as the number of interval N increases.

Table 6.1: *Uniform errors and orders of convergence of U_1 for Example 6.5.1.*

$(\varepsilon_1, \varepsilon_2) \in S$	Number of intervals N						
	64	128	256	512	1024	2048	4096
E_1^N	1.292e-1	5.671e-2	2.809e-2	1.318e-2	6.428e-3	3.245e-3	1.649e-3
r_1^N	1.1878	1.0135	1.0915	1.0361	0.98625	0.97648	-

Table 6.2: *Uniform errors and orders of convergence of U_2 for Example 6.5.1.*

$(\varepsilon_1, \varepsilon_2) \in S$	Number of intervals N						
	64	128	256	512	1024	2048	4096
E_2^N	5.499e-2	2.677e-2	1.246e-2	6.617e-3	3.023e-3	1.482e-3	7.867e-4
r_2^N	1.0381	1.1030	0.91375	1.1299	1.0288	0.91366	-

Table 6.3: *Uniform errors and orders of convergence of U_1 for Example 6.5.2.*

$(\varepsilon_1, \varepsilon_2) \in S$	Number of intervals N						
	64	128	256	512	1024	2048	4096
E_1^N	1.687e-2	7.297e-3	4.112e-3	1.896e-3	9.565e-4	4.801e-4	2.404e-4
r_1^N	1.2094	0.82749	1.1164	0.98777	0.99434	0.99759	-

The advantage of generating mesh by adaptive technique is that it does not require any *apriori* knowledge about the locations and widths of the boundary layers. This technique leads to an optimal parameter-uniform convergence corresponding to the upwind discretization, by equidistributing the proposed monitor function.

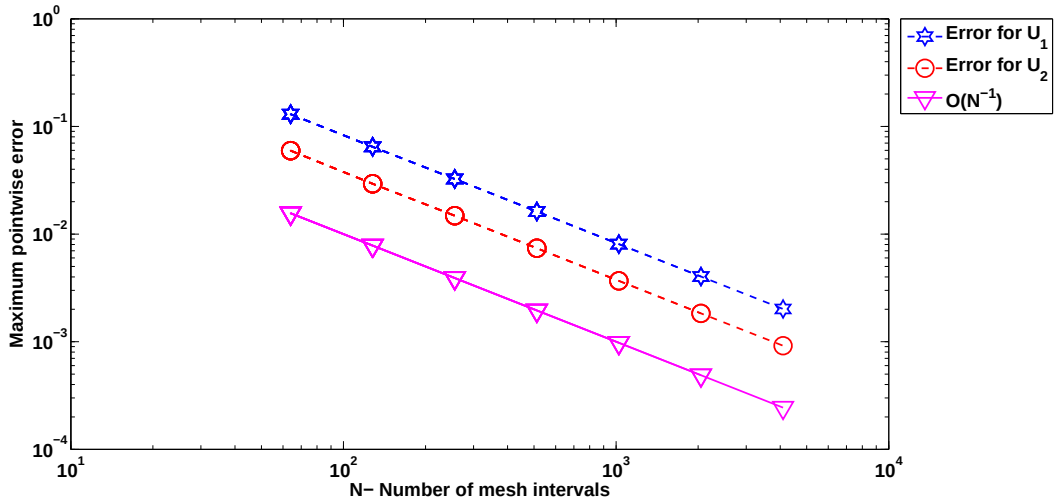

Figure 6.1: *Loglog plot of the maximum point-wise errors for Example 6.5.1 for* $\varepsilon_1 = 2^{-22}$ *and* $\varepsilon_2 = 2^{-16}$.

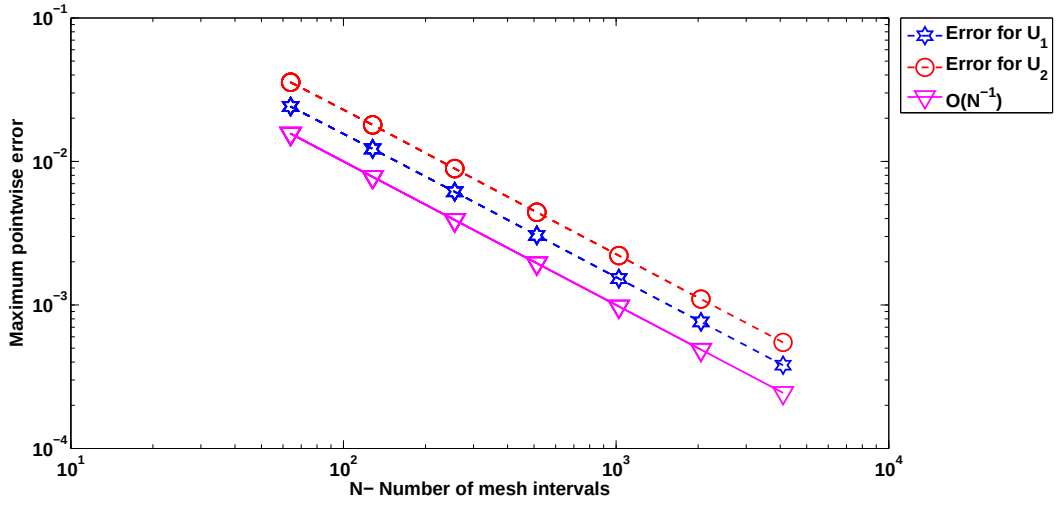

Figure 6.2: *Loglog plot of the maximum point-wise errors for Example 6.5.2 for* $\varepsilon_1 = 2^{-10}$ *and* $\varepsilon_2 = 2^{-22}$.

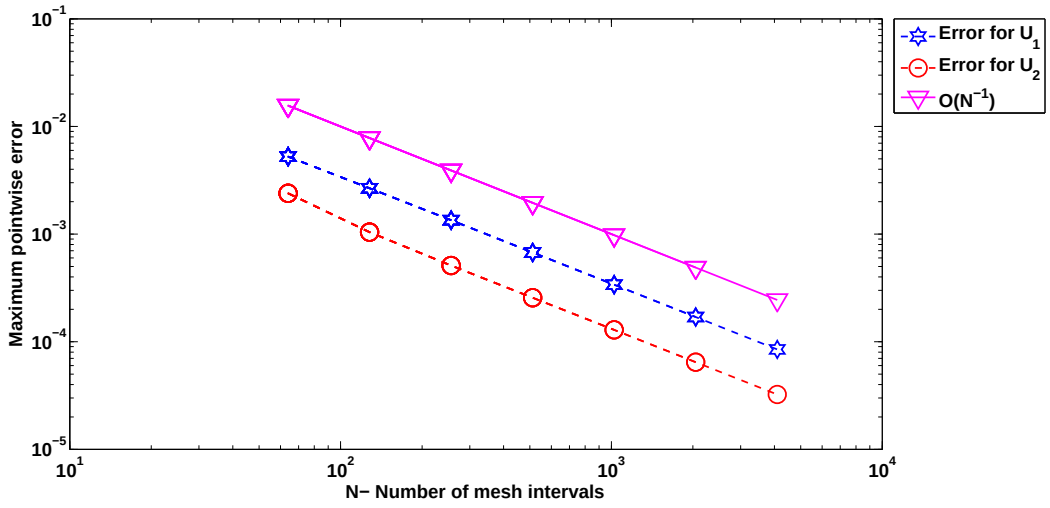

Figure 6.3: *Loglog plot of the maximum point-wise errors for Example 6.5.3 for* $\varepsilon_1 = 2^{-18}$ *and* $\varepsilon_2 = 2^{-22}$.

Table 6.4: *Uniform errors and orders of convergence of* U_2 *for Example 6.5.2.*

$(\varepsilon_1, \varepsilon_2) \in S$	Number of intervals N						
	64	128	256	512	1024	2048	4096
E_2^N	2.729e-2	1.221e-2	6.246e-3	3.170e-3	1.596e-3	8.010e-4	4.014e-4
r_2^N	1.1598	0.96798	0.97815	0.99007	0.99469	0.99677	-

6.6 Conclusion

In this section, the error analysis for the discretization of singularly perturbed weakly coupled system of BVPs of the form (6.1.1) is presented using the upwind finite difference scheme. The numerical solution is obtained on a suitable nonuniform adaptively generated mesh based on the idea of equidistribution principle. This solution can be extended globally by using the constant or piecewise linear interpolation of the numerical solution. The error analysis of the numerical solution is carried out by using maximum norm. It is shown that the errors are first-order convergent, which are independent of the singular perturbation parameters. Numerical solutions obtained for linear and semilinear

Table 6.5: *Uniform errors and orders of convergence of* U_1 *for Example 6.5.3.*

$(\varepsilon_1, \varepsilon_2) \in S$	Number of intervals N						
	64	128	256	512	1024	2048	4096
E_1^N	7.608e-3	3.301e-3	1.792e-3	8.832e-4	4.475e-4	2.219e-4	1.134e-4
r_1^N	1.2045	0.88105	1.0211	0.98070	1.0121	0.96746	-

Table 6.6: *Uniform errors and orders of convergence of U_2 for Example 6.5.3.*

$(\varepsilon_1, \varepsilon_2) \in S$	Number of intervals N						
	64	128	256	512	1024	2048	4096
E_2^N	3.696e-3	1.560e-3	7.551e-4	3.799e-4	1.896e-4	8.331e-5	4.531e-5
r_2^N	1.2447	1.0467	0.99098	1.0020	1.1869	0.87879	-

system of differential equations validate the efficiency of the proposed monitor function, which lead to the first-order parameter-uniform accuracy. The analysis provided here can be extended for more general class of systems, where all the convection coefficients are bounded away from zero by a constant. Therefore, the key result established here is that the numerical solution for weakly coupled system of convection-diffusion problems computed on adaptively generated meshes are first-order accurate to the exact solution.

Chapter 7

A Hybrid Scheme for Singularly Perturbed System of Reaction-Diffusion Robin type Boundary-Value Problems

This chapter deals with the study on system of singularly perturbed reaction-diffusion problems with the Robin or/ mixed type boundary conditions. The difference scheme is a combination of the classical central difference approximation and the cubic spline approximation on a piecewise-uniform Shishkin mesh defined in the whole domain. It is shown that the proposed scheme (*i.e.,* the central difference approximation for outer region and the cubic spline approximation for inner region of boundary layers) leads to almost second-order parameter-uniform convergence whereas the standard method (*i.e.,* the forward-backward approximation for the Robin boundary conditions and the central difference approximation for the differential equation) gives almost first-order convergence on Shishkin mesh provided that the perturbation parameters $\varepsilon_1, \varepsilon_2$ satisfy $\varepsilon_1, \varepsilon_2 \leq N^{-1}$, where N is the number of mesh intervals.

7.1 Introduction

Consider the following system of singularly perturbed Robin type reaction-diffusion problem:

$$\begin{cases} \mathcal{L}\boldsymbol{u}(x) \equiv -\boldsymbol{Eps}\ \boldsymbol{u}''(x) + \mathcal{B}(x)\boldsymbol{u}(x) = \boldsymbol{f}(x), \quad x \in \Omega, \\ M_{l_k}\boldsymbol{u}(0) \equiv \alpha_k u_k(0) - \beta_k u_k'(0) = A_k, \\ M_{r_k}\boldsymbol{u}(1) \equiv \gamma_k u_k(1) + \delta_k u_k'(1) = B_k, \quad k = 1, 2, \end{cases} \tag{7.1.1}$$

where $\mathcal{L} = (\mathcal{L}_1, \mathcal{L}_2)^T$, $\boldsymbol{Eps} = \text{diag}(\varepsilon_1, \varepsilon_2)$ with

$$\boldsymbol{u}(x) = \begin{pmatrix} u_1(x) \\ u_2(x) \end{pmatrix}, \quad \mathcal{B}(x) = \begin{pmatrix} b_{11}(x) & b_{12}(x) \\ b_{21}(x) & b_{22}(x) \end{pmatrix}, \quad \text{and} \quad \boldsymbol{f}(x) = \begin{pmatrix} f_1(x) \\ f_2(x) \end{pmatrix}.$$

Here $\varepsilon_1, \varepsilon_2$ are two singular perturbation parameters, where $0 < \varepsilon_1 \leq \varepsilon_2 \ll 1$. For convenience, define $M_l \boldsymbol{u}(0) = (M_{l_1} \boldsymbol{u}(0), M_{l_2} \boldsymbol{u}(0))^T$ and $M_r \boldsymbol{u}(1) = (M_{r_1} \boldsymbol{u}(1), M_{r_2} \boldsymbol{u}(1))^T$. It is assumed that the functions $b_{ij}(x) \in \mathcal{C}^3(\Omega)$ and $f_i(x) \in \mathcal{C}^2(\Omega)$ for $i, j = 1, 2$ and

$$\alpha_k, \beta_k \geq 0, \quad \alpha_k + \beta_k > 0, \quad \gamma_k > 0, \quad \delta_k \geq 0, \quad \text{for} \quad k = 1, 2.$$

In order to satisfy the standard maximum principle for the operator $\mathcal{L}$, assume that the matrix $\mathcal{B} = \{b_{ij}\}_{i,j=1}^2$ is a strictly diagonally dominant L_0-matrix (*i.e.,* diagonal entries are positive and off diagonal entries are non-positive) with

$$\min_{x \in \overline{\Omega}} \{b_{11}(x) + b_{12}(x), b_{21}(x) + b_{22}(x)\} > \beta > 0,$$

such that $\beta^* \geq |b_{ij}(x)|$ for $1 \leq i, j \leq 2$. These conditions immediately follow that the system of MBVPs (7.1.1) admits a unique solution $\boldsymbol{u}(x) \in \mathcal{C}^4(\Omega) \cap \mathcal{C}^1(\overline{\Omega})$ (see for *e.g.,* [17]) on $\overline{\Omega}$. In general, the solution $\boldsymbol{u}(x)$ exhibits boundary layers at both ends $x = 0, 1$.

The outline of this chapter is as follows: Section 7.2 provides *apriori* derivative bounds of the analytical solution. The decomposition into its smooth and singular components with their derivative bounds are also introduced here. The proposed cubic spline scheme is described in Section 7.3 for the discretization of (7.1.1). Then, this section introduces the piecewise-uniform Shishkin mesh for the system of two equations. This section also outlines the numerical discretization of (7.1.1), where the proposed cubic spline scheme is used to approximate the system of MBVPs inside the layer regions and also at the mixed boundary conditions. Section 7.4 is devoted to study the error and the stability analysis of the discretized operator. The main results, an almost second-order convergence using the proposed spline approximation, which is better than almost first-order uniform convergence for the forward-backward approximation for the mixed boundary conditions are also proved in this section using the supremum norm. Finally, Section 7.5 provides the numerical experiments to verify the rates of convergence predicted by the theoretical analysis.

7.2 Bounds for the Solution Derivatives and Decomposition of the Solution

In this section, the bounds for the continuous solution and its derivatives are provided. For the error analysis, we divide the solution into two components, namely the smooth

component and the singular component. Bounds for the smooth and the singular components are also provided. A boundary condition of mixed type causes a less severe boundary layer (see [74]). Therefore, we use the *apriori* bounds of the solution and its derivatives provided by [51] and [54].

Lemma 7.2.1. *Let* $\boldsymbol{u} = (u_1, u_2)^T$ *be the solution of the system (7.1.1). Then, its derivatives satisfy the following bounds:*

$$|u_1^{(k)}| \leq C(1+\varepsilon_1^{-k/2}), \qquad |u_2^{(k)}| \leq C(1+\varepsilon_2^{-k/2}), \quad \text{for } k = 1, 2,$$

and

$$|u_1^{(k+2)}| \leq C(\varepsilon_1^{-(k+2)/2}+\varepsilon_1^{-1}\varepsilon_2^{-k/2}), \qquad |u_2^{(k+2)}| \leq C(\varepsilon_1^{-k/2}\varepsilon_2^{-1}+\varepsilon_2^{-(k+2)/2}), \quad \text{for } k = 1, 2.$$

Proof. The proof of this lemma is given in [54]. ∎

We decompose the exact solution $\boldsymbol{u}$ into the smooth component $\boldsymbol{v}$ and the singular component $\boldsymbol{w}$ such that $\boldsymbol{u} = \boldsymbol{v} + \boldsymbol{w}$. For the analysis of the singular component, let us denote $\mathcal{E}_\mu(x) = \exp(-x\sqrt{\beta/\mu}) + \exp(-(1-x)\sqrt{\beta/\mu})$.

Solution of the problem (7.1.1) can be decomposed (see for *e.g.,* [52]) in a way such that $\boldsymbol{v} = (v_1, v_2)^T$ satisfies $\mathcal{L}\boldsymbol{v} = \boldsymbol{f}$ with $M_l\boldsymbol{v}(0) = \mathcal{B}(0)^{-1}\boldsymbol{f}(0)$ and $M_r\boldsymbol{v}(1) = \mathcal{B}(1)^{-1}\boldsymbol{f}(1)$, and $\boldsymbol{w} = (w_1, w_2)^T$ satisfies $\mathcal{L}\boldsymbol{w} = \boldsymbol{0}$ with $M_l\boldsymbol{w}(0) = \boldsymbol{A} - M_l\boldsymbol{v}(0)$ and $M_r\boldsymbol{w}(1) = \boldsymbol{B} - M_r\boldsymbol{v}(1)$ where $\boldsymbol{A} = (A_1, A_2)^T$, $\boldsymbol{B} = (B_1, B_2)^T$ and M_l, M_r are defined earlier.

The following derivative bounds for the smooth component $\boldsymbol{v}$ and the singular component $\boldsymbol{w}$ will be used in the error analysis.

Lemma 7.2.2. *The smooth component* $\boldsymbol{v}$ *satisfies the following estimates*

$$|v_1^k(x)| \leq C\big(1+\varepsilon_1^{(2-k)/2}\big), \quad |v_1^3(x)| \leq C(\varepsilon_2^{-1}+\varepsilon_1\mathcal{E}_{\varepsilon_1}(x)), \quad |v_2^k(x)| \leq C\big(1+\varepsilon_2^{(2-k)/2}\big), \tag{7.2.1}$$

for $k = 0, \cdots, 4$ *while the derivative bounds of the singular component* $\boldsymbol{w} = (w_1, w_2)^T$ *satisfy*

$$|w_1^{(k)}(x)| \leq C(\varepsilon_1^{-k/2}\mathcal{E}_{\varepsilon_1}(x) + \varepsilon_2^{-k/2}\mathcal{E}_{\varepsilon_2}(x)), \quad \text{for } k = 0, 1, 2, \tag{7.2.2}$$

$$|w_2^{(k)}(x)| \leq C\varepsilon_2^{-k/2}\mathcal{E}_{\varepsilon_2}(x), \quad \text{for } k = 0, 1, 2, \tag{7.2.3}$$

and

$$\varepsilon_1|w_1^{(k)}(x)| + \varepsilon_2|w_2^{(k)}(x)| \leq C(\varepsilon_1^{(2-k)/2}\mathcal{E}_{\varepsilon_1}(x) + \varepsilon_2^{(2-k)/2}\mathcal{E}_{\varepsilon_2}(x)), \qquad \text{for } k = 3, 4. \tag{7.2.4}$$

Proof. The proof of this lemma can be obtained from [51, 52]. ∎

In order to estimate the local truncation errors bound for the proposed hybrid scheme, we need the following derivative estimates of the layer term.

Lemma 7.2.3. *There exist two pair of decompositions of the singular component* $\boldsymbol{w}$ *namely* $(\boldsymbol{w}_{\varepsilon_1}, \boldsymbol{w}_{\varepsilon_2})$ *and* $(\widehat{\boldsymbol{w}}_{\varepsilon_1}, \widehat{\mathbf{w}}_{\boldsymbol{\varepsilon_2}})$, *such that* $\boldsymbol{w} = \boldsymbol{w}_{\varepsilon_1} + \boldsymbol{w}_{\varepsilon_2} = \widehat{\boldsymbol{w}}_{\varepsilon_1} + \widehat{\boldsymbol{w}}_{\varepsilon_2}$ *satisfies*

$$\begin{aligned} \varepsilon_1|w^{(2)}_{\varepsilon_1,1}(x)| + \varepsilon_2|w^{(2)}_{\varepsilon_1,2}(x)| &\leq C\ \mathcal{E}_{\varepsilon_1}(x), \\ |w^{(3)}_{\varepsilon_2,1}(x)| + |w^{(3)}_{\varepsilon_2,2}(x)| &\leq C\varepsilon_2^{-3/2}\mathcal{E}_{\varepsilon_2}(x), \end{aligned} \tag{7.2.5}$$

and

$$\begin{aligned} \varepsilon_1|\widehat{w}^{(2)}_{\varepsilon_1,1}(x)| + \varepsilon_2|\widehat{w}^{(2)}_{\varepsilon_1,2}(x)| &\leq C\ \mathcal{E}_{\varepsilon_1}(x), \\ \varepsilon_1|\widehat{w}^{(4)}_{\varepsilon_2,1}(x)| + \varepsilon_2|\widehat{w}^{(4)}_{\varepsilon_2,2}(x)| &\leq C\ \varepsilon_2^{-1}\mathcal{E}_{\varepsilon_2}(x), \end{aligned} \tag{7.2.6}$$

for all $x \in \overline{\Omega}$.

Proof. The proof of this lemma can be seen in [51]. ∎

7.3 Discrete Problem

In this section, we define the cubic spline approximation for the system of MBVPs (7.1.1). Here, the well-known piecewise-uniform Shishkin mesh for system of MBVPs is provided in a slightly modified way. The hybrid numerical scheme for the system (7.1.1) is also proposed here.

7.3.1 Cubic spline difference scheme

To define the cubic spline approximation on a general nonuniform mesh $\Omega^N \equiv \{0 = x_0 < x_1 < \cdots < x_N = 1\}$, with step size $h_i = x_i - x_{i-1},\ i = 1, \cdots, N$, we shall take the help of two equations (2.3.2) and (2.3.3) *i.e.,* one sided limits of the first-order derivatives with the condition of continuity, from Chapter 2. Let us define $M_{1,j}$ and $M_{2,j}$, as the double derivative of the spline approximation for u_1 and u_2. Then the following 'condition of continuity' for one sided first-order derivatives at the interior meshes hold true:

$$\frac{h_i}{6}M_{k,i-1} + \left(\frac{h_i + h_{i+1}}{3}\right)M_{k,i} + \frac{h_{i+1}}{6}M_{k,i+1} = \left(\frac{u(x_{i+1}) - u(x_i)}{h_{i+1}}\right) - \left(\frac{u(x_i) - u(x_{i-1})}{h_i}\right), \tag{7.3.1}$$

for $i = 1, \cdots, N-1$.

Substituting $M_{1,j}, M_{2,j}$ from $-\varepsilon_1 M_{1,j} + b_{11}(x_j)u_1(x_j) + b_{12}(x_j)u_2(x_j) = f_1(x_j),\ j = i, i \pm 1$ and $-\varepsilon_2 M_{2,j} + b_{21}(x_j)u_1(x_j) + b_{22}(x_j)u_2(x_j) = f_2(x_j),\ j = i, i \pm 1$ to the corresponding equations defined for u_1 and u_2 in (7.3.1), we obtain the following linear system

of equations of the discrete solution $\boldsymbol{U}_i = (U_{1,i},\, U_{2,i})^T$, for $i = 1, \cdots, N-1$,

$$\begin{cases} \left[\dfrac{-3\varepsilon_1}{h_i(h_i+h_{i+1})} + \dfrac{h_i}{2(h_i+h_{i+1})}b_{11}(x_{i-1})\right] U_{1,i-1} + \left[\dfrac{3\varepsilon_1}{h_i h_{i+1}} + b_{11}(x_i)\right] U_{1,i} + \\ \left[\dfrac{-3\varepsilon_1}{h_{i+1}(h_i+h_{i+1})} + \dfrac{h_{i+1}}{2(h_i+h_{i+1})}b_{11}(x_{i+1})\right] U_{1,i+1} + \left[\dfrac{h_i}{2(h_{i+1}+h_i)}b_{12}(x_{i-1})\right] U_{2,i-1} + \\ [b_{12}(x_i)]U_{2,i} + \left[\dfrac{h_{i+1}}{2(h_i+h_{i+1})}b_{12}(x_{i+1})\right] U_{2,i+1} = \\ \left[\dfrac{h_i}{2(h_i+h_{i+1})}\right] f_1(x_{i-1}) + f_1(x_i) + \left[\dfrac{h_{i+1}}{2(h_i+h_{i+1})}\right] f_1(x_{i+1}), \end{cases} \tag{7.3.2}$$

and

$$\begin{cases} \left[\dfrac{-3\varepsilon_2}{h_i(h_i+h_{i+1})} + \dfrac{h_i}{2(h_i+h_{i+1})}b_{22}(x_{i-1})\right] U_{2,i-1} + \left[\dfrac{3\varepsilon_2}{h_i h_{i+1}} + b_{22}(x_i)\right] U_{2,i} + \\ \left[\dfrac{-3\varepsilon_2}{h_{i+1}(h_i+h_{i+1})} + \dfrac{h_{i+1}}{2(h_i+h_{i+1})}b_{22}(x_{i+1})\right] U_{2,i+1} + \left[\dfrac{h_i}{2(h_i+h_{i+1})}b_{21}(x_{i-1})\right] U_{1,i-1} + \\ [b_{21}(x_i)]U_{1,i} + \left[\dfrac{h_{i+1}}{2(h_i+h_{i+1})}b_{21}(x_{i+1})\right] U_{1,i+1} = \\ \left[\dfrac{h_i}{2(h_i+h_{i+1})}\right] f_2(x_{i-1}) + f_2(x_i) + \left[\dfrac{h_{i+1}}{2(h_i+h_{i+1})}\right] f_2(x_{i+1}). \end{cases} \tag{7.3.3}$$

To discretize the mixed boundary conditions in (7.1.1) using expressions (2.3.2) and (2.3.3) we obtain that

$$\begin{cases} \left[\dfrac{3\varepsilon_1}{h_1}\left(\alpha_1 + \dfrac{\beta_1}{h_1}\right) + b_{11}(x_0)\beta_1\right] U_{1,0} + \left[\dfrac{-3\varepsilon_1\beta_1}{h_1^2} + \dfrac{b_{11}(x_1)\beta_1}{2}\right] U_{1,1} + \beta_1 b_{12}(x_0)U_{2,0} + \\ \dfrac{\beta_1 b_{12}(x_1)}{2}U_{2,1} = \dfrac{3\varepsilon_1 A_1}{h_1} + \beta_1 f_1(x_0) + \dfrac{\beta_1}{2}f_1(x_1), \\ \left[\dfrac{-3\varepsilon_1\delta_1}{h_N^2} + \dfrac{b_{11}(x_{N-1})\delta_1}{2}\right] U_{1,N-1} + \left[\dfrac{3\varepsilon_1}{h_N}\left(\gamma_1 + \dfrac{\delta_1}{h_N}\right) + b_{11}(x_N)\delta_1\right] U_{1,N} + \\ \dfrac{\delta_1 b_{12}(x_{N-1})}{2}U_{2,N-1} + \delta_1 b_{12}(x_N)U_{2,N} = \dfrac{3\varepsilon_1 B_1}{h_N} + \delta_1 f_1(x_N) + \dfrac{\delta_1}{2}f_1(x_{N-1}), \end{cases} \tag{7.3.4}$$

and

$$\begin{cases} \left[\dfrac{3\varepsilon_2}{h_1}\left(\alpha_2 + \dfrac{\beta_2}{h_1}\right) + b_{22}(x_0)\beta_2\right] U_{2,0} + \left[\dfrac{-3\varepsilon_2\beta_2}{h_1^2} + \dfrac{b_{22}(x_1)\beta_2}{2}\right] U_{2,1} + \beta_2 b_{21}(x_0)U_{1,0} + \\ \dfrac{\beta_2 b_{21}(x_1)}{2}U_{1,1} = \dfrac{3\varepsilon_2 A_2}{h_1} + \beta_2 f_2(x_0) + \dfrac{\beta_2}{2}f_2(x_1), \\ \left[\dfrac{-3\varepsilon_2\delta_2}{h_N^2} + \dfrac{b_{22}(x_{N-1})\delta_2}{2}\right] U_{2,N-1} + \left[\dfrac{3\varepsilon_2}{h_N}\left(\gamma_2 + \dfrac{\delta_2}{h_N}\right) + b_{22}(x_N)\delta_2\right] U_{2,N} + \\ \dfrac{\delta_2 b_{21}(x_{N-1})}{2}U_{1,N-1} + \delta_2 b_{21}(x_N)U_{1,N} = \dfrac{3\varepsilon_2 B_2}{h_N} + \delta_2 f_2(x_N) + \dfrac{\delta_2}{2}f_2(x_{N-1}). \end{cases} \tag{7.3.5}$$

By solving the above linear algebraic equations (7.3.2)- (7.3.5) of $U_{1,i}$, $U_{2,i}$, $i = 0, \cdots, N$, we get the approximate solution of $\boldsymbol{u}(x) = (u_1, u_2)^T$ at the nodal points $x_0, x_1, \cdots, x_N$.

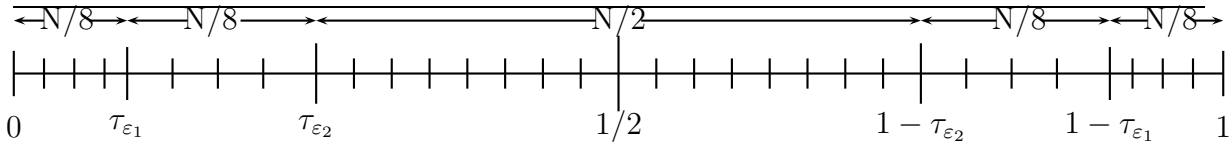

Figure 7.1: *Piecewise-uniform Shishkin Mesh for* $N = 32$.

7.3.2 The piecewise-uniform Shishkin mesh

The solution of (7.1.1) has two overlapping boundary layers near $x = 0$ and $x = 1$ for $0 < \varepsilon_1 \leq \varepsilon_2 \ll 1$. Hence, one need to define a comparatively finer mesh near the boundary layer regions and coarse mesh in the regular region which can be easily obtained by the piecewise-uniform Shishkin mesh. This mesh can be constructed by dividing the domain $\overline{\Omega}$ into five subintervals $[0, \tau_{\varepsilon_1}]$, $[\tau_{\varepsilon_1}, \tau_{\varepsilon_2}]$, $[\tau_{\varepsilon_2}, 1-\tau_{\varepsilon_2}]$, $[1-\tau_{\varepsilon_2}, 1-\tau_{\varepsilon_1}]$ and $[1-\tau_{\varepsilon_1}, 1]$ where τ_{ε_1} and τ_{ε_2} are known as transition points and defined as follows

$$\tau_{\varepsilon_2} = \min\left\{\frac{1}{8}, \tau_0\sqrt{\varepsilon_2}\,\ln N\right\}, \text{ and } \tau_{\varepsilon_1} = \min\left\{\frac{\tau_{\varepsilon_2}}{2}, \tau_0\sqrt{\varepsilon_1}\,\ln N\right\}, \tag{7.3.6}$$

where $\tau_0 \geq 2/\sqrt{\beta} > 0$ is a constant. Next, we subdivide $[\tau_{\varepsilon_2}, 1-\tau_{\varepsilon_2}]$ into $N/2$ mesh intervals and other subintervals by $N/8$ mesh intervals of uniform length, to get a piecewise-uniform mesh (see Figure 7.1: Piecewise-uniform Shishkin mesh for $N = 32$).

7.3.3 Robust hybrid numerical scheme

The difficulty with the proposed cubic spline approximation (7.3.2)-(7.3.5) is that it lacks stability, *i.e.,* it does not lead to a system of equations described by M-matrix in the outer coarse mesh region $[\tau_{\varepsilon_2}, 1-\tau_{\varepsilon_2}]$. However, if we use only (7.3.2)-(7.3.5) inside the layers, and the central difference approximation of the differential equation (7.1.1) to outside the layer, then the new system of equations do have a monotonicity property.

Therefore, the classical central difference scheme is used in $[\tau_{\varepsilon_2}, 1-\tau_{\varepsilon_2}]$ and the cubic spline scheme (7.3.2)-(7.3.5) is used in the regions $[0, \tau_{\varepsilon_2}]$ and $[1-\tau_{\varepsilon_2}, 1]$ to discretize the problem (7.1.1). This discrete problem can be written as to find $\boldsymbol{U} = (U_1, U_2)^T$ such that

$$[\mathcal{L}^N \boldsymbol{U}]_i \equiv \begin{pmatrix} \mathcal{L}_1^N \boldsymbol{U} \\ \mathcal{L}_2^N \boldsymbol{U} \end{pmatrix}_i = \begin{pmatrix} F_1 \\ F_2 \end{pmatrix}_i, \quad \text{for} \quad i = 1, \cdots, N-1, \tag{7.3.7}$$

where the discretized boundary conditions

$$M_l^N \boldsymbol{U}(0) = (M_{l_1}^N \boldsymbol{U}(0), M_{l_2}^N \boldsymbol{U}(0))^T \text{ and } M_r^N \boldsymbol{U}(1) = (M_{r_1}^N \boldsymbol{U}(1), M_{r_2}^N \boldsymbol{U}(1))^T, \tag{7.3.8}$$

are obtained from the relations (7.3.4), (7.3.5). Here $\mathcal{L}^N$, M_l^N and M_r^N are the discrete analogues of the continuous operators $\mathcal{L}$, M_l and M_r, respectively defined in (7.1.1).

Hence

$$\begin{cases} \mathcal{L}_1^N \boldsymbol{U} = r_{1,i}^- \, U_{1,i-1} + r_{1,i}^c \, U_{1,i} + r_{1,i}^+ \, U_{1,i+1} + q_{1,i}^- \, U_{2,i-1} + q_{1,i}^c \, U_{2,i} + q_{1,i}^+ \, U_{2,i+1}, \\ \mathcal{L}_2^N \boldsymbol{U} = r_{2,i}^- \, U_{2,i-1} + r_{2,i}^c \, U_{2,i} + r_{2,i}^+ \, U_{2,i+1} + q_{2,i}^- \, U_{1,i-1} + q_{2,i}^c \, U_{1,i} + q_{2,i}^+ \, U_{1,i+1}, \\ F_1 = F_{1,i}^- \, f_{1,i-1} + F_{1,i}^c \, f_{1,i} + F_{1,i}^+ \, f_{1,i+1}, \\ F_2 = F_{2,i}^- \, f_{2,i-1} + F_{2,i}^c \, f_{2,i} + F_{2,i}^+ \, f_{2,i+1}. \end{cases}$$

where, for $i = 1, \cdots, N/4-1$ and $i = 3N/4+1, \cdots, N-1$, the coefficients are obtained as

$$\begin{cases} r_{1,i}^- = \dfrac{-3\varepsilon_1}{h_i(h_i+h_{i+1})} + \dfrac{h_i}{2(h_i+h_{i+1})} b_{11}(x_{i-1}), \quad r_{1,i}^c = \dfrac{3\varepsilon_1}{h_i h_{i+1}} + b_{11}(x_i), \\ r_{1,i}^+ = \dfrac{-3\varepsilon_1}{h_{i+1}(h_i+h_{i+1})} + \dfrac{h_{i+1}}{2(h_i+h_{i+1})} b_{11}(x_{i+1}), \\ q_{1,i}^- = \dfrac{h_{i+1}}{2(h_i+h_{i+1})} b_{12}(x_{i-1}), \quad q_{1,i}^c = b_{12}(x_i), \quad q_{1,i}^+ = \dfrac{h_{i+1}}{2(h_i+h_{i+1})} b_{12}(x_{i+1}), \\ F_{1,i}^- = \dfrac{h_i}{2(h_i+h_{i+1})}, \quad F_{1,i}^c = 1, \quad F_{1,i}^+ = \dfrac{h_{i+1}}{2(h_i+h_{i+1})}, \\ r_{2,i}^- = \dfrac{-3\varepsilon_2}{h_i(h_i+h_{i+1})} + \dfrac{h_i}{2(h_i+h_{i+1})} b_{22}(x_{i-1}), \quad r_{2,i}^c = \dfrac{3\varepsilon_2}{h_i h_{i+1}} + b_{22}(x_i), \\ r_{2,i}^+ = \dfrac{-3\varepsilon_2}{h_{i+1}(h_i+h_{i+1})} + \dfrac{h_{i+1}}{2(h_i+h_{i+1})} b_{22}(x_{i+1}), \\ q_{2,i}^- = \dfrac{h_{i+1}}{2(h_i+h_{i+1})} b_{21}(x_{i-1}), \quad q_{2,i}^c = b_{21}(x_i), \quad q_{2,i}^+ = \dfrac{h_{i+1}}{2(h_i+h_{i+1})} b_{21}(x_{i+1}), \\ F_{2,i}^- = \dfrac{h_i}{2(h_i+h_{i+1})}, \quad F_{2,i}^c = 1, \quad F_{2,i}^+ = \dfrac{h_{i+1}}{2(h_i+h_{i+1})}, \end{cases} \tag{7.3.9}$$

and, for $i = N/4, \cdots, 3N/4$, the coefficients are given by

$$\begin{cases} r_{1,i}^- = \dfrac{-2\varepsilon_1}{h_i(h_i+h_{i+1})}, \quad r_{1,i}^c = \dfrac{2\varepsilon_1}{h_i h_{i+1}} + b_{11}(x_i), \quad r_{1,i}^+ = \dfrac{-2\varepsilon_1}{h_{i+1}(h_i+h_{i+1})}, \\ q_{1,i}^- = 0, \quad q_{1,i}^c = b_{12}(x_i), \quad q_{1,i}^+ = 0, \\ F_{1,i}^- = 0, \quad F_{1,i}^c = 1, \quad F_{1,i}^+ = 0, \\ r_{2,i}^- = \dfrac{-2\varepsilon_2}{h_i(h_i+h_{i+1})}, \quad r_{2,i}^c = \dfrac{2\varepsilon_2}{h_i h_{i+1}} + b_{22}(x_i), \quad r_{2,i}^+ = \dfrac{-2\varepsilon_2}{h_{i+1}(h_i+h_{i+1})}, \\ q_{2,i}^- = 0, \quad q_{2,i}^c = b_{21}(x_i), \quad q_{2,i}^+ = 0, \\ F_{2,i}^- = 0, \quad F_{2,i}^c = 1, \quad F_{2,i}^+ = 0, \end{cases} \tag{7.3.10}$$

along with the following coefficients corresponding to the mixed boundary conditions

$$\begin{cases} r^c_{1,0} = \dfrac{3\varepsilon_1}{h_1}\left(\alpha_1 + \dfrac{\beta_1}{h_1}\right) + b_{11}(x_0)\beta_1, \quad r^+_{1,0} = \dfrac{-3\varepsilon_1\beta_1}{h_1^2} + \dfrac{b_{11}(x_1)\beta_1}{2}, \quad q^c_{1,0} = \beta_1 b_{12}(x_0), \\ q^+_{1,0} = \dfrac{\beta_1 b_{12}(x_1)}{2}, \quad F^-_{1,0} = \dfrac{3\varepsilon_1 A_1}{h_1}, \quad F^c_{1,0} = \beta_1, \quad F^+_{1,0} = \dfrac{\beta_1}{2}, \end{cases} \tag{7.3.11}$$

$$\begin{cases} r^-_{1,N} = \dfrac{-3\varepsilon_1\delta_1}{h_N^2} + \dfrac{b_{11}(x_{N-1})\delta_1}{2}, \quad r^c_{1,N} = \dfrac{3\varepsilon_1}{h_N}\left(\gamma_1 + \dfrac{\delta_1}{h_N}\right) + b_{11}(x_N)\delta_1, \\ q^-_{1,N} = \dfrac{\delta_1 b_{12}(x_{N-1})}{2}, \quad q^c_{1,N} = \delta_1 b_{12}(x_N), \quad F^-_{1,N} = \dfrac{3\varepsilon_1 B_1}{h_N}, \quad F^c_{1,N} = \delta_1, \quad F^+_{1,N} = \dfrac{\delta_1}{2}, \end{cases} \tag{7.3.12}$$

and

$$\begin{cases} q^+_{2,0} = \dfrac{-3\varepsilon_2\beta_2}{h_1^2} + \dfrac{b_{22}(x_1)\beta_2}{2}, \quad q^c_{2,0} = \dfrac{3\varepsilon_2}{h_1}\left(\alpha_2 + \dfrac{\beta_2}{h_1}\right) + b_{22}(x_0)\beta_2, \\ r^c_{2,0} = \beta_2 b_{21}(x_0), \quad r^+_{2,0} = \dfrac{\beta_2 b_{21}(x_1)}{2}, \quad F^-_{2,0} = \dfrac{3\varepsilon_2 A_2}{h_1}, \quad F^c_{2,0} = \beta_2, \quad F^+_{2,0} = \dfrac{\beta_2}{2}, \end{cases} \tag{7.3.13}$$

$$\begin{cases} q^-_{2,N} = \dfrac{-3\varepsilon_2\delta_2}{h_N^2} + \dfrac{b_{22}(x_{N-1})\delta_2}{2}, \quad q^c_{2,N} = \dfrac{3\varepsilon_2}{h_N}\left(\gamma_2 + \dfrac{\delta_2}{h_N}\right) + b_{22}(x_N)\delta_2, \\ r^-_{2,N} = \dfrac{\delta_2 b_{21}(x_{N-1})}{2}, \quad r^c_{2,N} = \delta_2 b_{21}(x_N), \quad F^-_{2,N} = \dfrac{3\varepsilon_2 B_2}{h_N}, \quad F^c_{2,N} = \delta_2, \quad F^+_{2,N} = \dfrac{\delta_2}{2}. \end{cases} \tag{7.3.14}$$

The next section shows that the matrix corresponding to the proposed scheme satisfies the stability property.

7.4 Stability and Error Analysis

This section describes the truncation error analysis and the stability estimate for the proposed scheme. The main parameter-uniform convergence result is derived at the end of this section.

A straightforward derivation leads to the following truncation error (see [63]) of the hybrid scheme on the piecewise-uniform Shishkin mesh. Since the step lengths are uniform in each subinterval $(0, \tau_{\varepsilon_1})$, $(\tau_{\varepsilon_1}, \tau_{\varepsilon_2})$, $(1-\tau_{\varepsilon_2}, 1-\tau_{\varepsilon_1})$ and $(1-\tau_{\varepsilon_1}, 1)$, let us define the step length $h_i = h$ where the values of h will differ at each subinterval. For $i = 1, \cdots, N/8-1, N/8+1, \cdots, N/4-1$ and $3N/4+1, \cdots, 7N/8-1, 7N/8+1, \cdots, N-1$, one has

$$\begin{aligned} \tau_{i,\,u_1} \;=\; & \frac{\varepsilon_1 h^2}{8} u_1^{(iv)}(x_i) + r^+_{1,i}\, R_4(x_i, x_{i+1}, u_1) + r^-_{1,i}\, R_4(x_i, x_{i-1}, u_1) + \\ & \frac{\varepsilon_1}{4}\, R_2(x_i, x_{i+1}, u_1) + \frac{\varepsilon_1}{4}\, R_2(x_i, x_{i-1}, u_1) \;- \\ & -\frac{a_{11}(x_{i-1})}{4}\, R_4(x_i, x_{i-1}, u_1) - \frac{a_{11}(x_{i+1})}{4}\, R_4(x_i, x_{i+1}, u_1), \end{aligned} \tag{7.4.1}$$

and

$$\begin{aligned}\tau_{i,\ u_2} &= \frac{\varepsilon_2 h^2}{8}u_2^{(iv)}(x_i) + r_{2,i}^{+}\ R_4(x_i, x_{i+1}, u_2) + r_{2,i}^{-}\ R_4(x_i, x_{i-1}, u_2) + \\ &+\frac{\varepsilon_2}{4}\ R_2(x_i, x_{i+1}, u_2) + \frac{\varepsilon_2}{4}\ R_2(x_i, x_{i-1}, u_2)\ - \\ &-\frac{a_{22}(x_{i-1})}{4}\ R_4(x_i, x_{i-1}, u_2) - \frac{a_{22}(x_{i+1})}{4}\ R_4(x_i, x_{i+1}, u_2), \end{aligned} \tag{7.4.2}$$

where $\tau_{i,\ g}$ is the truncation error at the point x_i and $R_n(a, p, g)$ denotes the remainder of the Taylor series expansion for the function g.
For $i = N/8, 7N/8$, we can easily derive that

$$\begin{aligned}|\tau_{i,\ u_1}| &\leq\ C\varepsilon_1(h_i + h_{i+1})|u_1'''(x_i)|, \\ |\tau_{i,\ u_2}| &\leq\ C\varepsilon_2(h_i + h_{i+1})|u_2'''(x_i)|. \end{aligned} \tag{7.4.3}$$

For $i = N/4, \cdots, 3N/4$, the truncation errors are defined as

$$\tau_{i,\ u_1} = -\varepsilon_1 \left(\delta^2 - \frac{d^2}{dx^2}\right) u_1(x_i), \tag{7.4.4}$$

and

$$\tau_{i,\ u_2} = -\varepsilon_2 \left(\delta^2 - \frac{d^2}{dx^2}\right) u_2(x_i). \tag{7.4.5}$$

Now, the truncation error for $x_0 = 0$ satisfies

$$\tau_{0,\ u_1} = r_{1,0}^{c}\ u_{1,0} + r_{1,0}^{+}\ u_{1,1} + q_{1,0}^{c}\ u_{2,0} + q_{1,0}^{+}\ u_{2,1} - F_{1,0}^{-} - F_{1,0}^{c}\ f_{1,0} - F_{1,0}^{+}\ f_{1,1}.$$

Using (7.1.1) and the Taylor series expansion, we get

$$\tau_{0,\ u_1} = T_{0,0}\ u_1(x_0) + T_{1,0}\ u_1'(x_0) + T_{2,0}\ u_1''(x_0) + T_{3,0}\ u_1'''(x_0) + T_{4,0}\ u_1^{(iv)}(\xi),$$

where $\xi \in \Omega$, and

$$\begin{aligned} T_{0,0} &= r_{1,0}^{c} + r_{1,0}^{+} - \frac{3\varepsilon_1\alpha_1}{h_1} - F_{1,0}^{c}a_{11}(x_0) - F_{1,0}^{+}a_{11}(x_1), \\ T_{1,0} &= h_1 r_{1,0}^{+} + \frac{3\varepsilon_1\beta_1}{h_1} - \frac{\beta a_{11}(x_1)h_1}{2}, \\ T_{2,0} &= \frac{h_1^2 r_{1,0}^{+}}{2} + \varepsilon_1(F_{1,0}^{c} + F_{1,0}^{+}) - \frac{h_1^2 F_{1,0}^{+}a_{11}(x_1)}{2}, \\ T_{3,0} &= \frac{h_1^3 r_{1,0}^{+}}{3!} + \varepsilon_1 h_1 F_{1,0}^{+} - \frac{F_{1,\ 0}^{+}a_{11}(x_1)h_1^3}{3!}, \\ T_{4,0} &= \frac{h_1^4 r_{1,0}^{+}}{4!} + \frac{\varepsilon_1 h_1^2}{2}F_{1,0}^{+} - \frac{F_{1,0}^{+}a_{11}(x_1)h_1^4}{4!}. \end{aligned}$$

It can be easily checked that

$$T_{0,0}\ u_1(x_0) + T_{1,0}\ u_1'(x_0) = 0, \quad T_{2,0} = 0, \quad T_{3,0} = 0, \quad T_{4,0} = \varepsilon_1\beta_1 h_1^2\left(\frac{1}{4} + \frac{1}{24}\right).$$

Therefore, the truncation error for u_1 at x_0 is

$$|\tau_{0,\ u_1}| \leq C\varepsilon_1\beta_1 h_1^2 |u_{1,0}^{(iv)}|_{(x_0,x_1)}. \tag{7.4.6}$$

In an analogous way, the truncation error at x_N can be obtained as

$$|\tau_{N,\ u_1}| \leq C\varepsilon_1\delta_1 h_N^2 |u_{1,N}^{(iv)}|_{(x_{N-1},x_N)}.$$

Proceeding as like the error analysis for u_1, we can derive that

$$|\tau_{0,\ u_2}| \leq C\varepsilon_2\beta_2 h_1^2 |u_{2,0}^{(iv)}|_{(x_0,x_1)}, \quad \text{and} \quad |\tau_{N,\ u_2}| \leq C\varepsilon_2\delta_2 h_N^2 |u_{2,N}^{(iv)}|_{(x_{N-1},x_N)}. \tag{7.4.7}$$

In the convergence analysis, to define the transition points for piecewise-uniform Shishkin mesh we shall assume that

$$\tau_{\varepsilon_2} = \tau_0\sqrt{\varepsilon_2}\ln N < \frac{1}{8}, \quad \text{and} \quad \tau_{\varepsilon_1} = \tau_0\sqrt{\varepsilon_1}\ln N \leq \frac{\tau_{\varepsilon_2}}{2}, \tag{7.4.8}$$

because otherwise N^{-1} is exponentially small relatively to ε_2, which is very unlikely in practice. Again, for $\tau_{\varepsilon_2} = \tau_{\varepsilon_1}/2$, we have $\varepsilon_2 = O(\varepsilon_1)$ for which the analysis provided here can be extended in a direct way.

The point-wise errors of the numerical solution are examined by separately analyzing the errors of its smooth component and the singular component in each subinterval.

Lemma 7.4.1. *The truncation errors of the numerical solution corresponding to the solution* $\boldsymbol{u}$ *in the boundary layer regions* $[0, \tau_{\varepsilon_1})$ *and* $(1-\tau_{\varepsilon_1}, 1]$ *satisfy the following bounds:*

$$\begin{aligned} |\tau_{i,\ u_1}| &\leq C\tau_0^2 N^{-2}\ln^2 N, \quad \textit{for} \quad 0 \leq i \leq N/8-1, \quad \textit{and} \quad 7N/8+1 \leq i \leq N, \\ |\tau_{i,\ u_2}| &\leq C\tau_0^2 N^{-2}\ln^2 N, \quad \textit{for} \quad 0 \leq i \leq N/8-1, \quad \textit{and} \quad 7N/8+1 \leq i \leq N. \end{aligned} \tag{7.4.9}$$

Proof. To do the truncation error analysis of the decomposed solution, note that in the regions $[0, \tau_{\varepsilon_1})$ and $(1-\tau_{\varepsilon_1}, 1]$, the step length $h_i = h = 8N^{-1}\tau_0\sqrt{\varepsilon_1}\ln N$. Now using (7.2.1) and (7.2.4), we have from (7.4.6), (7.4.1)

$$\begin{aligned} |\tau_{i,\ u_1}| &\leq C\varepsilon_1 h^2 |u_1^{(iv)}| \leq C\varepsilon_1 h^2[|v_1^{(iv)}| + |w_1^{(iv)}|] \\ &\leq C\varepsilon_1 h^2\left[C(1+\varepsilon_1^{-1}) + C(\varepsilon_1^{-2}\mathcal{E}_{\varepsilon_1} + \varepsilon_1^{-1}\varepsilon_2^{-1}\mathcal{E}_{\varepsilon_2})\right] \\ &\leq Ch^2[1 + \varepsilon_1^{-1}\mathcal{E}_{\varepsilon_1} + \varepsilon_2^{-1}\mathcal{E}_{\varepsilon_2}] \\ &\leq Ch^2[1+\varepsilon_1^{-1}] \leq C\tau_0^2 N^{-2}\ln^2 N. \end{aligned}$$

Similarly, estimating the derivative bounds from (7.2.1) and (7.2.4), (7.4.2) and (7.4.7) yield

$$\begin{aligned}|\tau_{i,\ u_2}| &\leq C\varepsilon_2 h^2 |u_2^{(iv)}\ | \\ &\leq C\varepsilon_2 h^2 \left[C(1+\varepsilon_2^{-1}) + C(\varepsilon_1^{-1}\varepsilon_2^{-1}\mathcal{E}_{\varepsilon_1} + \varepsilon_2^{-2}\mathcal{E}_{\varepsilon_2})\right] \\ &\leq Ch^2(1+\varepsilon_1^{-1}) \leq C\tau_0^2 N^{-2}\ln^2 N.\end{aligned}$$

The error estimates for the region $(1-\tau_{\varepsilon_1}, 1]$ can be extended in an analogous way, which proves the result. ∎

Lemma 7.4.2. *The truncation errors in the outer region $(\tau_{\varepsilon_2}, 1-\tau_{\varepsilon_2})$ admit the following bounds*

$$\begin{aligned}|\tau_{i,\ u_1}| &\leq CN^{-\tau_0\sqrt{\beta}}, \quad \textit{for} \quad N/4 < i < 3N/4, \\ |\tau_{i,\ u_2}| &\leq CN^{-\tau_0\sqrt{\beta}}, \quad \textit{for} \quad N/4 < i < 3N/4.\end{aligned} \tag{7.4.10}$$

Proof. From the equation (7.4.4), we have for $N/4 < i < 3N/4$

$$\begin{aligned}|\tau_{i,\ u_1}| &= \varepsilon_1 \left|\left(\delta^2 - \frac{d^2}{dx^2}\right) u_1(x_i)\right| \leq |\tau_{i,\ v_1}| + |\tau_{i,\ w_1}| \\ &= \varepsilon_1 \left|\left(\delta^2 - \frac{d^2}{dx^2}\right) v_1(x_i)\right| + \varepsilon_1 \left|\left(\delta^2 - \frac{d^2}{dx^2}\right) w_1(x_i)\right|.\end{aligned}$$

Observe that, uniformity of the step lengths at $(\tau_{\varepsilon_2}, 1-\tau_{\varepsilon_2})$ give $h_i = h = 2N^{-1} - 4N^{-1}\tau_0\sqrt{\varepsilon_2}\ln N$. Hence from (7.2.1),

$$\varepsilon_1 \left|\left(\delta^2 - \frac{d^2}{dx^2}\right) v_1(x_i)\right| \leq C\varepsilon_1 h^2 |v_1^{(iv)}| \leq Ch^2(1+\varepsilon_1) \leq CN^{-2}.$$

For the singular component at $(\tau_{\varepsilon_2}, 1/2]$ using the bound at (7.2.2), we have

$$\begin{aligned}\varepsilon_1 \left|\left(\delta^2 - \frac{d^2}{dx^2}\right) w_1(x_i)\right| &\leq C\varepsilon_1 |w_1''|_{[x_{i-1}, x_{i+1}]} \\ &\leq C\varepsilon_1 [\varepsilon_1^{-1}\mathcal{E}_{\varepsilon_1} + \varepsilon_2^{-1}\mathcal{E}_{\varepsilon_2}] \\ &\leq C[\mathcal{E}_{\varepsilon_1} + \frac{\varepsilon_1}{\varepsilon_2}\mathcal{E}_{\varepsilon_2}] \leq C|\mathcal{E}_{\varepsilon_2}|_{[x_{i-1}, x_{i+1}]}.\end{aligned}$$

Now as $x_{i-1} \geq \tau_{\varepsilon_2}$ in $(\tau_{\varepsilon_2}, 1-\tau_{\varepsilon_2})$, so

$$|\mathcal{E}_{\varepsilon_2}|_{[x_{i-1}, x_{i+1}]} = |\mathcal{E}_{\varepsilon_2, i-1}| \leq 2\exp\left(-\tau_{\varepsilon_2}\sqrt{\frac{\beta}{\varepsilon_2}}\right) = 2\exp\left(-\tau_0\sqrt{\beta}\ln N\right) \leq 2N^{-\tau_0\sqrt{\beta}}. \tag{7.4.11}$$

Similarly for $x_i \in [1/2, 1-\tau_{\varepsilon_2})$ we have

$$\varepsilon_1 \left|\left(\delta^2 - \frac{d^2}{dx^2}\right) w_1(x_i)\right| \leq CN^{-\tau_0\sqrt{\beta}}.$$

For the error parts of u_2, we again consider $|\tau_{i,\ u_2}| \leq |\tau_{i,\ v_2}| + |\tau_{i,\ w_2}|$. Proceeding in a similar way used for v_1, it can be shown that $|\tau_{i,\ v_2}| \leq CN^{-2}$. For w_2, using (7.2.3) we have

$$|\tau_{i,\ w_2}| \leq C\varepsilon_2 |w_2''| \leq C|\mathcal{E}_{\varepsilon_2}|_{[x_{i-1},x_{i+1}]}.$$

Thereafter employing (7.4.11), we obtain $|\tau_{i,\ u_2}| \leq CN^{-\tau_0\sqrt{\beta}}$.
Hence the result follows. ∎

Lemma 7.4.3. *The truncation errors in the regions* $(\tau_{\varepsilon_1}, \tau_{\varepsilon_2})$ *and* $(1-\tau_{\varepsilon_2}, 1-\tau_{\varepsilon_1})$ *satisfy the following bounds*

$$\begin{aligned} |\tau_{i,\ u_1}| &\leq CN^{-\tau_0\sqrt{\beta}} + CN^{-2}\ln^2 N, \\ &\qquad \textit{for } i = N/8+1, \cdots, N/4-1, 3N/4+1, \cdots, 7N/8-1. \\ |\tau_{i,\ u_2}| &\leq CN^{-\tau_0\sqrt{\beta}} + CN^{-2}\ln^2 N, \\ &\qquad \textit{for } i = N/8+1, \cdots, N/4-1, 3N/4+1, \cdots, 7N/8-1. \end{aligned} \tag{7.4.12}$$

Proof. The meshes are uniform in the aforementioned regions. Hence, $h_i = h = 8\tau_0(\sqrt{\varepsilon_2} - \sqrt{\varepsilon_1})N^{-1}\ln N < 16\tau_0\sqrt{\varepsilon_2}N^{-1}\ln N < CN^{-1}$. Therefore, we have from (7.2.1)

$$|\tau_{i,\ v_1}| \leq C\varepsilon_1 h^2 |v_1^{(iv)}| \leq Ch^2\varepsilon_1(1+\varepsilon_1^{-1}) \leq CN^{-2}.$$

Now the decomposition $w_1 = w_{\varepsilon_1,1} + w_{\varepsilon_2,1}$ will be considered for the error analysis of the singular component. Note that $|\tau_{i,\ w_1}| \leq C[|\tau_{i,\ w_{\varepsilon_1,1}}| + |\tau_{i,\ w_{\varepsilon_2,1}}|]$. Therefore, a straightforward calculation shows that

$$|\tau_{i,\ w_{\varepsilon_1,1}}| \leq C\varepsilon_1 |w''_{\varepsilon_1,1}|_{[x_{i-1},x_{i+1}]} \leq C|\mathcal{E}_{\varepsilon_1}|_{[x_{i-1},x_{i+1}]}.$$

For $x_{i-1} \geq \tau_{\varepsilon_1}$, using the derivative bound from (7.2.6) for the above decomposition, we get

$$|\tau_{i,\ w_{\varepsilon_1,1}}| \leq C|\mathcal{E}_{\varepsilon_1,i-1}| \leq N^{-\tau_0\sqrt{\beta}}.$$

Again it follows from (7.2.6), that

$$|\tau_{i,\ w_{\varepsilon_2,1}}| \leq C\varepsilon_1 h^2 |w_{\varepsilon_2,1}^{(iv)}| \leq C\varepsilon_1 h^2 [\varepsilon_1^{-1}\varepsilon_2^{-1}\mathcal{E}_{\varepsilon_2}] \leq CN^{-2}\ln^2 N.$$

Therefore, we have

$$|\tau_{i,\ u_1}| \leq |\tau_{i,\ v_1}| + |\tau_{i,\ w_1}| \leq CN^{-2}\ln^2 N.$$

For u_2, the decomposition $u_2 = v_2 + w_{\varepsilon_1,2} + w_{\varepsilon_2,2}$ with the derivative bounds (7.2.1) and (7.2.6) leads to

$$|\tau_{i,\ v_2}| \leq C\varepsilon_2 h^2 |v_2^{(iv)}| \leq Ch^2(1+\varepsilon_2) \leq CN^{-2}.$$

Also

$$|\tau_{i,\ w_{\varepsilon_2,2}}| \leq C\varepsilon_2 h^2 |w_{\varepsilon_2,2}^{(iv)}| \leq C\varepsilon_2 h^2 [\varepsilon_2^{-2}\mathcal{E}_{\varepsilon_2}] \leq CN^{-2}\ln^2 N.$$

By an analogous argument provided for $\tau_{i,\ w_{\varepsilon_1,1}}$, we get

$$|\tau_{i,\ w_{\varepsilon_1,2}}| \leq C\varepsilon_2 |w''_{\varepsilon_1,2}| \leq C|\mathcal{E}_{\varepsilon_1}|_{[x_{i-1},x_{i+1}]} \leq CN^{-2}.$$

Hence, we have

$$|\tau_{i,\ u_2}| \leq CN^{-2}\ln^2 N,$$

which proves the result. ∎

Lemma 7.4.4. *The truncation errors at the transition points τ_{ε_1} and $1-\tau_{\varepsilon_1}$ satisfy*

$$\begin{aligned} |\tau_{i,\ u_1}| &\leq C\left(\sqrt{\frac{\varepsilon_1}{\varepsilon_2}}N^{-1} + N^{-\tau_0\sqrt{\beta}}\right),\ \textit{for } i = N/8, \quad 7N/8, \\ |\tau_{i,\ u_2}| &\leq C\left(\sqrt{\frac{\varepsilon_2}{\varepsilon_1}}N^{-1} + N^{-\tau_0\sqrt{\beta}}\right),\ \textit{for } i = N/8, \quad 7N/8. \end{aligned} \tag{7.4.13}$$

Proof. To prove this lemma, we shall use the solution decompositions used in the previous lemma. Note that, in this case $h_i + h_{i+1} \leq 16\tau_0\sqrt{\varepsilon_2}N^{-1}\ln N$. Hence

$$\begin{aligned} |\tau_{i,\ v_1}| &\leq C\varepsilon_1(h_i + h_{i+1})|v'''_1| \\ &\leq C\varepsilon_1\sqrt{\varepsilon_2}N^{-1}\ln N(1+\varepsilon_1^{-1/2}) \\ &\leq C\sqrt{\varepsilon_1}N^{-1}(\sqrt{\varepsilon_2}\ln N) \leq C\sqrt{\varepsilon_1}N^{-1}. \end{aligned}$$

By a similar technique, it is easy to show that $|\tau_{i,\ v_2}| \leq C\sqrt{\varepsilon_2}N^{-1}$. Now the derivative bound given in (7.2.5) yields

$$|\tau_{i,\ w_{\varepsilon_1,1}}| \leq C\varepsilon_1 |w''_{\varepsilon_1,1}|_{[x_{i-1},x_{i+1}]} \leq C|\mathcal{E}_{\varepsilon_1}|_{[x_{i-1},x_{i+1}]} \leq N^{-\tau_0\sqrt{\beta}},$$

and

$$\begin{aligned} |\tau_{i,\ w_{\varepsilon_2,1}}| &\leq C\varepsilon_1(h_i + h_{i+1})|w'''_{\varepsilon_2,1}| \\ &< C\varepsilon_1(\tau_{\varepsilon_1} + \tau_{\varepsilon_2})N^{-1}\varepsilon_2^{-3/2}\mathcal{E}_{\varepsilon_1}|_{[x_{i-1},x_{i+1}]} \\ &\leq C\varepsilon_1\varepsilon_2^{-1}N^{-1}\ln N\exp(-\tau_{\varepsilon_1}\sqrt{\beta/\varepsilon_2}) \leq C\varepsilon_1^{1/2}\varepsilon_2^{-1/2}N^{-1}. \end{aligned}$$

So

$$|\tau_{i,\ w_1}| \leq C(\varepsilon_1^{1/2}\varepsilon_2^{-1/2}N^{-1} + N^{-\tau_0\sqrt{\beta}}).$$

Similarly, we have

$$|\tau_{i,\ w_2}| \leq C(\varepsilon_2^{1/2}\varepsilon_1^{-1/2}N^{-1} + N^{-\tau_0\sqrt{\beta}}).$$

Hence the result follows. ∎

Lemma 7.4.5. *The truncation errors at the transition points τ_{ε_2} and $1-\tau_{\varepsilon_2}$ satisfy*

$$\begin{aligned} |\tau_{i,\ u_1}| &\leq C\left(\varepsilon_1\varepsilon_2^{-1/2}N^{-1} + N^{-\tau_0\sqrt{\beta}}\right),\ \textit{for } i = N/4, \quad 3N/4, \\ |\tau_{i,\ u_2}| &\leq C\left(\varepsilon_2^{1/2}N^{-1} + N^{-\tau_0\sqrt{\beta}}\right),\ \textit{for } i = N/4, \quad 3N/4. \end{aligned} \tag{7.4.14}$$

Proof. From the continuous derivative bounds appeared in (7.2.1), it follows that

$$|\tau_{i,\ v_1}| \leq C\varepsilon_1(h_i + h_{i+1})|v_1'''|_{[x_{i-1},x_{i+1}]} \leq C\varepsilon_1(h_i + h_{i+1})(\varepsilon_2^{-1} + \varepsilon_1^{-1}\mathcal{E}_{\varepsilon_1}).$$

Now taking $\tau_0 = 2/\sqrt{\beta}$, observe that

$$\tau_{\varepsilon_1} < \tau_{\varepsilon_2} \Rightarrow 2\varepsilon_1 < \varepsilon_2.$$

Again it can be shown (see [51]) that

$$\varepsilon_1^{-1/2}\mathcal{E}_{\varepsilon_1}(x) \leq 2\varepsilon_2^{-1/2}\exp(-x\sqrt{\beta/\varepsilon_2}) \leq 2\varepsilon_2^{-1/2}, \quad \text{for} \quad \sqrt{\varepsilon_2/\beta} \leq x \leq 1/2.$$

For sufficiently large N, we can have $|v_1'''| \leq C\varepsilon_2^{-1/2}$. Hence,

$$|\tau_{i,\ v_1}| \leq C\varepsilon_1(h_i + h_{i+1})|v_1'''|_{[x_{i-1},x_{i+1}]} \leq C\varepsilon_1\varepsilon_2^{-1/2}N^{-1}.$$

In an analogous manner, the derivative bound from (7.2.1) leads to

$$|\tau_{i,\ v_2}| \leq C\varepsilon_1(h_i + h_{i+1})|v_2'''|_{[x_{i-1},x_{i+1}]} \leq C\varepsilon_2^{1/2}N^{-1}.$$

Now using (7.2.2), we have

$$\begin{aligned}
|\tau_{i,\ w_1}| &\leq C|w_1''|_{[x_{i-1},x_{i+1}]} \\
&\leq C\varepsilon_1[\varepsilon_1^{-1}\mathcal{E}_{\varepsilon_1} + \varepsilon_1^{-2}\mathcal{E}_{\varepsilon_2}]_{[x_{i-1},x_{i+1}]} \\
&\leq C[\mathcal{E}_{\varepsilon_1} + \varepsilon_1\varepsilon_2^{-1}\mathcal{E}_{\varepsilon_2}]_{[x_{i-1},x_{i+1}]} \\
&= C|\mathcal{E}_{\varepsilon_2}|_{[x_{i-1},x_{i+1}]} = C|\mathcal{E}_{\varepsilon_2,i-1}|.
\end{aligned}$$

Noticing $x_{i-1} \geq \tau_{\varepsilon_2} - 8N^{-1}\tau_{\varepsilon_2}$, it follows that

$$|\tau_{i,\ w_1}| \leq C\exp(-\beta\varepsilon_2^{-1}\tau_{\varepsilon_2} + 8\beta N^{-1}{\varepsilon_2}^{-1}\tau_{\varepsilon_2}) \leq CN^{-\tau_0\sqrt{\beta}}.$$

Proceeding by an analogous way as like in w_1, we can derive that

$$|\tau_{i,\ w_2}| \leq CN^{-\tau_0\sqrt{\beta}}.$$

which proves the above lemma. ∎

Except the two inequalities (7.4.13) and (7.4.14), one can notice that the truncation errors are of order $O(N^{-2}\ln^2 N) + O(N^{-\tau_0\sqrt{\beta}})$. Therefore, to obtain the ε-uniform convergence of the proposed method, we shall use the discrete comparison principle using an adequate barrier function with the assumption $\tau_0\sqrt{\beta} \geq 2$ and $\varepsilon_1, \varepsilon_2 \leq CN^{-1}$. It leads to the truncation errors of order $O(N^{-2}\ln^2 N)$.

Definition 7.4.6. *(Discrete Comparison Principle) If the stiffness matrix associated with the hybrid scheme (7.3.9)-(7.3.14) of the discrete operator $\mathcal{L}^N$ is an M-matrix, then it satisfies that $[\mathcal{L}^N \boldsymbol{V}]_i \geq 0$, for $i = 1, \cdots, N-1$, with $M_l^N \boldsymbol{V}_0 \geq 0$ and $M_r^N \boldsymbol{V}_N \geq 0$, on Ω^N imply $\boldsymbol{V}_i \geq 0$, for $i = 0, \cdots, N$.*

The following lemma shows that the stiffness matrix of the discrete operator (7.3.7)-(7.3.8) leads to an M-matrix. A similar technique is used to show the stability of the discrete operator by Natesan and Deb [63].

Lemma 7.4.7. *Let us assume that $\varepsilon_2 = O(\varepsilon_1)$, i.e., there exists a positive number K such that $\varepsilon_2 \leq K\varepsilon_1$. Assume N_0 is the smallest positive integer which satisfies $32K\beta^*\tau_0^2 N^{-2}\ln^2 N < 3$, for $N \geq N_0$. Then, the following results hold true*

$$r_{1,i}^- < 0, \qquad r_{1,i}^+ < 0, \qquad r_{1,i}^c > 0, \qquad |r_{1,i}^c| - |r_{1,i}^-| - |r_{1,i}^+| \geq K_1 > 0,$$

$$r_{2,i}^- < 0, \qquad r_{2,i}^+ < 0, \qquad r_{2,i}^c > 0, \qquad |r_{2,i}^c| - |r_{2,i}^-| - |r_{2,i}^+| \geq K_2 > 0,$$

for $i = 0, \cdots, N$, where K_1 and K_2 are positive constants depending on the $\beta, \alpha_j, \beta_j, \gamma_j, \delta_j$ for $j = 1, 2$ and the mesh widths h_i for $i = 1, \cdots, N$. Therefore, the stiffness matrix of the proposed hybrid scheme defined by (7.3.9)-(7.3.14) satisfies a discrete comparison principle. Furthermore, the discrete solution is ε-uniform stable in the maximum norm.

Proof. From (7.3.10), it is clear that $r_{1,i}^- < 0$ and $r_{1,i}^+ < 0$ for $i = N/4, \cdots, 3N/4$. Also observe that $r_{1,i}^c > 0$ for all i.

For $i = 1, \cdots, N/8 - 1$ and $i = 7N/8 + 1, \cdots, N-1$, note that

$$r_{1,i}^- = \frac{-3\varepsilon_1}{h_i(h_i + h_{i+1})} + \frac{b_{11}(x_{i-1})}{4} < \frac{1}{128\tau_0^2 N^{-2}\ln^2 N}\left[-3 + 32K\beta^*\tau_0^2 N^{-2}\ln^2 N\right] < 0,$$

where $h_i = h_{i+1} = 8N^{-1}\tau_0\sqrt{\varepsilon_1}\ln N$.
For $i = N/8, N/8+1, \cdots, N/4-1, 3N/4+1, \cdots, 7N/8-1, 7N/8$, one can see that $h_i = 8N^{-1}\tau_0(\sqrt{\varepsilon_2} - \sqrt{\varepsilon_1})\ln N$. Hence the relations $\varepsilon_2 \leq K\varepsilon_1$ and $3 > 32K\beta^*\tau_0^2 N^{-2}\ln^2 N$ lead to

$$r_{1,i}^- = \frac{-3\varepsilon_1}{h_i(h_i + h_{i+1})} + \frac{b_{11}(x_{i-1})}{4} < \frac{\varepsilon_1}{128\tau_0^2\varepsilon_2 N^{-2}\ln^2 N}\left[-3 + 32K\beta^*\tau_0^2 N^{-2}\ln^2 N\right] < 0,$$

for sufficiently large $N \geq N_0$. By a similar technique, we can also show that $r_{1,i}^+ < 0$. Again the fact $\varepsilon_2 \geq \varepsilon_1$ implies that

$$r_{2,i}^- < 0, \quad r_{2,i}^+ < 0, \quad \text{and} \quad r_{2,i}^c > 0 \quad \text{for } i = 1, \cdots, N-1,$$

Now corresponding to the left boundary point $x_0 = 0$, observe that $h_1 = 8N^{-1}\tau_0\sqrt{\varepsilon_1}\ln N$. Hence from $b_{11}(x_1) \leq \beta^*$, we get

$$r_{1,0}^+ = \frac{-3\varepsilon_1\beta_1}{h_1^2} + \frac{b_{11}(x_1)\beta_1}{2} < \frac{\beta_1}{64\tau_0^2 N^{-2}\ln^2 N}\left[-3 + 32K\beta^*\tau_0^2 N^{-2}\ln^2 N\right] < 0.$$

In a similar manner, we can show that $r^-_{1,N} < 0$, $r^+_{2,0} < 0$, $r^-_{2,N} < 0$ and $r^c_{1,0} > 0$, $r^c_{1,N} > 0$, $r^c_{2,0} > 0$, $r^c_{2,N} > 0$.

On the other hand, for $i = N/4, \cdots, 3N/4$, it is clear that $|r^c_{1,i}| - |r^-_{1,i}| - |r^+_{1,i}| \geq \beta$. Now, for $i = 1, \cdots, N/4 - 1$ and $i = 3N/4 + 1, \cdots, N - 1$, we have

$$\begin{aligned}
|r^c_{1,i}| - |r^-_{1,i}| - |r^+_{1,i}| &= \frac{3\varepsilon}{h_i h_{i+1}} + b_{11}(x_i) - \frac{3\varepsilon}{h_i(h_i + h_{i+1})} + \frac{h_i b_{11}(x_{i-1})}{2(h_i + h_{i+1})} - \\
&\quad - \frac{3\varepsilon}{h_{i+1}(h_i + h_{i+1})} + \frac{h_{i+1} b_{11}(x_{i+1})}{2(h_i + h_{i+1})} \\
&= b_{11}(x_i) + \frac{h_i b_{11}(x_{i-1})}{2(h_i + h_{i+1})} + \frac{h_{i+1} b_{11}(x_{i+1})}{2(h_i + h_{i+1})} \\
&\geq \beta + \left[\frac{h_i}{2(h_i + h_{i+1})} + \frac{h_{i+1}}{2(h_i + h_{i+1})} \right] \beta = \frac{3}{2}\beta > 0.
\end{aligned}$$

Also

$$\begin{aligned}
|r^c_{1,0}| - |r^+_{1,0}| &= \frac{3\varepsilon_1}{h_1}\left(\alpha_1 + \frac{\beta_1}{h_1} \right) + b_{11}(x_0)\beta_1 - \frac{3\varepsilon_1 \beta_1}{h_1^2} + \frac{b_{11}(x_1)\beta_1}{2} \\
&= \frac{3\varepsilon_1}{h_1}\alpha_1 + \left[b_{11}(x_0) + \frac{b_{11}(x_1)}{2} \right] \beta_1 \\
&\geq \frac{3\varepsilon_1}{h_1}\alpha_1 + \frac{3}{2}\beta\beta_1 > 0,
\end{aligned}$$

and

$$\begin{aligned}
|r^c_{1,N}| - |r^-_{1,N}| &= \frac{3\varepsilon_1}{h_N}\left(\gamma_1 + \frac{\delta_1}{h_N} \right) + b_{11,N}\delta_1 - \frac{3\varepsilon_1 \delta_1}{h_N^2} + \frac{b_{11}(x_{N-1})\delta_1}{2} \\
&= \frac{3\varepsilon_1}{h_N}\gamma_1 + \left[\frac{b_{11}(x_{N-1})}{2} + b_{11}(x_N) \right] \delta_1 \\
&\geq \frac{3\varepsilon_1}{h_N}\gamma_1 + \frac{3}{2}\beta\delta_1 > 0.
\end{aligned}$$

By an analogous way, for $i = 0, N$, it can be shown that

$$|r^c_{2,0}| - |r^+_{2,0}| > 0, \text{ and } |r^c_{2,N}| - |r^-_{2,N}| > 0.$$

Hence, the discrete operator (7.3.7)-(7.3.8) is ε-uniform stable. ∎

Therefore, the discrete operator satisfies the discrete comparison principle and as a consequence, the discrete stability result can be obtained. The following theorem shows that in practice, the method (7.3.7)-(7.3.8) is almost second-order uniformly convergent on the piecewise-uniform Shishkin mesh.

Theorem 7.4.8. *Let $\boldsymbol{u}$ be the exact solution of the system (7.1.1) and $\boldsymbol{U}$ be the numerical solution obtained from the hybrid finite difference scheme (7.3.7)-(7.3.8). Then, under the conditions stated in Lemma 7.4.7 with $\varepsilon_2 = O(\varepsilon_1)$, $\varepsilon_1, \varepsilon_2 \leq N^{-1}$, we have the following parameter-uniform error estimate*

$$||\boldsymbol{u} - \boldsymbol{U}||_{\Omega^N} \leq C\left(N^{-2}\ln^2 N + N^{-\tau_0\sqrt{\beta}} \right), \quad i = 0, \cdots, N. \tag{7.4.15}$$

Proof. Define the barrier function $\mathbf{\Phi} = (\phi_1, \phi_2)^T$, such that

$$\mathbf{\Phi}(x_i) = C\left(N^{-2}\ln^2 N + N^{-\tau_0\sqrt{\beta}} + N^{-2}\frac{\tau_{\varepsilon_1}^2}{\sqrt{\varepsilon_1}}\psi_1(x_i) + N^{-2}\frac{\tau_{\varepsilon_2}^2}{\sqrt{\varepsilon_2}}\psi_2(x_i)\right)\begin{pmatrix}1\\1\end{pmatrix},$$

$i = 1, \cdots, N-1$, where

$$\psi_1(x) = \begin{cases} x/\tau_{\varepsilon_1}, & 0 \le x \le \tau_{\varepsilon_1}, \\ 1, & \tau_{\varepsilon_1} \le x \le 1-\tau_{\varepsilon_1}, \\ (1-x)/\tau_{\varepsilon_1}, & 1-\tau_{\varepsilon_1} \le x \le 1, \end{cases}$$

and

$$\psi_2(x) = \begin{cases} x/\tau_{\varepsilon_2}, & 0 \le x \le \tau_{\varepsilon_2}, \\ 1, & \tau_{\varepsilon_2} \le x \le 1-\tau_{\varepsilon_2}, \\ (1-x)/\tau_{\varepsilon_2}, & 1-\tau_{\varepsilon_2} \le x \le 1. \end{cases}$$

After simplification, it is easy to obtain that

$$\begin{aligned}[\mathcal{L}_1^N \mathbf{\Phi}(x_i)] \ &\ge C\left(N^{-2}\ln^2 N + N^{-\tau_0\sqrt{\beta}}\right)\left(r_{1,\,i}^- + r_{1,\,i}^c + r_{1,\,i}^+ + q_{1,\,i}^- + q_{1,\,i}^c + q_{1,\,i}^+\right) + \\ &+C\frac{\tau_{\varepsilon_1}^2}{\sqrt{\varepsilon_1}}\,N^{-2}\left([r_{1,\,i}^- + q_{1,\,i}^-]\psi_{1,i-1} + [r_{1,\,i}^c + q_{1,\,i}^c]\psi_{1,i} + [\,r_{1,\,i}^+ + q_{1,\,i}^+]\psi_{1,i+1}\right) + \\ &+C\frac{\tau_{\varepsilon_2}^2}{\sqrt{\varepsilon_2}}\,N^{-2}\left([r_{2,\,i}^- + q_{2,\,i}^-]\psi_{2,i-1} + [r_{2,\,i}^c + q_{2,\,i}^c]\psi_{2,i} + [\,r_{2,\,i}^+ + q_{2,\,i}^+]\psi_{2,i+1}\right).\end{aligned}$$

Therefore, using the truncation error bounds from Lemma 7.4.1-7.4.5, a calculation shows that

$$|\tau_{i,\,u_1}| = |L_1^N(\boldsymbol{U}-\boldsymbol{u})(x_i)| \le |\mathcal{L}_1^N\mathbf{\Phi}(x_i)|.$$

Similarly, for the second equation, one can have $|\tau_{i,\,u_2}| = |\mathcal{L}_2^N(\boldsymbol{U}-\boldsymbol{u})(x_i)| \le |\mathcal{L}_2^N\mathbf{\Phi}(x_i)|$. Now Lemma 7.4.7 implies that the stiffness matrix corresponding to the discrete operator $\mathcal{L}^N$ is an M-matrix. Hence the inverse of the discrete operator $\mathcal{L}^N$ is ε-uniformly bounded. Therefore, we obtain the required error bound

$$||\boldsymbol{U}_i - \boldsymbol{u}(x_i)|| \le ||\mathbf{\Phi}(x_i)|| \le C\left(N^{-2}\ln^2 N + N^{-\tau_0\sqrt{\beta}}\right). \qquad \blacksquare$$

In fact, the following theorem shows that a uniformly convergent global approximation of the numerical solution $\boldsymbol{U}$ can be constructed by forming piecewise linear interpolation of the numerical solution.

Theorem 7.4.9. *The numerical solution $\boldsymbol{U}$ of the hybrid scheme (7.3.7)-(7.3.8), which converges uniformly to the exact solution $\boldsymbol{u}$ of the continuous problem (7.1.1) satisfies the following global ε-uniform error estimate*

$$||\overline{\boldsymbol{U}} - \boldsymbol{u}|| \le C\left(N^{-2}\ln^2 N + N^{-\tau_0\sqrt{\beta}}\right),$$

where $\overline{\boldsymbol{U}}$ is the piecewise linear interpolant of $\boldsymbol{U}$ on $\overline{\Omega}$.

Proof. From the triangle inequality, we have

$$||\overline{\boldsymbol{U}} - \boldsymbol{u}\ || \leq ||\overline{\boldsymbol{U}} - \overline{\boldsymbol{u}}|| + ||\overline{\boldsymbol{u}} - \boldsymbol{u}||,$$

where $\overline{\boldsymbol{u}}$ is the piecewise linear interpolant of the values of $\boldsymbol{u}$ at the mesh points. Then, using the classical error estimate for linear interpolation, it is easy to prove that

$$||\overline{\boldsymbol{U}} - \boldsymbol{u}\ || \leq C\left(N^{-2}\ln^2 N + N^{-\tau_0\sqrt{\beta}}\right). \qquad \blacksquare$$

Remark 7.4.10. *One can notice that the construction of the transition parameters appeared in the piecewise-uniform Shishkin mesh (7.3.6) involved both the parameters ε_1 and ε_2 for the problem (7.1.1). Thereafter, we have carried out the convergence analysis using these two transition points. However, it is observed that the system of equations for discrete solution will satisfy the M-matrix property only when $\varepsilon_2 = O(\varepsilon_1)$. Hence, this condition suggests that it is sufficient to consider the system (7.1.1) using only one parameter, say ε_2. The corresponding discretized problem can be considered by dividing the domain into three parts $[0, \tau_{\varepsilon_2}]$, $[\tau_{\varepsilon_2}, 1-\tau_{\varepsilon_2}]$ and $[1-\tau_{\varepsilon_2}, 1]$ with one transition parameter τ_{ε_2}. This transition parameter will be chosen as $\min\{1/4, \tau_0\sqrt{\varepsilon_2}\ln N\}$. Thereafter, we may proceed to the convergence analysis, which is similar to the general convergence analysis provided in this chapter, by taking τ_{ε_2} as a transition point with sufficiently small ε_2.*

It should also be noted that the transition points are involving a constant $\tau_0 (\geq 2/\sqrt{\beta})$ in (7.3.6). This constant τ_0 can be chosen appropriately to get better convergence rate outside the layer regions (see Lemma 7.4.2). However, Theorem 7.4.8 suggests that the numerical solution $\boldsymbol{U}$ will converge with the rate of $O(N^{-2}\ln^2 N)$.

Remark 7.4.11. *Now consider the model problem (7.1.1) with a particular form of the mixed boundary conditions, defined as $\beta_k = \tilde{\beta}_k\sqrt{\varepsilon}$ and $\delta_k = \tilde{\delta}_k\sqrt{\varepsilon}$, where $\tilde{\beta}_k, \tilde{\delta}_k$'s are positive constants. Let us consider the general Shishkin mesh by assuming $\varepsilon_2 = \varepsilon_1 = \varepsilon$(say). We shall show that the cubic spline approximation inside the layer regions provides better approximation than the approximate model, where the forward and backward schemes are used at $x = 0, 1$, for the mixed boundary conditions respectively. In this case, we shall use the central difference approximation for the differential equation at the interior mesh points. Now, at $x = 0$ observe that*

$$\begin{aligned}
|(\alpha_k u_k(0) - \beta_k u_k'(0)) - (\alpha_k U_k(0) - \beta_k D^+U_k(0))| &= \sqrt{\varepsilon}\tilde{\beta}_k|u_k'(0) - D^+U_k(0)| \\
&\leq \left|\frac{\sqrt{\varepsilon}\tilde{\beta}_k}{h}\int_0^h (t-h)u_k''(t)dt\right| \\
&\leq Ch/\sqrt{\varepsilon} \leq CN^{-1}\ln N,
\end{aligned}$$

where the derivative bound of u_k is used from Theorem 7.2.1. The uniform convergence at the point $x = 1$ can be shown by a similar techique provided here. The derivation

of Lemma 7.4.7 implies that the standard approximation will also lead to an M-matrix. Hence, one can get $O(N^{-1}\ln N)$ as order of convergence for the standard method with the restricted choices of β_k, δ_k.

If we start the convergence analysis with the assumption $\boldsymbol{u}(x) \in \mathcal{C}^2(\Omega)$, then Lemma 7.4.2 implies that the truncation errors of the smooth component satisfy $|\tau_{i,\ v_1}| = \varepsilon_1 \left| \left(\delta^2 - \frac{d^2}{dx^2}\right) v_1(x_i) \right| \leq C\varepsilon_1 |v_1^{(ii)}| \leq CN^{-1}$, as $\varepsilon_1 \leq CN^{-1}$ and $|v_1^{(ii)}(x)| \leq C$. The same smoothness is required to derive $|\tau_{i,\ w_1}| \leq CN^{-\tau_0\sqrt{\beta}}$. But the assumption $\boldsymbol{u}(x) \in \mathcal{C}^2(\Omega)$ is not enough for the convergence of the standard method, i.e., for central difference approximation inside the layer regions, for e.g., *in $(0, \tau_{\varepsilon_1})$. One can observe that $|\tau_{i,\ w_1}| = \varepsilon_1 \left| \left(\delta^2 - \frac{d^2}{dx^2}\right) w_1(x_i) \right| \leq C\varepsilon_1 h^2 |w_1^{(iv)}| \leq C\tau_0^2 N^{-2} \ln^2 N$ from Lemma 7.4.1 if we assume $\boldsymbol{u}(x) \in \mathcal{C}^4(\Omega)$.*

Hence, we can conclude that, under the restricted choices of β_k, δ_k, we can at most expect $O(N^{-1}\ln N)$ as order of convergence of the standard method, whereas the proposed method provides order of convergence $O(N^{-2}\ln^2 N)$ for any choice of β_k, δ_k to mixed boundary conditions with the assumption $\boldsymbol{u}(x) \in \mathcal{C}^4(\Omega)$. So the proposed method is better than the standard one.

7.5 Numerical Results

This section presents the numerical experiments to confirm the theoretical results explained in the previous section. The numerical results are obtained by considering two test problems with the perturbation parameter $\varepsilon_2 = \varepsilon_1 = \varepsilon$ (see Remark 7.4.10). The maximum point-wise errors and the corresponding rates of convergence are given in tables.

Example 7.5.1. *Consider the following coupled system of reaction-diffusion MBVPs:*

$$\begin{cases} -\varepsilon u_1''(x) + 2(x+1)^2 u_1(x) - (1+x^3)u_2(x) = f_1(x), \quad x \in \Omega, \\ -\varepsilon u_2''(x) - 2\cos\left(\frac{\pi x}{4}\right) u_1(x) + 2.2e^{1-x} u_2(x) = f_2(x), \end{cases}$$

with

$$\begin{cases} u_1(0) - u_1'(0) = 2 - \dfrac{\exp(-1/\sqrt{\varepsilon}) - 1}{\sqrt{\varepsilon}(1+\exp(-1/\sqrt{\varepsilon}))}, \\ 2u_1(1) + u_1'(1) = 4 + \dfrac{1 - \exp(-1/\sqrt{\varepsilon})}{\sqrt{\varepsilon}(1+\exp(-1/\sqrt{\varepsilon}))}, \\ u_2(0) - 3u_2'(0) = 1 + 3e^{-1} + 3\dfrac{(1+\exp(-1/\sqrt{\varepsilon}))}{\sqrt{\varepsilon}(1-\exp(-1/\sqrt{\varepsilon})}, \\ u_2(1) + u_2'(1) = -4 - \dfrac{(1+\exp(-1/\sqrt{\varepsilon}))}{\sqrt{\varepsilon}(1-\exp(-1/\sqrt{\varepsilon})}. \end{cases}$$

Here $f_1(x)$ and $f_2(x)$ are chosen such a way that the exact solution of this problem becomes

$$u_1(x) = \frac{\exp((x-1)/\sqrt{\varepsilon}) + \exp(-x/\sqrt{\varepsilon})}{1+\exp(-1/\sqrt{\varepsilon})} + \cos^2 \pi x,$$

$$u_2(x) = \frac{\exp(-x/\sqrt{\varepsilon}) + \exp((x-1)/\sqrt{\varepsilon})}{1-\exp(-1/\sqrt{\varepsilon})} - x\exp(x-1).$$

Example 7.5.2. *Consider the coupled system of reaction-diffusion MBVPs:*

$$\begin{cases} -\varepsilon u_1''(x) + (5+2x)u_1(x) + (x-2)u_2(x) = -4-4x, \quad x \in \Omega, \\ -\varepsilon u_2''(x) - 2u_1(x) + (4-x^2)u_2(x) = 2x^2 - 12, \end{cases}$$

with

$$\begin{cases} u_1(0) - 2\sqrt{\varepsilon}u_1'(0) = 4,\ 2u_1(1) + \sqrt{\varepsilon}u_1'(1) = 1, \\ u_2(0) - \sqrt{\varepsilon}u_2'(0) = 1,\ u_2(1) + 3\sqrt{\varepsilon}u_2'(1) = 2. \end{cases}$$

In all these examples, maximum point-wise errors E_m^N and the corresponding rates of convergence r_m^N, of the discrete solution U_m, $m = 1, 2$ are computed by the formulas described in Chapter 2.

For Examples 7.5.1 and 7.5.2, the piecewise-uniform Shishkin meshes are constructed by taking $\beta = 1$, $\tau_0 = 2$ and the perturbation parameter ε is taken from the set

$$S = \{\varepsilon | \varepsilon = 2^0 N^{-1}, 2^{-1}N^{-1}, \cdots, 2^{-50}\},$$

where N is the number of mesh intervals.

Table 7.1: *Uniform errors and orders of convergence of U_1 by the proposed method for Example 7.5.1*

$\varepsilon \in S$	Number of intervals N							
	32	64	128	256	512	1024	2048	4096
E_1^N	1.509e-2	5.771e-3	1.939e-3	6.365e-4	2.020e-4	6.239e-5	1.887e-5	5.615e-6
r_1^N	1.3874	1.5736	1.6070	1.6558	1.6949	1.7251	1.7489	-

Tables 7.1 and 7.2 display the maximum ε-uniform errors and the corresponding orders of convergence of the computed solution U_m, $m = 1, 2$, for Example 7.5.1 using spline approximation. The standard method (the forward-backward approximation for the mixed boundary conditions respectively) is also used to compare the errors and the rates of convergence for this example which are shown in Tables 7.3 and 7.4. From Table 7.1 and Table 7.2, the monotonically decreasing behavior of ε-uniform errors can be observed as N increases. Tables 7.3 and 7.4 suggest that the standard method is

Table 7.2: *Uniform errors and orders of convergence of U_2 by the proposed method for Example 7.5.1*

$\varepsilon \in S$	Number of intervals N							
	32	64	128	256	512	1024	2048	4096
E_2^N	1.028e-2	3.984e-3	1.358e-3	4.473e-4	1.416e-4	4.371e-5	1.322e-5	3.936e-6
r_2^N	1.3678	1.5527	1.6021	1.6591	1.6961	1.7245	1.7489	-

also working well for Example 7.5.1. A similar behavior is observed for Example 7.5.2, where Tables 7.5 and 7.6 ensure almost second-order convergence for the numerical solution using proposed method, whereas standard technique suggests that one can get at most first-order convergence as depicted in Tables 7.7 and 7.8. Therefore, decreasing behavior of improved ε-uniform errors together with the second-order convergence upto logarithmic term is achieved for the proposed scheme using spline approximation. This shows that proposed technique provides better convergence than the existing one.

As a complement of these observations, Figures 7.2 and 7.3 display the plot of the number of mesh intervals N versus the maximum errors for Example 7.5.2. Here, for each $\varepsilon = 2^{-8}, 2^{-16}, 2^{-24}$, the number of subintervals N varies from $N = 32, \cdots, 4096$. These two graphs indeed show the comparison between the standard method and the proposed method (observe also the error scales). From the loglog plots, one can conclude that the standard method provides first-order accuracy upto logarithmic term whereas the proposed method is second-order convergent upto logarithmic factor.

Table 7.3: *Uniform errors and orders of convergence of U_1 by the standard method for Example 7.5.1.*

$\varepsilon \in S$	Number of intervals N							
	32	64	128	256	512	1024	2048	4096
E_1^N	2.011e-1	1.232e-1	7.224e-2	4.127e-2	2.317e-2	1.286e-2	7.066e-3	3.852e-3
r_1^N	0.70739	0.77015	0.80785	0.83229	0.84993	0.86381	0.87527	-

Table 7.4: *Uniform errors and orders of convergence of U_2 by the standard method for Example 7.5.1.*

$\varepsilon \in S$	Number of intervals N							
	32	64	128	256	512	1024	2048	4096
E_2^N	2.765e-1	1.493e-1	7.973e-2	4.290e-2	2.326e-2	1.265e-2	6.874e-3	3.724e-3
r_2^N	0.88928	0.90515	0.89405	0.88312	0.87885	0.87997	0.88420	-

Table 7.5: *Uniform errors and orders of convergence of U_1 by the proposed method for Example 7.5.2*

$\varepsilon \in S$	Number of intervals N							
	32	64	128	256	512	1024	2048	4096
E_1^N	6.281e-2	2.801e-2	1.094e-2	3.682e-3	1.159e-3	3.582e-4	1.083e-4	3.222e-5
r_1^N	1.1649	1.3557	1.5716	1.6672	1.6944	1.7255	1.7495	-

Table 7.6: *Uniform errors and orders of convergence of U_2 by the proposed method for Example 7.5.2*

$\varepsilon \in S$	Number of intervals N							
	32	64	128	256	512	1024	2048	4096
E_2^N	6.678e-2	2.785e-2	9.987e-3	3.241e-3	1.030e-3	3.186e-4	9.645e-5	2.869e-5
r_2^N	1.2616	1.4798	1.6235	1.6532	1.6935	1.7239	1.7489	-

7.6 Conclusions

In this chapter, we have proposed an efficient numerical scheme for singularly perturbed system of Robin type reaction-diffusion problems of the form (7.1.1) on the piecewise-uniform Shishkin mesh. It is shown theoretically and computationally that the newly proposed scheme is ε-uniformly convergent with almost second-order accuracy, whereas the well-known forward-backward approximation for the mixed boundary conditions and the central difference approximation for the differential equation at the interior points provide almost first-order convergence.

Table 7.7: *Uniform errors and orders of convergence of U_1 by the standard method for Example 7.5.2.*

$\varepsilon \in S$	Number of intervals N							
	32	64	128	256	512	1024	2048	4096
E_1^N	4.403e-1	2.611e-1	1.474e-1	8.177e-2	4.497e-2	2.465e-2	1.345e-2	7.301e-3
r_1^N	0.75379	0.82446	0.85081	0.86261	0.86692	0.87363	0.88223	-

Table 7.8: *Uniform errors and orders of convergence of U_2 by the standard method for Example 7.5.2.*

$\varepsilon \in S$	Number of intervals N							
	32	64	128	256	512	1024	2048	4096
E_2^N	3.975e-1	2.567e-1	1.532e-1	8.778e-2	4.923e-2	2.727e-2	1.496e-2	8.151e-3
r_2^N	0.63092	0.74464	0.80343	0.83427	0.85226	0.86557	0.87669	-

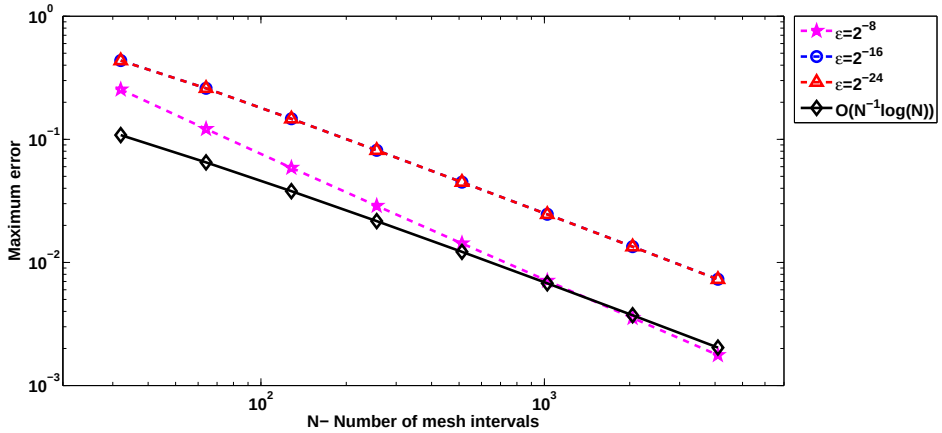

(a) For standard method

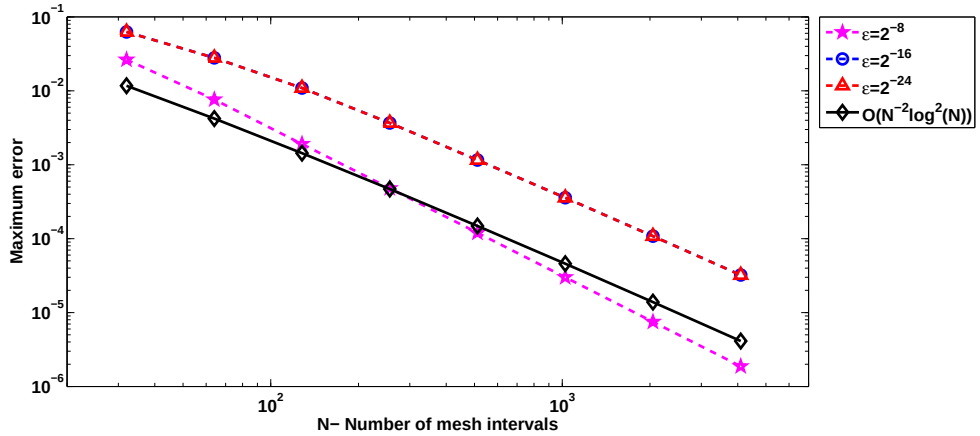

(b) For proposed method.

Figure 7.2: *Loglog plot of the maximum point-wise errors corresponding to U_1 for Example 7.5.2.*

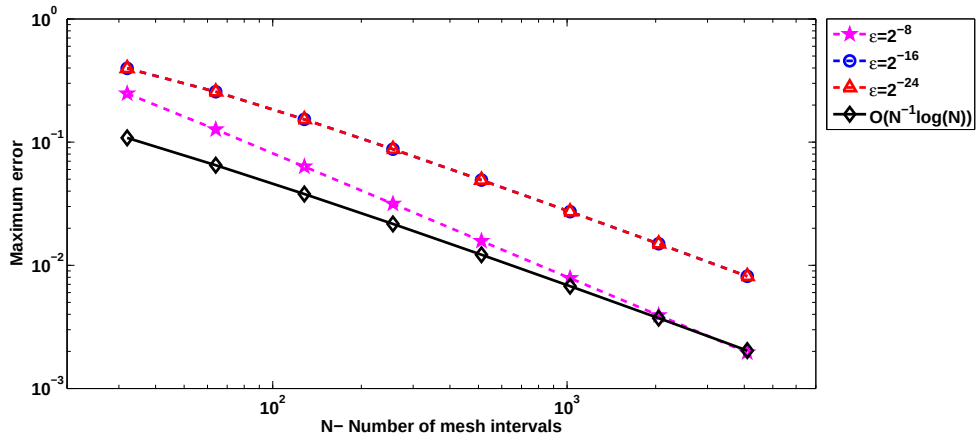

(a) For standard method

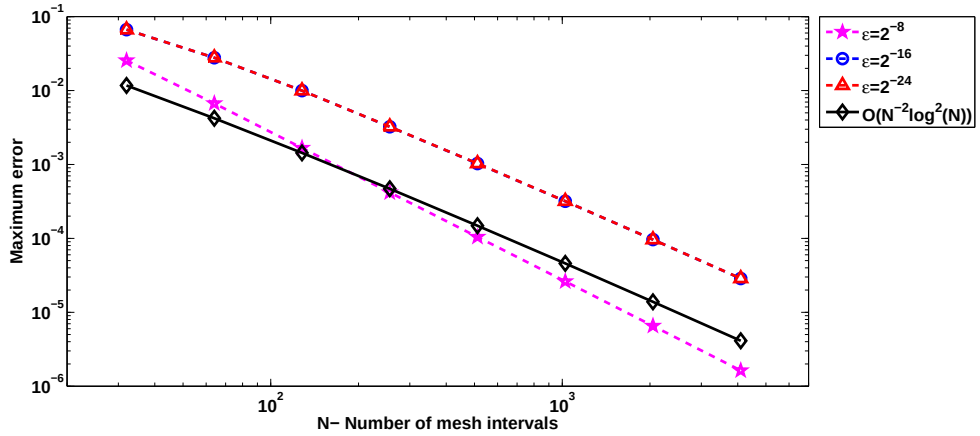

(b) For proposed method.

Figure 7.3: *Loglog plot of the maximum point-wise errors corresponding to U_2 for Example 7.5.2.*

Chapter 8

Summary and Future Scopes

This chapter summarizes the main results achieved in this dissertation. It also provides the scope of possible extensions of the present work and their further investigations.

8.1 Summary of the Results

The present thesis contributes to the study of developing parameter-uniform layer resolving techniques which are mainly concerned on the system of convection-diffusion and the system of reaction-diffusion problems using moving mesh methods. Another ε-uniform numerical method is discussed for solving SPPs on the well-known *apriori* chosen piecewise-uniform Shishkin mesh. The main results of this thesis with some important observations are highlighted below.

A uniformly convergent higher-order numerical scheme /or hybrid scheme is proposed and analyzed for a one-dimensional singularly perturbed Robin type reaction-diffusion problems. This scheme involves a spline approximation for the mixed boundary conditions on the equidistributed mesh. The mesh is obtained by the equidistribution of a positive monitor function involving the second-order derivative of the singular component of the solution. It is shown that the discrete solution obtained by this technique is second-order accurate in the discrete supremum norm, provided the perturbation parameter ε satisfies $\varepsilon \leq N^{-1}$, which is the most demandable case from practical point of view. It is also proved that the standard well-known technique *i.e.,* the forward, backward approximation at the left, right mixed boundary respectively and the central difference approximation for the differential equation provides first-order convergence. Theoretically, it is proved that the results obtained by the proposed scheme can be extended for a more larger class of Robin type reaction-diffusion problems than the model problem considered in this thesis.

Then, the concept of equidistribution principle is extended for a class of fourth-order ODEs. The problem is converted into a relatively simpler problem by reducing it into a system of second-order reaction-diffusion problems. A numerical technique is provided

to make the error estimates of the computed solution and its second-order derivative on the equidistributed mesh. It is found that the proposed numerical method converges ε-uniformly with first-order accuracy. The computational results show that this method is second-order convergent.

In case of a general system of singularly perturbed reaction-diffusion problems, a uniformly accurate numerical method is suggested by the mesh adaptation technique. An *apriori* error monitor function is obtained through the error analysis. This technique can be used to investigate a system of semilinear reaction-diffusion problems where the perturbation parameters are of different magnitudes. It is computationally observed that the proposed method is second-order accurate.

Again, a post-processing Richardson extrapolation technique is analyzed for solving singularly perturbed convection-diffusion problem on adaptively generated equidistributed mesh. It is proved both theoretically and computationally that the first-order convergence of standard upwind scheme can be raised to second-order ε-uniform convergence in the discrete supremum norm.

Next, a system of singularly perturbed weakly coupled convection-diffusion problems is studied using the mesh adaptation technique. Several suitable error monitor functions are derived from the sufficient condition of uniform convergence. A monitor function is suggested for the equidistribution of an initial primary chosen mesh which leads to the first-order parameter-uniform convergence for both the convection-diffusion and reaction-diffusion problems (given in [8, 9]) of scalar form. This is in fact an optimal error estimate corresponding to the upwind scheme. This technique is extended for a system of semilinear singularly perturbed weakly coupled convection-diffusion problems to obtain first-order convergence in the discrete supremum norm.

Finally, the idea of the hybrid scheme is successfully extended for a system of Robin type reaction-diffusion problems on the piecewise-uniform Shishkin mesh. It is proved both theoretically and computationally that the proposed hybrid scheme is almost second-order ε-uniform convergent. This method has an advantage on the standard method (using the forward-backward approximation) which produces almost first-order convergence for a particular class of system of MBVPs.

8.2 Scope for Future Work

This thesis has attempted to develop and analyze the mesh equidistribution and the mesh adaptation techniques to obtain parameter-uniform numerical approximations for the system of reaction-diffusion and the system of convection-diffusion problems exhibiting boundary layers. The higher-order accurate solutions are achieved by proposing a hybrid scheme and a post-processing technique. We now present some observations

about pertaining the possible extensions to more complex problems with smooth and nonsmooth data. Some of these major possibilities which will be carried out in the future with suitable model problems are listed below:

The proposed hybrid numerical scheme which is analyzed in **Chapter 2** and **Chapter 7** on the equidistributed mesh and the *apriori* chosen Shishkin mesh respectively can be used to study the following one-dimensional singularly perturbed Robin type convection-diffusion problem

$$\begin{cases} \mathcal{L}u(x) = -\varepsilon u''(x) + a(x)u'(x) + b(x)u(x) = f(x), \quad x \in \Omega, \\ M_l u(0) \equiv \alpha_1 u(0) - \beta_1 u'(0) = \gamma_1, \quad M_r u(1) \equiv \alpha_2 u(1) + \beta_2 \varepsilon u'(1) = \gamma_2. \end{cases} \tag{8.2.1}$$

The solution $u(x)$ of the problem (8.2.1) possesses a boundary layer at $x = 1$, if $a(x)$ has a positive lower bound (see [74]).

In **Chapter 3**, the mesh equidistribution technique is extended for a class of fourth-order ODEs. One may think of using the equidistribution technique for the fourth-order problems of different kinds. The following singularly perturbed third and fourth-order differential equations can be considered for mesh adaptation

$$\begin{cases} \mathcal{L}u(x) = -\varepsilon u'''(x) + a(x)u''(x) + b(x)u'(x) + c(x)u(x) = f(x), \quad x \in \Omega, \\ u(0) = p, \quad u'(0) = q, \quad u(1) = r, \end{cases} \tag{8.2.2}$$

and

$$\begin{cases} \mathcal{L}u(x) = -\varepsilon u^{iv}(x) - a(x)u'''(x) + b(x)u''(x) - c(x)u(x) = -f(x), \quad x \in \Omega, \\ u(0) = p, \quad u'(0) = q, \quad u(1) = -r, \quad u'(1) = -s. \end{cases} \tag{8.2.3}$$

Here the coefficient functions will be chosen in a way such that the problems (8.2.2) and (8.2.3) will have unique solution in $\overline{\Omega}$ (see [76, 82]).

In **Chapter 4**, the *apriori* error analysis is provided to obtain ε–uniform error estimate of a general singularly perturbed system of reaction-diffusion problems of type (4.1.1). The computational results suggest that the equidistribution of the proposed monitor function generated from the error analysis leads to second-order parameter-uniform convergence. To show the efficiency of the proposed monitor function, one needs to carry out the *aposteriori* error analysis by extending the numerical solution to the whole domain using the linear interpolation. This work will be carried out in future.

A post-processing technique known as Richardson extrapolation technique is discussed in **Chapter 5** to enhance the order of accuracy of the computed solution for singularly perturbed convection-diffusion problem. For our analysis, we have considered the convection coefficient as constant. Hence, the more general class of problems

will be investigated for the error analysis in our nearest future. Another well-known post-processing technique known as defect-correction technique on the adaptively generated meshes will be also inspected to obtain higher-order convergence for moving mesh methods.

Chapter 6 is devoted to the extension of the error monitor functions, proposed by Beckett and Mackenzie [9, 8] to the system of weakly coupled convection-diffusion problems. It has been computationally observed that this monitor function is also working well for a singularly perturbed system of convection-diffusion and reaction-diffusion problems of the following form

$$\begin{cases} -\varepsilon_1 u_1''(x) + b_{11}(x)u_1(x) + b_{12}u_2(x) = f_1(x), \quad x \in \Omega, \\ -\varepsilon_2 u_2''(x) - a_{22}(x)u_2'(x) + b_{21}(x)u_1(x) + b_{22}(x)u_2(x) = f_2(x), \\ u_1(0) = 0, \quad u_1(1) = 0, \quad u_2(0) = 0, \quad u_2(1) = 0. \end{cases} \tag{8.2.4}$$

A more general singularly perturbed system than (8.2.4) can be considered for future work.

This dissertation is mainly devoted on moving mesh methods to the system of one-dimensional convection-diffusion problems and the system of one-dimensional reaction-diffusion problems. However, the most realistic features can be observed in partial differential equations. Hence, it will be interesting to extend our analysis for the following singularly perturbed coupled system of parabolic initial-boundary-value problems:

$$\begin{cases} \dfrac{\partial \boldsymbol{u}}{\partial t} + \boldsymbol{\mathcal{L}u} = \boldsymbol{f}, \quad (x,t) \in G = \Omega \times (0,T), \\ \boldsymbol{u}(x,0) = \boldsymbol{0}, \quad x \in \overline{\Omega}, \\ \boldsymbol{u}(0,t) = \boldsymbol{u}(1,t) = \boldsymbol{0}, \quad t \in (0,T], \end{cases} \tag{8.2.5}$$

where

$$\boldsymbol{\mathcal{L}u} \equiv \boldsymbol{Eps}\frac{\partial^2 \boldsymbol{u}}{\partial x^2} + \boldsymbol{A}\frac{\partial \boldsymbol{u}}{\partial x} + \boldsymbol{Bu},$$

with $\boldsymbol{\mathcal{L}} = (\mathcal{L}_1, \cdots, \mathcal{L}_k)^T$, $\boldsymbol{Eps} = \text{diag}(\varepsilon_1, \cdots, \varepsilon_k)$, $\boldsymbol{A}(x) = \text{diag}(a_{11}(x), \cdots, a_{kk}(x))$, $\boldsymbol{B}(x) = (b_{ij}(x))_{k\times k}$, $\boldsymbol{f}(x,t) = (f_1(x,t), \cdots, f_k(x,t))^T$ and $\boldsymbol{u}(x,t) = (u_1(x,t), \cdots, u_k(x,t))^T$, for $x \in \Omega$. Here a few or all of the diagonal elements of $\boldsymbol{A}$ are zero and others are bounded by a constant. A couple of articles for the system of singularly perturbed elliptic and parabolic equations can be seen in Shishkin [80, 81].

Two-dimensional singularly perturbed problems also attracted by several authors for *e.g.,* Clavero et al. [19] and Clavero et al. [20]. One may think of extending the higher-order convergence techniques to solve the following two-dimensional model

convection-diffusion problem using mesh equidistribution:

$$\begin{cases} -\varepsilon \triangle u - \boldsymbol{A}.\nabla u = f(x,y), \quad (x,y) \in \mathcal{D} = (0,1)^2, \\ u = 0, \quad (x,y) \in \partial\mathcal{D}, \end{cases} \tag{8.2.6}$$

where $\boldsymbol{A} = (a_1, a_2)$ such that $a_1(x,y), a_2(x,y) \gg \varepsilon > 0$ and $\partial\mathcal{D}$ defines the boundary of $\mathcal{D}$. The source function $f(x,y)$ will be assumed sufficiently smooth. Now, define the inflow and outflow boundary

$$\partial\mathcal{D}_{in} = \{(x,y) \in \partial\mathcal{D} : y = 1\} \bigcup \{(x,y) \in \partial\mathcal{D} : x = 1\},$$

and

$$\partial\mathcal{D}_{out} = \{(x,y) \in \partial\mathcal{D} : y = 0\} \bigcup \{(x,y) \in \partial\mathcal{D} : x = 0\},$$

respectively. The two-dimensional problem (8.2.6) has boundary layers normal to $\partial\mathcal{D}_{out}$.

It is important to observe that the convergence of the model problems discussed in this thesis are based on the smoothness of the given data. Thus it will be more interesting and challenging to extend these techniques to problems with nonsmooth data resulting boundary and interior layers.

Bibliography

[1] V.B. Andreev. The Green function and a priori estimates for solutions of monotone three-point singularly perturbed difference schemes. *Differ. Equ.*, **37(7)**:923–933, 2001.

[2] A.R. Ansari and A.F. Hegarty. Numerical solution of a convection-diffusion problem with Robin boundary conditions. *J. Comput. Appl. Math.*, **156**:221–238, 2003.

[3] M.J. Baines, M.E. Hubbard, and P.K. Jimack. A moving mesh finite element algorithm for the adaptive solution of time-dependent partial differential equations with moving boundaries. *Appl. Numer. Math.*, **54(3-4)**:450–469, 2005.

[4] N.S. Bakhvalov. Towards optimization of methods for solving boundary value problems in the presence of boundary layers. *Zh. Vychisl. Mat. i Mat. Fiz.*, **9**:841–859, 1969 (In Russian).

[5] W. Bangerth and R. Rannacher. *Adaptive Finite Element Methods for Differential Equations*. Birkhäuser Verlag, Basel, 2003.

[6] R.K. Bawa and S. Natesan. A computational method for self-adjoint singular perturbation problems using quintic spline. *Comput. Math. Appl.*, **50(8-9)**:1371–1382, 2005.

[7] M.G. Beckett. *The robust and efficient numerical solution of singularly perturbed boundary value problem using grid adaptivity*. PhD thesis, University of Strathclyde, Strathclyde, U.K., 1998.

[8] M.G. Beckett and J.A. Mackenzie. Convergence analysis of finite difference approximations on equidistribted grids to a singularly perturbed boundary value problem. *Appl. Numer. Math.*, **35**:87–109, 2000.

[9] M.G. Beckett and J.A. Mackenzie. On a uniformly accurate finite difference approximation of a singularly perturbed reaction-diffusion problem using grid equidistribution. *J. Comput. Appl. Math.*, **131**:381–405, 2001.

[10] M.G. Beckett and J.A. Mackenzie. Uniformly convergent high order finite element solutions of a singularly perturbed reaction-diffusion equation using mesh equidistribution. *Appl. Numer. Math.*, **39**:31–45, 2001.

[11] C.M. Bender and S.A. Orszag. *Advanced Mathematical Methods for Scientists and Engineers*. McGraw-Hill, New York, 1978.

[12] C.J. Budd, W. Huang, and R.D. Russell. Adaptivity with moving grids. *Acta Numer.*, **18(1)**:111–241, 2009.

[13] A.W. Bush. *Perturbation Methods for Engineers and Scientists*. CRC Press, London, 1992.

[14] X. Cai and F. Liu. Uniform convergence difference schemes for singularly perturbed mixed boundary problems. *J. Comput. Appl. Math.*, **166**:31–54, 2004.

[15] G.F. Carey and H.T. Dinh. Grading functions and mesh redistribution. *SIAM J. Numer. Anal.*, **22(5)**:1028–1040, 1985.

[16] N.M. Chadha and N. Kopteva. A robust grid equidistribution method for a one-dimensional singularly perturbed semilinear reaction-diffusion problem. *IMA J. Numer. Anal.*, **31(1)**:188–211, 2011.

[17] K.W. Chang and F.A. Howes. *Nonlinear Singular Perturbation Phenomena: Theory and Applications*. Springer-Verlag, Newyork, 1984.

[18] K. Chen. Error equidistribution and mesh adaptation. *SIAM J. Sci. Comput.*, **15(4)**:798–818, 1994.

[19] C. Clavero, J.L. Gracia, and J.C. Jorge. A uniformly convergent alternating direction HODIE finite difference scheme for 2D time-dependent convection-diffusion problems. *IMA J. Numer. Anal.*, **26(1)**:155–172, 2006.

[20] C. Clavero, J.C. Jorge, F. Lisbona, and G.I. Shishkin. A fractional step method on a special mesh for the resolution of multidimensional evolutionary convection-diffusion problems. *Appl. Numer. Math.*, **27**:211–231, 1998.

[21] P. Das and S. Natesan. Higher order parameter uniform convergent schemes for Robin type reaction-diffusion problems using adaptively generated grid. *Int. J. Comput. Meth.*, **9(4)**:DOI 10.1142/S0219876212500521, 2012.

[22] C. de Boor. Good approximation by splines with variable knots. In *Spline functions and approximation theory (Proc. Sympos., Univ. Alberta, Edmonton, Alta., 1972)*, pages 57–72. Internat. Ser. Numer. Math., Vol. **21**. Birkhäuser, Basel, 1973.

[23] C. de Boor. Good approximation by splines with variable knots. II. In *Conference on the Numerical Solution of Differential Equations (Univ. Dundee, Dundee, 1973)*, pages 12–20. Lecture Notes in Math., Vol. **363**. Springer, Berlin, 1974.

[24] D. N. de G. Allen and R.V. Southwell. Relaxation methods applied to determine the motion, in two dimensions, of viscous fluid past a fixed cylinder. *Quart. J. Mech. Appl. Math.*, **8**:129–145, 1955.

[25] B.S. Deb and S. Natesan. Richardson extrapolation method for singularly perturbed coupled system of convection-diffusion boundary-value problems. *CMES: Computer Modeling in Engineering and Sciences*, **38(2)**:179–200, 2008.

[26] E.P. Doolan, J.J.H. Miller, and W.H.A. Schilders. *Uniform Numerical Methods for Problems with Initial and Boundary Layers*. Boole Press, Dublin, 1982.

[27] M. Van Dyke. *Perturbation Methods in Fluid Mechanics*. Academic Press, New York, 1964.

[28] V. Ervin and W. Layton. On the approximations of the derivatives of singularly perturbed boundary value problems. *SIAM J. Sci. Comput.*, **8(3)**:265–277, 1987.

[29] P.A. Farrell, A.F. Hegarty, J.J.H. Miller, E. O'Riordan, and G.I. Shishkin. *Robust Computational Techniques for Boundary Layers*. Chapman & Hall/CRC Press, Boca Raton, 2000.

[30] J. Filo and V. Pluschke. The porous medium equation in a two-component domain. *J. Differential Equations*, **247(9)**:2455–2484, 2009.

[31] B. Fornberg. Generation of finite difference formulas on arbitrarily spaced grids. *Math. Comp.*, **51(184)**:699–706, 1988.

[32] K.O. Friedrichs and W. Wasow. Singular perturbations of nonlinear oscillations. *Duke Math. J.*, **13**:367–381, 1946.

[33] E.C. Gartland. Graded mesh difference schemes for singularly perturbed two point boundary value problems. *Math. Comp.*, **51(184)**:631–657, 1988.

[34] P.W. Hemker, G.I. Shishkin, and L.P. Shishkina. ε-uniform schemes with high-order time-accuracy for parabolic singular perturbation problems. *IMA J. Numer. Anal.*, **20(1)**:99–121, 2000.

[35] P.W. Hemker, G.I. Shishkin, and L.P. Shishkina. High order accuracy decomposition of Richardson's method for a singularly perturbed elliptic reaction-diffusion equation. *Comput. Math. Math. Phys.*, **44(2)**:309–316, 2004.

[36] W. Huang, Y. Ren, and R.D. Russell. Moving mesh methods based on moving mesh partial differential equations. *J. Comput. Phys.*, **113(2)**:279–290, 1994.

[37] W. Huang and R.D. Russell. Analysis of moving mesh partial differential equations with spatial smoothing. *SIAM J. Numer. Anal.*, **34(3)**:1106–1126, 1997.

[38] M.K. Kadalbajoo and K.C. Patidar. A survey of numerical techniques for solving singularly perturbed ordinary differential equations. *Appl. Math. Comput.*, **130(2-3)**:457–510, 2002.

[39] M.K. Kadalbajoo and K.C. Patidar. Singularly perturbed problems in partial differential equations: a survey. *Appl. Math. Comput.*, **134(2-3)**:371–429, 2003.

[40] M.K. Kadalbajoo and Y.N. Reddy. Asymptotic and numerical analysis of singular perturbation problems: a survey. *Appl. Math. Comput.*, **30(3)**:223–259, 1989.

[41] R.B. Kellogg and A. Tsan. Analysis of some difference approximations for a singular perturbation problem without turning points. *Math. Comp.*, **32(1)**:1025–1039, 1978.

[42] N. Kopteva. Maximum norm a posteriori error estimates for a one-dimensional convection-diffusion problem. *SIAM J. Numer. Anal.*, **39(2)**:423–441, 2001.

[43] N. Kopteva. Maximum norm a posteriori error estimates for a 1D singularly perturbed semilinear reaction-diffusion problem. *IMA J. Numer. Anal.*, **27(3)**:576–592, 2007.

[44] N. Kopteva, N. Madden, and M. Stynes. Grid equidistribution for reaction-diffusion problems in one dimension. *Numer. Algorithms*, **40(3)**:305–322, 2005.

[45] N. Kopteva and M. Stynes. A robust adapive method for a quasilinear one-dimensional convection-diffusion problem. *SIAM J. Numer. Anal.*, **39(4)**:1446–1467, 2001.

[46] T. Linß. Sufficient conditions for uniform convergence on layer-adaptive grids. *Appl. Numer. Math.*, **37**:241–255, 2001.

[47] T. Linß. Uniform pointwise convergence of finite difference schemes using grid equidistribution. *Computing*, **66(1)**:27–39, 2001.

[48] T. Linß. Error expansion for a first-order upwind difference scheme applied to model convection-diffusion problem. *IMA J. Numer. Anal.*, **24(2)**:239–253, 2004.

[49] T. Linß. Analysis of an upwind finite-difference scheme for a system of coupled singularly perturbed convection-diffusion equations. *Computing*, **79(1)**:23–32, 2007.

[50] T. Linß. Analysis of a system of singularly perturbed convection-diffusion equations with strong coupling. *SIAM J. Numer. Anal.*, **47(3)**:1847–1862, 2009.

[51] T. Linß and N. Madden. Accurate solution of a system of coupled singularly perturbed reaction-diffusion equations. *Computing*, **73(2)**:121–133, 2004.

[52] T. Linß and N. Madden. Layer-adapted meshes for a linear system of coupled singularly perturbed reaction-diffusion problems. *IMA J. Numer. Anal.*, **29(1)**:109–125, 2009.

[53] N. Madden and M. Stynes. A uniformly convergent numerical method for a coupled system of two singularly perturbed linear reaction-diffusion problems. *IMA J. Numer. Anal.*, **23(4)**:627–644, 2003.

[54] S. Matthews, E. O'Riordan, and G.I. Shishkin. A numerical method for a system of singularly perturbed reaction-diffusion equations. *J. Comput. Appl. Math.*, **145(2)**:151–166, 2002.

[55] J.J.H. Miller, E. O'Riordan, and G.I. Shishkin. *Fitted Numerical Methods for Singular Perturbation Problems*. World Scientific, Singapore, 1996.

[56] J.J.H. Miller, G.I. Shishkin, B. Koren, and L.P. Shishkina. Grid approximatiom of a singularly perturbed boundary value problem modelling heat transfer in the case of flow over a fat plate with suction of the bounday layer. *J. Comput. Appl. Math.*, **166(1)**:221–232, 2004.

[57] P.D. Miller. *Applied Asymptotic Analysis*. American Mathematical Society, Rhode Island, 2006.

[58] J. Mohapatra and S. Natesan. Uniform convergence analysis of finite difference scheme for singularly perturbed delay differential equation on an adaptively generated grid. *Numer. Math. Theory Methods Appl.*, **3**(**1**):1–22, 2010.

[59] K.W. Morton. *Numerical Solution of Convection-Diffusion Problems*. Chapman & Hall, London, 1996.

[60] K. Mukherjee and S. Natesan. Optimal error estimate of upwind scheme on Shishkin-type meshes for singularly perturbed parabolic problems with discontinuous convection coefficients. *BIT*, **51**(**2**):289–315, 2011.

[61] K. Mukherjee and S. Natesan. Richardson extrapolation technique for singularly perturbed parabolic convection-diffusion problems. *Computing*, **92**(**1**):1–32, 2011.

[62] S. Natesan and R.K. Bawa. Second-order numerical scheme for singularly perturbed reaction-diffusion Robin problems. *JNAIAM J. Numer. Anal. Ind. Appl. Math.*, **2(3-4)**:177–192, 2007.

[63] S. Natesan and B.S. Deb. A robust computational method for singularly perturbed coupled system of reaction-diffusion boundary-value problems. *Appl. Math. Comput.*, **188(1)**:353–364, 2007.

[64] M.C. Natividad and M. Stynes. Richardson extrapolation for a convection-diffusion problem using a Shishkin mesh. *Appl. Numer. Math.*, **45(2-3)**:315–329, 2003.

[65] R.E. O'Malley. *Singular Perturbation Methods for Ordinary Differential Equations*. Springer-Verlag, New York, 1991.

[66] V. Pereyra and E.G. Sewell. Mesh selection for discrete solution of boundary value problems in ordinary differential equations. *Numer. Math.*, **23**:261–268, 1975.

[67] S. Polak, C. den Heijer, W.H. Schiders, and P. Markowich. Semi-conductor device modeling from the numerical point of view. *Int. J. Numer. Methods Eng.*, **24**:763–838, 1987.

[68] L. Prandtl. Uber flussigkeits-bewegung bei kleiner reibung. *In Verhandlungen, III Inter. Math. Kongresses, Tuebner, Leipzig*, pages 484–491, 1905.

[69] J.D. Pryce. On the convergence of iterated remeshing. *IMA J. Numer. Anal.*, **9(3)**:315–335, 1989.

[70] L.P. Shishkina P.W. Hemker, G.I. Shishkin. High-order time-accurate schemes for singularly perturbed parabolic convection-diffusion problems with robin boundary conditions. *Computational Methods in Applied Mathematics*, **2(1)**:3–25, 2002.

[71] Y. Qiu, D.M. Sloan, and T. Tang. Numerical solution of a singularly perturbed two-point boundary value problem using equidistribution: analysis of convergence. *J. Comput. Appl. Math.*, **116(1)**:121–143, 2000.

[72] Y. Ren and R.D. Russell. Moving mesh techniques based upon equidistribution, and their stability. *SIAM J. Sci. Statist. Comput.*, **13(6)**:1265–1286, 1992.

[73] W. Rodi. Turbulence models and their applications in hydraulics. *A.A. Balkema, ed., IAHR Monograph Series.*, 1993.

[74] H.G. Roos, M. Stynes, and L. Tobiska. *Robust Numerical Methods for Singularly Perturbed Differential Equations. Convection-Diffusion-Reaction and Flow Problems*. Springer-Verlag, Berlin, 2008.

[75] V. Shanthi and N. Ramanujam. A numerical method for boundary value problems for singularly perturbed fourth-order ordinary differential equations. *Appl. Math. Comput.*, **129(2-3)**:269–294, 2002.

[76] V. Shanthi and N. Ramanujam. A boundary value technique for boundary value problems singularly perturbed fourth-order ordinary differential equations. *Comput. Math. Appl.*, **47(10-11)**:1673–1688, 2004.

[77] G.I. Shishkin. A difference scheme for a singularly perturbed equation of parabolic type with a discontinuous initial condition. *Soviet Math. Dokl.*, **37(3)**:792–796, 1988 (In Russian).

[78] G.I. Shishkin. Approximation of solutions of singularly perturbed boundary value problems with a parabolic boundary layer. *U.S.S.R. Comput. Maths. Math. Phys.*, **29(4)**:1–10, 1989.

[79] G.I. Shishkin. A difference scheme for a singularly perturbed parabolic equation that is degenerate on the boundary. *Comput. Math. Math. Phys.*, **32(5)**:621–636, 1992.

[80] G.I. Shishkin. Grid approximation of singularly perturbed boundary value problems for systems of elliptic and parabolic equations. *Comput. Maths. Math. Phys.*, **35(4)**:429–446, 1995.

[81] G.I. Shishkin. Grid approximation of singularly perturbed systems of elliptic and parabolic equations with convective terms. *Differential Equations (Differ. Equ.)*, **34(12)**:1693–1704, 1998.

[82] S. Valamarthi and N. Ramanujam. An asymptotic numerical method for singularly perturbed third-order ordinary differential equations of convection-diffusion type. *Comput. Math. Appl.*, **44(5-6)**:693–710, 2002.

[83] R. Vulanovic. On a numerical solution of a type of singularly perturbed boundary value problem by using special discretization mesh. *Univ. u Novom Sadu Zb. Rad. Prirod.-Mat. Ser. Mat.*, **13**:187–201, 1983.

[84] W. Wasow. *On boundary layer problems in the theory of ordinary differential equations*. PhD thesis, New York University, New York, U.S.A., 1941.

[85] C. Zhongdi. Parameter-uniform finite dfference scheme for a system of coupled singularly perturbed convection-diffusion equations. *J. Syst. Sci. Complex.*, **18(4)**:498–510, 2005.

Peer Reviewed Publications

1. P. Das and S. Natesan, A uniformly convergent hybrid scheme for singularly perturbed system of reaction-diffusion Robin type boundary value problems, *J. Appl. Math. Comput.,* **41(1-2)**:447-471, 2013.
2. P. Das and S. Natesan, Higher order parameter uniform convergent schemes for Robin type reaction-diffusion problems using adaptively generated grid, *Int. J. Comput. Meth., Vol. 9, No. 4, 2012, DOI 10.1142/S0219876212500521.*

Submitted for Publication

1. P. Das and S. Natesan, A post-processing technique to obtain ε–uniform higher order accuracy for convection-diffusion problems on adaptively generated grid, *Communicated.*
2. P. Das and S. Natesan, A priori error estimate using grid adaptation technique for singularly perturbed system of reaction-diffusion boundary value problems, *Communicated.*
3. P. Das and S. Natesan, Robust numerical method for system of singularly perturbed convection-diffusion boundary-value problems through adaptively generated grid, *Communicated.*
4. P. Das and S. Natesan, Mesh adaptation for a class of singularly perturbed fourth order ordinary differential equations, *Communicated.*

Conference Proceedings

1. P. Das and S. Natesan, Parameter-uniform numerical method for a system of singularly perturbed convection-diffusion boundary-value problems on adaptively generated grid, *the International Conference on Advances in Modeling, Optimization and Computing (AMOC-2011), IIT Roorkee, Roorkee, India, December 5-7, 779-790, 2011.*